UiT The Arctic University of Norway

Faculty of Engineering Science and Technology

Sea Spray Icing Prediction: Integrating Experiments, Machine Learning, and Computational Fluid Dynamics.

SPICE: A machine learning model for prediction of sea spray icing.

Sujay Deshpande

A dissertation for the degree of Philosophiae Doctor (PhD) [May 2024]

A personal note

Thank you, Annie, for being with me through all of this, the encouragement, motivation, inspiration, and for everything else. Thank you Sia for all the beautiful memories so far and wish for many more to come.

आई बाबांचा आशीर्वाद...[1]

Words fall short to describe this long journey, and so does the list of people to thank. Deeply indebted to all family and friends who were a part of this, all from literal physical help during the experiments to helping me learn and brainstorming with me; for all the support from back in India, and all over the world; and for all the memories we shared and who continue to bless me from up there – we shall continue to be one, अहम् ब्रह्मास्मि[2].

Finally, to all PhD fellow colleagues at UiT suffering from stress, anxiety, and depression as a direct result of their work and workplace – keep on fighting for what you dreamt of at the start, don't let others put you down. Most importantly, don't let the PhD journey dictate your life, you are far better and stronger than the outcome. Carry on, as if nothing really matters[3], because it doesn't. And always remember, अपना time आएगा, तू नंगा ही तो आया है क्या घंटा लेकर जाएगा[4].

[1] In Marathi: With the blessings of my mother and father

[2] In Sanskrit: A spiritual belief from Indian Vedic Literature from the 6th century BCE indicating absolute oneness of the self with the universe. Each aspect of the universe, the ultimate reality, each individual in the non-physical form, the soul, are one and the same entity.

[3] Bulsara, Farrokh aka Freddy Mercury; Queen, 1975

[4] In Hindi (Mumbai dialect): I will succeed. You have come empty handed and will leave so. Da Silva Fernandes, Vivian Wilson aka Divine; Tewari, Ankur; and Singh, Ranveer; Gully Boy, 2019

Table of contents

List of Tables

Appendix 1

Appendix 2

Appendix 3

Appendix 4

[Unavailable in the restricted version of the thesis due to embargo]

Appendix 5

[Unavailable in the restricted version of the thesis due to embargo]

List of figures

Appendix 1

Appendix 2

Appendix 3

Appendix 4

[Unavailable in the restricted version of the thesis due to embargo]

Appendix 5

[Unavailable in the restricted version of the thesis due to embargo]

1. Abstract

Ice accretion is challenging for maritime and offshore operations in the Polar regions. Activities related to tourism, oil and gas exploration, fishing, and offshore wind energy are increasing in the arctic. Ice accretion on vessels and offshore structures pose a threat to structural integrity, vessel stability, and personnel safety in outdoor working environments. Freezing sea spray is the largest contributor to marine and offshore icing, attributing to 80-90% of offshore icing incidents.

Sea spray icing is a niche field with comparatively limited research. Theory related to this field is difficult to find from a single source and is spread throughout literature. Having no single source to refer to for theory and standards makes it challenging for new researchers in the field.

Models for prediction of sea spray icing are essential for safer maritime operations in the Arctic. Existing models have varying approaches and provide rather varying predictions, making it difficult to say which one is more accurate. Additionally, existing models are heavily dependent on existing empirical formulations developed from limited observations for important variables like spray flux, something pointed out to be the weakest link in any prediction model. Using these formulations, typically based on medium sized fishing vessels, limits the predictions to the type and size of vessel the formulations are based on. ISO35106 points this out with a comment that none of the current models can predict sea spray icing on a wide range of vessels.

Full-scale testing of sea spray icing poses significant challenges with respect to personnel safety in extreme weather conditions, as well as the costs associated with such testing. This has resulted in limited full-scale or laboratory data. This in turn makes it difficult for validating prediction models as well as for the development of new and better models.

Apart from different approaches, prediction models could have different purposes. Operational prediction models, or forecasting models, predict an icing rate for a given set of metocean conditions without any consideration of the type of vessel or structure. These could be best suited for taking precautionary actions in case heavy icing is forecasted. Comprehensive prediction models, on the other hand, can estimate the spatial distribution of icing over the vessel or structure surface for a set of metocean conditions. In other words, these can estimate the icing rates as a function of location on the surface. These are more suitable at the design stage to take anti-icing measures or design optimization of the vessel/structure itself to minimize icing or that of the heating systems.

The main objective of this PhD project was to develop a universal model for prediction of sea spray icing that could be able to predict icing on any vessel or offshore structure irrespective of its size, shape, or motion. After collecting extensive data from laboratory experiments, a forecasting type of model, SPICE, was developed ‘bottom-up’ from the experimental data using Machine Learning. An upgrade to this model is later made using Computational Fluid Dynamics to estimate some variables essential for prediction. This model, dubbed SPICE2, is a comprehensive prediction model and independent of any existing formulations for estimation of spray. SPICE2 was validated with icing measurements from a full-scale test.

The study presents a shift from the traditional modelling methods owing to the techniques used. The presented models show promising results with considerable scope for improvements in future research.

1.1. Main contributions

1. Consolidation of theory, standards, and existing prediction models in a single source.
2. Valuable sea spray icing data from the largest set of laboratory experiments to date.
3. SPICE (Sea sPray ICE): A machine learning model for prediction of sea spray icing. This is a forecasting model using empirical formulations of flux of choice but is flexibly designed to have room for users to use real time measurements of flux if available. The 'feature calculator' also gives room for estimating any missing variables required for prediction, albeit at the cost of accuracy.
4. SPICE2: An upgrade to SPICE using CFD to estimate ship specific parameters for prediction of icing rates and distribution of icing. This is a comprehensive prediction model that acts as a design tool for assessment of icing loads at specific locations on the vessel/ structure and would help optimally design active or passive anti-icing systems.

2. List of Publications

The list of papers for the PhD project, along with their publication status, and journal level according to the Norwegian Directorate for Higher Education and Skills are as follows:

- **Paper 1: Sea Spray Icing: The Physical Process and Review of Prediction Models and Winterization Techniques.**

(Status: Published. Journal level: 2, the highest level according to the Norwegian Directorate for Higher Education and Skills [1])

Deshpande Sujay, Sæterdal Ane, Sundsbø Per-Arne, 'Sea Spray Icing: The Physical Process and Review of Prediction Models and Winterization Techniques.' Journal of offshore Mechanics and Arctic Engineering, December 2021. Volume 143(6) / 061061. Paper number OMAE-20-1167. Published online: May 4, 2021. https://doi.org/10.1115/1.4050892

- **Paper 2: Experiments with Sea Spray Icing: Investigation of Icing Rates**

(Status: Published online. Journal level: 2, the highest level according to the Norwegian Directorate for Higher Education and Skills [1])

Deshpande Sujay, Sæterdal Ane, Sundsbø Per-Arne, 'Experiments with Sea Spray Icing: Investigation of Icing Rates.' Journal of offshore Mechanics and Arctic Engineering, February 2024, 146(1) / 011601. Paper number OMAE-22-1165. Published online: May 11, 2023. https://doi.org/10.1115/1.4062255

- **Paper 3: A machine learning model for prediction of marine icing**

(Status: Published online. Journal level: 2, the highest level according to the Norwegian Directorate for Higher Education and Skills [1])

Deshpande Sujay, 'A Machine Learning Model for Prediction of Marine Icing'. Journal of offshore Mechanics and Arctic Engineering, December 2024, 146(6) / 061601. Paper number OMAE-23-1029. Published online: March 1, 2024. https://doi.org/10.1115/1.4064108

- **Paper 4: Investigation into using CFD for estimation of ship specific parameters for the SPICE model for prediction of sea spray icing. Part 1: The proposal**

(Status: Submitted to journal for peer review.)

Deshpande Sujay, Sundsbø Per-Arne, 'Investigation into using CFD for estimation of ship specific parameters for the SPICE model for prediction of sea spray icing. Part 1: The proposal.' (To be submitted).

- **Paper 5: Investigation into using CFD for estimation of ship specific parameters for the SPICE model for prediction of sea spray icing. Part 2: Verification of Spice2 with full scale test**

(Status: Submitted to journal for peer review.)

Sundsbø Per-Arne, Deshpande Sujay 'Investigation into using CFD for estimation of ship specific parameters for the SPICE model for prediction of sea spray icing. Part 2: Verification of Spice2 with full scale test.' (To be submitted).

3. Objective of the PhD project

- *To develop a universal model for prediction of sea spray icing that can predict icing rates and distribution of icing on a wide range of vessels and structures, irrespective of the size, shape, and movement. The model should be:*
    - *Able to give icing rates at different locations on the same structure.*
    - *Independent of existing empirical flux formulations.*
    - *Based on a large set of icing data.*
    - *Able to also give forecasts for quick operational assessment.*

4. Introduction

4.1. The sea spray icing problem

Fishing and whaling have served as the main occupation in the arctic coastal regions for centuries [2]. Offshore activity has risen in the arctic and sub-arctic regions in the past few decades owing to oil and gas exploration. This is expected to rise further in the coming decades [3]. Tourism has also been increasing in this region with, for example, the increasing number of cruises to Svalbard [4]. Reduction of sea ice in the Arctic has opened shorter trade routes from Europe and North America to Asia through the Arctic. By the end of the century, even moderately-ice strengthened vessels are expected to be able to transit through the Arctic almost all year round [5].

In 1979, six fishing vessels sank killing 15 fishermen outside the coast of Hanstholm, Denmark in the North Sea, due to an icing incident lasting 24 hours. It was reported that heavy icing started as soon as the vessels started sailing upwind. The radar froze, antennas broke, and freezing on the wheelhouse windows led to

limited visibility. The windspeeds were 8-10 Beauforts (corresponding to 17-28 m/s [6]) and air temperature of -8°C; and it is reported that the surface of the ships was covered with six centimeters of ice within 12 hours. The severe conditions made it unfeasible to knock off the ice off the deck. It was also speculated that the life rafts were covered with ice preventing their release. [7]

Marine operations in freezing temperatures in the Arctic are challenging due to harsh weather conditions. Challenges due to ice accretion on vessels and structures have to be mitigated by taking appropriate actions for anti-icing or de-icing depending on the case. Ice accretion leads to additional weight on structures and could result in structural instability. Heavy icing loads on vessels can in extreme cases with lopsided ice loads, lead to capsizing or cause structural failures of the deck equipment. In other cases, critical systems like ventilation systems and escape doors can be blocked due to ice. Operational Health and Safety can be compromised due to slippery decks [8].

Sources of marine icing include supercooled fog, freezing rain, snow, and freezing sea spray. The most frequent and most significant source of icing is through freezing sea spray. The other sources are not considered to have any serious impact. Freezing sea spray is said to be accountable for 80-90% of all icing related incidents offshore [9], [10].

Traditionally, icing is tackled by deicing measures by mechanical means such as manually knocking the ice of the superstructure and deck. Anti-icing measures include heat tracing and chemical treatment of surfaces. If the areas prone to icing are available at available at the design stage, vessels and structures can be designed in a manner to minimize icing, prevent icing on critical equipment, or to optimize other anti-icing systems like heating [8].

Sea spray has two sources – the spray generated off wave crests due to wind, also called wind generated spray; and the spray generated due to ship impacting the wave or wave impacting the structure, also called the wave impact generated spray. Wind generated spray has proven to not have a significant contribution to icing compared to wave impact generated spray and can be ignored during predictions [11].

4.2. Necessity of icing predictions

Sea spray icing is the most common and severe form of icing and proves to be a challenge for operations in cold climate. The weight of accreted ice needs to be accounted for structural integrity. Vessels need to be stable in case of icing on the superstructure. Anti-icing systems like heat cables need to be optimally designed considering energy consumption. Critical equipment on the deck needs to be shielded against any possible icing. It is thus important to know, first of all, the expected icing rates in a given set of metocean conditions. In addition to the icing rates, it is as important to know the distribution of icing on the vessel's superstructure such that the dangers of icing can be mitigated at the design stage such that necessary design customizations could be done to reduce the impact of icing. Examples could include customization of the hull shape to reduce the spray generation or placing critical equipment in regions that are less prone to spray impact and eventually icing. Knowing the distribution also helps to analyze the stability of the vessel in icing conditions. Several international standards put down certain specific conditions for operations in cold climates, these are covered in the following sections.

4.3. Standards and regulations on sea spray icing

International standards like ISO 19906, ISO35106, DNVGL-OS-A201, and the Polar Code, put forward requirements for vessels and offshore installations operating in cold climate regions. Some of the important points related to sea spray icing and measures to mitigate challenges due to icing are discussed here, and generally suggest to 'take some action' against icing. It should be noted that these standards also talk about sea ice, for example, strengthening of the hull of vessels to avoid damage due to impact with sea ice. Such points related to sea ice are out of scope of the current study, all the more, as presence of sea ice actually reduces the spray generation, and thereby possibly resulting in lesser sea spray icing [8].

Winterization is the process to take measures for safe operations in cold climate, either during the design stage itself or during operations. Winterization measures related to icing are classified as anti-icing (prevention of ice formation) and deicing (removal of accreted ice). Winterization measures can also be classified as active measures (i.e., direct use of energy or physical force, for example, heating or hammering away the ice) and passive measures (for example, shielding, insulation, or coatings that prevent adhesion of ice).

Some of the relevant points from the aforementioned standards are as follows:

- Preference should be given to passive anti-icing measures [12]. These are measures that don't require any labor, activating procedure, or fuel/ electricity, for example, sheading, insulation, and surface coatings [8].
- A shielded location is the simplest and most reliable solution for anti-icing [12].
- Equipment requiring anti-icing measures should be as far as possible from the area prone to sea spray [12].
- A specific set of excess ice load conditions predefined by the standards must be applied for structural calculations to avoid structural failures [12].
- As such, ships should be designed to minimize ice accretion [13].
- Equipment critical for personnel safety should be completely functional under icing conditions and ideally should be kept ice free [12], [13], [14].
- Adequate stability should be retained in icing conditions in spite of the excess weight of accreted ice [12], [13], [14].
- Outdoor operations and analysis should be carried out for open and semi-open work areas in order to identify and take actions in potential problem areas due to overall exposure to temperature, wind, and icing [15].
- None of the current methods can predict sea spray icing accurately on a wide range of vessels [16].

4.3.1. Consequences of standards and regulations

- To avoid dangerous outdoor working environment, the possible need of hazardous manual removal of ice should be identified and reduced to a minimum.
- For designing the placement and shielding of critical equipment, locations on the vessel that are prone to icing needs to be identified. This requires knowing the distribution of icing over the structure at the design stage.

- To identify potential problem areas due to icing that might lead to dangerous working conditions, and consecutively, for taking appropriate measures, knowledge of icing rates at specific locations on a vessel or structure is important.
- In general, standards related to sea spray icing state that action needs to be taken against icing and point clearly towards knowing the distribution of icing in addition to the icing rates in given set of met-ocean conditions.

Paper 1 provides information on the existing standards in more detail. One type of requirements from standards deals with structural integrity of the vessel/ structure, for example, the ones outlining the maximum characteristics icing loads the vessel/ structure should be able to withstand while maintaining structural integrity (see Paper 1 - Table 1). The other type of requirements deals with the icing rates during operational conditions (see Paper 1 – Table 2). The latter are important for designing icing mitigation systems, like heating, and to give operators an idea of what conditions are to be expected to prepare them in taking appropriate actions. The universal model for prediction of sea spray icing, as mentioned in the objective in Section 3, should be able to give either of the assessment for a given set of met-ocean conditions. From a practical perspective, both assessments are relatively similar, since if the icing rate is known, the total load on the structure can be easily calculated. However, an important distinction is that, for the total load to be calculated, icing rates at individual locations on the structure, which would differ from each other depending on the local flux and other parameters, must be known. Existing models, except MARICE, are incapable of achieving this (see Table 1). On the other hand, only forecasting of icing rates for a given set of metocean conditions regardless of the type, size, and motion of vessels, is a quick and cheap way to give a general idea of the operational conditions, on the lines of weather forecasting.

4.4. A relevant research topic

Polar lows are severe storms in sub polar and polar regions with wind speeds above gale force occurring from October to May of which at least 20 cases have been reported each year since 1950 [17]. Strong winds that result in high waves which could result in large amounts of sea spray upon impact, in combination with freezing temperatures of the sub polar and polar winters are ideal conditions for heavy sea spray icing. Owing to the high frequency of these events and the potentially life-threatening consequences of sea spray icing in sever conditions, and in other less severe cases, the possibility of operational optimization through design of hulls and structures to minimize sea spray, avoiding the critical placing critical equipment in regions prone to sea spray icing, and possibility of other optimizations, such as that of heat systems through the knowledge of sea spray icing predictions makes sea spray icing a relevant research topic.

4.5. History of sea spray icing models

A considerable amount of research into sea spray icing was done in the 1960's-1980's. Early researchers gathered icing data mostly in the form of questionnaires from sailors from multiple countries, which was unfortunately not made publicly available [18], [19]. Several researchers have worked with the prediction problem and had very different approaches for determining the icing rates in a given set of met-ocean

conditions. Apart from the different approaches, the icing rates predicted by the different models also showed considerable variation, making it difficult to say which of the models is most accurate [20], [21]. Additionally, models also have some amounts of variation considering their applications; this is discussed in the following sections.

4.5.1. Forecasting vs Comprehensive Predictions

For the purpose of better understanding of the existing models, sea spray icing models could be divided into two broad categories as shown in Figure 1. The first category is termed as 'forecasting models' as these are capable of providing only the icing rates (either in terms of thickness or area density), similar to weather forecasts, for a given set of metocean conditions. The other category is termed as 'Comprehensive prediction models' which are capable of predicting the distribution of icing, in addition to the icing rates, on the surface of a vessel or structure depending on ship characteristics or size and shape of the structure. Forecasting models could be used to be better prepared in case of possible icing events. Prediction models however play a bigger role at the design stage of the vessels and critical sub-systems like placement of critical equipment or design of the heat tracing systems.

Forecasting models, though important for giving a quick assessment of the possible operational conditions, would give rather coarse predictions. This is due to the fact that the spray flux, which is an important variable for sea spray icing, depends on many factors like the size and shape of the vessel, the local ship-wave interaction, and not the least, the location on the vessel as the spray would not reach evenly to all parts of the ship. This would result in different amount of icing on different locations on the ship – making the prediction rather pointless, especially for design considerations. The generalization for forecasting would also require highly criticized [21], [22] empirical formulations for flux that do not necessarily hold true for all kinds of vessels and structures. Comprehensive prediction models on the other hand, would give icing loads at specific locations on the vessel or the structure for assessment of structural integrity and for optimal design of passive anti-icing measures. Having stated this fact, forecasting models are still important and used to give out icing alerts [23].

Some of the models are described in short in the following subsections.

4.5.2. Overland model

One of the earliest models for the forecasting of sea spray icing was the Overland model. The Overland model is a deterministic model that predicts the icing rate from basic physical parameters like wind speed, air and water temperatures, and salinity. The basis of this model was a set of 85 observations from intermediate size vessels (20-75m) and interviews with vessel operators [24]. Researchers have criticized the Overland model and argued that the results could not be replicated [25]. Overland et.al. 1986 themselves mention that the predicted icing rates with this model are similar to some studies by some unnamed Soviet and Japanese authors, but 5 times greater than one particular study by Mertins [26].

Despite this, due to the simplicity of the model, the Overland model has been widely used by the United States National Oceanic and Atmospheric Administration (NOAA) [27]. Being a forecasting type of model, the Overland model does not give any information about the distribution of icing over the structure.

4.5.3. Roebber & Mitten model

Roebber and Mitten 1987 were among those who found that the Overland model was too sensitive for water temperatures [28]. They modified the polynomial used by overland to incorporate this adjustment. This makes the Roebber & Mitten model as easy to use as the Overland model. Similar to that of the Overland model, this model does not give any information about the distribution of icing.

4.5.4. Stallabrass model

The Department of Transport, Ship Safety Branch, and the Canadian Research Council jointly proposed a research investigation into ship icing in 1968 as a result of the loss of three Canadian fishing vessels in preceding winters [9]. Stallabrass was critical to a previous model by Kachurin et. al. [29] that introduced time dependent effects stating this as 'unjustified' in view of uncertainties in measurements of various atmospheric and oceanic parameters and himself considered the icing process to be continuous, quasi-steady state process [9]. The Stallabrass model is a forecasting type of model and presents an equation for icing rate as a function of some basic parameters like wave height, relative wind speed, air temperature, and saturation vapour pressure. Additionally, the equilibrium temperature of the freezing surface is computed iteratively. This model is based on the 39 reported icing incidents specifically from fishing trawlers. Stallabrass concluded that each class of vessels should be treated separately due to differing sizes that could result into different icing rates. He also mentions that the scattered (inaccurate) nature of results from this model are attributed to size and design variations for the different fishing trawlers [9].

4.5.5. ICEMOD2

ICEMOD2 is a 2D numerical model that gives icing rates as a function of height on a vessel. It is an extension of the ICEMOD model developed for oil rigs at the Norwegian Hydrotechnical Laboratory (NHL) which is one of the first transient model [30]. ICEMOD2 attempts to model the brine film motion after spray impingement, and more complexities are added in terms of droplet trajectories around a cylinder. The model also considers wind generated spray. The model is based on flux measurements on a former trawler 'Endre Dyrøy'. An empirical relationship for the flux in terms of wave parameters, ship speed and heading, wind speed, and seawater density is provided for ship headings of 0°, 15°, and 45° from 10 (or 13 in one case) observations. Being a 2D model, it gives an idea of the distribution of ice at different heights. It however assumes equal icing on all surfaces at a given height, which is practically untrue as different regions on a ship are subjected to different spray flux. It was, however, a step towards understanding the distribution of icing on the surface. Being a numerical model that includes wind stress which is zero at the vertical stagnation line of the cylinders, the reliability of the model could not obtained by comparing the model results to that of the Endre Dyrøy measurements [30].

4.5.6. RIGICE04

RIGICE04 is a model developed at the University of Alberta in 2005, which is an extension of the previous RIGICE model. The newer version has been coded as an excel spreadsheet in visual basic. This makes the model very easy to implement if the excel file is obtained from the developers. The excel file is not openly available but can be obtained upon request. RIGICE04 is developed specifically for structures. Users have

to follow a specific guideline to input the metocean details and information about the structure. The model calculates icing thickness and the weight of ice on the structure as a function of height above the mean sea level in steps of 1m. Forest et.al. 2005 point out that the estimations of wave generated mass flux of spray from various Liquid Water Content (LWC) formulations available in literature vary greatly (from as low as 6.37×10^{-22} to as high as 44 kg/m^2/hr). The closest match for the LWC formulation for the semi-submersible drilling platform, Ocean Bounty, for which the model was developed, was from observations during experiments on Tarsuit island. This particular formulation was used since it matched an 'estimate' of 5-10 kg/m^2/hr of flux required to result in the observed amount of icing on the Ocean Bounty. They also mention that the equation used in RIGICE04 is from observations from one site only and that more field data is required to refine the result [31].

Availability of the excel file makes RIGICE04 relatively easy to implement. The spray flux formulation however was chosen from one set of observations at another location which was the closest match to estimates of flux required to obtain icing rates on one set of observations on Ocean Bounty. It makes it therefore difficult to say how accurate the icing predictions could be in a different set of weather conditions on a different platform. Additionally, RIGICE04 was developed specifically for structures, making it unusable for vessels, although rough estimates could be obtained for the purpose of comparison of different models.

4.5.7. MARICE

The MARICE model developed by Kulyakhtin 2014 [20] was the first, and until the development of the SPICE2 model, the only model that incorporated computational fluid dynamics (CFD) for parts of the models. Using CFD makes it possible for MARICE to provide a 3D spatial distribution of ice on a structure. However, CFD in MARICE is limited to computing heat transfer and wind flow around the structure. MARICE uses the same equations for spray mass flux as ICEMOD by Horjen and Vefsnmo 1985 [32] for testing the model, but any of the available flux formulations could be used [11]. A spray generation function was coded in Ansys using this equation which introduces spray droplets of predefined diameters at specific heights in the CFD domain at a vertical plain in front of the structure. For the demonstration of the method, the wind flow that carried the droplets to a ship was demonstrated [33]. This simulation, however, considered the ship as a stationary structure and the impingement of the artificially introduced droplets on the structure due to wind flow was computed. In addition, the MARICE model incorporates more complexities in terms of time-dependence and dynamics of the water film which showed to have a weak effect on ice growth compared to a steady state model [11].

Kulyakhtin 2014 points out that the choice of flux formulation is essential for icing predictions and mentions how using one flux formulation gave negligible icing, while another gave heavy icing in the location for lifeboats on the West Hercules drilling rig [11]. The dependence of the model on these empirical formulations which Kulyakhtin calls as the 'weakest links' in any prediction model, makes the results suitable for the type of vessel or structure and the prevailing metocean conditions that the spray flux formulation was based on. MARICE, however, paved the way for comprehensive prediction models using of CFD, albeit limited to a wind simulation, to estimate spatial distribution of ice in addition to icing rates on the structure.

4.5.8. MINCOG

The Marine Icing model for the Norwegian Coast guard (MINCOG) model developed by Samuelsen et.al. 2016 was, as the name suggests, a model based on historical weather and icing data and comparison with observations on the vessel KV Nordkapp of the Norwegian Coast Guard. The comparisons were made on one specific location on the vessel. The model is meant for general operational icing rate forecasts, similar to weather forecasts for precipitation. It does not provide the distribution of icing on the surface. Two different empirical formulations for spray flux were used and the one that best suited the case were incorporated along with additional historical data on wind and wave parameters. Samuelsen et.al. 2016 points out to the problems of applying empirical relationships for flux, as well as those between wind speeds and wave parameters. Although the use of MINCOG could be said to be similar to the Overland and Stallabrass models, wherein an icing rate is calculated from the metocean parameters without any information about the distribution of icing, its implementation is not as straightforward as the Overland and Stallabrass models making MINCOG difficult to implement for the purpose of a general forecast.

4.5.9. Comparison of sea spray icing models

Table 1 provides some details for comparison of the existing and proposed models.

Table 1: Some details about existing and the proposed models

Sr.nr.	Model	Ice distribution prediction	Ease of implementation (subjective)	Icing Based on	flux based on	Applications and openly known implementations
1	Overland [34]	None	Very easy	85 observations on intermediate size ships (20-75m)	N/A	Forecasting of icing rates in given met-ocean conditions (regardless of type and size of structure) by the United States National Oceanic and Atmospheric Administration (NOAA) [27] despite criticism (see section 4.5.2).
2	Roebber & Mitten	None	Very easy	Same as Overland	N/A	Academic research. Forecasting of icing rates (regardless of type and size of structure).
3	Stallabrass [35]	None	Relatively easy	39 observations on fishing trawlers of varying sizes	N/A	National Research Council (NRC) of Canada for prediction of icing rates on vessels [36] (regardless of type or size of ship). Unsure if utilized by the Dept. of Transport, Ship Safety Branch of the NRC.
4	ICEMOD2 [37]	2D (function of height)	Relatively complex	4 cylinders at different heights on a former trawler Endre Dyrøy	10-13 Observations on 4 collectors at different heights at 17.2m from the bow on a former trawler Endre Dyrøy	Academic research – for prediction of icing rates as a function of height on vessels (regardless of type and size of vessel).
5	RIGICE04 [38]	2D (function of height)	Relatively easy if excel file is available	Measurements on the semi-submersible drilling platform Ocean Bounty	Observations from an experiment on Tarsuit island	Academic research – for prediction of total icing loads on offshore structures. (Takes into consideration coarse dimensions of the structure.)

6	MARICE [39]	3D	Complex	Completely modelled	Any empirical formulation of choice	Academic research – Prediction of icing loads and spatial distribution of icing on offshore structures. Claimed to be applicable to vessels, but without consideration of vessel movement, effectively making it a stationary structure.
7	MINCOG [40]	None	Complex	Observations on one particular location on the vessel KV Nordkapp	Empirical formulations + historical weather data	Forecasting of icing rates for a given set of met-ocean conditions. Used by the Norwegian Meteorological Institute [41] regardless of the type and size of the vessel.
8	SPICE [21]	None	Very Easy	108K experimental datapoints	Up to user to use existing formulations or use live monitoring	Currently only academic research – Forecasting of icing rates for a given set of met-ocean conditions regardless of type and size of structure/ vessel.
9	SPICE2 [42]	3D	Complex due to use of CFD	108K experimental datapoints	CFD simulations	Currently only academic research – Prediction of icing rates (or total icing load) and spatial distribution for a given set of metocean conditions taking regard for the shape, size, and movement of the vessel/ offshore structure.

4.6. Need for an improved model

Upon close inspection of how existing models are designed and their applications, there is a large scope of improvement for sea spray icing predictions. Through the background study of existing models two types of models have been found as shown in Figure 1. For convention, these are hereafter referred to as P1 and P2 type of models. Operational forecasting models (P1 type) give a rough idea of what to expect in a given weather condition and could be said to be similar to weather forecasting. The P1 type of models do not take into account the design, size, shape, motion, etc. of the structure or the vessel, and predict a single value of icing rate for the given weather condition. The 'comprehensive prediction models' (P2 type) could be seen as a more robust tool that estimates the spatial distribution of icing over the surface, where different locations on the same structure in the same weather conditions could be subjected to different amounts of icing.

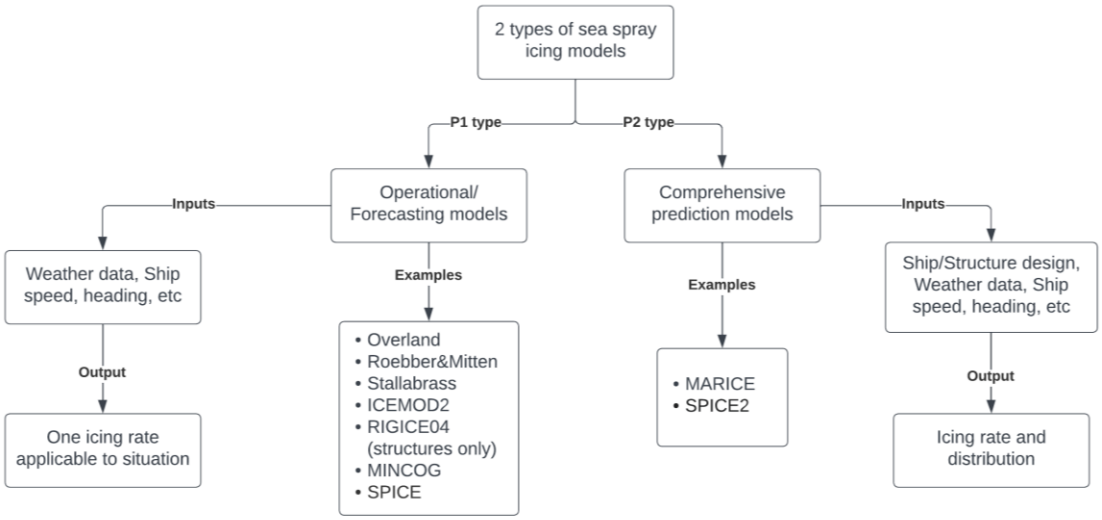

Figure 1: Types of sea spray icing prediction models

The evolution of sea spray icing prediction models over the past is shown in Figure 2. The first models have had the icing rate in focus, and not the distribution.

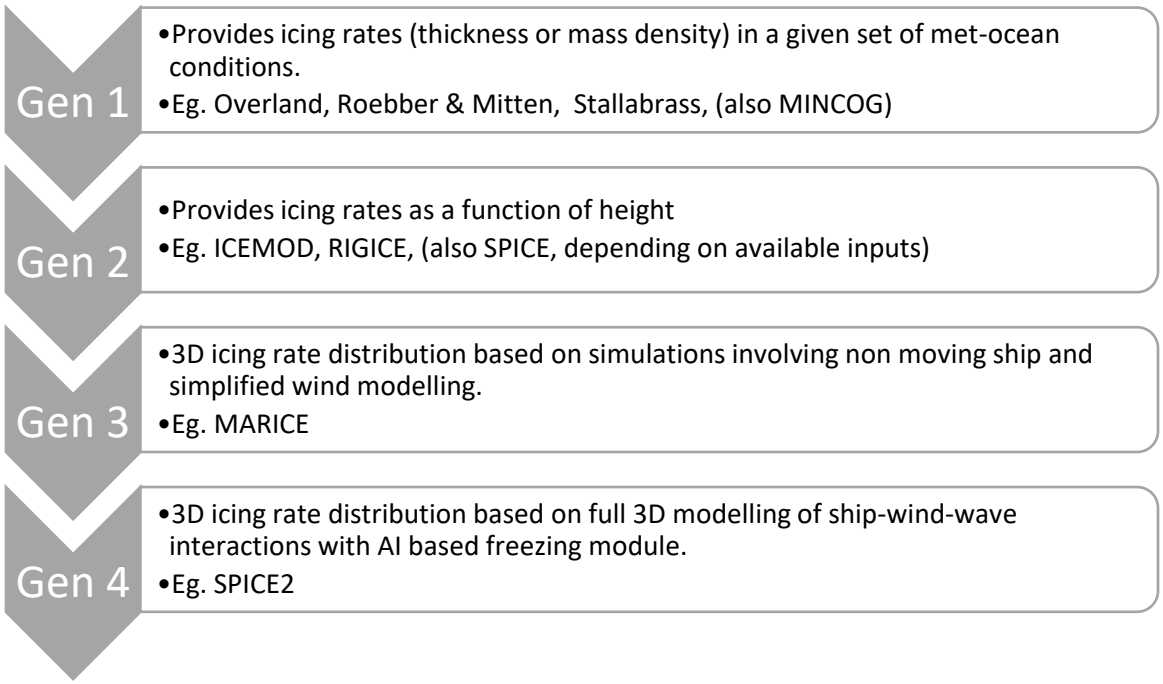

Figure 2: Development of sea spray icing models over time

Figure 1 clearly shows how the focus on the distribution of icing in addition to the icing rates is a relatively new.

Generation of spray is a stochastic process with many random variables having a role in the spray generation process. These variables include, but might not be limited to, wave height, wave period, ocean current, local ripples, ship speed, wind speed, design of the hull or structure, relative wind direction, ship

motions including roll, pitch, and heave, etc. One of the most detailed full-scale sea spray measurements was conducted by Ryerson, 1995. Measurement of droplet sizes and spray mass flux from 39 spray events were recorded. Ryerson themself mention that attempts at explaining all spray characteristics by their controlling parameters resulted in complex and insignificant relationships [43]. A corollary of this could be that spray generated, and thereby the resulting icing rates for even by a single vessel in similar met-ocean conditions, difficult to be empirically explained. However, all existing models use some forms of empirical formulations for spray generation making them at the most, limited to the type of vessel and the prevailing met-ocean conditions at the time of spray measurement.

The Overland model was criticized by Makkonen et.al. 1991 for being very sensitive to the seawater temperature and claimed to not being replicable [25]. The Overland model is however still used by the United States National Oceanic and Atmospheric Administration (NOAA) owing to its ease of implementation [27]. The Overland model and eventually the Roebber & Mitten model are based on observations on medium sized fishing vessels. The spray flux is dependent on many factors, including the size of ships. This makes the Overland and Roebber & Mitten models unreliable for other sizes of ships or structures.

The Stallabrass model is based on 39 icing events specifically from fishing trawlers. For the same reason mentioned previously, the Stallabrass model is unreliable for any vessels or structures of other sizes. For example, the spray flux generated by an impact of a much smaller vessel with the waves could be much lesser than that of a fishing trawler, leading to overestimation of icing rates for smaller vessels or under estimation of icing rates in case of larger vessels or structures.

ICEMOD2 is based on 10-13 flux measurements from a single trawler. Empirical relationships for flux are available for three specific ship headings and the icing rates are assumed to be equal at a given height. This could result in different parts of the vessel at the same height showing the same icing rates, which is incorrect as the amount of spray water impinging in various regions can vary greatly.

RIGICE04 uses an empirical formulation for spray generation from one experiment and extrapolates it to structures of different sizes. Additionally, it is developed specifically for structures such as oil rigs and cannot be used for vessels. The spatial distribution of ice is limited to 2D, giving one value of icing rate for each meter height of the structure.

The MINCOG model explores two different spray formulations and uses the one that suits the case study of the KV Nordkapp, making it limited to similar sized vessels to the KV Nordkapp. The MINCOG is the most recent model for prediction of sea spray icing and is an operational P1 type of model which makes it unusable for engineering applications such as predicting the total amount of ice and the spatial distribution on the surface.

MARICE is the only existing model that uses CFD. CFD is however only used for tracking the spray particles along with wind. A spray generation function that is based on any available formulation can be used. Additionally, the CFD simulation method considered the ship as a stationary object. The local wind speed near various surfaces could in reality vary due to the motion of the ship. The MARICE model is also time

dependent and adds complexity in terms of the water film motion. This makes implementation of the model rather complex.

Some researchers are of the opinion that time dependency adds 'unjustified complexity' to the model [9]. Horjen 2013 suggests that the ice accretion on a vessel structure is highly related to the mass flux of spray hitting the structure and therefore results of spray icing must be accompanied by the mass flux measurements on the same vessel [30]. This reinstates the opinion that sea spray icing models that use spray flux formulations cannot be generalized to other types of vessels or structures than the ones which the flux measurements were made on.

Horjen 2015 adds that no mathematical model can ever reproduce nature completely, and complicated models will not necessarily lead to more reliable results. He also mentions that spray impingement is a stochastic process and the only way to really test the validity of any icing model is by comparison with controlled laboratory experiments [44].

4.6.1. Inconsistency in prediction from existing models

A few sea spray icing prediction/ forecasting models already exist. Differences in the working of existing models makes direct comparison difficult. Limited full-scale and laboratory measurements prevent judging the accuracy of models. It thus makes it reasonable to compare the predictions of the models to each other to make a judgement on their accuracy.

The predicted icing rate from different models varies greatly. Empirical formulations for spray flux are inaccurate but are still used in all existing models, including MARICE [22]. Empirical equations for flux used in ICEMOD predicts 10 – 1000 times less spray flux than with the equations used in RIGICE04 [22]. This, in addition to any other model specific assumptions, contributes to severe inconsistencies in the prediction of icing with different models.

A comparison of the prediction of total ice load by Kulyakhtin 2014 on an offshore structure in a time series lasting approximately 30 days, showed, at the highest point, a variation from about 60 tons to about 120 tons depending on the model used[39].

The inconsistencies are also shown in Paper 3 – Figure 7 while comparing the results of SPICE to that of existing models. For example, in Case 1, the predictions vary from 4mm/hr to 35mm/hr for the same wind speed, and from 1.5mm/hr to 12mm/hr for the same flux [21].

It is difficult to say which of the models is most accurate. All existing models have a 'Top-Down' approach, wherein the model is constructed by selection of empirical formulations (limited spray or icing data) for important variables like spray flux that give similar icing rates to that of the case in question.

It is therefore important to have a model independent of any empirical formulations for important variables like flux. In addition, a model based on more data observations, either full-scale or from lab experiments is needed.

4.6.2. Summary of the rationale for warranting a new model and more data

- A universal model that predicts icing rates on a wide range of vessels and structures of differing shapes and sizes does not exist. It is essential that a model could be used for prediction of sea spray icing on any vessel or structure, independent of its shape, size, and met-ocean conditions. This cannot be achieved if the basis for the model is observation from a single vessel or a handful of similar vessels.
- Existing models serve different purposes (see Table 1 and Figure 1), and it is not straightforward to compare their accuracy to the limited full-scale or laboratory observations in literature.
- Limited full-scale and laboratory observations compel comparison of models to each other for determining accuracy. Kulyakhtin 2014 [39], Paper 3 – Figure 7, and Paper 4 – Figure 13 show large variations in the predicted icing rates from different models, thus raising the question of which model could be most accurate.
- Existing models are based on empirical formulations of flux that are based on a handful number of observations on specific vessels. It is obvious that the flux is heavily dependent on the size and shape of the vessel in addition to the prevalent met-ocean conditions, and also on the ship dynamics. Any model based on such empirical formulations of flux would be applicable, at the most, to the specific vessel the flux was measured on and in the specific met-ocean conditions at the time of measurement. This is also pointed out by Kulyakhtin 2014 who mentions that all existing models, including MARICE, use empirical equations to represent spray flux which might be inaccurate [22].
- Full scale measurements for sea spray icing are a rather extensive exercise involving large amounts of personnel, regulatory actors, and not least, capital intensive. Data from controlled laboratory experiments could be a solution for testing icing rates in a wide variety of met-ocean conditions.

4.7. Artificial Intelligence and Machine Learning

Artificial Intelligence (AI) and Machine Learning (ML) have significantly impacted various industries by acting as an advanced tool for data analysis, pattern recognition, and prediction. AI and ML are often used interchangeably to describe the development of systems and algorithms that learn from data and are used to make informed decisions. Although often used interchangeably, Machine Learning (ML) is a subset of Artificial Intelligence (AI) where an algorithm builds a model based on sample training data to make predictions without being explicitly hard-coded to perform the task [45]. The capability of AI systems to process vast amounts of information, identify intricate patterns, and leverage state-of-the-art ML techniques has become essential for modern problem solving.

AI and ML are increasingly applied to address complex challenges, optimize processes, and improve performance in diverse applications. A widely used application of ML is regression, a fundamental ML task focusing on predicting a continuous value based on a specified number of input variables. Several educational websites provide a simple example of prediction of housing prices based on various variables (called as features) like size, number of rooms, location, distance to the city center, etc., to explain this concept. A regression model trained on a dataset of historical housing prices and corresponding features can learn intricate relationships between these variables and the housing prices through techniques such

as gradient descent, regularization, and feature engineering. Similarly, a regression model that is trained on icing rates for corresponding variables that play a part in the icing process, could be used to predict the icing rate if the other variables are known. The model can learn the intricate relationship between variables such as spray flux, wind speed, air temperature, etc., to predict an icing rate where formulating empirical relationships seem to be insignificant.

The integration of AI/ML into regression tasks offers numerous advantages. These technologies can capture complex relationships and nonlinear dependencies between input variables and the target value through techniques like deep learning with neural networks, kernel methods, or decision tree ensembles. ML models exhibit robustness in handling noisy data, adaptability to new information, and continuous improvement through techniques like cross-validation, hyperparameter tuning, and model evaluation metrics such as mean squared error or R-squared.

However, challenges arise when applying AI/ML regression models. Ensuring data quality through preprocessing techniques like data cleaning, normalization, or feature scaling is crucial. Proper feature selection using techniques like feature selection or dimensionality reduction is essential to avoid irrelevant or redundant features. Addressing missing data using imputation methods and mitigating overfitting or underfitting through regularization techniques such as L1 or L2 regularization or early stopping are necessary for reliable predictions [46].

Furthermore, domain expertise and contextual understanding play a pivotal role in interpreting the outputs of the regression model and making informed decisions. Techniques such as interpretability methods, model explainability, or visualizations enhance the understanding of the model's internal workings and provide transparency [47].

AI has emerged as an indispensable tool in regression tasks, empowering researchers and practitioners to predict continuous values based on input variables using advanced ML techniques. The ability to extract insights from data, capture complex relationships using diverse algorithms, and adapt over time can open up new opportunities for the prediction of sea spray icing if sufficiently large quantities of structured icing data is available.

4.8. Computational Fluid Dynamics

Computational Fluid Dynamics (CFD) is a widely used computational technique for analyzing and simulating fluid flow phenomena. It combines principles from fluid mechanics, applied mathematics, and computer science to predict and visualize fluid behavior in various real-world scenarios. By employing mathematical equations to simulate fluid flow, CFD enables engineers and researchers to gain valuable insights, optimize designs, and make informed decisions.

Fundamentally, CFD involves solving the governing equations of fluid flow, which are based on the principles of conservation of mass and momentum. These equations, known as the Navier-Stokes equations, mathematically describe the motion of fluids and can be expressed as follows for incompressible flow:

Continuity Equation:

$$\nabla \cdot v = 0$$ *Ref:* [48] *Eq. (1)*

This equation signifies the conservation of mass, stating that the rate of mass change within a control volume is equal to the net mass flux across its boundaries. Here, *v* represents fluid velocity.

Momentum Equations:

$$\frac{\partial v}{\partial t} + (v \cdot \nabla v)v = -\nabla p + v\nabla^2 v$$ *Ref:* [48] *Eq. (2)*

These equations describe the conservation of momentum in incompressible flow. The left-hand side represents the temporal and convective acceleration of the fluid, while the right-hand side comprises the pressure gradient ($-\nabla p$) and the viscous forces ($v\nabla^2 v$). Here, *v* represents the kinematic viscosity.

Solving these equations entails computationally demanding processes due to their complexity and the need for iterative methods. CFD employs numerical techniques like the finite volume method to discretize the governing equations into a computational grid. Subsequently, the equations are iteratively solved over discrete cells or elements to obtain approximate solutions.

CFD software packages utilize sophisticated algorithms and solvers to simulate fluid flow, enabling engineers and researchers to visualize flow patterns, pressure distributions, temperature variations, and other fluid properties of interest. These simulations aid in optimizing designs, evaluating performance, and predicting the behavior of fluid systems under different conditions. CFD is a powerful computational tool for studying and analyzing fluid flow phenomena. By numerically solving the governing equations, CFD allows for the prediction and visualization of fluid behavior across diverse applications. In case of prediction models for sea spray icing, MARICE was previously the only model to use CFD in some form. MARICE used CFD to track flow of particles due to wind, the spray particles however were introduced artificially in the domain with a user defined function based on existing spray formulations [11]. None of the existing models use CFD for spray generation.

4.8.1. Continuous phase approach for spray modelling

Paper 4 delves into simulating spray generation and using averaged values from the simulation in the AI model. The continuous phase approach is employed in CFD simulations to model sprays, where the dispersed liquid phase is treated as a continuous medium as opposed to Discrete Phase Modelling (DPM) where each spray droplet is treated individually. The continuous phase approach could be suitable when the droplet size is small compared to the grid size, and when the focus is on capturing the averaged behavior of the spray. Dynamics of water droplets have proven to be effectively modelled at microscopic scales [49]. While modelling the spray generated due to the impact of a vessel with waves, there are two completely different scales involved. Individual cells of the computational grid for capturing individual droplets due to the vessel-wave impact would need to be in the range of millimeters or even micrometers. This would make the simulation impractically expensive. Additionally, in such a case where millions of droplets would be generated, the effect of individual droplets could be ignored and an averaged behavior from a continuous phase model could provide satisfactory understanding of the phenomenon.

Recently, Smoothed Particle Hydrodynamics (SPH) was also studied to capture the wave impact spray [50]. SPH is a computational method wherein the fluid continuum is represented as several Lagrangian particles. SPH is a relatively new technique compared to traditional CFD and visualizations for simulations with SPH could be more 'appealing'. However, SPH can be computationally expensive for large scale simulations. All particles in the simulation have a standard size, which would not necessarily represent the spread of spray droplet diameters. Due to computational limitations, larger sized droplets would have to be used which are again, a representation of several smaller droplets just like while using the continuous phase approach.

Treating spray as a continuous phase allows for efficient computation by eliminating the need to track individual droplets. Instead, a fraction representing the liquid volume is tracked within each computational cell using the Volume of Fluid (VOF) method. This approach significantly reduces the computational cost compared to DPM or SPH, especially for large-scale spray simulations. The continuous phase approach enables the analysis of the averaged behavior of the spray, providing valuable insights into the overall spray pattern, dispersion, and interaction with the surrounding flow. It provides an averaged representation of the spray behavior focusing on the macroscopic properties. The VOF method tracks the volume fraction of liquid within each computational cell. Since it does not have to track individual particles, it is computationally more efficient. SPH models are generally inefficient at higher Reynolds numbers [51]. At higher wind speeds, the wind flow around the vessel or structure would cause severe turbulence, and thus higher Reynolds numbers. This might lead to inaccuracy in estimating the flux at various surfaces at higher wind speeds. Traditional CFD approaches use turbulence modelling that is effective at high Reynolds numbers. Treating the spray as a continuum does, however, lead to a certain degree of mesh dependency which is generally aimed to be reduced in any CFD simulation.

Simulating generation of spray with either method is relatively new and to the best of the author's knowledge has been attempted once each (SPH by Mintu et.al. 2021 and VOF in Paper 4). Using these approaches over heavily criticized existing empirical formulations [20] is a paradigm shift in how the icing problem is approached and future research efforts could focus on refining the modeling techniques to improve accuracy and calibration with the help of full-scale measurements.

4.9. Need for more and new data

Availability of experimental and full-scale icing data is necessary to build and verify sea spray icing models. The 1960s-1980s saw extensive work in gathering icing data for use in prediction of dangerous icing events [19]. In one study that had not been made public, around 7000 questionnaires responses from multiple countries were collected to gather icing data [19]. Samuelsen et.al. 2017 report a few cases from the past where the icing data has been made available. For precious estimation of icing rates, information of various metocean parameters and ship characteristics during the icing events are ideally required, but none of the available datasets have detailed information about these parameters [19]. Ryerson 1995 gave a detailed description of 39 spray events and the total ice accreted in an icing event for 100 hours [43]. Another case with metocean and ship parameters was presented by Samuelsen et.al. 2017 wherein 37 cases are presented with the corresponding icing data [19]. An attempt to use this data for verification of the new model was done in Paper 3, however it was found that comparing icing rates estimated by various

models to that of these two datasets, as presented, did not serve the purpose of validation for a real case. A complete reasoning for this is found in Paper 3.

Detailed full-scale measurements of sea spray icing are expensive [20]. Literature thus has a limited number of such full-scale measurements, and since the most well-known ones described above too have been deemed to be not detailed enough for full-scale verification, the next best option is controlled laboratory experiments. Dehghani-Sanji et.al. 2019 presented an experimental study for sea spray icing that analyzed mass and thickness with 12 unique sets of measurements. This study included 2 variations each of atmospheric temperature, salinity, spray period, spray duration, and 3 variations of wind speed. The results of this study were presented in the form of icing rates per hour for individual conditions. This was a huge step forward for the availability of the results for verification. However, there existed some limitations, for example, the temperature in the freezing room varied by 4°C during the tests and this was not accounted for in the results. The experiment did not include sea temperature as a variable which was measured at 17°C in the pipe just before the nozzle inside the freezing room [52]. All models use seawater temperature in the modelling even though the effect of seawater is limited. Spray droplets do undergo cooling inflight, but starting with such a high temperature could be a source of error. Some more limitations are presented in Paper 2. Paper 2 presents results form a new set of experiments wherein many of the limitations from the Dehghani-Sanji et.al. 2019 experiment are improved upon. Additionally, a greater number of variables and tests are presented, and the data is recorded every second to account for the variations in the temperature inside the freezing room.

5. Paper 1

5.1. Summary

In view of several existing models for prediction of sea spray icing, a state-of-the-art study was conducted to understand the approach existing models use. Sea spray icing is a niche field with comparatively limited available literature. This article, first of all, compiles information about the sea spray icing process to create a much needed, comprehensive and consolidated resource for researchers in this field of study. The article discusses the international standards and regulations related to ice accretion. The objectives of a prediction model for sea spray icing are discussed keeping the international standards as a reference. Variables that play a role in the icing process are discussed and how existing models approach the prediction problem are studied. The methodologies incorporated by various existing models are compared, and it is seen why the different approaches and goals of these models make it difficult for direct comparison of existing models. Finally, the anti-icing and deicing technologies to mitigate the challenges faced due to sea spray icing are delved into.

The findings from this article show the enormous potential for improvement in sea spray icing predictions and these findings are used to formulate the requirements for more data, and a new model that is capable of making predictions on a universal basis and not limited to a type of vessel or structure. Some of the main findings of this article pertaining to objectives for sea spray icing predictions that are used for further investigations are as follows:

- A prediction model should be able to provide spatial distribution of ice in addition to icing rates.

- Distribution of ice cannot be determined by generalized theoretical models, and using CFD is essential for determining distribution.
- Modelling dynamic ship-sea-wind interactions have potential in this field.
- Models for spray generation have to be improved, and ideally modelled with CFD for individual vessels and structures.
- Prediction models should be capable of predicting sea spray icing on a universal basis for a large variety of vessels and structures.
- Existing models suffer from lack of experimental verification.
- More experimental and full-scale data is required.

5.2. Main contributions

- Consolidation of theory, standards, and existing prediction models in a single source.
- Stating the requirements for a comprehensive prediction model based on international standards.
- Pointing out the need for more experimental data.

5.3. Literature cited

Paper 1 cites the following literature:

[3] [4] [5] [20] [53] [54] [9] [10] [55] [12] [16] [56] [57] [58] [59] [60] [61] [28] [32] [30] [31] [11] [19] [62] [63] [27] [25] [64] [65] [13] [66] [33] [67] [68] [69] [70] [71] [72] [73] [74] [43] [75] [2] [76] [77] [78] [79] [80] [81] [82] [83] [84] [85] [86] [87] [88] [89] [90] [91] [92] [93] [94] [95] [96] [97] [98] [99] [100] [101] [102] [103] [104] [105] [106] [107] [108] [109] [110] [111] [112] [113]

6. Paper 2

6.1. Summary

Paper 2 presents results from eight controlled laboratory experiments comprising of 20 unique tests, each of which gives the variation of icing rates due to a separate independent variable that affects icing rates, in addition to one more experiment for repeatability analysis. This is the greatest number of variables tested for sea spray icing in a single study, making it, to date, the largest experimental study of sea spray icing. The variables tested were substrate material (or thermal conductivity), wind speed, atmospheric temperature, seawater temperature, spray flux (by varying pressure), spray duration, spray period or frequency of spray, and seawater salinity.

Paper 1 found that existing models for prediction of sea spray icing suffered from a general lack of experimental validation. Researchers had pointed out to the general lack of data for in this field of research [20]. Full scale measurements are expensive and rather complex to perform [20]. Detailed spray and icing measurements were performed by Ryerson 1995 [43], however, this and some other full-scale measurements available, are not detailed enough for the purpose of validation of computational results [75]. A reasoning for this is also provided in Paper 3. There have also been a limited number of laboratory

tests for sea spray icing in the past [52], [92]. Paper 2 puts forth a few limitations of the experiments performed by Dehghani-Sanij et.al. 2019 and improves upon these.

The experimental results presented in Paper 2 first of all provide invaluable data about icing rates and its dependence on the selected variables. Detailed accounts of the experimental setup, selection of variables, and measurement techniques are provided to maintain the replicability of the experiments for verification purposes. Valuable insights and challenges faced during the experimental work are provided for giving a heads-up for similar experiments in the future.

For each experiment, the variation of icing rate throughout the one-hour period of each test and the weight of accreted ice are presented along with detailed information of other variables. Differences in the icing rates due to different measuring techniques are provided. Ice accretion on the test plate is not uniform and icing rates are provided for different regions of the plate along with the icing rate computed from the weight of accreted ice assuming uniform icing. As the ice thickness was measured only at the end of each test, the icing rate by thickness for different regions was available only at the end of each test. Similarly, icing rates were observed to vary with time in the initial stages, and thus, icing rates were also provided separately for, including, and excluding the first 15 minutes. Details of the average set and real temperatures are provided for each experiment along with the mass of spray water impinging on the plate or simply, the spray mass flux during each test.

The repeatability experiment showed minor variation in the icing rates even under controlled laboratory conditions, throwing some light on how complex full scale sea spray icing studies could be. Most of the experiments showed higher icing rates in the initial stages or the first few sprays after which the icing rates were more or less constant. The transition from the start to the tendency of the icing rate becoming constant could be seen in the form of a knee-bend on the plot of icing rates vs time. The location or the time of occurrence of this knee-bend varied depending on the configuration of the test variables for individual tests; the latest of which was approximately 15 minutes from the start.

Some conclusions could be drawn from these experiments. For example, the material played no role in icing rates after the initial few sprays. Thus, in case the icing rate or the weight of ice accreted has to be estimated over a considerably large amount of time, the effect of the substrate material could be neglected. Other variables like air temperature and wind speed showed clear tendencies towards their effect on the icing rate. Attempts were made to compute the change in icing rate due to these variables alone. This was however rather complex as many variables together affect the icing rate and stating values like, for example, x kg/m^2/hr change in icing rate for a unit change in temperature would be additionally dependent on the wind speed. In any refrigeration mechanism, the temperature fluctuates between some upper and lower thresholds. Variation of temperature, especially in the freezing room, affected the icing rates also in experiments where the air temperature was not a variable. Additionally, spray duration and spray period were independent variables, but flux was a definite covariate while experimenting with these. The significant number of covariates prevented a thorough conclusion of the effect of each variable on the icing rate. The experiment with varying flux by changing the pump pressure was considered unsatisfactory, however, several different values of flux were in fact tested through variation of other variables like spray duration and spray period.

The dependence of the icing rate on multiple variables, the fact that some variables like temperature and flux could not be precisely controlled in the experiments that needed them to be constant, gave rise to multiple covariates due to which the effect of each independent variable on the icing rate could not be determined precisely by straight forward empirical relationships. Owing to the large amount of data collected from these experiments, it was suggested to use advanced techniques like machine learning for further analysis.

6.2. Main contributions

- Valuable sea spray icing data from the largest set of laboratory experiments to date.
- Proved that material of the substrate affects the icing rates only in the initial stages of the onset of icing.

6.3. Literature cited

Paper 2 cites the following literature:

[114] [20] [8] [11] [30] [31] [19] [61] [9] [24] [43] [92] [52] [115] [33] [116] [64] [102] [117] [118] [119] [120] [121] [10] [122] [123] [124] [125] [126] [127] [128] [129] [130] [58] [131] [132] [18] [67]

6.4. Additional supporting information

6.4.1. Correlation of experimental variables to real events

Paper 2 – Table 1 shows the list of the eight tested variables in the experiments, namely material, windspeed, atmospheric temperature, seawater temperature, gauge pressure (flux), spray duration, spray period, and salinity. Some variables would not have an effect on the outcome whether tested in the lab or in a real-world offshore scenario, while others would. Material, spray duration, spray period, and salinity could be considered to have a direct and equal correlation in a lab vs real-world situation. The seawater temperature was controlled with the help of heat exchangers (see Paper2 – Figure 1). In reality, the seawater temperature could vary a slightly as a function of the depth from the water surface, which could play a minor role in case of heavy vessels with a relatively larger draft. The atmospheric temperature in a lab fluctuated a bit due to the freezing mechanism. These local and quick variations would not be seen in a real-world situation. The flux was varied with changing the pressure of the pump. Although this would not affect the outcome in a lab vs real-world scenario in terms of the actual flux, the possible difference in droplet sizes might affect the icing rate. Additionally, as flux plays an important role in the determination of the icing rates, the problem in a real-world scenario is that the flux can never be measured at absolute all locations on the vessel's /structure's surface. Wind speed is also a variable that highly affects the icing rates. In most real-world situations, u_{10} (wind speed at a height of 10m from the mean sea level) is available, while it is the local wind speed at specific locations which affects the local icing rates. In the experiments, the measured wind speeds were close to the plate's surface (9mm above the plate) and vary from 0 – 6m/s. To estimate the equivalent u_{10} for this case, Eq. (3) could be used where u_z is the wind speed at height $z = 9mm$ measured above the plate, $u_{z0} = u_{10}$ is the equivalent wind speed u_{10} at height $z_0 = 10m$; assuming the roughness length $z^* = 0.001m$ assuming the case to be similar to a ground with

surface covered with an ice sheet [133]; thus giving the equivalent u_{10} for the experiments from 0 – 25.15m/s for measured local wind speeds of 0 – 6m/s.

$$\frac{u_z}{u_{z0}} = \frac{\ln(z/z^*)}{\ln(z_0/z^*)} \qquad \textit{Ref:}\ [134] \qquad \textit{Eq. (3)}$$

6.4.2. Shortcomings of experimental setup in relation to a real offshore situation

One of the main shortcomings of the experimental setup is the water run-off effect on the icing rate. When the spray impacts a surface, especially in large amounts, not all the water freezes and some of the water remains in a liquid state and flows away due to gravity, wind, or vessel movement. The plate that represents the freezing surface in the experiments in stationary and vertical. Although the water runoff effect for this particular situation is captured during the experiments, the icing rates for another situation, for example, a horizontal/ tilted or a dynamic surface could vary. For example, if the plate was horizontal, it could happen that the water that dripped down in case of the vertical plate, would accumulate on the surface and freeze as time passes – leading to higher icing rates. On the other hand, accumulation of large quantities of seawater or movement of the plate could actually prevent the freezing and could result in a lower icing rate. How the orientation and dynamics would affect the icing rate depends on individual situations all of which are not captured with the current experimental setup.

7. Paper 3

Paper 3 presents a machine learning model for the prediction of sea spray icing dubbed as SPICE (Sea sPray ICE prediction model).

7.1. Background

The experiments presented in Paper 2 along with ten additional repetitions of certain tests performed in the aftermath of Paper 2 provided data from a total of 30 tests. Some variables like wind speed remained constant for the eternity of one individual test whereas other variables like air temperature were transient. Since data was recorded each second, icing rates were available for 108K datapoints for combinations of eight different independent variables. Owing to the large amount of data, new technologies involving machine learning were studied to see if these could identify hidden patterns, learn the intricacies in the data, and if so, be used to create a model that could predict the icing rate given that the user had knowledge of the other independent variables.

Data processing by making the available data suitable for use in modelling was a considerable task. The data collection procedure is described in detail in Paper 2. Data was collected from multiple sources like the data logger, anemometer, and manual recording. This data had to be structured in a way that was first of all easy to understand and store logically, similar to a ‘relational database’ which proved useful when additional experiments were performed, and data had to be added to the database. Additionally, a clone of the data was structured in the form of a ‘data warehouse’ which could be used for the purpose of analysis and modelling. Standard procedures for cleaning the data were followed.

7.2. Summary

Paper 2 concluded that the material did not have any effect on the icing rate after the first few sprays. The first 15 minutes were omitted from further analysis. The other seven independent variables that affect icing (also called features) and the icing rate by weight measured with the load cell (also called the target) were kept for further analysis. As a preliminary feature engineering, the measured wind speeds were converted into a new feature based on wind power law for extending the range of confident predictions. Once the data was in the correct format, exploratory data analysis was carried out to understand the correlation between individual features and the target. Discussions on the inclusion of certain features are presented. The dataset consists of all the data from the 30 experiments, although different parameters were tested individually by varying them between experiments, all parameters were recorded for all experiments. This led to a situation where between different set of experiments, some variables remained constant while others varied during the same set of experiments – a typical situation with controlled and independent variables favorable for causal analysis and machine learning. The dataset is randomly divided into training and testing datasets where training data constitutes of 80% (86,400) of the datapoints and the testing data constitutes of 20% (21,600) of the datapoints. The training dataset is used to train machine learning models whereas the test dataset is used to test the performance of predictions with these models. Initially four different ML models are constructed and their performance of predicting icing rates in the test dataset is analyzed based on three metrics: mean absolute error (MAE), r2 (r squared) error, and mean squared error (MSE). The XGBoost regressor model showed the best performance with satisfactory metrics and showing wind speed and flux as the dominant features for the prediction of icing rates.

Although the model showed great results predicting the icing rates in the test dataset, it was soon discovered that some features like wind speed that remained constant throughout an individual test created challenges. A discussion into why the model did not perform well for feature values in between those tested is presented. To tackle this, two feature engineering techniques are applied. These techniques capture the most important classifications made by a tree-based algorithm and convert them into equations which are a combination of multiple features. New features calculated from these equations are added to the dataset and a new model is trained. This new model, dubbed SPICE, not only showed better metrics to that of the standard model without feature engineering, but also was able to predict icing rates for feature values in between those that were tested. Analysis of the new model showed that the equation consisting of a multiple of wind speed, air temperature, and flux was the dominant feature, over individual features. A discussion on how this is analogous to the physical process is presented, where for example, only low temperatures would not cause icing if there were no water impinging on the surface.

Next, several models were trained excluding some of the original features to study the inclusion or exclusion of certain less important features. Including all the original features showed the best metrics and thus all original features were retained.

Some features like air and water temperatures, and wind speed is easy to measure or have access to from various sources. Other features like spray duration and period, and more importantly, the spray flux, are not directly accessible. For this purpose, a ‘feature calculator’ is provided to the users wherein unavailable features are estimated with existing empirical formulations. The user can choose between any of the formulations which suit the case or input the values from their own measurements. Existing formulations

for flux for example, are also dependent on the vessel speed and heading. This allows the user to input these instead of flux. The icing rate predictions from SPICE are compared with five other existing sea spray icing models for a set of metocean conditions. Additionally, the variation of predictions by using different flux formulations are presented.

The results from SPICE are attempted to be compared with two available full-scale datasets. However, the analysis points out some shortcomings of these full-scale datasets and a discussion is presented on why these datasets cannot be used for validation of any prediction model. However, predictions of SPICE are compared with five other existing models using metocean and spray data from one of the datasets.

The concluding discussion includes how the SPICE model can be implemented and suggestions for further improvement of the model. Advantages of the SPICE model over existing models are discussed where one argument is that SPICE is built 'Bottom-Up' with a large set of experimental data such that the icing rates predicted by SIPCE, unlike existing models, are experimentally validated. This is of added importance as full scale icing measurements proved to be ineffective for validation.

Finally, the severe limitations of using existing empirical formulations for important features like estimation of flux and are discussed and using other approaches for their estimation are suggested. Overall, it is suggested to keep the use of the feature calculator to a minimum by researching into alternatives such as using newer techniques to measure flux in real time or using CFD to estimate flux.

Detailed flowcharts for easier replication of the model are provided. Availability of the experimental data to build the model and some advanced techniques in Object Oriented Programming (OOP) and ML prevent the model from being easily replicated. However, any user with access to the object format of the SPICE model already constructed in this study can use the model with a few lines of basic coding in python for entering the metocean data, making the model extremely user-friendly. The model would be made available for all users upon request.

7.3. Main contributions

- Developed a first of its kind machine learning model – SPICE, for prediction of sea spray icing. Having been built 'bottom-up' from experimental data, the model could be said to be more accurate than existing models.
- Proves that a combination of air temperature, wind speed, and spray flux is most crucial to icing predictions and icing in general.
- Easy to use, and extremely flexible model that can be easily incorporated into a ship's onboard systems.
- Inclusion of a feature calculator for estimating missing inputs.
- Unlike existing models, the flexibility allows users to choose the most appropriate formulation for estimating missing variables, and also has options for manual inputs in case users wish to adopt their own methods for estimating the required inputs.
- Presents drawbacks of using existing empirical formulations for estimating important variables like flux.
- Presents challenges of attempting validation from existing full-scale datasets.

- Comparison of sea spray icing predictions with existing models.

7.4. Literature cited

Paper 3 cites the following literature:

[22] [135][136] [36] [137] [138] [40] [139] [140] [8] [141] [142] [143] [144] [145] [146] [133] [147] [148] [149] [150] [151] [152] [153] [154] [155] [156] [157] [158] [159] [160] [161] [162] [163] [164] [165] [37] [166] [167] [168] [169] [170] [39] [171] [172] [173] [38] [174] [175] [176] [177] [34] [35]

8. Paper 4

Paper 4 presents a hybrid CFD-ML model for the prediction of icing rates and the distribution of icing over a moving vessel, which can also be implemented for stationary structures. This model, dubbed SPICE2, is an upgrade to SPICE wherein some of the inputs for the ML model are estimated with CFD. SPICE2 is capable of providing the spatial distribution of ice in addition to the icing rates. In addition, the method presented makes it independent of any existing formulations.

8.1. Background

Paper 3 presented a model for prediction of icing rates for a given set of metocean conditions. One of the most important variables that affect the icing rate was found to be the spray flux. Errors in the prediction of icing rates due to errors in estimation of spray flux was first pointed out by Kulyakhtin 2014, who names existing formulations for spray flux as the 'weakest link' for any sea spray icing model. This was also seen in Paper 3, where using different existing formulations gave different results for icing rates. It is argued that these existing formulations are empirically generated from limited number of observations from individual vessels in a given set of met ocean conditions, making these, at best, limited to the type of vessel the formulations are based on. Ryerson 1995 made some detailed full scale spray measurements which show vastly differing spray flux measured on the same vessel and themselves mention that attempts at generating statistical relationships with the metocean conditions gave 'complex and insignificant results' [43]. Researches have however been using these empirical formulations for estimating important variables like spray flux, either by selecting the best suited formulation for their case (like Samuelsen et. al. 2017 [19]), or by selecting one at random (like Kulyakhtin 2014 [11]). Models using these formulations are argued to be inefficient for use in a universal model that could predict icing for a large number of structures or vessels. This is also pointed out in ISO35106 which states that none of the current methods can predict sea spray icing on a wide range of vessels [16].

The SPICE model presented in Paper 3 has a 'feature calculator' which is used to estimate variables such as spray duration, spray period, spray flux, and local wind speeds, which are not directly available for measurement. The use of the feature calculator was suggested to be kept at a minimum to retain accuracy of predictions. Paper 4 presents a method where these variables are estimated from CFD simulations for further use in prediction of icing rates with the ML model.

8.2. Summary

Paper 4 uses Flow-3D for the CFD simulation. Some of the highlights of the simulations include a 2-phase simulation with a wave inlet boundary condition for water and a custom inlet boundary condition that introduces air as a second fluid at a velocity governed by the wind power law over the water line. The simulation uses the vessel (lifeboat) as a moving object. Probes at various locations on the lifeboat monitor the fraction of fluid in the containing cell at each timestep. The fraction of fluid is literally the fraction of water inside individual computational cells at any given timestep and can be considered to be representative of a large number of spray droplets inside each cell as a continuum.

Signal processing techniques like locating signal peaks are used to locate the peak, start and end of sprays. This data is further used to calculate the mean spray duration and mean spray period at each probe. Large amounts of water splashing at one location at once can mechanically wash away accreted ice or prevent ice formation. Historical data from the observations of Ryerson 1995 are used to form an assumption of the percentage of water required in each cell for it to be enough for 'wave washing'. A new method for calculation of flux from the effective fraction of fluid after considering the wave washing criterion is presented. These three variables in addition to the mean wind speeds measured at the probes are then run through the SPICE model presented in Paper 3.

The resulting model that uses CFD for estimation of the four aforementioned variables in addition to the air temperature, water temperature, and salinity from weather data or other forms of measurement are run through the previously presented SPICE model, thus providing icing rates at the different probe locations. The complete method using CFD and the ML model in combination is dubbed SPICE2. To the best of the author's knowledge, this is the first study in this field of study that attempts to use CFD for the purpose of estimating spray flux on a vessel due to wave impact. In reality, spray generation into separate droplets happens at a much smaller scale compared to the size of the vessel and is thus challenging to model it in CFD due to computational limitations. The continuous phase approach presented in this study shows promising results as an alternative to using empirical formulations, however, the method is mesh dependent. Mesh independence is usually a goal for CFD simulations and as a suggestion for future work, developing the method for mesh independence is suggested.

8.3. Main contributions

- The presented model, SPICE2, is a comprehensive sea spray icing prediction model that is capable of predicting icing rates and the spatial distribution of icing on any given vessel or structure, moving or stationary.
- The only model till date which is independent of existing formulations for estimation of critical variables required for predictions making it suitable for icing predictions on a wide range of vessels and structures, as called for by ISO35106.

8.4. Literature cited

Paper 4 cites the following literature:

[20] [58] [9] [178] [33] [19] [21] [16] [179] [11] [43] [8] [180] [6] [181] [67] [182] [183] [184] [31] [10] [12] [13] [185] [186] [187] [188][189] [190]

8.5. Additional supporting information

Note: As Papers 4 and 5 are parts of the same study, the discussion in this section is valid for both, Paper 4, and Paper 5.

Spray generation is a complex process impacted by many uncertain variables which cannot be reproduced fully by existing models and is not yet well understood [34], [35]. It is seen in Paper 3 how important knowing the flux is for accurate prediction of icing rates. The varying approaches researchers have used in the past to tackle the issue of the spray generation and flux measurement (also mentioned in Paper 1 – Section 5 and Paper 3 – Section 6.3.7) points to the fact that there is no single generally accepted way to either resolve the spray generation, or to measure the spray flux. Researchers have described the uncertainty of flux as the weakest link in prediction models [21], [22]. Paper 4 presents a method attempting to estimate the impact generated sea spray flux using CFD, which, to the authors best knowledge, has not been attempted before in comparable studies. Though the icing rate predictions in Paper 5 using the method described in Paper 4 show promising results, it is not verified that the method presented in Paper 4 gives an accurate estimation of spray flux itself. Rather, it is a proposal and a modest first attempt to show that estimation of flux with the help of CFD is possible, and a call for further research into this direction, ideally verifying the flux estimation from CFD with full-scale measurements.

8.5.1. Short overview of existing methods of spray generation used in modelling

Over the years, researchers in the field of icing have attempted to solve the flux problem with different approaches, mostly by measuring incoming spray water and trying to formulate an empirical equation about the Liquid Water Content (LWC) in the spray, based on the observations. These empirical equations were further used for estimating the possible amount of water impinging on the freezing surface in sea spray icing prediction/ forecasting models.

The models by Overland and Roebber & Mitten are statistical based on observations of icing thickness and do not use any form of flux for the estimation of icing, but rather developing a ‘predictor’ that is a function of windspeed, freezing point of seawater, and air and sea temperatures [34][35].

The Stallabrass model uses existing estimates for Liquid Water Content (LWC) in a spray, mean droplet sizes, and collection efficiency (ratio of the actual to the total possible water impingement) derived from experiments to propose an expression for the amount of water imping on the surface [36].

RIGICE04 uses spray flux densities from empirical formulations developed by Zakrzewski [164] using flux measurements from the Tarsuit Island [191], as these matched the study’s observations on the Ocean Bounty, but other measurements were also considered [38]. Regardless of the flux formulation used, mass per unit volume of a single spray cloud was expressed in terms of Liquid Water Content (LWC). The LWC was later translated into number of drops of an assumed droplet diameter in a small segment in front of the icing surface. Using a droplet trajectory model, the vertical distribution at the freezing surface was computed [38].

The ICEMOD2 model uses a similar procedure as RIGICE04 for the estimation of spray flux using empirical formulations for LWC based on a trawler and collection efficiency and feeding it into a droplet trajectory model [37].

The MINCOG model also uses empirical formulations for spray flux along with the collection efficiency and formulations for mean spray duration from observations to estimate the water available for freezing at the surface. A droplet trajectory model was used for estimating in-flight cooling of the droplets, but being a forecasting type of model, not for estimating icing distribution [40].

The MARICE model is open to flux estimation in two ways. However, both methods use empirical formulations for the flux itself as an initial input in the CFD simulations. One way is to prescribe the time averaged flux directly on the vessel/ structure surface [39] and the other way is to prescribe the flux as droplets with a certain mean diameter on a surface offset from the freezing surface and tracking their trajectories due to wind [39][138].

As it can be seen, all current models, use some form of empirical formulations for generation of spray for modelling. Existing formulations for spray flux are based on a limited number of studies on individual vessels in a certain weather condition. It can be safely stated that these formulations based on observations on, for example, one ship, or one structure, cannot be used for generalization to all types of vessels and structures. Researchers have been using the limited available formulations available in literature, and choosing the one that most closely matches their observations, while maintaining that, in principle, any formulation could be used [38][39][40].These empirical formulations have been called the weakest link in sea spray icing prediction models, but are however being used time and again, even for models that are designed for estimating icing arbitrary vessels/structures.

In one of the studies having the most detailed and the greatest number of measurements of spray flux, Ryerson 1995 clearly discourages the use of empirical formulations by stating that attempts to make a general equation for spray flux from the spray measurements was complex and insignificant [148].

8.5.2. Cloud-based vs surface-based approach

As it can be understood from Section 8.5.1, flux can be resolved or prescribed in two different ways. The first way is the ‘cloud-based’ approach where the magnitude of the spray cloud is estimated as a start. The spray is then subjected to the wind flow in the simulation, from which, the flux is measured at the surface of the vessel/structure. On the other hand, in a ‘surface-based’ approach, empirical formulations are used to directly estimate the flux on the surface. It is however to be noted that existing models using the cloud-based approach also use empirical formulations to estimate the spray cloud itself.

In the models considered in Section 8.5.1, this cloud-based approach is used in RIGICE04 and ICEMOD2 models, whereas the surface-based approach is used by the Stallabrass and the MINCOG models. MARICE is open to both approaches having used the surface-based approach in the study where the model is presented [39], while also demonstrating the use of the cloud-based approach in another study [138].

By the nature of the method, any attempts to use the surface-based approach would always require empirical formulations for spray flux for estimating the water impinging on the surface. The cloud-based

approach on the other hand, has a potential to be completely independent of empirical flux formulations as research progresses. Paper 4 uses the cloud-based approach in a modest first attempt where the generation is independent of any existing empirical formulations.

8.5.3. Pros and cons of this paper

The pros and cons of this paper are already discussed in Paper 4 – Section 6. The most important issues are discussed in the following paragraphs in the current section to highlight the challenges faced.

As already mentioned in Paper 4, the biggest drawback of Paper 4 is that the spray flux estimated from the CFD simulation was not measured in a real full-scale case. Paper 5 compares the icing rate observations from a full-scale test to that predicted with SPICE2, where the CFD method presented in Paper 4 is used to estimate, amongst other variables, the spray flux at certain locations on the lifeboat. The results show promising comparisons of the icing rate. However, the verification of the presented CFD model would only hold true if the flux, rather than the icing rate is compared. The flux was unfortunately not measured during the test described in Paper 5. A separate and new full-scale test planned for the lifeboat used in Paper 4 was planned in March 2020 in Svalbard as a part of a larger exercise in the SARex Svalbard project [192], which had to be called off due to the Covid pandemic. This resulted in the lack of data for tuning and verification of the CFD model presented in Paper 4. Paper 3 – Section 7.2 describes some shortcomings of existing openly available datasets for using them for the purpose of validation. The lack of verification, at least for case of spray flux, downgrades the overall model.

On the other hand, SPICE2 which uses the flux results from the CFD simulation in combination of the ML model does indeed make promising predictions for the icing rate verified against full scale measurements. Paper 3 – Sections 7.2 and 8.1 point out how ineffective it is to use empirical formulations for the estimation of flux for a universal model that can predict icing rates for a wide variety of vessels and structures. The method presented in Paper 4 does overcome the issue of empirical formulations and makes the model independent of these and is a good starting point for research in this direction.

The paper uses a wave washing threshold, the value of which stems from measurements from the Ryerson 1995 data. Using this value as the wave washing threshold, as stated in the paper, is a pure assumption of the threshold level required for wave washing. This too, like flux, needs to be verified through full scale tests. On the other hand, the paper demonstrates how the wave washing threshold needs to be used in conjunction with the ML model and makes space for this. Without the wave washing threshold, the ML model would predict very heavy icing in the area of the vessel that is submerged under water due to the large amounts of incoming fluid as the ML model is not trained for deicing.

Another drawback of the Paper 4, which is also mentioned in Paper 4 - Section 6, is the large grid size that one could argue would not accurately represent the spray. The ship-sea dynamics and generation of droplets after a wave impact happen at very different scales. Dynamics of single droplet generation at the scale of a few millimeters has been demonstrated to be computable with CFD [193]. Researchers in the field of sea spray icing also have begun studies into trajectories of individual droplets [194], however the generation of the droplets itself is not a part of the study. It is well known that CFD simulations are mesh dependent and accuracy of the model would indeed increase with a finer mesh. For the simulation in

Paper 4, a decision was made on the grid size considering the balance between computational time and demonstration of the method. In retrospect, in the view of missing verifications against full scale flux measurements, a mesh dependence study would have given a clearer picture of how much variation in the estimation of flux could be expected with a variation in the grid size.

Although the mesh dependence would be interesting suggestion for continuation of the study and development of the method, focus on resolving individual droplets for the case of prediction of sea pray icing on a vessel or a large structure, for example with an extremely fine mesh using techniques similar to that presented by Zhou et.al.2021 [193] would require simulation resources beyond comprehension using contemporary technology, make the simulation unnecessarily complex, and to a certain extent is also unnecessary in macroscopic terms. The balance between accuracy and computational expense is thus indeed an important consideration. However, in the end stages of the project, another method of using scalars for sea spray generation in CFD was coarsely explored in Paper 5. Either method from papers 4 and 5, if and when verified against full scale flux measurements, would completely set aside the need to look into microscopic droplet levels for sea spray generation.

8.5.4. A perspective on modelling of sea spray generation

When a moving vessel impacts against an incoming wave or a wave, impacts against a vessel or a structure, the wave-vessel/structure impact causes the wave to break into a jet of water droplets in the form of a spray. This sea spray constitutes of water droplets of varying diameters, which also affects how wind would carry these droplets. The spray generation is dependent on many known and unknown parameters and each individual spray event would be different to a point that it could be considered stochastic. Extremely accurate modelling of each spray event, or over a period of time would not be possible or even necessary. In essence, any attempts to model sea spray for the prediction of sea spray icing would be limited to an estimate.

It is however important that the estimates of flux to be applicable for a universal model to predict icing and distribution on arbitrary vessels or structures of different sizes and shapes, must be made for individual subjects rather than in terms of empirical formulations. One of the most important points from the discussion in Paper 3 is quoted here:

“Ryerson from their detailed study of flux and icing measurements mentions that the observed flux data were attempted to be written as general equations as a function of other parameters, but most relationships were complex and not significant [148]. This observation clearly discourages the use of any formulations for the estimation of spray flux. Despite this, researchers have been using a handful of available flux formulations. Models using these formulations, often in the form of LWC, would, at most, predict icing rates for similar ships and the exact locations as ones from the flux measurements. Any attempts to generalize these types of ice prediction models over different types and sizes of ships or structures or use them to estimate the distribution of ice would provide inaccurate results. This effectively deems all theoretical models as inaccurate or limited to very specific cases. The problem was visible while attempting to validate models against full-scale data, since the ice thickness and flux were measured at different locations. This calls for a radical change in how future models approach the estimation of spray flux.” [21]

This was the inspiration to start research into a method that could be universally applicable for any arbitrary vessel/ structure. Paper 4 presents a proposal for solving the flux problem in a new direction using fluid continuum approach in CFD. The method makes the model completely independent of the heavily criticized empirical formulations. It comes, however, with other challenges, mainly concerned with the verification against full-scale measurements. The challenges with the method are openly discussed to aid future and ongoing research address these to improve the flux estimations. One possible improvement is the use of scalars for spray generation in CFD simulations. This was delved into, albeit rather coarsely, towards the end of the project and is partially used in the simulation in Paper 5.

9. Paper 5

9.1. Background

Challenges related to using existing full-scale data from literature for the purpose of validation of prediction models were covered in Paper 3. Since SPICE2 is vessel specific, it is essential to have the 3D model of the vessel for the icing and distribution predictions. This makes validating the model from external icing measurements impossible. The predicted icing rates by SPICE2 in Paper 4 were compared to predictions with existing models which are not capable of providing distribution. In 2020, full-scale icing tests were planned to be carried out on the Miriam lifeboat from Paper 4 but were unfortunately cancelled due to Covid. Sundsbø et.al. 2018 had carried out a full-scale icing test on another similar lifeboat from Harding [195]. In 2023, partial results from this originally confidential report, and the 3D model of the lifeboat from the test were made available for the validation of SPICE2. Due to permissions regarding usage of data from these full-scale tests, the presentation of Spice2 and its validation had to be separated into different papers.

9.2. Summary

The model of the Harding lifeboat was run through the SPICE2 method with simulation inputs that of the met-ocean conditions during the test duration. The predictions from SPICE2 are compared with the measurements from the full-scale icing test by Sundsbø et.al. 2018. The icing measurements from this test were more detailed than those which were previously investigated in Paper 3. This made it possible for a direct comparison of the predicted and measured icing rates. The icing measurements made available were as a range of icing rates and not exact measurements. SPICE2 showed satisfactory predictions for a majority of probe locations where the predicted icing rates at individual locations were within the measured range. An alternate source of spray data using scalars in the CFD simulations was discovered to be as useful as the one presented in Paper 4 due to problems with some of the outputs from the CFD software. Icing rates predicted with SPICE2 were compared directly to the measured icing rates. The upgrade of SPICE2 from SPICE involves an intermediate step of estimating spray data from CFD before icing predictions are made with the ML model. Since spray data was not measured during the full-scale tests, this could not be validated, and ideally needs to be done as a part of future research. The final output of the SPICE2 model, which is the icing rates, however, showed satisfactory comparison with the measured icing rates at various probe locations.

9.3. Literature cited

Paper 5 cites the following literature:

[20] [58] [9] [178] [33] [19] [21] [8] [16] [195] [42] [67] [43] [196] [197]

9.4. Additional supporting information

Note: As Papers 4 and 5 are parts of the same study, refer Section 8.5 for the supporting information. Section 8.5 is valid for both, Paper 4, and Paper 5.

10. Concluding discussion

Some of the achievements of the current PhD project are as follows:

- Paper 1: Compilation of literature related to the sea spray icing phenomenon, international standards related to the topic, and comparison of various modelling approaches in a single document which can be used by the industry and researchers alike for the purposes of learning about the topic and as a starting point to future research in this field.
- Paper 2: The greatest number of independent variables that affect icing rates experimentally tested.
- Paper 3: A prediction model that implements new techniques including machine learning and feature engineering, making the model experimentally validated. This is extremely important considering limited full-scale studies and difficulties of using these for model validation. It is a dynamically designed forecasting model wherein the user is able to use flux formulations that best suit their case or even use real time flux measurements. Missing variables required for prediction of icing can be estimated through a 'feature calculator'.
- Paper 4: A truly universal prediction model capable of predicting icing rates with the distribution on an arbitrary moving vessel, which is completely independent of existing empirical formulations that have been criticized and termed as the 'weakest link' for sea spray icing prediction models by past researchers.
- Spice and Spice2 together fill all the objectives of for a new model as defined in Section 3.
- Paper 5: Validation of the presented model by comparison with full-scale measurements.

10.1. Suggestions for future work

Each paper individually provides advantages, limitations, and scope for improvement in the methods used in those papers. Four of the main scopes for improvement and suggestions for future research are as follows:

- Conducting full-scale studies is difficult and expensive. Controlled laboratory experiments are also time and energy consuming but proved to be doable. Machine learning models have been shown to capture intricacies and hidden patterns in the data but cannot confidently predict icing rates for values outside the range of the training data. More tests and consecutively more data would

improve the range of predictions allowing continuous improvement of models as and when new data is obtained.

- Existing formulations for important variables like spray flux have time and again been criticized for their inaccuracy during generalization. A method to estimate spray flux using CFD has been developed in this study and showed promising results with the predicted icing rates. The validation ideally needs to be done directly with spray data for which more full-scale measurements are necessary. In general, future research should focus on methods to estimate spray flux for a wide range of vessels and structures.
- Although models based on a limited number of full-scale observations have been criticized, full-scale observations are essential for validation of models. Many more and detailed full-scale observations are suggested for validation of sea spray icing models.
- Availability of real time flux measurement at strategic locations on the vessel or structure can help eliminate all uncertainties related to the estimation of flux used in SPICE. For example, even though CFD simulations on individual vessels is argued to be better than using limited observations on a single vessel, there will always be some limitations with simulating a stochastic process like sea spray, for example, the local underwater currents, rouge waves, and the fact that the simulation can be performed only for one pair of relative vessel heading with respect to waves. This method would, of course, be limited to operational situations. Research into measurement of real time spray flux are suggested for future research.

10.2. Practical requirements for the model

The current research project presents, in essence, two separate models: SPICE, a forecasting type of model (see Section 4.5.1, Figure 1, Figure 2) which is a purely ML model presented in Paper 3; and SPICE2, a comprehensive prediction model (see Section 4.5.1, Figure 1, Figure 2) which is a hybrid ML-CFD model and an extension of SPICE wherein some of the input variables are estimated with CFD as opposed to either a direct input to the ML model with all variables known (for e.g. through live monitoring), or by using the feature calculator for missing required variables, which necessitates the use of empirical formulations.

10.2.1. Practical requirements for using SPICE for forecasting

The practical requirements for SPICE would depend on the application. The model itself is completely ready and with the availability (currently restricted – see Section 10.3) of the model, one would be able to predict icing rates if all input variables are available. Input variables, especially flux, is not usually readily available. In certain use cases like, for example, real-time icing rate predictions, real-time flux measurements using a method of choice can be used. However, this is not applicable to all user cases, like for example, when a prediction needs to be done ahead of time in order to take necessary precautions or for sending out warnings. In this case, the feature calculator (see Paper 3), which is currently programmed in python, needs to be used where missing obligatory variables required for prediction by the ML model are estimated as per the given algorithm. Other inputs related to weather, could be either fed directly or gathered through a suitable weather forecast Application Programming Interface (API).

In either user case, some amount of programming would be necessary to design the software around the specific user case, integration of the model with other measurement systems, and the Graphical User Interface (GUI) for their end user.

Besides these factors, further testing like the ones presented in Paper 2, but with more variation in the variables, and retraining the model with the combined data would help increase the range of confident predictions (see Paper 3). Especially for a user case in which the total icing load in a long period of time is required, data from deicing tests which could be used to train the model for negative icing rates would be required.

10.2.1. Practical requirements for using SPICE2 for comprehensive predictions

For comprehensive predictions including prediction of icing rates, as well as the distribution of icing on the surface of the vessel/ structure, SPICE2 uses CFD simulations in addition to the ML model. In addition to the practical requirements for SPICE, comprehensive predictions with SPICE2 would require CFD simulations to be done on each individual vessel or structure for the required met-ocean conditions for the prediction, necessitating the availability of the 3D model of the subject and would require knowledge and availability of a CFD software.

Since each individual vessel or structure would result in different flux, ideally, the current method, or as a matter of fact, any method for estimating flux needs to be verified against multiple dissimilar vessels and structures of varying sizes and shapes. Full scale tests for verification, as mentioned earlier, are extremely time consuming, and capital and labor intensive. It could also be possible that if the flux is measured and verified for one vessel would not hold true for another vessel of a different size. This does not imply that flux validations against full scale measurements should not be done. Gathering full scale flux data from multiple types of vessels/ structures, additionally in varying met ocean conditions with several variables is not something that can be easily practically achieved. On the other hand, if the model is verified with a limited number of full-scale flux measurements, but a comparatively large number of icing measurement from varying vessel/ structure types, which can be assessed comparatively easily would provide a reasonable verification of the method and the model.

10.3. Continuation of the work done in this PhD project

The machine learning model developed in this PhD project, SPICE, predicts the icing rate based on 7 different variables given as input. Some of the variables can be used from the weather data and others are computed from any available data with the help of existing formulations. SPICE2 computes the other unavailable variables through CFD making the model independent of existing formulations and thereby universal, such that it could be used for any vessel or structure independent of its size or shape. SPICE itself would be completely independent in case flux data from real-time measurements is fed to the model.

The SPICE model developed in this research is disseminated through the already published Paper 3, for which, the experimental data collection is already disseminated through paper 2, while papers 4 and 5 are intended to be submitted soon. Although the data collection procedure and the flowchart for the development of the model is made publicly available through the publications, the actual model and the

training data is withheld due to the ongoing commercialization of research project with UiT and Norinnova. UiT has retained the rights over the model.

The SPICE model in its current form exists as a pickled binary object – a common practice for developers of machine learning models. The feature calculator used in SPICE and all related programming exists as a python code. Anyone familiar with python and machine learning would be able to use the pickled object without much support, and availability of the complete python code would enable even users unfamiliar to programming to manipulate input variables and make icing predictions. Details of how to use the model with valid inputs are provided in Paper 3. However, sharing of the model to interested parties is, at least at the time of writing, due to the ongoing project, should go through a request directly to UiT.

The model is intended for a variety of end users. The commercialization of research project is looking into industry partners who would be interested in further development and application of the model. The framework of the end-product where the model would be used, irrespective of the outcome of the commercialization of research project, would have to be developed around the model. In other words, development of the 'software tool' for the end user depends heavily on the application of the model and could involve either SPICE or SPICE2 including a Graphical User Interface (GUI) for the end user, and integrations with weather data providers through Application Programming Interfaces (APIs). Some of the suggested user cases are as follows:

- Marine vessel and offshore structure designers for estimating the icing loads on the vessel/ structure to make design considerations to support structural integrity and for optimal design of passive anti-icing measures.
- Shipping companies and offshore operators for operational forecasts to take precautionary measures in terms of operational safety.
- Vessel operators for deciding on the most optimal sailing route to avoid heavy icing, and thereby saving fuel by avoiding additional weight of ice.
- Designers of anti-icing equipment, for example, heat tracing systems to optimize the heating based on the predicted icing, leading to greener operations by saving energy consumption for heating.
- Certification agencies to control the designs for vessels/ structures operating in cold climates.

11. References

[1] Norwegian Directorate for Higher Education and Skills, "NORWEGIAN REGISTER FOR SCIENTIFIC JOURNALS, SERIES AND PUBLISHERS." Accessed: Apr. 29, 2024. [Online]. Available: https://kanalregister.hkdir.no/publiseringskanaler/Om.action?request_locale=en

[2] T. S. Jørgensen, "Influence of ice accretion on activity in the northern part of the Norwegian Continental Shelf.," Report No. STF88F82016, Offshore Testing and Research Group, Trondheim, Norway (1982), 1982.

[3] AMAP, *Arctic Oil and Gas 2007. Arctic Monitoring and Assessment Programme (AMAP).*, xiii. Oslo, Norway, 2007.

[4] The Barents Observer, "Norway considers size limitation on passenger ships sailing at Svalbard," Dec. 17, 2019.

[5] N. Melia, K. Haines, and E. Hawkins, “Sea ice decline and 21st century trans-Arctic shipping routes,” *Geophys Res Lett*, vol. 43, no. 18, pp. 9720–9728, Sep. 2016, doi: 10.1002/2016GL069315.

[6] N. M. L. and A. UK, “The Beaufort Scale,” 2010.

[7] Fiskeritidende, “They will never forget that day in February 1979. (originally in Danish).” Accessed: Jul. 10, 2023. [Online]. Available: https://fiskeritidende.dk/nyheder/gl-fiskeritidende/de-glemmer-aldrig-den-dag-i-februar-1979/

[8] S. Deshpande, A. Sæterdal, and P.-A. Sundsbø, “Sea Spray Icing: The Physical Process and Review of Prediction Models and Winterization Techniques,” *Journal of Offshore Mechanics and Arctic Engineering*, vol. 143, no. 6, pp. 1–12, Dec. 2021, doi: 10.1115/1.4050892.

[9] Stallabrass, “Trawler Icing - a Compilation of Work Done At N. R. C.,” *Mechanical Engineering Report MD-56, N.R.C. No. 19372 (National Research Council, Ottawa Canada)*, 1980.

[10] *ISO 19906:*, 2nd ed. Petroleum and natural gas industries – Arctic offshore structures, 2019.

[11] A. Kulyakhtin and A. Tsarau, “A time-dependent model of marine icing with application of computational fluid dynamics,” *Cold Reg Sci Technol*, vol. 104–105, pp. 33–44, Aug. 2014, doi: 10.1016/j.coldregions.2014.05.001.

[12] DNVGL-OS-A201, “OFFSHORE STANDARD DNV GL AS Winterization for cold climate operations (Edition July 2015),” 2015.

[13] Polar Code, “International Code for ships operating in Polar waters,” *IMO: International Maritime Organization*, 2017.

[14] ISO, *ISO - ISO 19901-3:2014 - Petroleum and natural gas industries — Specific requirements for offshore structures — Part 3: Topsides structure*. 2014.

[15] N. (Working Environment), “NORSOK S-002:2018+AC,” 2021.

[16] *ISO 35106: Petroleum and natural gas industries — Arctic operations — Metocean, ice, and seabed data*. 2017.

[17] M. Zahn and H. von Storch, “A long-term climatology of North Atlantic polar lows,” *Geophys Res Lett*, vol. 35, no. 22, Nov. 2008, doi: 10.1029/2008GL035769.

[18] R. D. Brown and P. Roebber, “The Scope of the ice accretion problem in Canadian waters related to offshore energy and transportation.,” Canadian Climate Centre Report 85-13, 1985.

[19] E. M. Samuelsen, K. Edvardsen, and R. G. Graversen, “Modelled and observed sea-spray icing in Arctic-Norwegian waters,” *Cold Reg Sci Technol*, vol. 134, pp. 54–81, Feb. 2017, doi: 10.1016/j.coldregions.2016.11.002.

[20] A. Kulyakhtin, “Numerical Modelling and Experiments on Sea Spray Icing,” Doctoral thesis. Department of Civil and Transport Engineering. Norwegian University of Science and Technology (NTNU), Norway, 2014.

[21] S. Deshpande, “A Machine Learning Model for Prediction of Marine Icing,” *Journal of Offshore Mechanics and Arctic Engineering*, vol. 146, no. 6, Dec. 2024, doi: 10.1115/1.4064108.

[22] A. Kulyakhtin, “Numerical Modelling and Experiments on Sea Spray Icing,” Doctoral thesis. Department of Civil and Transport Engineering. Norwegian University of Science and Technology (NTNU), Norway, 2014. [Online]. Available: http://hdl.handle.net/11250/277036

[23] J. Flannery, “Tragedy leads to better icing alerts,” SoundingsOnline.

[24] J. E. Overland, C. H. Pease, R. W. Preisendorfer, and A. L. Comiskey, “Prediction of Vessel Icing,” *Journal of Climate and Applied Meteorology*, vol. 25, no. 12, pp. 1793–1806, Dec. 1986, doi: 10.1175/1520-0450(1986)025<1793:POVI>2.0.CO;2.

[25] L. Makkonen, R. D. Brown, and P. T. Mitten, “Comments on ‘Prediction of Vessel Icing for Near-Freezing Sea Temperatures,’” *Weather Forecast*, vol. 6, no. 4, pp. 565–567, Dec. 1991, doi: 10.1175/1520-0434(1991)006<0565:COOVIF>2.0.CO;2.

[26] H. O. Mertins, “Icing on fishing vessels due to spray.,” Mar. Obs., 38, 1968.

[27] S. Mintu, D. Molyneux, and D. Oldford, “State-of-the-Art Review of Research on Ice Accretion Measurements and Modelling,” in *Arctic Technology Conference*, Offshore Technology Conference, Oct. 2016. doi: 10.4043/27422-MS.

[28] P. Roebber and P. Mitten, *Modelling and measurement of icing in Canadian waters*. Report (Canadian Climate Centre), no. 87-15., 1987.

[29] L. G. Kachurin, L. I. Gashin, and I. A. Smirnov, “Icing Rate of Small Displacement Fishing Boats under Various Hydro-meterological Conditions.,” *Meterologiya i Gidrologia*, vol. 3, pp. 50–60, 1974.

[30] I. Horjen, “Numerical modeling of two-dimensional sea spray icing on vessel-mounted cylinders,” *Cold Reg Sci Technol*, vol. 93, pp. 20–35, Sep. 2013, doi: 10.1016/j.coldregions.2013.05.003.

[31] T. W. Forest, E. P. Lozowski, and R. Gagnon, “Estimating marine icing on offshore structures using RIGICE04,” in *Proceedings of the International Workshop on Atmospheric Icing on Structures (IWAIS), Montreal, Canada.*, 2005.

[32] Horjen and Vefsnmo, “A numerical sea spray icing model including the effect of a moving water film.,” in *Proceedings. Int. Workshop on Offshore Winds and Icing, Halifax, pp. 152-164.*, 1985.

[33] A. Kulyakhtin, O. Shipilova, B. Libby, and S. Løset, “Full-scale 3D CFD Simulation of Spray Impingement on a Vessel Produced by Ship-wave Interaction,” *Proc. of the 21st IAHR Intl. Symposium on Ice (2012)*, pp. 1129–1141, 2012.

[34] J. E. Overland, C. H. Pease, R. W. Preisendorfer, and A. L. Comiskey, “Prediction of Vessel Icing,” *Journal of Climate and Applied Meteorology*, vol. 25, no. 12, pp. 1793–1806, Dec. 1986, doi: 10.1175/1520-0450(1986)025<1793:POVI>2.0.CO;2.

[35] P. Roebber and P. Mitten, *Modelling and measurement of icing in Canadian waters*. Report (Canadian Climate Centre), no. 87-15., 1987.

[36] Stallabrass, "Trawler Icing - a Compilation of Work Done At N. R. C.," *Mechanical Engineering Report MD-56, N.R.C. No. 19372 (National Research Council, Ottawa Canada)*, 1980.

[37] I. Horjen, "Numerical modeling of two-dimensional sea spray icing on vessel-mounted cylinders," *Cold Reg Sci Technol*, vol. 93, pp. 20–35, Sep. 2013, doi: 10.1016/j.coldregions.2013.05.003.

[38] T. W. Forest, E. P. Lozowski, and R. Gagnon, "Estimating marine icing on offshore structures using RIGICE04," in *Proceedings of the International Workshop on Atmospheric Icing on Structures (IWAIS), Montreal, Canada.*, 2005.

[39] A. Kulyakhtin and A. Tsarau, "A time-dependent model of marine icing with application of computational fluid dynamics," *Cold Reg Sci Technol*, vol. 104–105, pp. 33–44, Aug. 2014, doi: 10.1016/j.coldregions.2014.05.001.

[40] E. M. Samuelsen, K. Edvardsen, and R. G. Graversen, "Modelled and observed sea-spray icing in Arctic-Norwegian waters," *Cold Reg Sci Technol*, vol. 134, pp. 54–81, Feb. 2017, doi: 10.1016/j.coldregions.2016.11.002.

[41] V. Os, "Warns of danger of icing on ships (In Norwegian)," University of Tromsø Newsletter. Accessed: Apr. 10, 2024. [Online]. Available: https://uit.no/nyheter/artikkel?p_document_id=560838&p_dim=88131

[42] S. Deshpande and P. Sundsbø, "Investigation into using CFD for estimation of ship specific parameters for the SPICE model for prediction of sea spray icing. Part 1: The proposal," *Submitted to journal for peer-review*, pp. 1–20, 2024.

[43] C. C. Ryerson, "Superstructure spray and ice accretion on a large U.S. Coast Guard cutter," *Atmos Res*, vol. 36, no. 3–4, pp. 321–337, May 1995, doi: 10.1016/0169-8095(94)00045-F.

[44] I. Horjen, "Offshore drilling rig ice accretion modeling including a surficial brine film," *Cold Reg Sci Technol*, vol. 119, pp. 84–110, 2015, doi: 10.1016/j.coldregions.2015.07.006.

[45] C. M. Bishop, "Pattern Recognition and Machine Learning," *Pattern Recognition and Machine Learning*, Dec. 2006, doi: 10.1007/978-0-387-45528-0.

[46] S. Schelter, F. Biessmann, T. Januschowski, D. Salinas, S. Seufert, and G. Szarvas, "On Challenges in Machine Learning Model Management," *Bulletin of the IEEE Computer Society Technical Committee on Data Engineering*, pp. 5–13, 2018.

[47] P. Kumar and M. Sharma, "Data, Machine Learning, and Human Domain Experts: None Is Better than Their Collaboration," *Int J Hum Comput Interact*, vol. 38, no. 14, pp. 1307–1320, Aug. 2022, doi: 10.1080/10447318.2021.2002040.

[48] H. K. Versteeg and W. Malaskekera, *An Introduction to Computational Fluid Dynamics: The Finite Volume Method*. 1995. doi: 10.2514/1.22547.

[49] X. Yu, Y. Zhang, R. Hu, and X. Luo, “Water droplet bouncing dynamics,” *Nano Energy*, vol. 81, p. 105647, Mar. 2021, doi: 10.1016/j.nanoen.2020.105647.

[50] S. Mintu, D. Molyneux, and B. Colbourne, “Full-scale SPH simulations of ship-wave impact generated sea spray,” *Ocean Engineering*, vol. 241, p. 110077, Dec. 2021, doi: 10.1016/J.OCEANENG.2021.110077.

[51] A. Nasreldeen, L. Fan, and K. Liu, “Smooth PArticle Hydrodynamics (SPH),” *Penn State University College of Earth and Mineral Science Department of Energy and Mineral Engineering*, 2017.

[52] A. Dehghani-Sanij, M. Mahmoodi, S. R. Dehghani, Y. S. Muzychka, and G. F. Naterer, “Experimental investigation of vertical marine surface icing in periodic spray and cold conditions,” *Journal of Offshore Mechanics and Arctic Engineering*, vol. 141, no. 2, pp. 1–40, 2019, doi: 10.1115/1.4041394.

[53] E. M. Samuelsen, “Prediction of ship icing in Arctic waters Observations and modelling for application in operational weather forecasting,” UiT, The Arctic University of Norway (Doctoral thesis), 2017.

[54] C. C. Ryerson, “Ice protection of offshore platforms,” *Cold Reg Sci Technol*, vol. 65, no. 1, pp. 97–110, Jan. 2011, doi: 10.1016/j.coldregions.2010.02.006.

[55] M. Mahmood and A. Revenga, “DESIGN ASPECTS OF WINTERIZED AND ARCTIC LNG CARRIERS – A CLASSIFICATION PERSPECTIVE,” in *Proceedings of OMAE2006, 25th International Conference on Offshore Mechanics and Arctic Engineering, June 4-9, 2006, Hamburg, Germany*, 2006, pp. 1–8.

[56] M. Polakis, P. Zachariadis, and J. O. de Kat, “The Energy Efficiency Design Index (EEDI),” in *Sustainable Shipping*, Cham: Springer International Publishing, 2019, pp. 93–135. doi: 10.1007/978-3-030-04330-8_3.

[57] Y. hang Hou, K. Kang, and X. Liang, “Vessel speed optimization for minimum EEOI in ice zone considering uncertainty,” *Ocean Engineering*, vol. 188, p. 106240, Sep. 2019, doi: 10.1016/j.oceaneng.2019.106240.

[58] E. P. Lozowski, K. Szilder, and L. Makkonen, “Computer simulation of marine ice accretion,” *Philosophical Transactions of the Royal Society of London. Series A: Mathematical, Physical and Engineering Sciences*, vol. 358, no. 1776, pp. 2811–2845, Nov. 2000, doi: 10.1098/rsta.2000.0687.

[59] J. Ashcroft, “Potential ice and snow accretion on North Sea rigs and platforms,” *MarineTechnical Note no. 1, British Meteorological Office, Bracknell*, 1985.

[60] Romagnoli, “Ice growth modelling for icing control purposes of offshore marine units employed by the petroleum industry,” in *Int. Association for Hydraulic Re posium on Ice, Sapporo, pp. 486-497.*, 1988.

[61] J. E. Overland, “Prediction of Vessel Icing for Near-Freezing Sea Temperatures,” *Weather Forecast*, vol. 5, no. 1, pp. 62–77, Mar. 1990, doi: 10.1175/1520-0434(1990)005<0062:POVIFN>2.0.CO;2.

[62] SR. Dehghani, GF. Naterer, and Y. S. Muzychka, “3-D trajectory analysis of wave-impact sea spray over a marine vessel,” *Cold Reg Sci Technol*, vol. 146, no. November 2017, pp. 72–80, Feb. 2018, doi: 10.1016/j.coldregions.2017.11.016.

[63] S. R. Dehghani, Y. S. Muzychka, and G. F. Naterer, “Numerical Solution of Rapid Freezing of Sea Water on Cold Substrates,” in *Volume 8: Polar and Arctic Sciences and Technology; Petroleum Technology*, American Society of Mechanical Engineers, Jun. 2017, pp. 1–8. doi: 10.1115/OMAE2017-62191.

[64] A. Dehghani-sanij, Y. S. Muzychka, and G. F. Naterer, “Analysis of Ice Accretion on Vertical Surfaces of Marine Vessels and Structures in Arctic Conditions,” in *Volume 7: Ocean Engineering*, American Society of Mechanical Engineers, May 2015, pp. 1–7. doi: 10.1115/OMAE2015-41306.

[65] A. R. Dehghani-Sanij, S. MacLachlan, G. F. Naterer, Y. S. Muzychka, R. D. Haynes, and V. Enjilela, “Multistage cooling and freezing of a saline spherical water droplet,” *International Journal of Thermal Sciences*, vol. 147, p. 106095, Jan. 2020, doi: 10.1016/j.ijthermalsci.2019.106095.

[66] DNV, “RULES FOR CLASSIFICATION Ships Part 6 Additional class notations Chapter 6 Cold climate,” no. July, 2015.

[67] W. P. Zakrzewski, “Icing of Fishing Vessels. Part I: Splashing a Ship With Spray.,” in *Proceedings of the 8th Int. IAHR Symposium on Ice, Iowa City, August 18–22, 1986, Vol. 2 (1986), pp. 179-194*, 1986.

[68] Dehghani, Muzychka, and Naterer, “Water breakup phenomena in wave-impact sea spray on a vessel,” *Ocean Engineering*, vol. 134, pp. 50–61, Apr. 2017, doi: 10.1016/j.oceaneng.2017.02.013.

[69] D. Saha, S. R. Dehghani, K. Pope, and Y. Muzychka, “The Extent of Water Sheet Breakup on a Vertical Surface,” in *Arctic Technology Conference*, Offshore Technology Conference, Oct. 2016. doi: 10.4043/27404-MS.

[70] Ryerson, “Icing Management for Coast Guard Assets,” U.S. Army Engineer Research and Development Center, Hanover, New Hampshire, USA, 2013.

[71] E. Fuentes, H. Coe, D. Green, G. de Leeuw, and G. McFiggans, “Laboratory-generated primary marine aerosol via bubble-bursting and atomization,” *Atmos Meas Tech*, vol. 3, no. 1, pp. 141–162, Feb. 2010, doi: 10.5194/amt-3-141-2010.

[72] R. Lewis and E. Schwartz, *Sea Salt Aerosol Production: Mechanisms, Methods, Measurements and Models—A Critical Review*, vol. 152. in Geophysical Monograph Series, vol. 152. Washington, D. C.: American Geophysical Union, 2004. doi: 10.1029/GM152.

[73] I. Horjen and S. Vefsnmo, “A Kinematic and Thermodynamic Analysis of Sea Spray (in Norwegian), Offshore Icing—Phase II. Norwegian Hydrodynamic Laboratory (NHI). Report STF60 F85014,” 1985.

[74] E. L. Andreas, “Time constants for the evolution of sea spray droplets,” *Tellus, Series B*, vol. 42 B, no. 5, pp. 481–497, Nov. 1990, doi: 10.3402/tellusb.v42i5.15241.

[75] A. Bodaghkhani, S.-R. Dehghani, Y. S. Muzychka, and B. Colbourne, “Understanding spray cloud formation by wave impact on marine objects,” *Cold Reg Sci Technol*, vol. 129, pp. 114–136, Sep. 2016, doi: 10.1016/j.coldregions.2016.06.008.

[76] J. Stallabrass, “ICING OF FISHING VESSELS IN CANADIAN WATERS.,” DME/NAE Quarterly Bull., 1975 (1) (1975) Ottawa, Canada, 1975.

[77] G. S. H. Lock, *The growth and decay of ice.* Cambridge University Press, 1990.

[78] S. R. Dehghani, G. F. Naterer, and Y. S. Muzychka, "Droplet size and velocity distributions of wave-impact sea spray over a marine vessel," *Cold Reg Sci Technol*, vol. 132, pp. 60–67, Dec. 2016, doi: 10.1016/j.coldregions.2016.09.013.

[79] A. R. Dehghani-Sanij, S. R. Dehghani, G. F. Naterer, and Y. S. Muzychka, "Sea spray icing phenomena on marine vessels and offshore structures: Review and formulation," *Ocean Engineering*, vol. 132, pp. 25–39, Mar. 2017, doi: 10.1016/j.oceaneng.2017.01.016.

[80] Y. Borisenkov and V. Panov, "Basic results and prospects of research on hydrometeorological conditions of sihpboard icing," *Issled. Fiz. Prin Obledeneniya Sudov, Leningrad (1972), CRREL Draft Translation TL411, 1974*, 1972.

[81] A. Kulyakhtin, L. E. Kollar, S. Løset, and M. Farzaneh, "Numerical Simulations of 3D Spray Flow in a Wind Tunnel with Application of O'Rourke's Interaction Algorithm and Its Validation," in *Proc. of the 21st IAHR Intl. Symposium on Ice (2012)*, 2012.

[82] M. Breuer, N. Jovičić, and K. Mazaev, "Comparison of DES, RANS and LES for the separated flow around a flat plate at high incidence," *Int J Numer Methods Fluids*, vol. 41, no. 4, pp. 357–388, Feb. 2003, doi: 10.1002/fld.445.

[83] J. Fröhlich and D. von Terzi, "Hybrid LES/RANS methods for the simulation of turbulent flows," *Progress in Aerospace Sciences*, vol. 44, no. 5, pp. 349–377, Jul. 2008, doi: 10.1016/j.paerosci.2008.05.001.

[84] S. R. Dehghani, M. H. Saidi, A. A. Mozafari, and A. Ghafourian, "Particle Trajectory in a Bidirectional Vortex Flow," *Particulate Science and Technology*, vol. 27, no. 1, pp. 16–34, Jan. 2009, doi: 10.1080/02726350802611366.

[85] S. R. Dehghani, Y. S. Muzychka, and G. F. Naterer, "Droplet trajectories of wave-impact sea spray on a marine vessel," *Cold Reg Sci Technol*, vol. 127, pp. 1–9, Jul. 2016, doi: 10.1016/j.coldregions.2016.03.010.

[86] C. H. Lee and R. D. Reitz, "An experimental study of the effect of gas density on the distortion and breakup mechanism of drops in high speed gas stream," *International Journal of Multiphase Flow*, vol. 26, no. 2, pp. 229–244, Feb. 2000, doi: 10.1016/S0301-9322(99)00020-8.

[87] P. S. O'Rourke, "Collective drop effects on vaporizing liquid sprays.," United States, 1981.

[88] L. E. Kollár and M. Farzaneh, "Modeling the evolution of droplet size distribution in two-phase flows," *International Journal of Multiphase Flow*, vol. 33, no. 11, pp. 1255–1270, Nov. 2007, doi: 10.1016/j.ijmultiphaseflow.2007.04.002.

[89] Makkonen, "Models for the growth of rime, glaze, icicles and wet snow on structures," *Philosophical Transactions of the Royal Society of London. Series A: Mathematical, Physical and Engineering Sciences*, vol. 358, no. 1776, pp. 2913–2939, Nov. 2000, doi: 10.1098/rsta.2000.0690.

[90] K. J. Finstad, E. P. Lozowski, and E. M. Gates, “A Computational Investigation of Water Droplet Trajectories,” *J Atmos Ocean Technol*, vol. 5, no. 1, pp. 160–170, Feb. 1988, doi: 10.1175/1520-0426(1988)005<0160:ACIOWD>2.0.CO;2.

[91] W. Gao, D. W. Smith, and D. C. Sego, “Freezing Temperatures of Freely Falling Industrial Wastewater Droplets,” *Journal of Cold Regions Engineering*, vol. 14, no. 3, pp. 101–118, Sep. 2000, doi: 10.1061/(ASCE)0887-381X(2000)14:3(101).

[92] J. Stallabrass and P. Hearty, “The Icing of cylinders in conditions of simulated freezing sea spray,” 1967.

[93] A. Dehghani-Sanij, Y. S. Muzychka, and G. F. Naterer, “Predicted Ice Accretion on Horizontal Surfaces of Marine Vessels and Offshore Structures in Arctic Regions,” in *Volume 8: Polar and Arctic Sciences and Technology; Petroleum Technology*, American Society of Mechanical Engineers, Jun. 2016, pp. 1–9. doi: 10.1115/OMAE2016-54054.

[94] L. Makkonen, “Salinity and growth rate of ice formed by sea spray,” *Cold Reg Sci Technol*, vol. 14, no. 2, pp. 163–171, Aug. 1987, doi: 10.1016/0165-232X(87)90032-2.

[95] P. Schwerdtfeger, “The Effect of Finite Heat Content and Thermal Diffusion on the Growth of a Sea-Ice Cover,” *Journal of Glaciology*, vol. 5, no. 39, pp. 315–324, Jan. 1964, doi: 10.3189/S0022143000029051.

[96] A. Kulyakhtin, S. Kulyakhtin, and S. Løset, “The role of the ice heat conduction in the ice growth caused by periodic sea spray,” *Cold Reg Sci Technol*, vol. 127, pp. 93–108, Jul. 2016, doi: 10.1016/j.coldregions.2016.04.001.

[97] L. Makkonen, “Solid fraction in dendritic solidification of a liquid,” *Appl Phys Lett*, vol. 96, no. 9, p. 091910, Mar. 2010, doi: 10.1063/1.3306728.

[98] R. Z. Blackmore, L. Makkonen, and E. P. Lozowski, “A new model of spongy icing from first principles,” *Journal of Geophysical Research: Atmospheres*, vol. 107, no. D21, p. AAC 9-1-AAC 9-15, Nov. 2002, doi: 10.1029/2001JD001223.

[99] J. S. Wettlaufer, M. G. Worster, and H. E. Huppert, “the phase evolution of Young Sea Ice,” *Geophys Res Lett*, vol. 24, no. 10, pp. 1251–1254, May 1997, doi: 10.1029/97GL00877.

[100] M. Schremb, I. V. Roisman, and C. Tropea, “Normal impact of supercooled water drops onto a smooth ice surface: experiments and modelling,” *J Fluid Mech*, vol. 835, pp. 1087–1107, Jan. 2018, doi: 10.1017/jfm.2017.797.

[101] G. Wilbur, B. MacMillan, K. M. Bade, and I. Mastikhin, “MRI monitoring of sea spray freezing,” *Journal of Magnetic Resonance*, vol. 310, p. 106647, Jan. 2020, doi: 10.1016/j.jmr.2019.106647.

[102] K. F. Jones and E. L. Andreas, “Sea spray concentrations and the icing of fixed offshore structures,” *Quarterly Journal of the Royal Meteorological Society*, vol. 138, no. 662, pp. 131–144, Jan. 2012, doi: 10.1002/qj.897.

[103] W. ; Kays, M. ; Crawford, and B. Weigand, *Convective Heat and Mass Transfer. 4th Edition*. 2004.

[104] T. S. Jørgensen, “Sea spray characteristics on a semi-submersible drilling rig - STF60 F 85015,” 1985.

[105] I. Horjen, S. Loeset, and S. Vefsnmo, “Icing Hazards On Supply Vessels And Stand-by Boats - STF60 A86073,” 1986.

[106] I. Muzik and A. Kirby, “Spray overtopping rates for Tarsiut Island: model and field study results,” *Canadian Journal of Civil Engineering*, vol. 19, no. 3, pp. 469–477, Jun. 1992, doi: 10.1139/l92-057.

[107] V. V. Borisenkov, Y.P., Zablockiy, G.A., Makshtas, A.P., Migulin, A.I., Panov, “On the approximation of the spray-cloud dimensions (In Russian). Arkticheskii I Antarkticheskii Nauchno-Issledovatelskii Institut.,” 1975.

[108] H. E. B. Børs, S. Løset, K. Iden, M. Reistad, K. Harstveit, B. Nygård, “Goliat Environmental/ Icing Evaluation Study. 25/08,” 2009.

[109] C. Anandharamakrishnan, J. Gimbun, A. G. F. Stapley, and C. D. Rielly, “Application of Computational Fluid Dynamics (CFD) Simulations to Spray-Freezing Operations,” *Drying Technology*, vol. 28, no. 1, pp. 94–102, Dec. 2009, doi: 10.1080/07373930903430843.

[110] E. Villeneuve, D. Harvey, D. Zimcik, R. Aubert, and J. Perron, “Piezoelectric Deicing System for Rotorcraft,” *Journal of the American Helicopter Society*, vol. 60, no. 4, pp. 1–12, Oct. 2015, doi: 10.4050/JAHS.60.042001.

[111] S. A. Kulinich and M. Farzaneh, “Ice adhesion on super-hydrophobic surfaces,” *Appl Surf Sci*, vol. 255, no. 18, pp. 8153–8157, Jun. 2009, doi: 10.1016/j.apsusc.2009.05.033.

[112] Ulstein Group, “X-Bow.” Accessed: Feb. 19, 2020. [Online]. Available: https://ulstein.com/innovations/x-bow

[113] P. Guest and R. Luke, “Mariners Weather Log Vol. 49, No. 3, December 2005.” Accessed: Sep. 07, 2020. [Online]. Available: https://www.vos.noaa.gov/MWL/dec_05/ves.shtml

[114] E. M. Samuelsen and R. G. Graversen, “Weather situation during observed ship-icing events off the coast of Northern Norway and the Svalbard archipelago,” *Weather Clim Extrem*, vol. 24, no. 9293, p. 100200, Jun. 2019, doi: 10.1016/j.wace.2019.100200.

[115] A. Kulyakhtin and S. Løset, “Sea spray icing : in-cloud evaporation . Semi- analytical and numerical investigations .,” in *The 14th International Workshop on Atmospheric Icing of Structures, Chongqing, China, May 8 - May 13, 2011 SEA*, Chongqing, China, 2011.

[116] A. Hyldgård, D. Mortensen, K. Birkelund, O. Hansen, and E. V. Thomsen, “Autonomous multi-sensor micro-system for measurement of ocean water salinity,” *Sens Actuators A Phys*, vol. 147, no. 2, pp. 474–484, Oct. 2008, doi: 10.1016/J.SNA.2008.06.004.

[117] S. Brohez, C. Delvosalle, and G. Marlair, “A two-thermocouples probe for radiation corrections of measured temperatures in compartment fires,” *Fire Saf J*, vol. 39, no. 5, pp. 399–411, Jul. 2004, doi: 10.1016/J.FIRESAF.2004.03.002.

[118] CSGNetwork, “Water Density Calculator.” Accessed: Sep. 14, 2022. [Online]. Available: http://www.csgnetwork.com/h2odenscalc.html

[119] Matlab_Documentation, “Filtering and Smoothing Data - MATLAB & Simulink - MathWorks Nordic.” Accessed: Aug. 16, 2022. [Online]. Available: https://se.mathworks.com/help/curvefit/smoothing-data.html

[120] R. D. Brown and T. Agnew, “Characteristics of marine icing in Canadian waters.,” in *Proceedings of the International Workshop on Offshore Winds and Icing*, 1985, pp. 78–94.

[121] X. Chang *et al.*, “Research on ultrasonic-based investigation of mechanical properties of ice,” *Acta Oceanologica Sinica*, vol. 40, no. 10, pp. 97–105, 2021, doi: 10.1007/s13131-021-1890-3.

[122] M. C. Ortiz, L. A. Sarabia, M. S. Sánchez, and A. Herrero, “Quality of Analytical Measurements: Statistical Methods for Internal Validation,” in *Comprehensive Chemometrics*, vol. 1, Elsevier, 2009, pp. 17–76. doi: 10.1016/B978-044452701-1.00090-9.

[123] S. Ferraris and L. M. Volpone, “ALUMINIUM ALLOYS IN THIRD MILLENNIUM SHIPBUILDING: MATERIALS, TECHNOLOGIES, PERSPECTIVES.,” *The Fifth International Forum on Aluminium Ships.*, Oct. 2005.

[124] S. SUZUKI, R. MURAOKA, T. OBINATA, S. ENDO, T. HORITA, and K. OMATA, “Steel Products for Shipbuilding,” *JFE TECHNICAL REPORT, 2:41*, Mar. 2004.

[125] VikingNorsafe, “VIKING Norsafe Life-Saving Equipment Norway AS MATHILDA-74,” VIKING Doc. No.: TSB-0045, Rev. No. 3, Mar. 2021.

[126] RolledMetalProducts, “Aluminum 5052 data sheet.” 2017.

[127] A. A. Bhatti, Z. Barsoum, H. Murakawa, and I. Barsoum, “Influence of thermo-mechanical material properties of different steel grades on welding residual stresses and angular distortion,” *Materials & Design (1980-2015)*, vol. 65, pp. 878–889, Jan. 2015, doi: 10.1016/j.matdes.2014.10.019.

[128] G. B Vaggar, S. C Kamate, and P. V Badyankal, “Thermal Properties Characterization of Glass Fiber Hybrid Polymer Composite Materials,” *International Journal of Engineering & Technology*, vol. 7, no. 3.34, p. 455, Sep. 2018, doi: 10.14419/ijet.v7i3.34.19359.

[129] S. Wang and J. Qiu, “Enhancing thermal conductivity of glass fiber/polymer composites through carbon nanotubes incorporation,” *Compos B Eng*, vol. 41, no. 7, pp. 533–536, Oct. 2010, doi: 10.1016/j.compositesb.2010.07.002.

[130] L. Li, Y. Liu, Z. Zhang, and H. Hu, “Effects of thermal conductivity of airframe substrate on the dynamic ice accretion process pertinent to UAS inflight icing phenomena,” *Int J Heat Mass Transf*, vol. 131, pp. 1184–1195, Mar. 2019, doi: 10.1016/J.IJHEATMASSTRANSFER.2018.11.132.

[131] P. Dawson and S. L. Dawson, “Sharing successes and hiding failures: ‘reporting bias’ in learning and teaching research,” *https://doi.org/10.1080/03075079.2016.1258052*, vol. 43, no. 8, pp. 1405–1416, Aug. 2016, doi: 10.1080/03075079.2016.1258052.

[132] I. Horjen and S. Vefsnmo, “Mobile platform stability (MOPS) subproject 02 - icing (MOPS Report No. 15).,” 1984.

[133] E. S. Miles, J. F. Steiner, and F. Brun, “Highly variable aerodynamic roughness length (z0) for a hummocky debris-covered glacier,” *Journal of Geophysical Research: Atmospheres*, vol. 122, no. 16, pp. 8447–8466, Aug. 2017, doi: 10.1002/2017JD026510.

[134] G. M. Masters, *Renewable and Efficient Electric Power Systems.* Hoboken, New Jersey: Wiley-Interscience, 2004.

[135] J. Stallabrass, “Meteorological and oceanographic aspects of trawler icing off the Canadian east coast.,” 1971.

[136] E. P. Lozowski, K. Szilder, and L. Makkonen, “Computer simulation of marine ice accretion,” *Philosophical Transactions of the Royal Society of London. Series A: Mathematical, Physical and Engineering Sciences*, vol. 358, no. 1776, pp. 2811–2845, Nov. 2000, doi: 10.1098/rsta.2000.0687.

[137] W. P. Zakrzewski, “Splashing a ship with collision-generated spray,” *Cold Reg Sci Technol*, vol. 14, no. 1, pp. 65–83, Jun. 1987, doi: 10.1016/0165-232X(87)90045-0.

[138] A. Kulyakhtin, O. Shipilova, B. Libby, and S. Løset, “Full-scale 3D CFD Simulation of Spray Impingement on a Vessel Produced by Ship-wave Interaction,” *Proc. of the 21st IAHR Intl. Symposium on Ice (2012)*, pp. 1129–1141, 2012.

[139] L. Battisti, R. Fedrizzi, A. Brighenti, and T. Laakso, “Sea Ice and Icing Risk for Offshore Wind Turbines,” in *OWEMES 2006*, Citavecchia, Italy: OWEMES, 2006, pp. 20–22.

[140] A. R. Dehghani-Sanij, S. R. Dehghani, G. F. Naterer, and Y. S. Muzychka, “Sea spray icing phenomena on marine vessels and offshore structures: Review and formulation,” *Ocean Engineering*, vol. 132, pp. 25–39, Mar. 2017, doi: 10.1016/j.oceaneng.2017.01.016.

[141] R. D. Brown and P. Roebber, “The Scope of the ice accretion problem in Canadian waters related to offshore energy and transportation.,” Canadian Climate Centre Report 85-13, 1985.

[142] *ISO 35106: Petroleum and natural gas industries — Arctic operations — Metocean, ice, and seabed data*. 2017.

[143] A. Bodaghkhani, S.-R. Dehghani, Y. S. Muzychka, and B. Colbourne, “Understanding spray cloud formation by wave impact on marine objects,” *Cold Reg Sci Technol*, vol. 129, pp. 114–136, Sep. 2016, doi: 10.1016/j.coldregions.2016.06.008.

[144] S. Deshpande, A. Sæterdal, and P.-A. Sundsbø, “Experiments With Sea Spray Icing: Investigation of Icing Rates,” *Journal of Offshore Mechanics and Arctic Engineering*, vol. 146, no. 1, Feb. 2024, doi: 10.1115/1.4062255.

[145] S. Li, J. Qin, and R. Paoli, “Data-Driven Machine Learning Model for Aircraft Icing Severity Evaluation,” *Journal of Aerospace Information Systems*, vol. 18, no. 11, pp. 876–880, Nov. 2021, doi: 10.2514/1.I010978.

[146] S. Li, J. Qin, M. He, and R. Paoli, “Fast Evaluation of Aircraft Icing Severity Using Machine Learning Based on XGBoost,” *Aerospace*, vol. 7, no. 4, p. 36, Mar. 2020, doi: 10.3390/aerospace7040036.

[147] G. M. Masters, *Renewable and Efficient Electric Power Systems.* Hoboken, New Jersey: Wiley-Interscience, 2004.

[148] C. C. Ryerson, “Superstructure spray and ice accretion on a large U.S. Coast Guard cutter,” *Atmos Res*, vol. 36, no. 3–4, pp. 321–337, May 1995, doi: 10.1016/0169-8095(94)00045-F.

[149] D. Chicco, M. J. Warrens, and G. Jurman, “The coefficient of determination R-squared is more informative than SMAPE, MAE, MAPE, MSE and RMSE in regression analysis evaluation,” *PeerJ Comput Sci*, vol. 7, pp. 1–24, Jul. 2021, doi: 10.7717/PEERJ-CS.623/SUPP-1.

[150] T. Chen and C. Guestrin, “XGBoost: A Scalable Tree Boosting System”, doi: 10.1145/2939672.2939785.

[151] F. Pedregosa FABIANPEDREGOSA *et al.*, “Scikit-learn: Machine Learning in Python Gaël Varoquaux Bertrand Thirion Vincent Dubourg Alexandre Passos PEDREGOSA, VAROQUAUX, GRAMFORT ET AL. Matthieu Perrot,” *Journal of Machine Learning Research*, vol. 12, pp. 2825–2830, 2011, Accessed: Mar. 06, 2023. [Online]. Available: http://scikit-learn.sourceforge.net.

[152] S. Chowdhury, Y. Lin, B. Liaw, and L. Kerby, “Evaluation of Tree Based Regression over Multiple Linear Regression for Non-normally Distributed Data in Battery Performance”.

[153] J. A. Colton and K. M. Bower, “Some misconceptions about R2,” *International Society of Six Sigma Professionals, EXTRAOrdinary Sense*, vol. 3, no. 2, pp. 20–22, 2002.

[154] A. Bodaghkhani, Y. S. Muzychka, and B. Colbourne, “Three-Dimensional Numerical and Experimental Simulation of Wave Run-Up Due to Wave Impact with a Vertical Surface,” *Journal of Fluids Engineering, Transactions of the ASME*, vol. 140, no. 8, pp. 1–12, 2018, doi: 10.1115/1.4039369.

[155] S. Lundberg, “SHAP documentation - Rev.45b85c18.” Accessed: Mar. 07, 2023. [Online]. Available: https://shap.readthedocs.io/en/latest/example_notebooks/overviews/Be%20careful%20when%20interpreting%20predictive%20models%20in%20search%20of%20causal%C2%A0insights.html

[156] G. Dong and H. Liu, *Feature Engineering for Machine Learning and Data Analytics*. CRC Press - Taylor and Francis Group , 2018.

[157] J. H. Friedman and B. E. Popescu, “Predictive Learning via Rule Ensembles,” *Source: The Annals of Applied Statistics*, vol. 2, no. 3, pp. 916–954, 2008, doi: 10.1214/07-AOAS.

[158] T. McConaghy, “FFX: Fast, Scalable, Deterministic Symbolic Regression Technology,” pp. 235–260, 2011, doi: 10.1007/978-1-4614-1770-5_13.

[159] D. Cote, “Demonstrating the power of feature engineering .” Accessed: Mar. 07, 2023. [Online]. Available: https://medium.com/@dave.cote.msc/demonstrating-the-power-of-feature-engineering-part-ii-how-i-beat-xgboost-with-linear-regression-e63aeb6a15f8

[160] C. Molnar, *Interpretable Machine Learning . A guide for making Black Box models Explainable*. https://christophm.github.io/interpretable-ml-book/, 2023. Accessed: Mar. 07, 2023. [Online]. Available: https://christophm.github.io/interpretable-ml-book/

[161] C. Molnar, "Python package for RuleFit." Accessed: Mar. 07, 2023. [Online]. Available: https://github.com/christophM/rulefit/blob/master/LICENSE

[162] T. McConaghy, "Python package for FFX," Solido Design Automation Inc. Accessed: Mar. 07, 2023. [Online]. Available: https://github.com/natekupp/ffx/blob/master/LICENSE

[163] J. Bergstra, B. Komer, C. Eliasmith, D. Yamins, and D. D. Cox, "Hyperopt: a Python library for model selection and hyperparameter optimization," *Comput Sci Discov*, vol. 8, no. 1, p. 014008, Jul. 2015, doi: 10.1088/1749-4699/8/1/014008.

[164] W. P. Zakrzewski, "Icing of Fishing Vessels. Part I: Splashing a Ship With Spray.," in *Proceedings of the 8th Int. IAHR Symposium on Ice, Iowa City, August 18–22, 1986, Vol. 2 (1986), pp. 179-194*, 1986.

[165] N. M. L. and A. UK, "The Beaufort Scale," 2010.

[166] T. S. Jørgensen, "Sea spray characteristics on a semi-submersible drilling rig - STF60 F 85015," 1985.

[167] I. Horjen, "Numerical modeling of time-dependent marine icing, anti-icing and de-icing," Trondheim University, Norway, 1990.

[168] B. Massey and J. Ward-Smith, *Mechanics of Fluids*, Eighth. Taylor & Francis, 2006.

[169] A. Kovrova, C. Korotun, and V. Panov, "Gidrometeorologicheskiye usloviya obledeneniya na sudakh v arkticheskikh moryakh. (Hydrometeorological conditions of icing on ships in the Arctic seasa)," *Arkticheskii i Antarkticheskii Nauchno-lssledovatiel'skii lnstitut, Leningrad*, 1969.

[170] L. R. Aksjutin, "Icing of Ships. Leningrad: Sudostroenye (in Russian)," p. 126, 1979.

[171] Ryerson, "Icing Management for Coast Guard Assets," U.S. Army Engineer Research and Development Center, Hanover, New Hampshire, USA, 2013.

[172] Y. P. Borisenkov, "On the theory of spray icing of ships. In: Arkticheskii i Antarkticheskii Nauchno-Issledovatelskii Institut. Trudy 298. Leningrad: Gidrometeoizdat (in Russian), 34-43.," 1972.

[173] E. M. Samuelsen, "Prediction of ship icing in Arctic waters Observations and modelling for application in operational weather forecasting," UiT, The Arctic University of Norway (Doctoral thesis), 2017.

[174] I. Horjen and S. Vefsnmo, "A Kinematic and Thermodynamic Analysis of Sea Spray (in Norwegian), Offshore Icing—Phase II. Norwegian Hydrodynamic Laboratory (NHI). Report STF60 F85014," 1985.

[175] L. Makkonen, R. D. Brown, and P. T. Mitten, "Comments on 'Prediction of Vessel Icing for Near-Freezing Sea Temperatures,'" *Weather Forecast*, vol. 6, no. 4, pp. 565–567, Dec. 1991, doi: 10.1175/1520-0434(1991)006<0565:COOVIF>2.0.CO;2.

[176] A. Kulyakhtin and S. Løset, “Sea spray icing : in-cloud evaporation . Semi- analytical and numerical investigations .,” in *The 14th International Workshop on Atmospheric Icing of Structures, Chongqing, China, May 8 - May 13, 2011 SEA*, Chongqing, China, 2011.

[177] L. Makkonen, “Salinity and growth rate of ice formed by sea spray,” *Cold Reg Sci Technol*, vol. 14, no. 2, pp. 163–171, Aug. 1987, doi: 10.1016/0165-232X(87)90032-2.

[178] W. P. Zakrzewski, “Splashing a ship with collision-generated spray,” *Cold Reg Sci Technol*, vol. 14, no. 1, pp. 65–83, Jun. 1987, doi: 10.1016/0165-232X(87)90045-0.

[179] S. Deshpande, A. Sæterdal, and P.-A. Sundsbø, “Experiments With Sea Spray Icing: Investigation of Icing Rates,” *Journal of Offshore Mechanics and Arctic Engineering*, vol. 146, no. 1, Feb. 2024, doi: 10.1115/1.4062255.

[180] A. Kulyakhtin, O. Shipilova, and M. Muskulus, “Numerical simulation of droplet impingement and flow around a cylinder using RANS and LES models,” *J Fluids Struct*, 2014, doi: 10.1016/j.jfluidstructs.2014.03.007.

[181] B. Massey and J. Ward-Smith, *Mechanics of Fluids*, Eighth. Taylor & Francis, 2006.

[182] Flow-3D, “Flow-3D® Version 12.0 (2019).” Flow Science, Inc., Santa Fe, NM, 2019.

[183] LicetStudios, “Ship in Storm | Cruise Ship Climbing Up Big Waves.” [Online]. Available: https://www.youtube.com/watch?v=j2sxfx3SSCQ

[184] LicetStudios, “Ship in Storm | WARSHIP Hit By Monster Wave Near Antarctica [4K].” [Online]. Available: https://www.youtube.com/watch?v=TYe2tkXgPqs

[185] Y. Jin, H. Zhou, L. Zhu, and Z. Li, “Dynamics of Single Droplet Splashing on Liquid Film by Coupling FVM with VOF,” *Processes 2021, Vol. 9, Page 841*, vol. 9, no. 5, p. 841, May 2021, doi: 10.3390/PR9050841.

[186] S. Wang and C. Guedes Soares, “Review of ship slamming loads and responses,” *Journal of Marine Science and Application*, vol. 16, no. 4, pp. 427–445, 2017, doi: 10.1007/s11804-017-1437-3.

[187] Flow-3D, “Flow-3D® Version 12.0 (2019).” Flow Science, Inc., Santa Fe, NM, 2019.

[188] C. W. Hirt and J. M. Sicilian, “A POROSITY TECHNIQUE FOR THE DEFINITION OF OBSTACLES IN RECTANGULAR CELL MESHES,” in *International Conference on Numerical Ship Hydrodynamics, 4th*, Washington DC, 1985.

[189] G. WEI, “A FIXED-MESH METHOD FOR GENERAL MOVING OBJECTS IN FLUID FLOW,” *Modern Physics Letters B*, vol. 19, no. 28n29, pp. 1719–1722, Dec. 2005, doi: 10.1142/S021798490501030X.

[190] V. Yakhot, S. A. Orszag, S. Thangam, T. B. Gatski, and C. G. Speziale, “Development of turbulence models for shear flows by a double expansion technique,” *Physics of Fluids A: Fluid Dynamics*, vol. 4, no. 7, pp. 1510–1520, Jul. 1992, doi: 10.1063/1.858424.

[191] I. Muzik and A. Kirby, “Spray overtopping rates for Tarsiut Island: model and field study results,” *Canadian Journal of Civil Engineering*, vol. 19, no. 3, pp. 469–477, Jun. 1992, doi: 10.1139/l92-057.

[192] SARex-Svalbard, “About SARex 2019-2020,” SARex-Svalbard.

[193] Y. Jin, H. Zhou, L. Zhu, and Z. Li, “Dynamics of Single Droplet Splashing on Liquid Film by Coupling FVM with VOF,” *Processes 2021, Vol. 9, Page 841*, vol. 9, no. 5, p. 841, May 2021, doi: 10.3390/PR9050841.

[194] SR. Dehghani, GF. Naterer, and Y. S. Muzychka, “3-D trajectory analysis of wave-impact sea spray over a marine vessel,” *Cold Reg Sci Technol*, vol. 146, no. November 2017, pp. 72–80, Feb. 2018, doi: 10.1016/j.coldregions.2017.11.016.

[195] P.-A. Sundsbø and T. Jakobsen, “Sea Spray Icing on Goliat Lifeboat. 2018. (Confidential),” 2018.

[196] P.-A. Sundsbø, T. Jakobsen, and R. Safer, “FF1200 Test report Sea Spray Icing on Goliat Lifeboat, Palfinger Marine Safety AS, Palfinger report 5583(Confidential),” 2018.

[197] P. Sundsbø, “Full scale measurement & modelling of sea spray icing caused by wind-ship-sea interaction (Unpublished working paper),” 2024.

12. Appendix 1: Paper 1

Sea spray icing: The physical process, and review of prediction models and winterization techniques

Sujay Deshpande[1]*, Ane Sæterdal[2], Per-Arne Sundsbø[1]

[This is a reprint of the accepted version of the article. Reprinted with permission from ASME. Strictly for the use of inclusion in the PhD thesis. DOI of published version: https://doi.org/10.1115/1.4050892**]**

Abstract—Ice accretion on marine vessels and offshore structures is a severe hazard in the Polar Regions. There is increasing activities related to oil and gas exploration, tourism, cargo transport, and fishing in the Arctic. Ice accretion can cause vessel instability, excess load on marine structures and represents a safety risk for outdoor working environment and operations. Freezing sea spray is the main contributor to marine icing.

For safe operations in cold climate, it is essential to have verified models for prediction of icing. Sea spray icing forecast models have improved. Empirical and theoretical models providing icing rates based may be useful as guidelines. For predicting the distribution of icing on a surface at the design stage, Computational Fluid Dynamics has to be applied along with a freezing module. State-of-the-art models for numerical simulation of sea spray icing are still not fully capable of modelling complex ship-sea-wind interactions with spray generation and impact of shipped water. Existing models include good understanding of spray flow effects and freezing. Further development should focus on developing models for dynamic ship-sea-wind interactions, in particular including spray generation, effects of shipped water and distribution of icing on the vessel surface. More experimental and full-scale data is needed for development and verification of new and improved models. Models that estimate ice distribution may improve the winterization design process and reduce effort required for deicing. Improved methods for de-icing and anti-icing will reduce the impact of sea spray icing and increase safety for marine operations in cold waters.

Keywords—Sea spray icing, prediction models, winterization, CFD, review, state-of-the-art, numerical models, arctic operations, cold climate, anti-icing, deicing.

1. INTRODUCTION

Fishing has been the main activity in arctic waters for centuries. The past few decades has seen a growth in offshore oil and gas activity in the arctic and sub-arctic cold regions ,and it is expected to further rise in the arctic regions in Alaska [1]. There is also substantial increase in tourism in the region like cruises to

[1] Dept. of Building, Energy and Material Technology, UiT, The Arctic University of Norway.
[2] Department of Computer Science and Computational Engineering, UiT, The Arctic University of Norway.
* Corresponding author: Sujay Deshpande.
email: sujay.r.deshpande@uit.no
Address: C/o UiT, Campus Narvik, Lodve Langesgate 2, 8514, Narvik, Norway.

Svalbard [2]. Due to the decline of Arctic sea ice, shorter trade routes through the Arctic are anticipated to bloom [3].

Operations in the Arctic are challenging due to the harsh weather conditions. Ice accretion on vessels can cause blockage of critical systems like the ventilation system and escape doors, and cause hazardous working conditions on-board due to slippery decks [4]. In extreme situations, a lopsided ice load may lead to the capsizing in case of smaller vessels [5] or structural failures of deck equipment [6].

Icing can occur due to various reasons such as supercooled fog, freezing rain, snow, and freezing sea spray. Freezing sea spray is the most frequent and the most significant form of icing, and the other three causes are not considered to have any serious impact [7], [8]. Freezing sea spray caused 80 – 90% of all offshore icing incidents [4]. For design and operational purposes, it is crucial to have models for prediction of sea spray icing.

Winterization includes design and operational measures concerning safe operability and maintainability in a cold climate. Safe offshore operations in icing conditions rely on marine ice warning forecast, proper operational routines and vessel/ structural design for ice impact and ice load. Marine ice warning forecast models predict approximate icing rates with available metocean data. Operational routines include everything from favourable manoeuvres, deicing (ice removal) and avoiding marine icing weather zones. Most common design measures concerning sea spray icing have been shielding critical equipment on vessels and offshore structures, heat tracing, a favourable arrangement of deck equipment and to some extent minimising details that may cause marine ice accumulation [9]. In general, prevention is better than cure, and so, international standards put emphasis on anti-icing methods, i.e. methods for prevention of ice formation, especially design measures that prevent the formation of ice. In addition, standards call for adequate stability during icing events [10], [11]. This makes it necessary for marine design engineers to estimate the icing amount, and especially the distribution of icing on the vessel/ offshore structure already at the design stage.

Data of marine ice accumulation can be obtained from climatic atlases, site measurements from rigs in the area, coastal stations and ships [8]. Such data is knowledge-based/deterministic and typically provides general estimates for icing loads, icing rates. Sometimes the variation of icing rate with height above sea level is available. Distribution of icing on the surface of arbitrary ships/ structures cannot be estimated from such historical data. The distribution of marine ice should be modelled for individual vessels and structures for proper design and winterization with respect to marine icing. The distribution of sea spray ice may be found through full-scale measurements or numerical modelling. However, performing offshore full-scale measurements of sea spray icing is resource-intensive and risky. Numerical modelling of sea spray icing is still in the developing phase and not fully applicable for all engineering purposes [8]. An example of the uncertainty of prediction can be seen in the comparison of three different models presented by Kulyakhtin and Tsarau, 2014 (Figure 7) where the predicted icing load on a stationary vertical cylinder with a diameter of 90m and height of 30m varied by a factor of almost 100% at one point of time. Additionally, in case of ships, it is essential to predict the distribution of icing on the superstructure for stability analysis. It can be seen from Table 4 that the distribution of icing on the superstructure is missing from many models. MARICE simulates a stationary ship instead of ideally considering the motion of the ship for calculating the icing distribution. Owing to the variation of the icing prediction from various models and

the lack of comparison against full-scale measurements, and especially icing distribution, it is difficult to say which model is most reliable.

The focus on 'green' technologies and reduction of energy consumption has increased in the recent years. The International Maritime Organisation (IMO) has introduced an Energy Efficiency Design Index (EEDI) to reduce the environmental impact of ships. The EEDI sets a minimum energy efficiency level per capacity mile for different categories of ships and acts as a benchmark for comparison. The reference energy efficiency level for new ships is tightened every five years by 10%. EEDI regulations do not apply to ice-breaking cargo ships, but do apply to all other ships operated in cold regions [12]. The fuel efficiency of the vessel can be severely impacted due to ice loads [13]. Improvement in anti-icing design measures will lead to higher fuel efficiency for vessel operating in cold climate and reduce the energy consumption for eventual de-icing. This might enable ship designers to achieve a higher rating in the EEDI and thereby contributing to IMOs goals of reducing the environmental impacts of ships. Advancements in technology has resulted in development of autonomous vessels. Autonomous vessels intended for operations in cold waters will be exposed to icing. There is a need for anti-icing design measures and having autonomous de-icing systems on board. For developing improved and anti-icing designs, we need verified models to predict the distribution of sea spray icing on the structure.

Modelling of sea spray icing is a niche field and limited number of researchers have worked on this topic. The physical process of sea spray icing is complex and is divided into several sub processes for modelling purposes. This has led to information scattered across multiple scientific articles and necessitates the need to gather information about the all the involved sub processes in one place.

Parallel development of numerical models for prediction of marine icing had begun since the 1980s due to the increasing exploration of natural resources in the North Sea [14]. Some of the existing prediction models are the Ashcroft model [15], Romagnoli model [16], the Overland model [17], the RIGICE model [18] by Roebber and Mitten, and the ICEMOD model [19] by Horjen and Vefsnmo [14]. Two of these models have been further developed over the years by adding more details giving rise to ICEMOD2 [20] and RIGICE04 [21]. More recently, some other models have been developed like the MARICE model [22], the MINCOG model [23] and the model at the Memorial University of Newfoundland, Canada [24], [25].

The Overland model is a deterministic model for icing rates based on basic physical parameters [26]. Though it has limitations [27], the Overland model is used by the United States National Oceanic and Atmospheric Administration (NOAA) owing to its simplicity [26]. ICEMOD and RIGICE are theoretical models that have not been sufficiently verified by field measurements [26]. ICEMOD02 suggests that the relative wind direction has the most significant impact on vessel icing [20]. RIGICE04 is coded as an Excel spreadsheet with Visual Basic 6 subroutines making it easy to use [21]. Although the new version of RIGICE seems to be more accurate than the previous versions of RIGICE, there is a need for more verification of the model with field data [21]. Researchers at the Memorial University of Newfoundland, Canada have developed a 1-D model for the icing process on vertical surfaces [28]. There has been further progress with this research, like the study of 3-D trajectory analysis of wave impact spray [24] and freezing of water droplets [29]. Of the considered models, MARICE is the only numerical model using Computational Fluid Dynamics (CFD) for the sea spray icing process. It is probably the first and currently only model to attempt modelling the distribution of icing on an arbitrary surface. MARICE uses CFD to solve the droplet dynamics

and heat transfer. It involves both, the freezing and melting processes with the help of an additional freezing module [22].

This paper gives an insight into the processes involved in sea spray icing. A summary of ice management requirements by international standards is presented. The modelling approach of some state-of-the-art sea spray icing models towards individual sub-processes is studied. Objectives of developing a sea spray icing model are summarised and how far the existing models hold true to these objectives are discussed. Examples of what each model is capable of can help readers chose the most appropriate model based on their requirement. Improvements for future sea spray icing models are suggested. In addition, ice management techniques relevant for anti-icing and deicing of vessels and offshore structures are presented. Prediction models considered in this review represent rather different concepts and is therefore hard to compare them in a case study. Thus, comparison of results from these models are limited.

2. Standards and Regulations related to ice accretion

There are several standards stating requirements for vessels and offshore installations for operations in cold-climate regions. The contents of the most widely used relevant standards pertaining to ice accretion are summarised in this section.

Winterization measures are classified as anti-icing (prevention of ice formation) and deicing (removal of accumulated ice), and further as active measures (direct use of energy, for example, heating or physical force) and passive measures (for example sheading or insulation) [10]. Preference should be given to passive anti-icing measures, and a shielded location is the simplest and most reliable solution for anti-icing. Equipment requiring anti-icing measures should be as far as possible from the area prone to sea spray. [10]. As such, ships should be designed to minimize ice accretion [30].

Standards state that equipment crucial for personnel safety and the functioning of the vessel has to be completely functional under icing conditions and ideally should be kept ice-free either with active or passive anti-icing measures. Some examples include deck drains and scuppers, helicopter deck, deck cranes, mooring equipment, motor, lighting, escape ways, doors and hatches, firefighting system, fire and gas alarm systems, Public Address/ General Alarm (PA/GA) system, life raft/ Marine Evacuation Systems (MES), lifeboats, Escape, Evacuation and Rescue (EER) craft, antennae, ballast tanks, ventilation systems, pressure/ vacuum relief arrangements, Global Maritime Distress and Safety System (GMDSS) and Emergency position-indicating radio beacon station (EPIRB). Additionally, any overboard discharges should not lead to icing [8], [10], [30].

Adequate stability should be retained under icing conditions due to the excess weight of the accredited ice [8], [10], [30]. Some standards specify icing loads that have to be used while calculating the stability of vessels. An example of the specified ice loads can be seen in

Table .

Table 1: Icing load for decks, gangways, deckhouse tops and other horizontal surfaces [10]

Icing load (kg/m2) to be applied to decks, gangways, deckhouse tops and other horizontal surfaces1			
Height from Waterline (WL)	**From forward extremity to 50m aft of the Forward Perpendicular (FP)**	**50 to 100m aft of the FP**	**>100m aft of the FP**
> 24m	10	10	10
> 18 to 24m	30	30	30
>12 to 18m	40	30	30
>6 to 12m	80	40	30
0 to 6m	120	60	30
1For the purpose of this rule, the Waterline (WL) shall be taken as the Summer Load Line			

In general, sea-spray icing or marine icing may occur if the air temperature is less than the freezing point of seawater. Table 2 gives guidelines for the relationship between sea spray icing rates and metocean conditions, mainly based on vessel icing events and to some extent, site measurements. These guidelines are only rough estimates since the occurrence of sea spray icing depends on vessel characteristics.

Table 2: Icing intensity classification [8]

Icing intensity	**Ice Accumulation (mm/h)**	**Air temperature (°C)**	**Wind speed (m/s)**	**Water temp (°C)**
Slow	< 10	0 to -3	Any	< 8
		< -3	< 7	< 8
Fast	10 - 30	-3 to -8	7 - 15	< 8
Very fast	> 30	< -8	> 15	< 8

2.1. Winterized class ship qualifiers

International standards classify winterized class ships into three main qualifiers based on the level of design environmental conditions (the weather extremes that the ship should withstand for safe operations) – Basic, Cold, and Polar [10], [31] as shown in Table 3.

Table 3: Classification qualifiers of winterized ships [31]

Winterized class Qualifier	**Purpose**	**Air temperature (td)**	**Sea water temperature**	**Wind speed**
Basic	Occasional short operations in cold climate	≤ −10°C	+4°C (without ice class) -2°C (with ice class)	20 m/s
Cold	Regular extended operations in cold climate	-15°C to -30°C	+2°C (without ice class) -2°C (with ice class)	20 m/s
Polar	Year-round operations in extreme cold climate of the polar regions	< -25°C	-2°C	20 m/s
Where td is the lowest statistical mean daily average air temperature in area of operation over 20 years, And 'ice class' refers to classification in light or drifting sea ice.				

It can be concluded from Table 2 and Table 3 that all winterized class ships, irrespective of their qualifier as Basic, Cold, or Polar, have to be designed to withstand or remain within operational safety limits of 'very fast' icing intensity of ice accumulation rates greater than 30 mm/hour. The operational safety can be achieved by a combination of extra factor of safety during structural and stability calculations and active deicing systems.

The polar code additionally categories polar ships into various categories and ice classes depending on their ability of operation in ice waters. This categorization is however not relevant for the current study which concerns sea spray icing.

2.2. Standards related to the measurement of ice

Standards for Arctic operations also suggest which parameters should be physically recorded after sea spray icing events. These parameters are the thickness of ice accretion on several surfaces covering at least two different elevations, the weight of ice per length or surface area, frequency and height of wave splash, associated conditions (anti-icing/deicing measures), photographic documentation, the lowest and highest elevation of observed sea spray icing [11]. Additionally, other physical parameters such as air and seawater temperature, wind speed and direction, vessel pitch and heave amplitudes, vessel or structure characteristics affecting the wave response and interaction, structure position, speed and heading, presence of sea ice, and wind information at local data points have to be recorded [11].

3. Objectives of prediction of sea spray icing

Sea spray icing is common in cold climate operations and is the most severe form of offshore icing [4], [11]. For offshore structures, icing loads have to be accounted for in the design to avoid structural failures due to the weight of the accreted ice [8], [10]. In the case of vessels, adequate stability should be maintained in case of icing on the superstructure [10], [30]. It is thus necessary to have ice load and distribution predictions at the design stage.

To the best of the authors' knowledge, there is only one numerical model using CFD for sea spray icing predictions– the MARICE model. It uses CFD to determine where spray droplets might impact on the structure.

Other widely used sea spray icing models like RIGICE and ICEMOD are theoretical models, whereas the model presented by Overland, 1990 is deterministic, neither of these uses CFD [26]. Overland, 1990 provides guidelines and icing rates that may be used as an input for CFD for calculating the distribution of icing. However, Makkonen et. al., 1991 give a robust summary of how the assumptions in the Overland, 1986 and the updated Overland, 1990 model are faulty and mention that the model could not be replicated [27]. Some researchers have been critical to the use of CFD for sea spray icing predictions due to the numerous variables that are difficult to parameterise and the time scales involved [23].

Numerical estimates of sea spray icing must account for the following processes [11]:

- Spray generation
- Spray transport and drift
- Spray collision, freezing, melting and run-off
- Effect of the structure motions when relevant

The last point – Effect of structure motions, is a critical aspect to consider while CFD modelling involving ships. The ship-sea interaction leads to pitching and rolling of the ship. This affects the flow of the generated spray with respect to the ship's structure. The MARICE sea spray icing model considers the ship as a stationary object in the spray impingement model [32]. Neither does the 3-D trajectory analysis of wave-impact sea spray over a marine vessel [24] consider the effect of the motion of the ship due to the ship-sea interaction in the spray flow trajectory models.

The MARICE model uses the equation of Zakrzewski [33] for the spray generation [32]. This model was developed for a medium-sized fishing vessel [33]. The results may vary if the model is applied to vessels of other sizes. The method suggested by Overland [17] is traditionally used for estimation of sea spray ice on small-to-medium size vessels. None of the current methods can predict sea spray icing on a wide range of vessels [11]. Also, verification of the models against full-scale data is extremely limited [11].

The objectives of a sea spray icing CFD can be listed as follows:

- To approximate spray generation, transport, impingement and freezing while considering the motion of the vessel or structure in waves.
- The model should conform well with full-scale data.

- The model should give detailed distribution and amount of icing on the structure's surface.
- A single model should be applicable to all types of vessels and offshore structures.

3.1. Use of the CFD model as an Engineering tool

An applicable CFD-model for numerical modelling of sea spray icing has to be based on the forecast metocean parameters such as wind speed, air temperature, and sea temperature; and include a ship or offshore model. The number of metocean parameters, numerical limitations and our understanding of included processes, to some extent limits the expected prediction accuracy. However, there is a potential for the development of a CFD-modelling tool that enables prediction of the distribution of sea spray icing on offshore ships and structures.

A CFD sea spray icing model applicable to offshore engineering must be capable of modelling:

- prevailing ice pattern/ development
- ship/sea interaction and sea spray generation
- relative distribution of ice accretion-, no ice- and deicing zones

4. Processes involved in Sea spray icing

The occurrence and development of sea spray icing depend on a complex correlation between environmental parameters and vessel characteristics. The environmental parameters are wind speed, air temperature, water temperature, freezing temperature of water and wave characteristics. Vessel characteristics include ship manoeuvring characteristics like speed, heading, and handling and ship design characteristics like size, shape, cold-soaking, freeboard, and topside equipment. Sea spray icing may occur if the air temperature is less than the freezing point of seawater. At normal ocean water salinity, considered to be 35 ‰, water freezes at −1,9 °C. For icing to occur, the spray needs to be deposited on the vessel surface and cooled below the freezing point. In general, there is sparse with well-documented measurements of sea spray icing on vessels, and the uncertainty regarding combined effects and factors involved is relatively high.

The complete process of sea spray icing may be divided into three sub-processes, as shown in Figure [4]. First, the interaction between structure and the waves leads to the breaking of the wave and formation of a cloud of small water droplets that move upwards in the planes of interaction. This stage is called spray generation. Next, the water droplets get carried with the wind, and as a result of the particle momentum and wind flow around the structure, some water droplets impinge on the structure. Cooling of the water droplets might take place in this stage. The final stage involves the thermodynamics of the freezing and icing process.

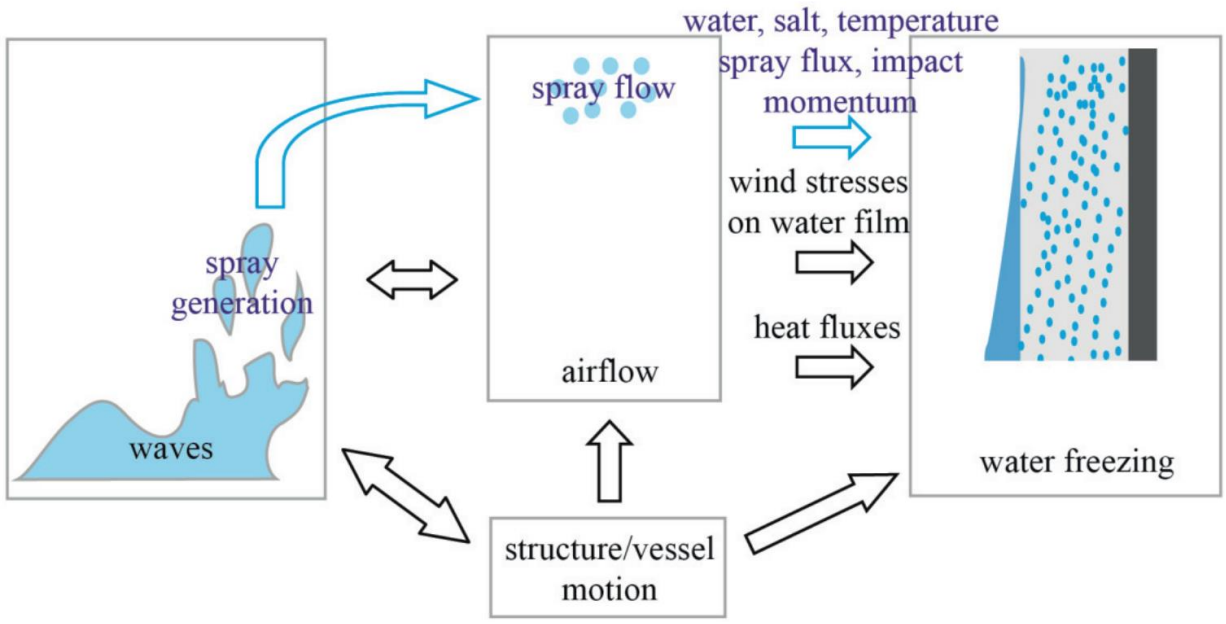

Figure 1: Processes involved in sea spray icing [4]

In the final stage, the water impinges on the structure's surface freezes and creates an ice film on the surface. Over time, this ice film grows in size on account of the continuous impingement of water droplets from consecutive spray events.

Another sub-process that is consequential to the overall icing process is the melting due to various reasons like wave washing. In this review, MARICE is the only model to consider the melting process [22].

Wave impact generated spray, or impact spray, is the most significant source of sea spray icing, whereas wind-generated spray does not contribute as much to the icing [4], [33]. Thus, most modern models ignore the effects of the wind-generated spray. An exception is the updated ICEMOD2 that includes the effects of wind-generated spray [20].

Further sections show how existing models deal with each of the sub-processes and the main findings from these models.

5. Spray generation

5.1. Process of spray generation

During the pitching motion of a vessel moving in waves, the bow of the ship slams into the water and jets a sheet of water into the air along the perimeter of the bow. The impact of the ship's bow with water forms a sheet of water that jets vertically upwards. The jet velocity and the angle of attack directly affect the height, width, and area of the water sheet and its breakup [34], [35]. Air entrainment further leads to the breakup of the water sheet into droplets [34], [36].

Figure 2: Spray generation and entrainment [36]

5.2. A complex process

The generation of spray is a complex process including numerous uncertain variables and cannot be reproduced by existing models [22]. The phenomenon of spray generation is not yet well understood [26]. All the existing models for sea spray icing use either direct measurement or empirical equations for the generation of sea spray. For example, investigation of the spray generation was beyond the scope of the study for the MARICE model [4].

5.3. Wind-generated spray

Besides the spray generated from ship-sea interaction, a small amount of spray is also generated due to wind interacting with waves. Wind speeds of over 4m/s cause wave breaking leading to wind-generated spray [37], [38]. Other researchers determined that wind-generated spray occurs at wind speeds over 9m/s [26], [39], [40]. Kulyakthin argues that the wind-generated spray does not have a significant contribution to icing and can be neglected in sea spray icing calculations [22].

5.4. Measurement of spray parameters

The spray generation is heavily dependent on the ship geometry and leads to the necessity of direct measurement of spray and icing for individual ship classes [41]. Full-scale measurements of characteristics of spray generation like spray event duration, Liquid water content (LWC) in the spray cloud, time-averaged and instantaneous spray flux, drop number concentration and droplet size distribution (DSD) were quantified for the first time on a vessel – the Coast Guard Cutter (CGC) Midgett by Ryerson in 1995 [41]. However, large variations were expected due to practical limitations in measurement techniques [41]. These measurements were not detailed enough to be used for validation of computational results [42].

Scaled laboratory measurements of water sheet breakup were carried out by researchers at the Memorial University of Newfoundland, Canada, to study the distribution of the spray upon impact on a vertical surface. However, techniques for extrapolation of results from scaled experiments about spray generation to full-scale values need to be developed further [35].

5.5. Size and distribution of droplets within the spray

Size of individual droplets affects their trajectory, flight time, in-air cooling, evaporation rate during the flight, the volume of the droplet, collection efficiency at the surface of the structure and eventually the ice formation. [43], [44]. The drop number concentration (drops per unit volume of spray) affects the rate of freezing [44]. Higher drop concentration results in slower cooling [43]. Rate of in-flight cooling of droplets by convection is higher for lower drop concentration in a spray cloud due to increased humidity [41], [45].

Researchers have experimented with CFD models using droplets of a single size represented by the mean volume diameter (MVD) and also with variable droplets sizes over a spectrum. Uncertainty of spray MVD at the input resulted in errors of several orders of magnitude in the spray inflow. Approximation of the DSD spectrum using constant droplet size equal to MVD resulted in up to 100% error in collection efficiency in some areas of the ship [32]. In recent studies, Kulyakthin considered the spray MVD to be varying from 250 to 2500 µm [32], whereas Dehghani considered the droplet size varying from 0.3mm to 7mm [46]. The distribution of droplet sizes in the spray cloud is such that the largest and the smallest droplets do not rise as high vertically as the medium-sized droplets do [46].

5.6. Liquid water content (LWC)

The LWC is a crucial spray characteristic [41] and can be considered a variable that is most dependent on the size and type of ship. It is the mass of water in a spray cloud per unit amount of dry air [47].

The LWC on a medium-sized fishing vessel was measured to be 4600g/m3 [48] and Ryerson measured the LWC on the CGC Midgett ranging from 1.1 to 1162.9 g/m3 for 39 spray events with a mean of 64.1 g/m3 [41]. The exact LWC per spray event is extremely difficult to predict.

5.7. Modelling of the generation of sea spray

The generation of spray is a complex process including numerous uncertain variables and cannot be reproduced by existing physical models [22]. Current CFD models do not simulate the spray generation process, but use the functions given by Zakrzewski given in [33] for the inputs for spray height and LWC and the empirical equations of Ryerson given in [41] for the droplet size distribution [24], [32]. The spray particles are initialized either at a plane perpendicular to the direction of the ship's motion, as in the MARICE model [32] or at the contour of the bulwark [24] as shown in Figure 3.

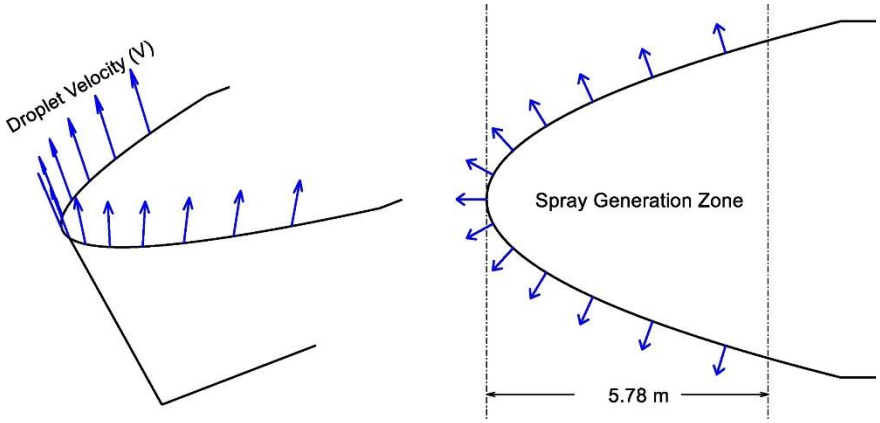

Figure 3: Droplet initial positions [24]

DNS (Direct Numerical Simulation) of ship-wave interaction is not currently viable, and individual processes need to be modelled separately. SPH (Smoothed Particle Hydrodynamics) can be used in addition to traditional CFD methods for accurate and cost-efficient modelling of spray generation. [35].

The spray generation function used in current CFD models for sea spray icing is based on measurements on a medium-sized fishing vessel [33], and thus, the results may vary if the model is used on vessels of other size or geometry.

5.8. Effect of sea ice

As seen in earlier sections, wave impact generated sea spray is the primary source of sea spray icing. In case of seas with an ice cover, there is just a small channel created by an icebreaker that ships sail through without much interaction with the surrounding solid ice. Since there is limited interaction of the vessel with waves, it can be noted that the spray generation is limited if there is an ice cover on the sea surface [11].

6. Spray flow

The second stage of the sea spray icing process involves the flow of the generated water droplets from the point of impact to the structure. It is complicated to separate the spray generation and the spray flow process [4].

The generated spray is entrained with the wind and is carried over to the ship's superstructure as a cloud [41].

Figure 4: Spray flow as a cloud [36]

Before proceeding to the freezing problem, it is essential to determine the number of droplets from the spray cloud that hit the surface of the structure. Modelling these fine droplets next to large geometries like a vessel is problematic [47].

6.1. Airflow and particle trajectories

Empirical relationships might not be suitable for complex structures and necessitate the use of CFD to model the spray flow [49]. In CFD models or other types of particle trajectory models, the vessel is divided into surfaces to calculate the droplet impingement on each subdivision [24], [32]. Standard CFD procedures calculate airflow around the structure by solving the Navier-Stokes equations. The MARICE model uses Reynolds Averaged Navier Stokes (RANS) simulations with RNG $k-\varepsilon$ turbulence model to calculate the airflow, and Lagrangian particle tracking is used to track the flow of the initialized water droplets. [22], [32]. Prediction of complex separated unsteady flows is better with Large Eddy Simulations (LES) compared to RANS, and thus, LES can be used for a more detailed study of the airflow, especially in the wake regions [50]. LES simulations need a much finer grid than RANS simulations and can lead to much

higher computational costs. Hybrid RANS/LES models have been suggested to improve accuracy by reducing computational costs [51].

On the other hand, some researchers believe that meshing a large domain like a vessel and working with minute spray particles simultaneously make CFD solutions of wave-impact spray unachievable [24]. Thus, another approach to estimate the droplet trajectories numerically without CFD was developed with a trajectory model like the one developed by Dehghani in [52]. The application of this trajectory model to predict trajectories of sea spray particles is demonstrated by Dehghani in [53] and [24].

6.2. The motion of the ship

The trajectories of the spray particles are highly dependent on the airflow around the structure. In case of ships, the instantaneous airflow around the structure changes with the motion of the ship in waves. Numerical estimates of sea spray icing must consider the effects of the motion of the structure [11]. However, both, Kulyakthin [32] and Dehghani [24] have considered the ship as a stationary object over the water surface for their spray flow analysis and droplet trajectory analysis respectively. Kulyakthin considered the yaw of the ship in one study, albeit as a stationary ship with a prescribed angle to the spray generation plane, but this does not affect the airflow around the ship with time [32].

6.3. Droplet size dependence

In numerical models, the droplet sizes are considered in two ways. Either all the droplets are assumed to be of the same size equal to the MVD of the spray, or a spectrum of droplet sizes (Droplet size distribution or DSD) can be specified. Both methods are used and compared in MARICE. The results show that the collection efficiency calculated on certain surfaces can be different in both methods [32].

CFD simulations with a single droplet size show that smaller droplets tend to produce a more uniform spray inflow than larger droplets. A wrong assumption of droplet diameter for simulations with a single droplet size can lead to errors in several orders of magnitude. Smaller droplets flow easily with the wind around the superstructure, whereas larger droplets tend to fall on the front portion of the ship [32].

6.4. Wind speed

The wind speed can directly affect the nature of airflow around and over the structure and thus affect the regions on the surface where the droplets might land. Varying wind speed can alter the flow of the droplets and eventually, the icing on the structure.

Stronger wind causes the spray to be lifted higher. Although sea spray icing is usually observed up to 15-20m above the surface of the sea, there have been reports of sea spray icing at 60m heights. [8].

CFD simulations agree and show that higher wind speeds lift droplets higher, and result in lower collection efficiency. Assumption of constant wind speed highly overestimates the spray inflow in the front of the structure. A stochastic approach with random fluctuations in velocity gives more accurate results for spray flow in the wake regions of the superstructure [32].

The wind speed directly affects the evaporative heat-transfer coefficient [23], which affects the in-flight cooling of the spray droplets.

6.5. Secondary droplet breakup and interaction

The larger droplets formed during the wave impact on the structure undergo a secondary break up into smaller droplets during the flight. Detailed analysis of the mechanisms of this secondary breakup was done by Lee in [54] and Dehghani in [34]. Kulyakthin argued that this secondary breakup processes could be neglected due to the small sizes of the spray droplets [4].

On the other hand, smaller droplets tend to fuse to form larger droplets by coalescence, and this can change the droplet size and dynamics. Modelling of droplet coalescence and interaction for marine icing problems cannot be carried out properly with the current knowledge of spray generation and turbulent properties of airflow. [4]. However, droplet interactions only weakly affect the LWC and can be neglected in calculations [49].

6.6. Droplet interactions

During the travel of the spray droplets from the point of formation to surface impact, the individual droplets might interact with other droplets in the spray.

Droplet interactions and coalescence can be modelled with the probabilistic theory of O'Rourke given in [55] [4].

A theoretical model to simulate the droplet motion was developed by Kollar in [56]. This model takes into account several processes that affect the droplet size and motion, like droplet collision, coalescence, and turbulent dispersion of the dispersed phase. Kulyakthin concluded that with the limited current knowledge about spray generation, droplet interaction and coalescence cannot be appropriately modelled, and thus, abandoned the modelling of spray coalescence [4].

6.7. Droplet impingement and Collection efficiency

Ice accretion on a structure's surface starts and continues as long as the water droplets in the spray impinge on the surface. It is thus essential to predict the number of droplets from the spray that hit the surface. Some droplets are carried away from the surface due to factors like wind and turbulence. The collection efficiency is defined as the spray inflow rate per unit area on the ship's surface to the spray inflow rate per unit area of the injection plane [32]. In simple terms, collection efficiency is the number of spray particles hitting the surface compared to the number of spray particles that are present as input in the model. Stallabrass gave empirical equations to estimate the collection efficiency on cylinders and rectangular surfaces [7]. Practically determining the collision efficiency is complex and challenging [47], [57]. Several theoretical models for calculating impingement of droplet surfaces are compared by Finstad [58]. For the calculation of collection efficiency, Finstad et.al. have suggested assuming the spray cloud have droplets of a constant diameter equal to the MVD [58]. The ice accretion calculations are hardly affected due to a certain degree of inaccuracy in the calculation of collection efficiency [20].

7. Freezing process

The final process in the sea spray icing phenomenon is the freezing process. The droplets that impinge on the freezing surface form a film of water that, over some time, freezes. During consequent spray events, the frozen layer increases in thickness due to the additional drops of water.

It is the combination of freezing air temperatures, cold seawater, and strong winds, that amount to significant icing. The general conditions for icing can be said to be air temperatures below the freezing point of the saline water for local salinity levels, seawater temperature below 8°C, and wind speeds of over 10m/s [8].

7.1. In-flight cooling

Spray droplets are supercooled below the freezing temperature without change of phase, and freezing occurs after the droplets hit the surface [4], [59]. Droplets under $40\mu m$ reach thermal equilibrium with the environment, and those over $300\mu m$ do not see a change in temperature from their initial state. The droplets in the range from 40-$300\mu m$ are small enough to reach thermal equilibrium, but whether they do so, depends on the flight time [40]. Stallabrass suggests that at temperatures below $-18℃$, spray droplets freeze in-flight and do not adhere to the surface [60].

The MARICE model neglects the in-flight cooling for simplicity and considers droplet temperatures to be equal to freezing temperature [22]. Recently, Dehghani-Sanij studied the cooling and freezing of saline spherical droplets intending to use the results in sea spray icing models [29]. They conclude that in-flight cooling and freezing of spray droplets does take place and have presented a semi-analytical technique using the Stefan-type condition [29]. How this technique is included in their 3D-trajectory analysis is yet to be seen.

7.2. Formation and growth of ice layer and the effects of salinity

After a spray event, when the droplets hit the surface, a liquid film is formed on the surface. This film of water freezes and forms a layer of ice. The ice layer grows in thickness over time. At each spray event, a new water film is formed over the surface of the existing ice, and this film moves due to gravity. Ice accretion occurs in the interface between liquid and pre-existing ice or a cold surface. The phase change from liquid to ice is driven by the heat balance when the temperature difference exceeds the freezing point of the liquid. The latent heat released during freezing dissipates through the colder medium by conduction [22].

Salinity is a significant factor in determining the growth rate of the ice on the freezing surface [61]. The freezing process is complex and gets more complicated due to the salinity of the seawater. Compared to fresh water spray, the icing rate due to saline water spray is always lower, and the ratio of icing rate due to fresh water spray to the icing rate due to saline water spray is a function of the air temperature and spray salinity [62]. The effect of spray salinity on the icing rate was presented by Makkonen, 1987 (Figure 5).

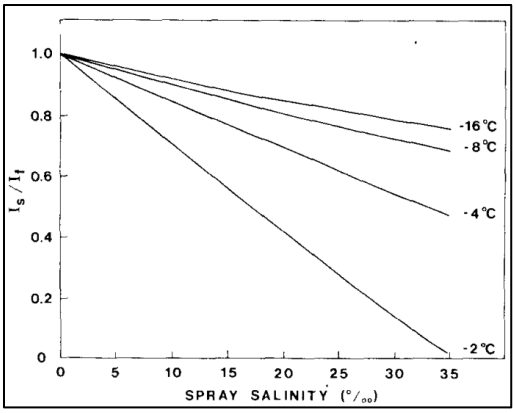

Figure 5: Ratio of icing rate of saline spray icing to icing rate of pure spray icing [62]

The freezing temperature of the saline water film depends on the salinity of the water film, which is not necessarily equal to the salinity of the incoming spray [63]. Salt rejection from ice results in higher salinity of the run-off water. This affects the salt balance of the water film on the icing surface. Higher salinity of the water film on the surface prevents it from freezing. The next spray event dilutes the brine film and causes further freezing. This cycle repeats itself for each incoming spray [61], [64]. The temperature of the brine layer decreases while the temperature of the ice increase during the freezing process. As ice accumulates, the temperature of the ice and size of the brine pockets decreases further from the seawater-ice interface. The rate of ice accretion is largest at the start of each freezing interval, at maximum thermal capacity [25].

Cooling of a liquid below its freezing temperature results in its solidification in the form of growing dendrites (tree-like microscopic structures). The solidified mass has liquid entrapped in these dendrites. This phenomenon leads to the formation of spongy ice. The ratio of the frozen volume to the total volume including the entrapped liquid is known as the solid fraction [65]. Further reduction in air temperature decreases the sponginess and the accredited ice can reach zero sponginess or 'dry' icing. Blackmore et. al., 2002 developed a model to predict the sponginess of accredited ice for freshwater. Though salinity is not a condition for spongy icing, this model can be easily extended to include the effects of salinity due to observations with sea spray icing [66]. The brine-spongy ice is assumed to be a homogenous two-phase medium, when the temperature differences are small, due to the fast freezing process [25]. The two phases consist of brine pockets and pure ice evenly distributed. Salt rejection during the freezing process occurs internally to the brine pockets, and externally to the brine layer. Kulyakthin argues that the salinity of the water film increases due to salt rejection, resulting in a change in the freezing temperature [4]. Dehghani on the other hand, argues that the rapid freezing causes complete solute trapping, making the salinity constant. The diffusion rate of solute in the brine layer is about 250 times slower than that of the heat into the brine layer [67].

An icing event begins when the atmospheric temperature decreases below the freezing point of the saline water in the presence of wind, and it stops if the temperature rises above the freezing point or in the absence of wind for over 12 hours[21]. The thermodynamics and the growth of this ice layer are analysed by several researchers [14], [20]–[23], [25], [62], [68], [69].

7.3. Heat and Mass balance

Theoretical models have been developed to estimate the thickness of the ice formed. The spray water hitting the surface freezes, evaporates, or runs off, as shown in Figure 6: Schematic of the sea spray ice accretion process and heat balance Figure 6.

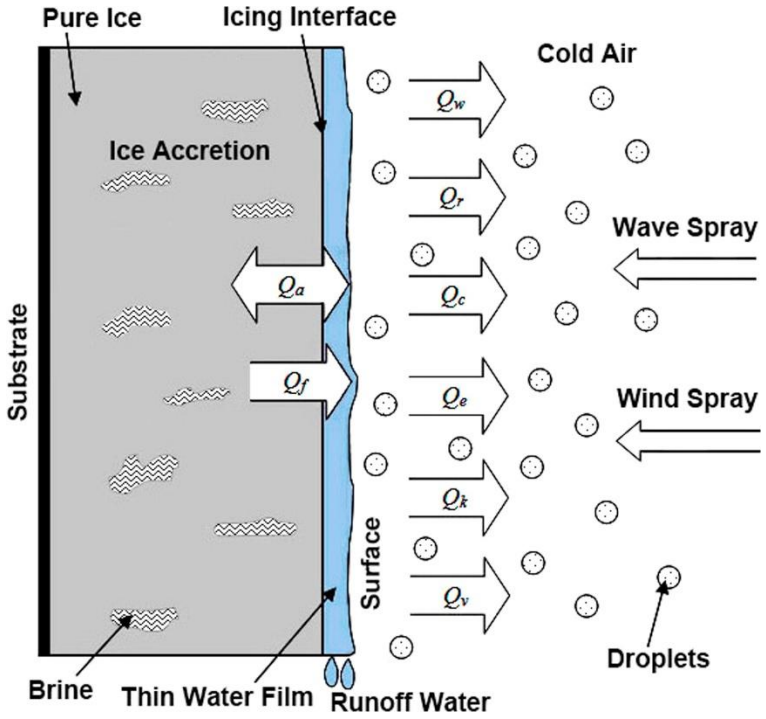

Figure 6: Schematic of the sea spray ice accretion process and heat balance [28]

Mass balance equations are used to compute the thickness of the ice layer and the thickness of the water film [28]. A model to predict the rate of icing is suggested by [28] where empirical relations were used for determining the freezing and run-off fractions of the mass flux, whereas the mass fraction for evaporation was assumed to be negligible. The rate of icing is also predicted with the help of heat balance equations from the thermodynamic process, as shown in Figure 6 [28].

Freezing of the spray particles at the surface involves four main heat fluxes – convection, evaporation, heat capacity of the incoming spray and radiant heat flux [20], [22]. The empirical equation for the sponginess of the accreted ice is given in the RIGICE04 model suggests that the sponginess decreases linearly between $-25℃$ $-5℃$ and the ice is solid at the freezing temperature [21]. As the brine-spongy ice has a varying temperature and thereby composition, the thermal conductivity varies along with the thickness of the ice layer [25].

7.4. Effects of wind and atmospheric temperature on freezing

Icing occurs when the atmospheric temperature is below the freezing temperature of the saline seawater. Severe sea spray icing usually begins at wind speeds of 8m/s to 10m/s [8].

Spray droplets can be supercooled below the freezing point; however, they do not freeze before hitting the structure [59].

According to Jones, small droplets in moderate to high wind speeds cause small ice accumulations, whereas large droplets at higher wind speeds cause high icing rates [70].

A simulation with constant MVD and varying wind speeds showed that higher wind speed does not necessarily lead to more icing [32].

Wind influences the water film, and further studies should investigate and include the effects of wind shear on the ice/water film. MARICE neglects the wind shear stress [22].

The heat transfer coefficient is independent of the temperature but varies due to the wind speed and geometry of the structure [71]. The energy balance equation is used in this case for obtaining the distribution of heat transfer coefficients on the surface of the structure [22].

7.5. Water film motion

When spray water hits a surface, a film of water is formed over the surface before it starts freezing as shown in Figure 6. The film moves due to gravity and other forces like wind acting on the water film. This movement of the water film can be modelled for estimating the spatial distribution of the liquid water, and in turn, the ice on the surface [4]. MARICE, RIGICE04, and ICEMOD use different water film models but give similar results indicating that the choice of water film models is not essential [22]. In addition, the steady model of Makkonen [62] that does not include water film motion predicts a similar ice accretion rate to MARICE. Thus, this steady model can be used to avoid computationally expensive numerical methods for resolving the water film dynamics [22].

7.6. Wave washing

Besides the sea spray, there might be a large continuous mass of water that splashes directly over the deck and other surfaces of a ship. Despite near-freezing temperatures, the latent heat of the splashing mass of water can be sufficient to avoid freezing if this water flows off the surface quickly. Also, wave washing causes melting and flushing off of ice that has already formed on the surface [8].

Regions on the structure where sea waves impact directly are less prone to icing due to direct washing away of the formed ice [4].

8. Comparison of sea spray icing models

Current sea spray icing models use widely differing approaches to predict the icing rates or in addition the distribution of icing on the vessel surface. In addition, each model uses a different test approach for verification purposes. The different test objects used in the model, and the fact that testing carried out in different metocean conditions would give different results, makes it difficult to give a direct comparison of results from all the models. It is however essential for the readers to know what each model uses as a basis for the modelling of the various sub-processes, and the nature of the results that could be obtained from various models. Such a comparison of four recent sea spray icing models is provided in Table 4.

Table 4: Comparison of modelling procedures of sea spray icing models

Sr. nr.	Modelling	ICEMOD2 [20]	RIGICE04 [21]	MARICE [22]	MINCOG [23]
1	**Author/s**	Horjen, 2013	Forest et.al., 2005	Kulyakhtin and Tsarau, 2014	Samuelsen et.al. 2016
2	**Concept**	Numerical model - 2D	Numerical model	3D CFD model for spray flow + numerical freezing module	Numerical model
3	**Sea spray generation**	Formulation from data from Jørgensen, 1985 [72] and Hjoren, 1986 [73] (ICEMOD)	Formulation from data from Tarsuit island experiment [74]	Equations of Horjen and Vefsnmo, 1985 [39] (ICEMOD)	Formulation from data from Borisenkov, 1975 [75] and Horjen, 1986 [73]
4	**Spray flow due to wind**	Not considered	Not considered	CFD	Not considered
5	**Water film dynamics**	Yes	Not considered	Yes	Not considered
6	**Ice distribution on the surface in addition to the icing rate**	On a cylindrical object	No distribution model	Over stationary vessels	No distribution model
7	**Motion of vessel**	No	No	No	No
8	**Verification of model against full-scale measurements**	Against field measurements on cylinders mounted on a vessel	Against field measurements on a semi-submersible	Against field measurements on a semi-submersible	Against field measurements on a rectangular plate mounted on a vessel

RIGICE and MINCOG give only the icing rates, but do not model the distribution of ice on the structure. ICEMOD2 and MARICE give the distribution of icing on the structure in addition to the icing rates. ICEMOD2 provides the horizontal and vertical distribution of icing on a cylinder. It is, however, unsure if this distribution model is applicable to any arbitrary surface. MARICE on the other hand, can provide the distribution of icing over any arbitrary surface in 3D. It can be noted that none of the models model the motion of the vessel. Considering the structure or a vessel as a stationary object, like in MARICE, can be applicable for large vessels and structures, like oil rigs, where the motion of the structure in waves is low. For smaller vessels however, the motion of the vessel in waves is significantly high and has to be considered for accurate results of the spray flow and icing distribution model. In addition, none of the models actually model the spray generation process when the waves hit the surface, but use formulations based on empirical data.

Kulyakthin, 2014 presents a graphical comparison of total ice load on a 90 meter diameter cylinder calculated with MARICE, ICEMOD [76], and RIGICE04 in [22].

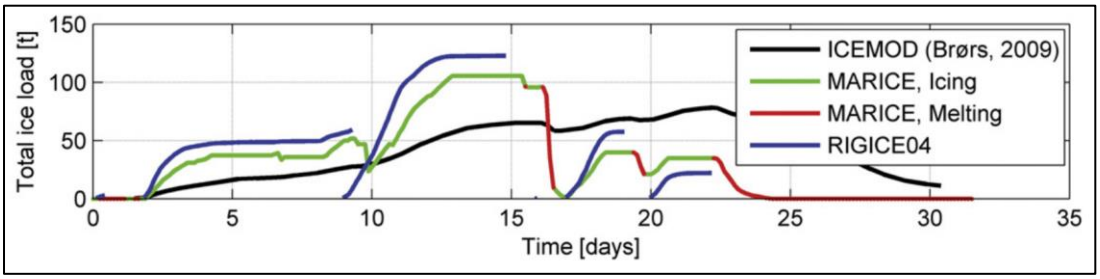

Figure 7: Comparison of total ice load on a 90m diameter cylinder calculated with various models [22]

Introducing CFD, MARICE is the probably the first, and currently, the only model attempting to give the distribution of icing in addition to the icing rate on an arbitrary surface. MARICE uses CFD for the distribution along with a freezing module as a user defined function [22]. Freezing of spray particles and the build-up of ice layer using CFD is also demonstrated by Anandharamakrishnan et. al., 2009 [77]. Numerical modelling using CFD seems to be promising for predicting the distribution of icing on vessels and marine structures.

9. Anti-icing and deicing techniques

Estimating the amount of accreted ice by prediction models can contribute to anti-icing measures on vessels and offshore structures. However, no measure prevent the risk of icing entirely. This section gives an overview of the commonly used anti-icing and deicing techniques.

Anti-icing methods are applied to prevent the creation of ice, while deicing describes the process of removing ice, as explained in [10]. Approaches for anti- and deicing are roughly divided into the categories; thermal, mechanical, chemical, design and other methods as shown in Figure 8. Several measures fall into multiple categories, i.e. sea spray can both result in mechanical removal of pre-existing ice and reduce ice by its thermal heating capacity.

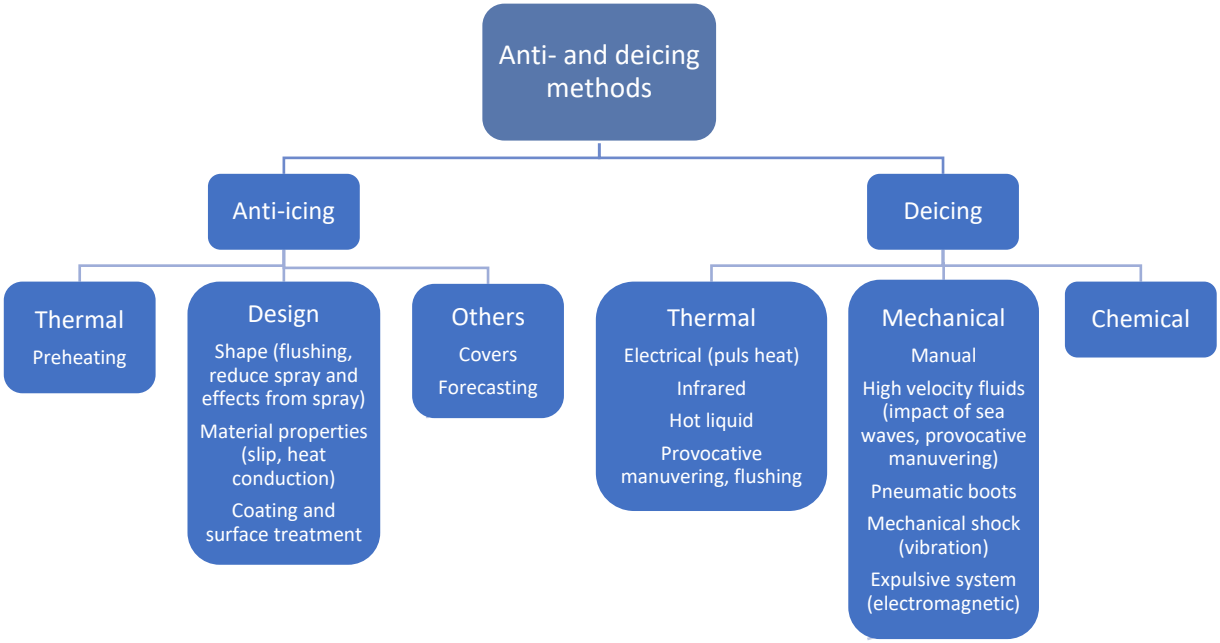

Figure 8: Anti-icing and deicing methods

9.1. Chemical methods

Chemical methods for deicing are widely used for roads, runways and in aviation. Commonly used deicing chemicals are sodium chloride, calcium chloride, magnesium chloride, potassium chloride, calcium magnesium acetate, and urea [78]. The key drawbacks of these methods are environmental issues and corrosion. Besides, chemical residues can be a safety hazard causing slippery decks, and be a potential health risk to personnel handling chemicals.

9.2. Thermal methods

Thermal methods for anti- and deicing are commonly used for ice-free entrances and walkways. Heating can be applied through mediums like electrical wires, heated pipes, hot water, moist heated air or hot air. Preheating when the risk of icing is small or over a large area can be expensive and wasteful. Intermittent heating or pulse heating is more efficient compared to constant heat (Ryerson, 2011) Heat loss to the substrate is reduced by positioning the system closer to or on the surface. In some situations, it could be sufficient to heat a thin layer between ice and substrate, resulting in ice removal by gravity or facilitating manual removal.

High-volume, low-pressure systems is another method for ice removal. If the method is combined with heat, it is even more efficient. Utilizing the external fire sprinkler system for deicing is an example of this method. Similarly wave-washing, naturally occurring or increased by provocative manoeuvring, are examples of high-volume with seawater temperature. Hot water can be an effective deicing tool, but one major concern is the risk of refreezing when the process is completed.

Infrared emitters can transfer heat to be absorbed by the ice or substrate as a deicing or anti-icing measure. Challenges include the dependence of an absorbent substrate, potential overheating of materials, and the rare possibility of the emitter acting as an ignition source [6].

9.3. Mechanical methods

Mechanical methods for deicing include methods like manual deicing, high-velocity fluids, piezoelectric actuators, expulsive systems, pneumatic boots and waves slamming against a structure. Accreted ice is forcefully separated from the substrate.

Manual deicing methods include using handheld tools to remove ice, such as mallets, crowbars, ice scrapes, and shovels. Historically, manual deicing was the standard solution to ice accumulation, and it remains a frequently used method (Ryerson, 2011). (Guest, 2005) emphasises the use of wooden tools for manual removal as these are less damaging to the ship and equipment. Manual labour requires human resources and is prone to accidents and injuries on personnel, equipment and surfaces. Besides, it is time-consuming and can only be utilized in areas accessible to the crew. Nevertheless, manual deicing can serve as an essential backup or supplementary to other measures (Ryerson, 2011).

High-velocity fluids can remove substantial amounts of ice mechanically. The method is useful, but requires high pressure and can be rough on the substrate. Paint, coatings, and insufficiently fastened elements can be unattached or worn off. High-velocity fluids can, for instance, be a combination of air and water, or either exclusively. If the liquid used is water, the run-off system needs to be effective. Steam lances were commonly used in the past because of the ready availability of steam from engine boilers [78]. Provocative vessel manoeuvring can increase the amount of crashing waves and thereby remove ice.

Another mechanical deicing method is using piezoelectric actuators. By distorting or accelerating the substrate, i.e. with vibrations, the increased stress breaks the bond between the ice and the substrate [78]. This technology is primarily developed for aviation and is advantageous over small areas (Ryerson, 2011).

Similarly, expulsive systems deice by accelerating the substrate to supersede the adhesion strength between ice and substrate. This method releases the ice and allows wind or gravity to disperse of it. The acceleration can be achieved by placing electromagnetic coils under a flexible metal skin or glueing a thin, flexible sandwich of conductors and dielectric materials to the protected surface [6]. According to Ryerson, the expulsive systems are energy efficient compared to traditional thermal systems and have the capacity to remove large masses of ice. Disadvantages are the risk of damaging personnel or equipment when the ice is accelerated from the surface. Care should also be taken to plan further removal if the ice is not instantaneously thrown from the ship [6].

Pneumatic boots are commonly known from aviation, where the leading edge of wings can be deiced by inflating the flexible surface [6]. This technology could be explored for areas on ships, such as handrails.

9.4. Design and other methods

Special designed coating may be used to reduce the adhesion strength between the ice and substrate. No known material completely prevents ice accumulation, but some coatings are believed to provide reduced

adhesion [79]. Super-hydrophobic surfaces are often used for coating. As a passive anti-icing method, it does not involve daily labour, an activating procedure, or fuel/electricity. The coating can increase the efficiency of other methods (Guest, 2005), such as heating and physical removal. The coated surface can be slippery and thereby prove a safety hazard (Guest, 2005). Limitations to the coating method are, i.e. that coatings have a restricted life expectancy and therefore require regular maintenance. The performance also decreases with time (Ryerson, 2011). The substrate is crucial to the coating finish, and consequently, the coating can provide significantly different results based on the underlying material. Due to incomplete guidelines on how to test the adhesion strength, it is difficult to gauge the coating performance [6].

Soft and hard shell enclosures or covers are possible anti-icing methods. Life-saving equipment can be protected, but the added barrier this causes for accessibility needs to be addressed compared to the risk of icing. Covers also include shielding important areas like walkways and stairs. Sheltering working areas has additional benefits of improved working environment by reducing the wind and exposure. Covers often need to be manually deiced (Ryerson, 2011).

Structural design is perhaps the most effective tool for reducing icing hazards [6]. Initially, the priority should be to minimize the spray caused by wave-structure interaction by altering the shape. If the freeboard height is above the spray cloud, this will significantly reduce icing, but this is not always an option. Limiting the areas where seawater can adhere and freeze is also crucial. Convex surfaces, small objects, and riggings are elements prone to icing. It is, for instance, possible to reduce the surface area exposed to icing of several cables by wrapping these together in a flexible cover. Efficient draining from surfaces leaves less water to freeze. This also applies to, i.e. sprinkler systems, which should be designed for drainage after use and without areas where the water can linger.

One example of utilising design as an anti-icing measure is the Ulstein Group's invention; the X-bow. The inverted bow, according to the company, results in reduced bow impact and slamming, which consequently reduces spray [80].

Manoeuvring decisions can reduce icing. Guest and Lucke recommend steaming downwind to minimise sea spray. Also, a position downwind from a landmass is preferable, as the waves close to shore are relatively small despite high wind speed [81].

10. Application of anti-/deicing methods

It should be emphasized that anti- and deicing measures may be inadequate in the face of severe icing conditions. Ultimately, the best anti-icing strategy is to avoid high-risk situations. A new marine icing forecast model was developed by Samuelsen to predict icing rates [5]. The prediction model is today implemented in Norwegian weather forecasting.

Ideally, several methods for deicing and anti-icing may be combined, utilizing the benefits of each technique. Prioritising functions on the vessel/structure help decide their importance, and thereby where to focus the anti- and deicing efforts. Ryerson, 2011 presented a table of functional areas versus potential ice protection technology solution for a platform 11 [6]. Table 5 presents suggested anti-and deicing

methods for key areas on a ship. Favourable design is an all-encompassing method and is therefore not included in the table.

Similarly, manual removal of ice is discouraged due to safety concerns and not included. Outdoor work priority zones are areas with regular traffic during normal operation. Escape routes and emergency equipment, communication and windows for navigation have been singled out because they are considered a high priority.

Table 5: Suggested anti- and deicing methods for areas/functions on a ship.

	Deck/ topside	**Work Priority zones**	**Deck Equipment**	**Escape routes and emergency equipment**	**Communication equipment**	**Vents, hatches, in/outlets**	**Windows (for navigation)**
Electrical heating	0	X	0	X	X	0	X
Heated liquid	X	X	X	X		X	X
Coating	0	0			0	0	0
Covers		X	X	0	0	0	
High-velocity fluid	X	X	0	X		0	X
Chemicals	0	0		0		0	0
Expulsive system	0					0	
X indicates a stronger match than 0, and no symbol indicates no match.							

The table does not consider cost or compare the alternatives. Recommended systems need to be evaluated and customized to individual vessels. Anti-icing and deicing measures can increase the design and construction cost but are likely to improve the working conditions and reduce the operational expenses and risk in cold climate.

11. Summary

Meteorological sea spray icing forecast models and empirical models based on analysis of vessel icing events provide icing rate estimates and to some extent vertical ice distribution, from metocean parameters. This is useful for operational purposes and for estimating the impact from marine icing. However, for design purposes, we need verified models to predict the generation of sea spray and distribution of ice on vessels and offshore structures.

The main objective for numerical modelling of sea spray icing on marine vessels and offshore structures is to estimate icing/melting rates and to model the distribution of ice on the structure. This depends on reliable metocean data for the given operational waters and numerical modelling of sea spray, icing and melting based on dynamic ship-sea-wind interactions. State of art numerical models for sea spray icing, like MARICE model vessels/ rigs as stationary objects. It is thus more applicable to icing on larger ships and rigs, than for small and medium sized vessels with more movements and comprehensive ship-sea interactions. Spray generation is at most, based on empirical data and effects from vessel movements and shipped water is not included.

In this review MARICE is the only model using CFD for modelling of the distribution of spray particles around the vessel caused by relative wind. The strongpoints of current sea spray icing models are the modelling and understanding of spray flow and the freezing process, i.e. effects that are close to an atmospheric concept. There is also a positive development in marine ice warning forecast models, which in general will contribute to improve ice prediction. However, the way sea spray generates and enters the railing on a ship is of crucial importance for further improvement of sea spray icing models. The biggest limitations are probably the lack of modelling of the ship-sea-wind interactions with spray generation and impact of shipped water on freezing and melting. This requires rather complex CFD modelling of ship-dynamics in wind and waves. It would be interesting to study the results of the MARICE model when the appropriate motion of the ship is taken into consideration. In addition, the heat exchange and temperature distribution along the ship should be included. The development of improved and verified CFD models for simulation of sea spray icing will depend on additional full-scale and laboratory testing.

On marine vessels and offshore structures intended for operations in arctic climate, outdoor operations such as ice and snow removal by hand must be identified and reduced to a minimum. For practical, safety, environmental and economic reasons anti-icing through most possible beneficial design should be preferred before de-icing. Further, utilizing the latent heat content of seawater through sprinkling or enable shipped water to flush along the sides of the vessel may represent a potential for improved de-icing and anti-icing methods.

Some potentials for further development of sea spray icing prediction models can be summarised as follows:

Development of models for sea spray icing including icing distribution for ship/structural design purpose.

Ice distribution cannot be determined by generalized theoretical models. It is thus essential that numerical models using CFD are used for determining the distribution and impact of sea spray on the structure as in the MARICE model.

Modelling concepts for dynamic ship-sea-wind interaction are currently not available and must be further studied.

Models for spray generation have to be improved and ideally, a model for dynamic spray generation based on ship design and ship-sea-wind interaction has to be developed. This may be modelled by using CFD.

Models should be capable of predicting sea spray icing on general basis, for a large variety of vessels and marine structures.

Improve freezing-melting dynamics and include effects from shipped water.

Collect more experimental data from full-scale measurements and laboratory setup.

Verification of the prediction models against full-scale data is limited, further verification is needed.

Finally, any model may not be more accurate or precise than the weakest link in the modelling chain. However, there is a potential for developing a CFD model that simulates main trends in the distribution of sea spray icing.

12. References

[1] AMAP, *Arctic Oil and Gas 2007. Arctic Monitoring and Assessment Programme (AMAP).*, xiii. Oslo, Norway, 2007.

[2] The Barents Observer, "Norway considers size limitation on passenger ships sailing at Svalbard," Dec. 17, 2019.

[3] N. Melia, K. Haines, and E. Hawkins, "Sea ice decline and 21st century trans-Arctic shipping routes," *Geophys. Res. Lett.*, vol. 43, no. 18, pp. 9720–9728, Sep. 2016, doi: 10.1002/2016GL069315.

[4] A. Kulyakhtin, "Numerical Modelling and Experiments on Sea Spray Icing," Doctoral thesis. Department of Civil and Transport Engineering. Norwegian University of Science and Technology (NTNU), Norway, 2014.

[5] E. M. Samuelsen, "Prediction of ship icing in Arctic waters Observations and modelling for application in operational weather forecasting," UiT, The Arctic University of Norway (Doctoral thesis), 2017.

[6] C. C. Ryerson, "Ice protection of offshore platforms," *Cold Reg. Sci. Technol.*, vol. 65, no. 1, pp. 97–110, Jan. 2011, doi: 10.1016/j.coldregions.2010.02.006.

[7] Stallabrass, "Trawler Icing - a Compilation of Work Done At N. R. C.," *Mech. Eng. Rep. MD-56, N.R.C. No. 19372 (National Res. Counc. Ottawa Canada)*, 1980.

[8] *ISO 19906:*, 2nd ed. Petroleum and natural gas industries – Arctic offshore structures, 2019.

[9] M. Mahmood and A. Revenga, "DESIGN ASPECTS OF WINTERIZED AND ARCTIC LNG CARRIERS – A CLASSIFICATION PERSPECTIVE," in Proceedings of OMAE2006, 25th International Conference on Offshore Mechanics and Arctic Engineering, June 4-9, 2006, Hamburg, Germany, 2006, pp. 1–8.

[10] DNVGL-OS-A201, "OFFSHORE STANDARD DNV GL AS Winterization for cold climate operations (Edition July 2015)," 2015. [Online]. Available: https://rules.dnvgl.com/docs/pdf/dnvgl/OS/2015-07/DNVGL-OS-A201.pdf.

[11] ISO 35106: Petroleum and natural gas industries — Arctic operations — Metocean, ice, and seabed data. 2017.

[12] M. Polakis, P. Zachariadis, and J. O. de Kat, “The Energy Efficiency Design Index (EEDI),” in *Sustainable Shipping*, Cham: Springer International Publishing, 2019, pp. 93–135.

[13] Y. hang Hou, K. Kang, and X. Liang, “Vessel speed optimization for minimum EEOI in ice zone considering uncertainty,” *Ocean Eng.*, vol. 188, p. 106240, Sep. 2019, doi: 10.1016/j.oceaneng.2019.106240.

[14] E. P. Lozowski, K. Szilder, and L. Makkonen, “Computer simulation of marine ice accretion,” *Philos. Trans. R. Soc. London. Ser. A Math. Phys. Eng. Sci.*, vol. 358, no. 1776, pp. 2811–2845, Nov. 2000, doi: 10.1098/rsta.2000.0687.

[15] J. Ashcroft, “Potential ice and snow accretion on North Sea rigs and platforms,” *Mar. Note no. 1, Br. Meteorol. Off. Brac.*, 1985.

[16] Romagnoli, “Ice growth modelling for icing control purposes of offshore marine units employed by the petroleum industry,” 1988.

[17] J. E. Overland, “Prediction of Vessel Icing for Near-Freezing Sea Temperatures,” *Weather Forecast.*, vol. 5, no. 1, pp. 62–77, Mar. 1990, doi: 10.1175/1520-0434(1990)005<0062:POVIFN>2.0.CO;2.

[18] P. Roebber and P. Mitten, *Modelling and measurement of icing in Canadian waters*. Report (Canadian Climate Centre), no. 87-15., 1987.

[19] Horjen and Vefsnmo, “A numerical sea spray icing model including the effect of a moving water film.,” 1985.

[20] I. Horjen, “Numerical modeling of two-dimensional sea spray icing on vessel-mounted cylinders,” *Cold Reg. Sci. Technol.*, vol. 93, pp. 20–35, Sep. 2013, doi: 10.1016/j.coldregions.2013.05.003.

[21] T. W. Forest, E. P. Lozowski, and R. Gagnon, “Estimating marine icing on offshore structures using RIGICE04,” in *Proceedings of the International Workshop on Atmospheric Icing on Structures (IWAIS), Montreal, Canada.*, 2005, no. June.

[22] A. Kulyakhtin and A. Tsarau, “A time-dependent model of marine icing with application of computational fluid dynamics,” *Cold Reg. Sci. Technol.*, vol. 104–105, pp. 33–44, Aug. 2014, doi: 10.1016/j.coldregions.2014.05.001.

[23] E. M. Samuelsen, K. Edvardsen, and R. G. Graversen, “Modelled and observed sea-spray icing in Arctic-Norwegian waters,” *Cold Reg. Sci. Technol.*, vol. 134, pp. 54–81, Feb. 2017, doi: 10.1016/j.coldregions.2016.11.002.

[24] S. Dehghani, G. Naterer, and Y. S. Muzychka, “3-D trajectory analysis of wave-impact sea spray over a marine vessel,” *Cold Reg. Sci. Technol.*, vol. 146, no. November 2017, pp. 72–80, Feb. 2018, doi: 10.1016/j.coldregions.2017.11.016.

[25] S. R. Dehghani, Y. S. Muzychka, and G. F. Naterer, “Numerical Solution of Rapid Freezing of Sea Water on Cold Substrates,” in *Volume 8: Polar and Arctic Sciences and Technology; Petroleum Technology*, Jun. 2017, pp. 1–8, doi: 10.1115/OMAE2017-62191.

[26] S. Mintu, D. Molyneux, and D. Oldford, “State-of-the-Art Review of Research on Ice Accretion Measurements and Modelling,” in *Arctic Technology Conference*, Oct. 2016, no. March 2017, doi: 10.4043/27422-MS.

[27] L. Makkonen, R. D. Brown, and P. T. Mitten, “Comments on ‘Prediction of Vessel Icing for Near-Freezing Sea Temperatures,’” *Weather Forecast.*, vol. 6, no. 4, pp. 565–567, Dec. 1991, doi: 10.1175/1520-0434(1991)006<0565:COOVIF>2.0.CO;2.

[28] A. Dehghani-sanij, Y. S. Muzychka, and G. F. Naterer, “Analysis of Ice Accretion on Vertical Surfaces of Marine Vessels and Structures in Arctic Conditions,” in *Volume 7: Ocean Engineering*, May 2015, pp. 1–7, doi: 10.1115/OMAE2015-41306.

[29] A. R. Dehghani-Sanij, S. MacLachlan, G. F. Naterer, Y. S. Muzychka, R. D. Haynes, and V. Enjilela, “Multistage cooling and freezing of a saline spherical water droplet,” *Int. J. Therm. Sci.*, vol. 147, p. 106095, Jan. 2020, doi: 10.1016/j.ijthermalsci.2019.106095.

[30] Polar Code, “International Code for ships operating in Polar waters,” *IMO Int. Marit. Organ.*, 2017, [Online]. Available: http://www.imo.org/en/mediacentre/hottopics/polar/pages/default.aspx.

[31] DNV, “RULES FOR CLASSIFICATION Ships Part 6 Additional class notations Chapter 6 Cold climate,” no. July, 2015.

[32] A. Kulyakhtin, O. Shipilova, B. Libby, and S. Løset, “Full-scale 3D CFD Simulation of Spray Impingement on a Vessel Produced by Ship-wave Interaction,” *Proc. 21st IAHR Intl. Symp. Ice*, pp. 1129–1141, 2012.

[33] W. P. Zakrzewski, “Icing of Fishing Vessels. Part I: Splashing a Ship With Spray.,” 1986.

[34] Dehghani, Muzychka, and Naterer, “Water breakup phenomena in wave-impact sea spray on a vessel,” *Ocean Eng.*, vol. 134, pp. 50–61, Apr. 2017, doi: 10.1016/j.oceaneng.2017.02.013.

[35] D. Saha, S. R. Dehghani, K. Pope, and Y. Muzychka, “The Extent of Water Sheet Breakup on a Vertical Surface,” Oct. 2016, doi: 10.4043/27404-MS.

[36] Ryerson, “Icing Management for Coast Guard Assets,” U.S. Army Engineer Research and Development Center, Hanover, New Hampshire, USA, 2013.

[37] E. Fuentes, H. Coe, D. Green, G. de Leeuw, and G. McFiggans, “Laboratory-generated primary marine aerosol via bubble-bursting and atomization,” *Atmos. Meas. Tech.*, vol. 3, no. 1, pp. 141–162, Feb. 2010, doi: 10.5194/amt-3-141-2010.

[38] R. Lewis and E. Schwartz, *Sea Salt Aerosol Production: Mechanisms, Methods, Measurements and Models—A Critical Review*, vol. 152. Washington, D. C.: American Geophysical Union, 2004.

[39] I. Horjen and S. Vefsnmo, “A Kinematic and Thermodynamic Analysis of Sea Spray (in Norwegian), Offshore Icing—Phase II. Norwegian Hydrodynamic Laboratory (NHI). Report STF60 F85014,” 1985.

[40] E. L. Andreas, “Time constants for the evolution of sea spray droplets,” *Tellus, Ser. B*, vol. 42 B, no. 5, pp. 481–497, Nov. 1990, doi: 10.3402/tellusb.v42i5.15241.

[41] C. C. Ryerson, “Superstructure spray and ice accretion on a large U.S. Coast Guard cutter,” *Atmos. Res.*, vol. 36, no. 3–4, pp. 321–337, May 1995, doi: 10.1016/0169-8095(94)00045-F.

[42] A. Bodaghkhani, S.-R. Dehghani, Y. S. Muzychka, and B. Colbourne, “Understanding spray cloud formation by wave impact on marine objects,” *Cold Reg. Sci. Technol.*, vol. 129, pp. 114–136, Sep. 2016, doi: 10.1016/j.coldregions.2016.06.008.

[43] T. S. Jørgensen, “Influence of ice accretion on activity in the northern part of the Norwegian Continental Shelf.,” Report No. STF88F82016, Offshore Testing and Research Group, Trondheim, Norway (1982), 1982.

[44] J. Stallabrass, “ICING OF FISHING VESSELS IN CANADIAN WATERS.,” DME/NAE Quarterly Bull., 1975 (1) (1975) Ottawa, Canada, 1975.

[45] G. S. H. Lock, *The growth and decay of ice.* Cambridge University Press, 1990.

[46] S. R. Dehghani, G. F. Naterer, and Y. S. Muzychka, “Droplet size and velocity distributions of wave-impact sea spray over a marine vessel,” *Cold Reg. Sci. Technol.*, vol. 132, pp. 60–67, Dec. 2016, doi: 10.1016/j.coldregions.2016.09.013.

[47] A. R. Dehghani-Sanij, S. R. Dehghani, G. F. Naterer, and Y. S. Muzychka, “Sea spray icing phenomena on marine vessels and offshore structures: Review and formulation,” *Ocean Eng.*, vol. 132, pp. 25–39, Mar. 2017, doi: 10.1016/j.oceaneng.2017.01.016.

[48] Y. Borisenkov and V. Panov, “Basic results and prospects of research on hydrometeorological conditions of sihpboard icing,” *Issled. Fiz. Prin Obledeneniya Sudov. Leningr. (1972), CRREL Draft Transl. TL411, 1974*, 1972.

[49] A. Kulyakhtin, L. E. Kollar, S. Løset, and M. Farzaneh, “Numerical Simulations of 3D Spray Flow in a Wind Tunnel with Application of O’Rourke’s Interaction Algorithm and Its Validation,” 2012.

[50] M. Breuer, N. Jovičić, and K. Mazaev, “Comparison of DES, RANS and LES for the separated flow around a flat plate at high incidence,” *Int. J. Numer. Methods Fluids*, vol. 41, no. 4, pp. 357–388, Feb. 2003, doi: 10.1002/fld.445.

[51] J. Fröhlich and D. von Terzi, “Hybrid LES/RANS methods for the simulation of turbulent flows,” *Prog. Aerosp. Sci.*, vol. 44, no. 5, pp. 349–377, Jul. 2008, doi: 10.1016/j.paerosci.2008.05.001.

[52] S. R. Dehghani, M. H. Saidi, A. A. Mozafari, and A. Ghafourian, “Particle Trajectory in a Bidirectional Vortex Flow,” *Part. Sci. Technol.*, vol. 27, no. 1, pp. 16–34, Jan. 2009, doi: 10.1080/02726350802611366.

[53] S. R. Dehghani, Y. S. Muzychka, and G. F. Naterer, “Droplet trajectories of wave-impact sea spray on a marine vessel,” *Cold Reg. Sci. Technol.*, vol. 127, pp. 1–9, Jul. 2016, doi: 10.1016/j.coldregions.2016.03.010.

[54] C. H. Lee and R. D. Reitz, “An experimental study of the effect of gas density on the distortion and breakup mechanism of drops in high speed gas stream,” *Int. J. Multiph. Flow*, vol. 26, no. 2, pp. 229–244, Feb. 2000, doi: 10.1016/S0301-9322(99)00020-8.

[55] P. S. O’Rourke, “Collective drop effects on vaporizing liquid sprays.,” United States, 1981. Accessed: Aug. 11, 2020. [Online]. Available: https://www.osti.gov/biblio/5201366.

[56] L. E. Kollár and M. Farzaneh, “Modeling the evolution of droplet size distribution in two-phase flows,” *Int. J. Multiph. Flow*, vol. 33, no. 11, pp. 1255–1270, Nov. 2007, doi: 10.1016/j.ijmultiphaseflow.2007.04.002.

[57] Makkonen, “Models for the growth of rime, glaze, icicles and wet snow on structures,” *Philos. Trans. R. Soc. London. Ser. A Math. Phys. Eng. Sci.*, vol. 358, no. 1776, pp. 2913–2939, Nov. 2000, doi: 10.1098/rsta.2000.0690.

[58] K. J. Finstad, E. P. Lozowski, and E. M. Gates, “A Computational Investigation of Water Droplet Trajectories,” *J. Atmos. Ocean. Technol.*, vol. 5, no. 1, pp. 160–170, Feb. 1988, doi: 10.1175/1520-0426(1988)005<0160:ACIOWD>2.0.CO;2.

[59] W. Gao, D. W. Smith, and D. C. Sego, “Freezing Temperatures of Freely Falling Industrial Wastewater Droplets,” *J. Cold Reg. Eng.*, vol. 14, no. 3, pp. 101–118, Sep. 2000, doi: 10.1061/(ASCE)0887-381X(2000)14:3(101).

[60] J. Stallabrass and P. Hearty, “The Icing of cylinders in conditions of simulated freezing sea spray,” 1967.

[61] A. Dehghani-Sanij, Y. S. Muzychka, and G. F. Naterer, “Predicted Ice Accretion on Horizontal Surfaces of Marine Vessels and Offshore Structures in Arctic Regions,” in *Volume 8: Polar and Arctic Sciences and Technology; Petroleum Technology*, Jun. 2016, pp. 1–9, doi: 10.1115/OMAE2016-54054.

[62] L. Makkonen, “Salinity and growth rate of ice formed by sea spray,” *Cold Reg. Sci. Technol.*, vol. 14, no. 2, pp. 163–171, Aug. 1987, doi: 10.1016/0165-232X(87)90032-2.

[63] P. Schwerdtfeger, “The Effect of Finite Heat Content and Thermal Diffusion on the Growth of a Sea-Ice Cover,” *J. Glaciol.*, vol. 5, no. 39, pp. 315–324, Jan. 1964, doi: 10.3189/S0022143000029051.

[64] A. Kulyakhtin, S. Kulyakhtin, and S. Løset, “The role of the ice heat conduction in the ice growth caused by periodic sea spray,” *Cold Reg. Sci. Technol.*, vol. 127, pp. 93–108, Jul. 2016, doi: 10.1016/j.coldregions.2016.04.001.

[65] L. Makkonen, “Solid fraction in dendritic solidification of a liquid,” *Appl. Phys. Lett.*, vol. 96, no. 9, p. 091910, Mar. 2010, doi: 10.1063/1.3306728.

[66] R. Z. Blackmore, L. Makkonen, and E. P. Lozowski, “A new model of spongy icing from first principles,” *J. Geophys. Res. Atmos.*, vol. 107, no. D21, p. AAC 9-1-AAC 9-15, Nov. 2002, doi: 10.1029/2001JD001223.

[67] J. S. Wettlaufer, M. G. Worster, and H. E. Huppert, “the phase evolution of Young Sea Ice,” *Geophys. Res. Lett.*, vol. 24, no. 10, pp. 1251–1254, May 1997, doi: 10.1029/97GL00877.

[68] M. Schremb, I. V. Roisman, and C. Tropea, “Normal impact of supercooled water drops onto a smooth ice surface: experiments and modelling,” *J. Fluid Mech.*, vol. 835, pp. 1087–1107, Jan. 2018, doi: 10.1017/jfm.2017.797.

[69] G. Wilbur, B. MacMillan, K. M. Bade, and I. Mastikhin, “MRI monitoring of sea spray freezing,” *J. Magn. Reson.*, vol. 310, p. 106647, Jan. 2020, doi: 10.1016/j.jmr.2019.106647.

[70] K. F. Jones and E. L. Andreas, “Sea spray concentrations and the icing of fixed offshore structures,” *Q. J. R. Meteorol. Soc.*, vol. 138, no. 662, pp. 131–144, Jan. 2012, doi: 10.1002/qj.897.

[71] W. . Kays, M. . Crawford, and B. Weigand, *Convective Heat and Mass Transfer. 4th Edition*. 2004.

[72] T. S. Jørgensen, “Sea spray characteristics on a semi-submersible drilling rig - STF60 F 85015,” 1985.

[73] I. Horjen, S. Loeset, and S. Vefsnmo, “Icing Hazards On Supply Vessels And Stand-by Boats - STF60 A86073,” 1986.

[74] I. Muzik and A. Kirby, “Spray overtopping rates for Tarsiut Island: model and field study results,” *Can. J. Civ. Eng.*, vol. 19, no. 3, pp. 469–477, Jun. 1992, doi: 10.1139/l92-057.

[75] V. V. Borisenkov, Y.P., Zablockiy, G.A., Makshtas, A.P., Migulin, A.I., Panov, “On the approximation of the spray-cloud dimensions (In Russian). Arkticheskii I Antarkticheskii Nauchno-Issledovatelskii Institut.,” 1975.

[76] H. E. B. Børs, S. Løset, K. Iden, M. Reistad, K. Harstveit, B. Nygård, “Goliat Environmental/ Icing Evaluation Study. 25/08,” 2009.

[77] C. Anandharamakrishnan, J. Gimbun, A. G. F. Stapley, and C. D. Rielly, “Application of Computational Fluid Dynamics (CFD) Simulations to Spray-Freezing Operations,” *Dry. Technol.*, vol. 28, no. 1, pp. 94–102, Dec. 2009, doi: 10.1080/07373930903430843.

[78] E. Villeneuve, D. Harvey, D. Zimcik, R. Aubert, and J. Perron, “Piezoelectric Deicing System for Rotorcraft,” *J. Am. Helicopter Soc.*, vol. 60, no. 4, pp. 1–12, Oct. 2015, doi: 10.4050/JAHS.60.042001.

[79] S. A. Kulinich and M. Farzaneh, “Ice adhesion on super-hydrophobic surfaces,” *Appl. Surf. Sci.*, vol. 255, no. 18, pp. 8153–8157, Jun. 2009, doi: 10.1016/j.apsusc.2009.05.033.

[80] Ulstein Group, “X-Bow,” 2020. https://ulstein.com/innovations/x-bow (accessed Feb. 19, 2020).

[81] P. Guest and R. Luke, “Mariners Weather Log Vol. 49, No. 3, December 2005,” 2005. https://www.vos.noaa.gov/MWL/dec_05/ves.shtml (accessed Sep. 07, 2020).

13. Appendix 2: Paper 2

Experiments with sea spray icing: Investigation of icing rates

Sujay Deshpande*, Ane Sæterdal, Per-Arne Sundsbø

[This is a reprint of the accepted version of the article. Reprinted with permission from ASME. Strictly for the use of inclusion in the PhD thesis. DOI of published version: https://doi.org/10.1115/1.4062255]

Dept. of Building, Energy and Material Technology, UiT, The Arctic University of Norway.
*Corresponding author: Sujay Deshpande.
Address: C/o UiT, Campus Narvik, Lodve Langesgate 2, 8514, Narvik, Norway.
email: sujay.r.deshpande@uit.no

Abstract

Sea spray icing on ships and marine structures depends on a complex correlation between metocean parameters and vessel characteristics. Sea spray icing rates have mostly been investigated and given as a function of general metocean parameters. The existing models suffer from lack of experimental data. More experimental data is required for better prediction models and understanding of the icing process. This paper presents results from a comprehensive cold laboratory study of the dependence and trends of sea spray icing rates related to 8 parameters. Experiments were performed simulating sea spray from a nozzle towards a vertical surface in freezing environment. This study presents 20 unique tests structured into 8 experiments, each of which focusses on change in icing rates due to one independent variable. Results showed that the sea spray rates dependence of the investigated parameters comply with existing knowledge, however preliminary analysis points out various unintentional covariates for most experiments which calls for further investigations. This is the greatest number of variables tested in one set of experiments to date and serve as valuable sea spray icing data experimental data – a limitation for the evaluation of previous models that pointed out to the lack of enough icing measurements in this field of research.

Keywords: Sea spray icing, icing on ships and offshore structures, experimental icing data, icing rates.

1. Introduction

Arctic and Sub-Arctic regions have seen a growth in marine and offshore operations in terms of fishing, aquaculture installations, oil and gas exploration, and more recently, tourism. Marine operations in cold climate have numerous challenges out of which, sea spray icing has been pointed out to be a major challenge. Sea spray icing, possibly in combination with snow [1], has been attributed to 80-90% of all offshore icing incidents [2]. Icing predictions are essential for safe marine operations. Winterization of vessels and offshore structures includes anti-icing and de-icing procedures that require estimation of expected icing already at the design stage [3].

Previously, researchers have presented models for the prediction of sea spray icing [4]–[9]. A recent review article suggests need for improvement of these models and points out to the lack of enough full-scale and laboratory experimental data studying sea spray icing [3].

Full scale measurements for sea spray icing were carried out by some researchers [10], [11]. However, large variations were expected due to limitations in measurement techniques and the measurements were not detailed enough for validation of computational results [3]. Laboratory experiments were conducted by Stallabrass & Hearty, 1967 for studying sea spray icing in cylinders [12]. Variation of atmospheric temperature was the only variable in this experiment. In reality, sea spray icing is a complex process including numerous uncertain variables [3].

Deghani-Sanij et.al., 2019 presented an experimental study for sea spray icing that analyzed mass and thickness due to sea spray icing with 12 unique sets of measurement. This was a major step forward into experimentation with multiple variables for sea spray icing. The experiment consisted of two variations each of atmospheric temperature and salinity, 3 variations of wind speeds, and 2 variations of a combination of spray duration and spray period. This experiment did not include sea temperature as a variable which was measured at 20.9°C in the water tank outside the freezing room, and about 17°C measured in pipe just before the nozzle inside the freezing room. The temperature in the freezing rooms during the experiments varied by 4°C during the tests. [13]

The current study presents results from a set of 20 unique tests in which 8 different variables identified to affect sea spray icing were tested under controlled conditions in the cold climate laboratory at UiT, The Arctic University of Norway, Campus Narvik. The study is divided into 9 different experiments (8 variables + 1 repeatability) with either 3 or 4 tests included in each experiment. In each experiment, one variable is varied for individual tests while keeping the others constant to study the effects of individual variables on icing rates. The results of the tests are presented in the form of icing rates on a vertical plate in terms of weight and thickness. In a first, the time dependency of icing rates in the initial stages of an icing event is presented. Some parameters are difficult to be kept constant even under laboratory conditions and thus the difference between ideal and practical conditions are presented for every test. The variation due to different measurement methods is part of the study. The results presented in this article illustrates how icing rates could vary the selected variables and methods of measurement. However, owing to the relatively large scope of the experiments, detailed level of measurements, and the fact that many of the variables cannot be kept constant even under controlled laboratory conditions, it is not straightforward to investigate the connection to existing sea spray models based on metocean parameters. However, the provided experimental data of the icing process show important trends that would be useful for further analysis. The complete lab setup and lessons learned during the experimental work and data collection are shared to assist improvements during any similar experiments in the future. Data analysis with the help of machine learning, interpretation of the results in terms of metocean conditions and ship characteristics, and comparison of results with existing models is suggested as a progression for this study.

2. Selection of variables

Sea spray icing is a complex process involving many variables, some of which are difficult to measure to full extent or be controlled in an experimental setup. Different researchers also had very different approaches to prediction models and selection of governing variables in the icing process.

The simplest of the models is an empirical model presented by Overland 1986 based on statistical analysis of metocean data, that predicts the icing thickness rate (cm/hr) from wind speed (U_{10}), air and sea

temperatures, and the freezing point of water, that is a function of salinity [8], [10]. Stallabrass 1980 presented a stationary theoretical model for the prediction of icing thickness rate (mm/hr) using wave height, relative wind speed, temperature of icing surface, air temperature, spray droplet temperature at impingement, sea temperature, thermal conductivity of air, Nusselt number for wind flow, density of water, specific heat of water, droplet diameter, latent heat of vaporization, barometric pressure, specific heat of dry air, vapour pressure at air temperature and at droplet temperature at impingement [9]. Kulyakhtin 2014, used a hybrid theoretical and numerical model for predicting icing thickness rates in the MARICE model using density of accreted ice, latent heat of fusion of pure ice, ratio of entrapped liquid mass to mass of ice accretion, thermal conductivity of water, freezing temperature of water film, water film thickness, specific heat capacity of water film, spray flux on freezing surface, spray temperature at generation, heat transfer coefficient at air-water interface, air temperature, thermal conductivity of water, liquid water content (LWC) [4]. The ICEMOD2 model presented by Horjen 2013 predicted the icing rate in terms of ice mass ($kg/m^2/s$) using wind speed (U_{10}), height above the mean sea level, significant wave height, vessel speed, relative wind heading, density of water, spray frequency, spray duration, and vessel direction with respect to waves as the main parameters [5]. Forest et.al. 2005, in the RIGICE04 model, predict the total ice accretion mass on offshore structures with variables including spray frequency, significant wave height, LWC, mass of water in one spray, height above the mean sea level, velocity of water droplets, spray duration, salinity, air temperature, sponginess of accreted ice, wind speed [6].

Laboratory setups favour controlled experiments and detailed measurements, but does not enable modelling of ship characteristics as wave generation, long spray flights with cooling of airborne spray droplets etc. Therefore, this experimental study was focused on basic fluid mechanics parameters and fluid properties governing sea spray icing, and what may be modelled and measured in the confined lab. These variables could be categorised into two categories: metocean parameters and parameters dependent on ship characteristics. The metocean parameters include *atmospheric temperature, sea temperature, wind speed, and salinity*. The parameters that are dependent on ship and wave characteristics include *spray flux, spray frequency and spray duration*. *Wind speed* may also be considered as a parameter depending on ship characteristics since the ship design and wind direction highly affects the near-surface wind conditions and cooling of the surface. Material was the lone parameter identified that is only ship/ structure specific.

Kulyakhtin 2011 has shown that changes in humidity inside a droplet cloud has no significant effect upon the droplet temperature [14]. Humidity was hence not considered as a variable. Most of the existing sea spray icing models mentioned above use droplet diameter as a variable. Ryerson 1995, measured the droplet size spectrum and the LWC close to the spray impact location on the 115m Coast Guard Cutter wherein 39 spray events were sampled [11]. It is difficult to determine if a spray generated due to the impact of any random vessel with waves would confirm with these spectra of droplet sizes from the observations from one ship. Researchers have investigated the use of mean volume diameter (MVD) as an estimation for the complete spectrum of droplet sizes, and Kulyakthin 2012 concluded that uncertainty in the spray MVD can result is errors of several orders of magnitude [15]. Therefore, the droplet size was not included in this study. However, the nozzle and pressure combinations were selected in the range of droplet sizes that were presented in previous research. Details of the selection of the nozzle are outlined in section 3.1.

3. Experimental Setup

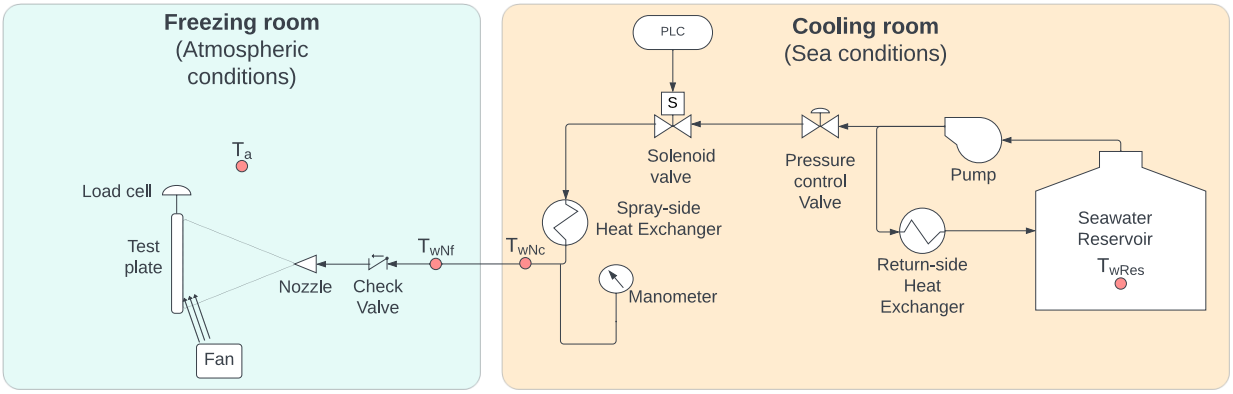

Figure 1: Schematic of experimental setup

The experimental setup consisted of 2 rooms. The first room (right side in Figure), called the 'cooling room', simulated the cold sea conditions and was set between +2°C and +6°C throughout all the experiments. The second room (left side in Figure), called the 'freezing room' simulated the freezing air conditions and was set between -15°C to -5°C depending on the experiments.

Seawater was stored in a 1000 litre reservoir in the cooling room. A pump was used to build up the flow in the system. Pressure in the system was measured about 1.5m before the nozzle and was controlled with the help of a control valve. A solenoid valve, controlled by a PLC (Programmable Logic Controller), was used to simulate periodic spray conditions. This helped to set the spray duration and period. A return pipe returned the seawater back to the reservoir from the pump since the pump was in continuous operation. Temperature measurement after the pump showed that there was a significant rise in the temperature of seawater at the output of the pump. A heat exchanger on the return side helped maintain the temperature of seawater in the reservoir. Another heat exchanger before the nozzle ensured that the seawater temperature through the nozzle was as close to the set water temperature in the room. The line then proceeded to the nozzle through a check valve in the freezing room. The intermittent spray conditions made in necessary to have a check valve to prevent air entering the system when the solenoid valve turned off, the absence of which resulted in reduction of flow through the nozzle over time. Finally, the freezing room had the test plate at a distance of 2 meters from the nozzle, on which the ice accretion was measured. The weight of ice was measured as a function of the output voltage from the load cell in a data logger. In addition to the schematic, there were numerous thermocouples that were strategically placed throughout the system and connected to the datalogger outside of both rooms.

Additionally, there was a cross-flow fan of a length greater than the plate to simulate near-surface wind. This fan was placed in close proximity to the plate in a manner that the whole plate was subjected to the airflow.

Figure shows the schematic of the experimental setup and the images from the setup can be seen in Figure 2, Figure 3, and Figure 4.

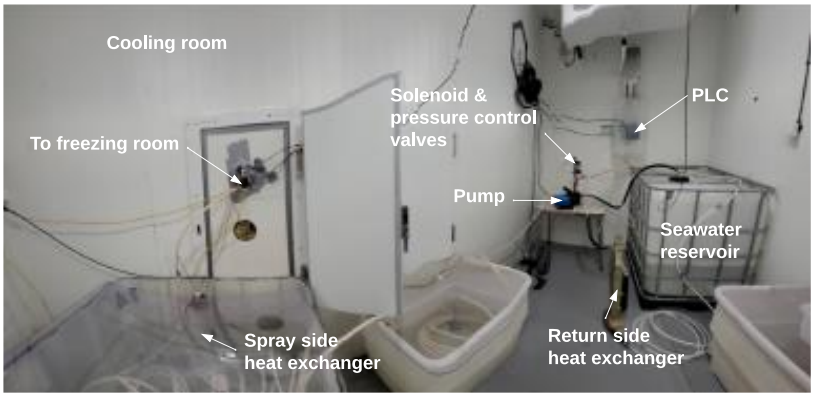

Figure 2: Cooling room setup

Figure 3: Freezing room setup

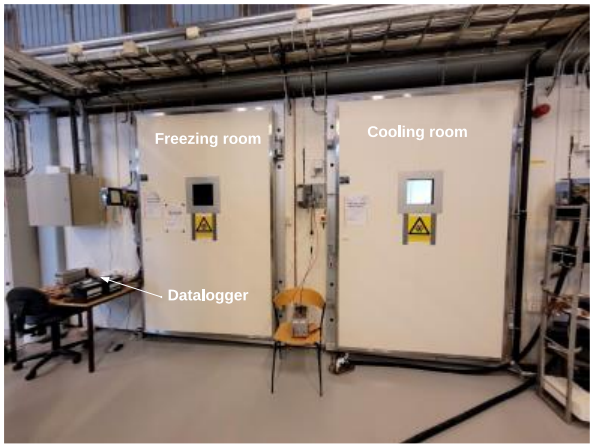

Figure 4: Cold climate laboratory at UiT, The Arctic University of Norway - Campus Narvik

3.1. Spray nozzle

Selection of the spray nozzle and operational pressure for experiments with sea spray icing controls droplet sizes, flow rate and distribution of the spray.

The experimental setup presented by Deghani-Sanij et.al., 2019 with respect to the nozzle, wind, and the plate, allowed for droplets that were only carried by the wind to impinge on the plate. In reality, there is a wide spectrum, of droplets within a spray cloud after interaction of a vessel with waves. Larger droplets tend to fall rapidly back in the water or in the forward part of the vessel whereas smaller droplets are carried by the wind to the aft part. The experiment used a nozzle and pressure combination that produced droplets of DV0.5 (Median Volume Diameter) approximately 975µm [13]. Droplets with diameters greater than 400µm are too large to be lifted by the turbulence [4], this value was however computed from wind generated spray. This could suggest that larger diameter droplets never reached the test plate, as it was not the momentum of the droplets, but the wind that carried the droplets to the plate. It is thus a possibility that the results of this experiment might be more useful for the aft regions of the ship than the forward regions since a CFD simulation by Kulyakhtin et.at. 2012 suggests a difference in the flow rate distribution of as much as $1x10^4$ between the forward and aft part of the ship [15].

Droplets of size 250 -500 µm are the primary reason for the spray flux at the aft, and sides of the vessel [2], this however depends on the size and design of the vessel. The nozzle used for the current experiments have a rated DV0.5 of 520µm ,410µm, and 350µm, at 1, 2, and 3 bars respectively. 3 bar pressure was the maximum that could be achieved with the available pump at the location of measurement (Figure). The nozzle was full-cone nozzle with a rated spray angle of 30°. Owing to the setup of the current experiment presented in Figure , most of the droplets within the full spectrum could be assumed to be impacting the plate due to the momentum of the particles exiting the nozzle.

4. Test structure

The test structure is presented in Table . The study comprised of 20 unique tests divided into 9 experiments. The first experiment, experiment 0, was conducted to study the repeatability of the tests under the same set conditions. The next 8 experiments with experiment numbers 1-8 are main experiments. In each experiment, 3 tests (4 in case of wind speed) were conducted by varying one variable while keeping the others constant. In each row in Table , the highlighted column shows the variable for the particular experiment.

Table 1: Experiment structure

Exp. Nr.	Constants / Varibles	Material	Wind speed (m/s)	Atmospheric temperature (°C)	Seawater temperature (°C)	Gauge Pressure (bar)	Spray duration (seconds)	Spray period (seconds)	Salinity (ppt)
0	**Repetition**	Aluminium	0 m/s	-9°C	+4°C	3 bar	0.25 s	9 s	32.45 ppt
1	**Material**	1. Aluminium 2. Steel 3. Fibreglass	0 m/s	-9°C	+4°C	3 bar	0.25 s	9 s	32.45 ppt
2	**Wind speed (m/s)**	Aluminium	1. 0 m/s 2. 2 m/s 3. 4 m/s 4. 6 m/s	-9°C	+4°C	3 bar	0.25 s	9 s	32.9 ppt
3	**Atmospheric temperature (°C)**	Aluminium	6 m/s	1. -5°C 2. -9°C 3. -15°C	+4°C	3 bar	0.25 s	9 s	32.9 ppt
4	**Seawater temperature (°C)**	Aluminium	6 m/s	-9°C	1. 2°C 2. 4°C 3. 6°C	3 bar	0.25 s	9 s	32.9 ppt
5	**Gauge Pressure (bar)**	Aluminium	6 m/s	-9°C	+4°C	1. 1 bar 2. 2 bar 3. 3 bar	0.25 s	9 s	32.9 ppt
6	**Spray duration (seconds)**	Aluminium	6 m/s	-9°C	+4°C	3 bar	1. 0.25 s 2. 0.5 s 3. 1 s	9 s	32.9 ppt
7	**Spray period (seconds)**	Aluminium	6 m/s	-9°C	+4°C	3 bar	0.25 s	1. 3 s 2. 6 s 3. 9 s	32.9 ppt
8	**Salinity (ppt)**	Aluminium	6 m/s	-9°C	+4°C	3 bar	0.25 s	9 s	1. 0.03 ppt 2. 32.45 ppt 3. 32.90 ppt

Some variables mentioned in Table have underlying parameters that were the actual subjects of the test. The variation of the test plate material corresponds to the change in thermal conductivity and the change in pressure corresponds to the change in spray flux. The unit used for salinity is ppt (parts per thousand) which is the same as psu (practical salinity unit) used by oceanographers [16].

For all experiments, the distance between the nozzle and the plate, or the minimum spray flight distance, was constant at 2m. Video analysis showed that, in case of 3 bar pressure, the approximate flight time or the time required for the spray to reach the plate from the nozzle was 0.3 seconds giving an approximate ejection velocity of 6.66m/s. Atmospheric pressure measured inside the freezing room, located approximately at an altitude of 120m over the mean sea level, at -9°C with a multi-function ventilation meter was 97.5KPa. Changes in this value over the course of the study are not taken into consideration.

Some fluctuations were observed during the experiments. For example, the recorded temperatures showed slightly variation from the set temperatures and varied by about 1-2°C during each test due to the manner in which the refrigeration system controlled the temperature in the cold climate lab. This topic is discussed in detail in the results section for individual experiments.

5. Test procedure

The test procedure started with ensuring that the plate temperatures (using thermocouples glued in holes on the plate at a distance of 0.5mm from the surface facing the spray) and the water temperature in the reservoir were stable and as close to the set temperatures in the freezing room and the cooling room respectively. In addition, it was ensured that all other parameters are adjusted in accordance with the set test conditions. Recording the data logger was started. The pump was started at this point. The PLC was programmed to give a continuous spray for the first couple of minutes to ensure removing that all air pockets from the spray line. This ensured minimum variation of water exiting the nozzle throughout the experiment. During the initial continuous spray, there was a drainage system (Figure 5) that diverted the spray to the water collection tank and ensured that the spray does not come in contact with the plate.

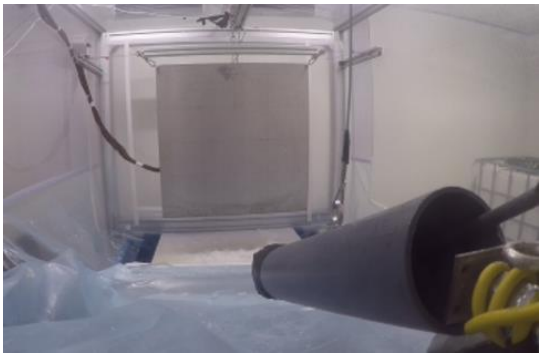

Figure 5: Spray drainage system

After the start of pulsating spray, the drain cover was removed with the help of a pulley mechanism. The pulley mechanism helped to remove the drain cover without entering the freezing room, without which, opening and closing of the freezing room resulted in excessive vibrations of the test plate, and thereby resulting in excessive noise in the weight data. This marked the start of the test period of 1 hour. The spray continued for exactly one hour, at the end of which, the pump was switched off. This marked the end of the test. The plate was allowed to rest for a few minutes to dampen the vibrations caused by the pulsating spray for recording the total ice weight (including ice stalactites under the plate). Next, the ice stalactites were scraped with a sharp metal plate, ensuring as close as possible, that no ice on the projected surface area of the plate was removed. The plate was again allowed to rest for some minutes for recording the reading of ice weight without the ice stalactites. This step marked the end of the test. Figure 8 provides details of the time intervals pertaining to the test.

6. Measurements and Data analysis

Table 2 presents a list of all variables used for the current study. It includes nomenclature, description, the source of measurement, and the formulae used for calculation, if any.

Table 2: Nomenclature & data source

Symbol	Unit of measurement	Description	Source of measurement	Formula/ Reference
u_{set}	m/s	set wind speed	hot wire anemometer	Figure 6
T_{aSet}	°C	set air temperature in freezing room	set in cold climate lab	-
T_{wSet}	°C	set seawater reservoir temperature (set air temperature in cooling room)	set in cold climate lab	-
p_{gauge}	bar	gauge pressure measured approximately 1.5 meters before the nozzle	manometer	-
t_s	sec	spray duration	set in PLC	-
t_p	sec	spray period or time between two consecutive sprays	set in PLC	-
T_{aMean}	°C	mean air temperature in freezing room for the duration of each test	thermocouple/ data logger	avg over 1 hour
T_{wRes}	°C	Temperature of seawater in reservoir	thermocouple/ data logger	-
T_{wNc}	°C	mean temperature of seawater measured before nozzle in cooling room for the duration of each test	thermocouple/ data logger	avg over 1 hour
T_{wNf}	°C	Mean temperature of seawater measured before nozzle in freezing room for the duration of each test	thermocouple/ data logger	avg over 1 hour
T_{wMean}	°C	Mean temperature of seawater out of nozzle	thermocouple/ data logger	$(T_{wNc+} T_{wNf})/2$
$\dot{m}_{plate}$	kg/hr	mass of seawater impinging the plate per hour	physical measurement	Figure 7
Q_{plate}	kg/m²/hr	mass flux of seawater impinging the plate per hour	calculation	$(\dot{m}_{plate})/(A_p)$
s_{ppt}	ppt	salinity	Conductivity meter	-
ρ_i	kg/m³	density of sea spray ice (assumed = 900 kg/m³)	literature	[4], [17], [18]
A_p	m²	surface area of each test plate (= 0.49m²)	physical measurement	-
w_{ice15}	kg	total weight of ice in first 15 mins of test (from 10 min moving avg curve of ice weight)	Load cell/ data logger	Figure 9
w_{iceX15}	kg	total weight of ice excluding first 15 mins of test (from 10 min moving avg curve of ice weight)	Load cell/ data logger	Figure 9
w_{ice60}	kg	total weight of ice in 1 hour of the test (from 10 min moving avg curve of ice weight)	Load cell/ data logger	Figure 9
w_{tot}	kg	total weight of ice in 1 hour of the test (measured average after end of each test)	Load cell/ data logger	Figure 8
w_{plate}	kg	weight of ice in 1 hour of the test without ice stalactites (after scraping ice hanging below plate surface projected area) (measured average after end of each test)	Load cell/ data logger	Figure 8
r_{ice15}	kg/m²/hr	effective icing rate for first 15 mins of each test	calculation	$w_{ice15}*4/A_p$
r_{iceX15}	kg/m²/hr	effective icing rate excluding 15 mins of each test	calculation	$w_{iceX15}*(4/3)/A_p$
r_{ice60}	kg/m²/hr	effective icing rate for each test calculated from 10 min moving avg of total ice weight	calculation	w_{ice15}/A_p
r_{tot}	kg/m²/hr	effective icing rate for each test calculated from avg total ice weight measured after test	calculation	w_{tot}/A_p

r_{plate}	kg/m²/hr	effective icing rate for each test calculated from avg ice weight without ice stalactites measured after test	calculation	w_{plate}/A_p
i_p	mm/hr	icing rate assuming uniform ice layer, calculated from ice weight without ice stalactites	calculation	$w_{plate}/A_p/\rho_i/1000$
i_{25}	mm/hr	icing rate considering all 25 points	physical measurement	Figure 11
i_{6-}	mm/hr	icing rate considering upper 6 points (low icing region)	physical measurement	Figure 11
i_{6+}	mm/hr	icing rate considering lower 6 points (heavy icing region)	physical measurement	Figure 11

Some measurements that do not have an obvious explanation in Table 2, are detailed out below.

6.1. Wind speed (u_{set})

A cross-flow fan of a length greater than the test plate was used to simulate the influence of wind on and near the freezing surface. The placement of the fan is shown in Figure 6.

The wind speed was measured with the help of a hot wire anemometer 9mm over the surface of the plate as shown in Figure 6. Wind speed was measured as an average of several readings at the top and the bottom of the plate. The difference in the wind speeds measured at the top and bottom varied by approximately 5% and was assumed constant over the entire surface of the plate.

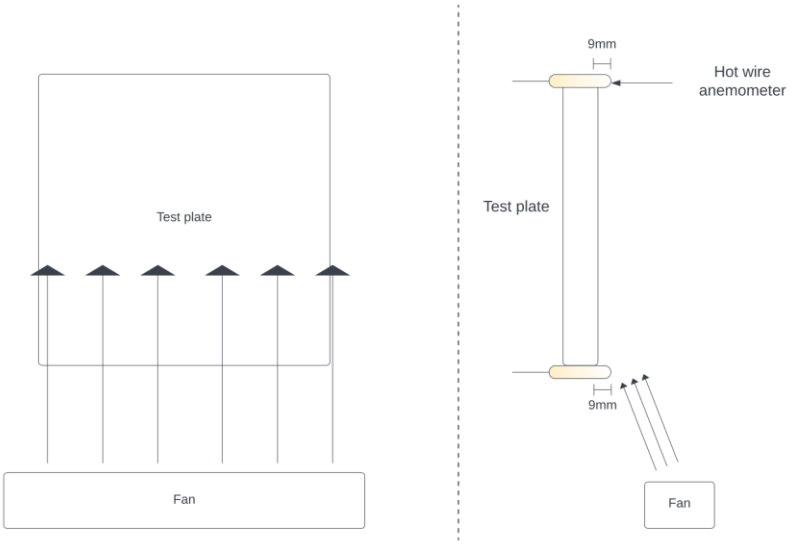

Figure 6: Schematic of windspeed measurement

The measurement of wind speeds in the experiment presented by Deghani-Sanij et.al., 2019 took place at a distance of 40cm from the fan, which was 2.1m from the plate, given that the distance between the fan and the test plate was 2.5m [13]. Wind speed measurements in the setup for the current study shown in Figure 6, were measured at the plate, which is a more accurate measurement for the wind speed affecting the freezing surface.

6.2. Temperatures

Temperatures were measured with the help of thermocouples and recorded every second with a datalogger. The locations of measuring probes for air and seawater temperatures are shown in Figure . The air temperature in the freezing room was monitored with a thermocouple suspended close to the setup, but away from the spray.

Temperature of seawater was monitored in the reservoir (T_{wRes}), but not used during the analysis owing to the rise in temperature due to the pump. Instead, seawater temperatures were measured close to the nozzle. The seawater temperature close to the nozzle was measured with a thermocouple inserted perpendicularly in the pipe, about 10cm upstream of the nozzle inside the freezing room (T_{wNf}). The intermittent stagnation of seawater in the freezing room due to periodic spray was expected to lower the seawater temperature out of the nozzle compared to the temperature of seawater in the reservoir. Thermocouple readings can be affected by radiation errors [19]. Since the pipe in this location was constantly exposed to the freezing temperatures, despite of the insulation, the readings for the sea temperature at the nozzle could have been lower than the actual values. Thus, another measurement of the seawater temperature was taken about 1.5m upstream of the nozzle, but this one in the cooling room (T_{wNc}). The actual temperature would lie somewhere in between the seawater temperature measured upstream of the nozzle in the freezing room (T_{wNf}) and the one measured upstream of the nozzle in the cooling room (T_{wNc}) and thus, the actual seawater temperature exiting the nozzle (T_{wMean}) was considered to be the average of these two readings.

6.3. Mass of seawater impinging the plate per hour ($\dot{m}_{plate}$)

The setup for measuring the mass of seawater impinging on the plate is shown in Figure 7. The setup was run for all combinations of the input variables (wind speeds, pressure, spray duration, spray period) used in the test, each for 15 minutes, with the first batch of seawater with 32.45ppt salinity. The setup consisted of a frame with inner dimensions of that of the test plate (0.7m x 0.7m). A plastic water retainer collected all the spray water and drained it through a hole at the bottom into a collection bin. The mass of water collected in a collection bin was measured. This mass was multiplied by 4 to give the mass per hour.

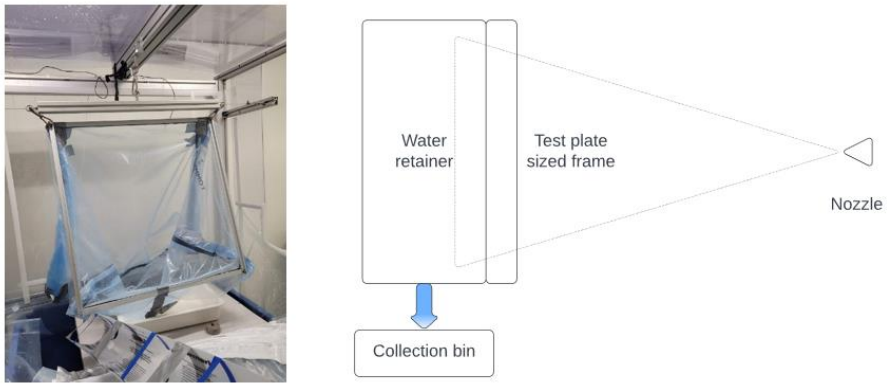

Figure 7: Setup and schematic for spray flux measurement

Measurements using the method used by Dehghani-Sanij et. al. 2018 to measure spray flux by collecting the water after hitting the plate in the small container [13], showed about 11.4% lesser flux than the current method shown in Figure 7. In the current method, 100% of the spray droplets that would have hit the plate are measured, whereas in the method described by Dehghani-Sanij et. al. 2018, some droplets that bounce back after hitting the plate are not captured, thus giving a lower value of flux than actually hits the plate. This difference in the measurement techniques is especially important due to the difference in the setup of the spray nozzle and the plate in both experiments (see Figure). In the experiment by Dehghani-Sanij et. Al. 2018, the nozzle was directed upwards, parallel to the plate, with a DV0.5 of 975µm, and the droplets that hit the plate were purely due to wind, and not the momentum of the droplets coming out of the nozzle. In section 3.1, it was suggested that it is possible that relatively larger droplets would be unable to be carried by the wind to the plate. This could have resulted in only the smaller droplets actually hitting the plate. In this case, the spray flux measurement technique applied by Dehghani-Sanij et. Al. 2018 would be valid, although, the results from such a setup would be more appropriate only for the aft parts of the vessel where the droplets might reach mainly due to being carried by the wind. In the setup for the current study, the spray nozzle faces the plate, thereby taking also the relatively larger droplets to the plate due to momentum. The flux measurement technique used in this case (Figure 7) is more appropriate for the current setup.

The tests were carried out with two samples of seawater and one of freshwater. Measurements for the mass of impinging seawater per hour ($\dot{m}_{plate}$) were done at ambient room temperature with the seawater sample with 32.45ppt salinity. Since the density of water changes with salinity and temperature, assuming the volume of water hitting the plate during measurements and the tests remaining constant, the percentage difference in $\dot{m}_{plate}$ during the measurements and the tests is solely due to the difference in the density. Table 3 shows how neglecting the changes in the density causes only a negligible error in $\dot{m}_{plate}$ of a maximum of 0.45% for both seawater samples and 1.54% for the sole test with freshwater. It is however to be noted that this applies only for the calculations of the mass flux and not the mass of accreted ice, since the mass of ice is directly measured with the help of a load cell. The densities in Table 3 are obtained from an open source density calculator [20].

Table 3: Density difference in various water samples

	Water sample	Salinity (ppt)	Approx. Temp.	Density (kg/m³)	Error due to neglecting difference in density (%)
During Measurement of $\dot{m}_{plate}$	Sample 1	32.45	25°C	1015.63	-
During icing tests	Sample 1	32.45	2°C	1019.779	0.41
	Sample 2	32.895		1020.242	0.45
	Fresh water	0.03		999.992	-1.54

6.4. Weights from datalogger

The data logger registered the output voltage from the load cell throughout the duration of the whole test, in addition to some periods before and after the actual test duration. 11 calibration tests confirmed

a 0.001mV/gm increase in the output voltage from the load cell. This calibration was used to calculate the ice weights from the raw data. A sample raw data from one of the tests is shown in Figure 8. To reduce the effects of the noise in the data, there were periods before and after the actual test duration for measuring weights. Before the actual test starts, there is a period to measure the average start weight of the plate. After the actual test duration, average weight is taken before and after scraping of ice stalactites, providing the basis for the calculation of w_{tot} and w_{plate} respectively.

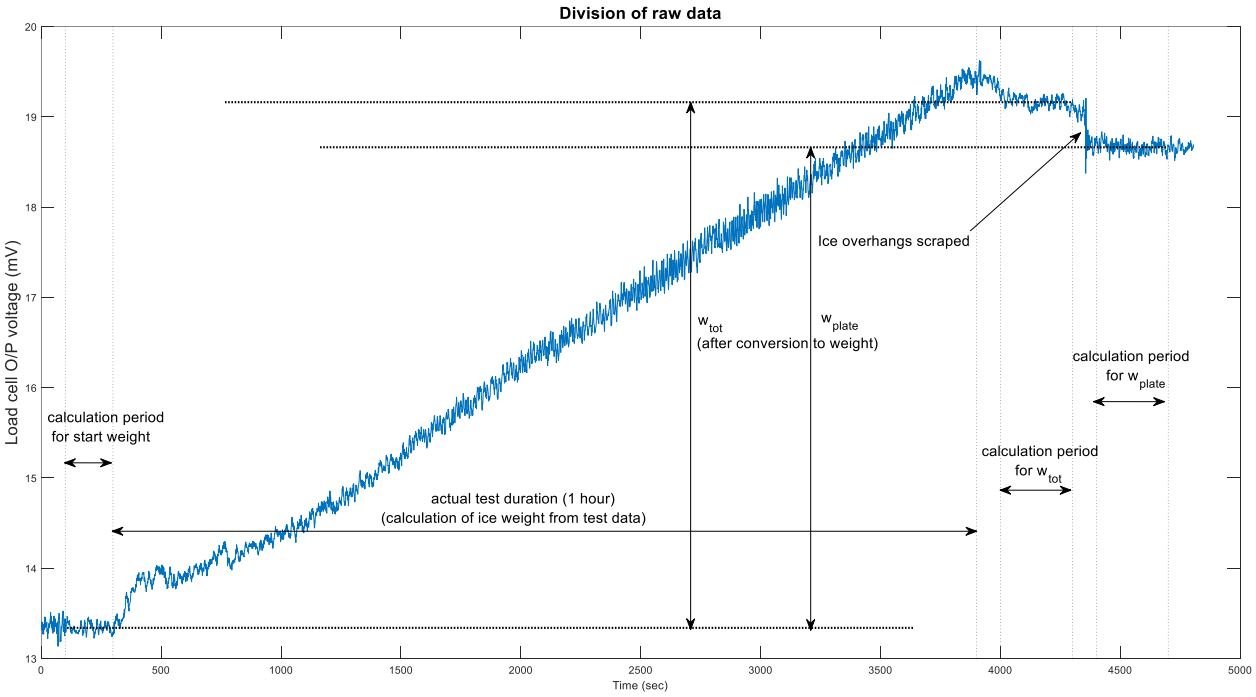

Figure 8: Timewise division of raw data from data logger (example of Experiment 7, test 1 with 3sec spray period)

Next, processing of the actual test data was carried out and is explained in the next section.

6.5. Data processing of weight measurements

Raw data for the actual test duration shown in Figure 8 was extracted and processed further to remove noise from the data. After experimenting with several curve smoothing algorithms and spans, it was concluded that the Robust Locally Weighted Scatterplot Smoothing (RLOWESS) algorithm [21] with a span of 600 timesteps (10 minutes) gave the bet fit for the raw data.

In Figure 9, the output voltage from the raw data is first converted to weight and then smoothed with the aforementioned function (blue curve). Due to the noise in the data, the start was not necessarily at 0gms. This data was then zero-adjusted, i.e., the start of this curve was moved to 0gms. The resulting red curve in Figure 9 was considered to be the ice weight curve for individual tests. Figure 9 also shows the calculation procedure for the rest of the weights that were not covered in Figure 8.

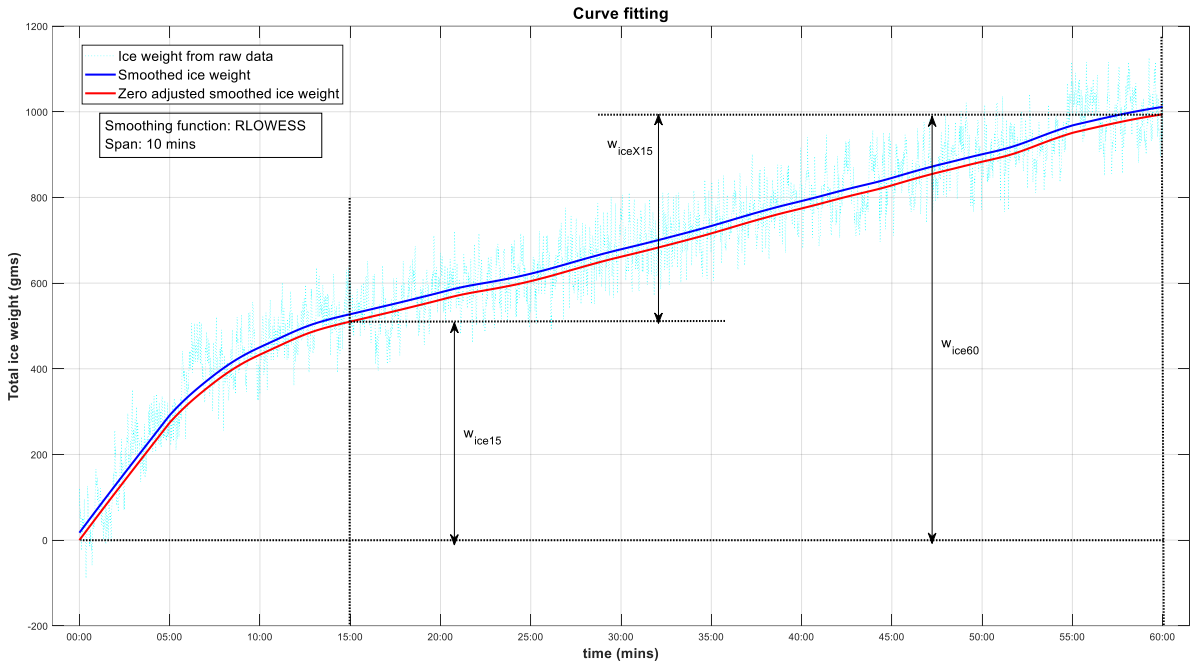

Figure 9: Noise reduction of weight data (example from experiment 2, test 1 for 0 wind speed)

Most calculations required the actual weight on the plate from Figure 9. However, it is the area density (mass per unit area) of ice accretion that is of more interest, for which another calculation was performed. As shown in Figure 10, the zero adjusted ice weight in grams from Figure 9 is first converted to kgs, and then, the mass per unit area is calculated by dividing this with the area of the plate. The icing rate is then calculated by taking the difference in the mass per unit area of consecutive points (per second) and converting the rate to per hour. Since the icing rate is calculated from the time averaged weight of ice accreted over 10 minutes, the icing rate too would be the time averaged icing rate over ten minutes.

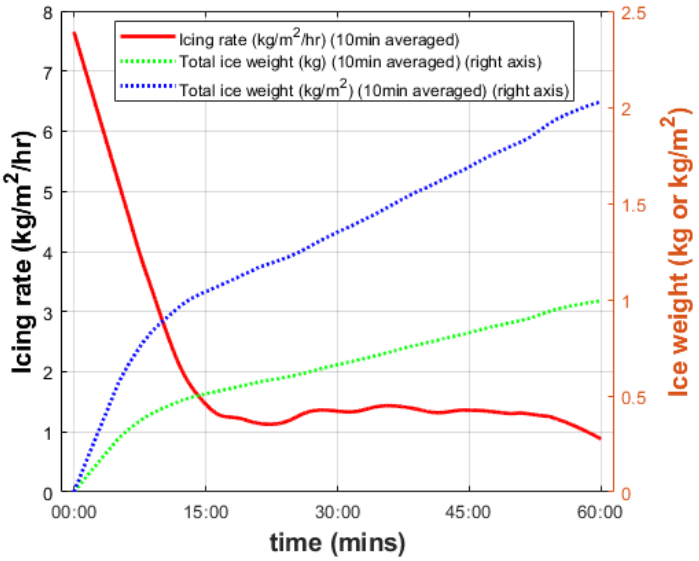

Figure 10: Calculating ice weight per unit area and time averaged icing rates.

6.6. Ice Weight measurements and icing rates

Figure 8 and Figure 9 show the 5 different weights measured for each test and Figure 10 shows the icing rate and ice weight per unit area calculated from the instantaneous total weight of ice on the plate. Most tests showed high icing rate in the initial stages of the test and that quickly declined to a near constant icing rate for the rest of the test. This is clearly spotted in Figure 10, where a knee-bend can be observed for the icing rate. It is later seen in 7.3 how this knee-bend is more visible for lower wind speeds. The reason for this is due to the difference in the thermal conductivities of the plate material and the ice layer and is explained in further detail in 7.2.

As shown in Table 4, r_{ice15} gives the effective icing rate for the first 15 minutes of the test. r_{iceX15} gives the effective icing rate excluding the first 15 minutes of the test. The knee-bend was observed at different times for different test conditions. The knee-bend that was furthest from the start was approximately at 15 minutes. Thus, it was decided to keep 15 minutes as the split time for all tests. Taking different initial time periods would obviously show a difference in the initial effective icing rates. w_{plate} gives the ice weight without ice stalactites after one hour. w_{ice60} and w_{tot} are the weight of total ice on the plate after one hour with ice stalactites. The difference is purely due to the difference in the methods of calculation as shown in Figure 8 and Figure 9. Icing rates (r) in $kg/m^2/hr$ with corresponding prefixes are then calculated as shown in Table 2.

There is a reason for inclusion of all different measurements of icing rates in the analyses that can be attributed to the application. Knowledge about the development of the initial icing rate could prove to be applicable for anti-icing methods using heat, pulse heating, or vibration. Using icing rates that exclude the few initial minutes or those that consider the entire 60 min test duration could simplify long-term estimations for icing. Since the icing rates seem to be much higher in the initial stages of a maximum of 15 minutes, the effect of this high icing rate would disappear for longer test periods. In real conditions, the mean duration for icing events is 15 hours with a standard duration of 13 hours [2], [22]. The icing rates with and without ice stalactites, again depend on the application. Estimation of ice accretion on large surfaces would require the icing rates without ice stalactites as the water forming the ice stalactites would flow to the next 'cell'. Icing rates with ice stalactites would be necessary for estimation of ice accretion where development of ice stalactites is a possibility. In the analyses for individual experiments, the 3 different icing rates after 60 minutes are visualised as an error bar, in Plot 3 of each experiment result figure, for example, in Figure 12 – Plot 3. The median of these 3 values is plotted, and the error bar shows the 2 extreme values.

6.7. Plate divisions and thickness measurements

Each of the 3 plates used in the experiments was divided into a grid of 25 divisions as shown in Figure 11. Since the plates were oriented vertically during the tests, icing observed in the lower parts was higher than that of the upper parts as the water film slides down due to gravity before freezing. This results in different icing rates in different regions on the plate. The icing rate measured by weight could not differentiate between the different regions. For determination of the icing rate by thickness however, at total of 75 measurements were done over the plate, 3 in each division with the depth probe of a vernier calliper. In case of very uneven ice build-up, the extremities or peaks were excluded, and the mean of multiple

measurements was recorded for each of the 75 points. For measurements up to approximately 7-8mm of ice thickness with seawater, the probe could relatively easily pierce the ice. For larger thicknesses, holes had to be bored to take the thickness measurements. An ultrasonic thickness gauge proved of little help for measuring the ice thickness. The reason for this could have been air bubbles in the sea spray ice and the uneven nature of the ice layer that prevented good contact with the probe, in addition to the brine pockets. If using an ultrasonic thickness gauge, it is suggested that the ice surface be gently polished [23], for example, with the probe or a finger, to flatten out the surface. This method could be used if the ice surface is relatively smooth and the ice is without entrapped air bubbles.

4 different thickness measurements are presented in Plot 4 of all the experiments, for e.g., in Figure 12 – Plot 4. These include the mean of all 75 measurements in all 25 divisions of the whole plate, a mean of 18 measurements from each of the 6 divisions of the low icing region and the heavy icing region, and finally a thickness estimation assuming uniform ice layer, calculated from the weight of ice on the plate without ice stalactites (w_{plate}) assuming an ice density of 900 kg/m^3 [4]. Icing intensity is classified into slow, fast, and very fast icing depending on icing rates, which are <10, 10-30, and >30 mm/hr respectively [3], [24]. These intensities are indicated in the same plots.

It should be noted that the ice density was not measured during this experiment, and that literature provides different values of sea spray ice density. Ryerson and Gow, 2000 observed sea spray ice densities between 693-917 kg/m^3. Stallabrass, 1980 assumed an ice density of 890 kg/m^3 [9] ,whereas several other researchers assumed an ice density of 900 kg/m^3 [4], [17], [18] . The value of 900 kg/m^3 is used in the current article only for the purpose of calculation of icing rate assuming uniform ice layer, calculated from ice weight without ice stalactites (i_p).

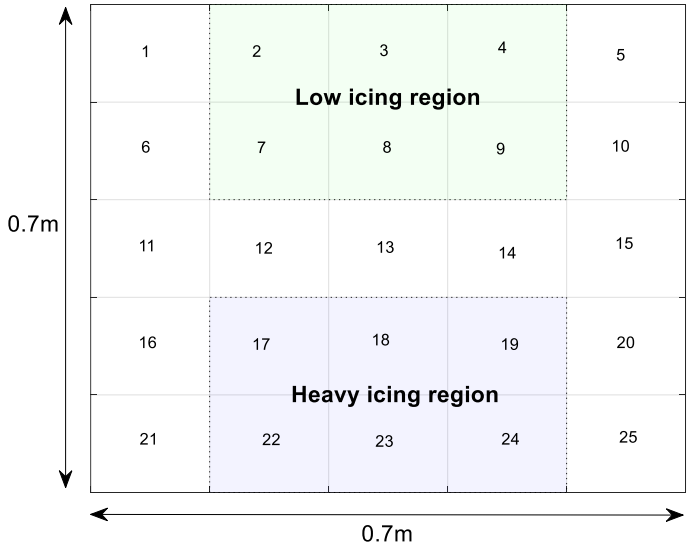

Figure 11: Plate divisions for thickness measurements

7. Results

7.1. Experiment 0: Repeatability

Repeatability is the precision of analytical measurements [25]. An ideal experiment has to be inherently repeatable. However, practically, some variables are difficult to hold constant throughout multiple readings. For testing the repeatability of the current study, 3 readings were taken in with the same set conditions. The measured air and seawater temperatures however, showed some variation. It is thus necessary to find out the amount of variation to be expected in a reading if taken multiple times. The repeatability was tested under one of the set conditions otherwise tested. The set conditions for Experiment 0 - the repeatability test are shown in Table and the results are shown in Figure 12 and Table 4.

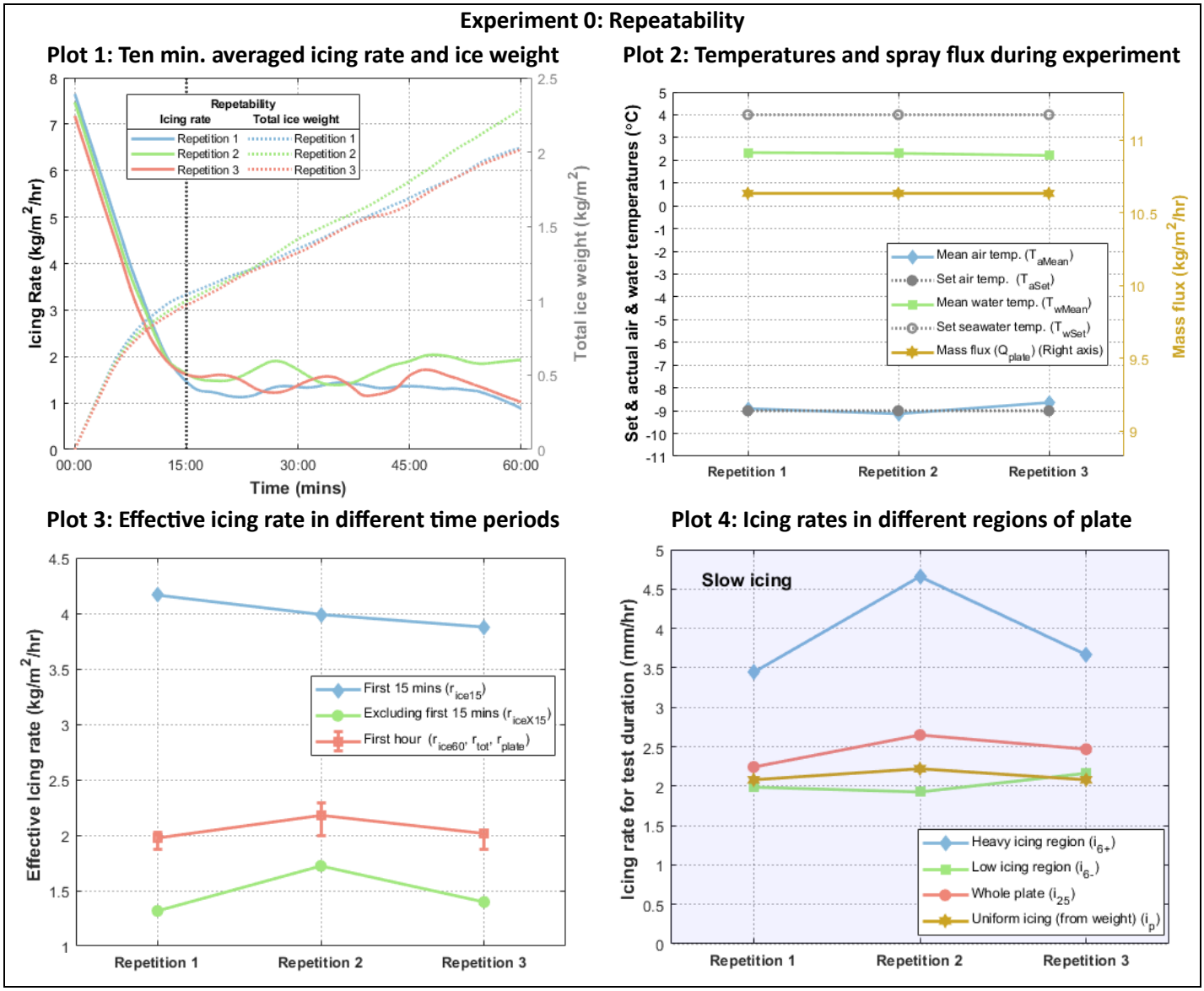

Figure 12: Exp. 0 - Ice weights, temperature & spray flux variations, and icing rates for 3 repetitions with same set conditions.

Figure 12 - Plot 1, shows the variation in the icing rates and the weight of accreted ice during the duration of the three repetitions. Some variations, albeit minor, are visible from this figure. Figure 12 - Plot 2 shows the variations in the mean of measured temperatures in each test. The mean air temperatures show a small variation of less than a degree from the set temperatures. The seawater temperature is about 2°C lower than the set water temperature for each test. Figure 12 – Plots 3 and 4 show minor variations also in the icing rates.

Table 4: Repeatability analysis (Exp. 0)

Test parameters												
Exp nr	Rep nr	Set Parameters								Measured values		
		material	u_{set}	T_{aSet}	T_{wSet}	p_{gauge}	t_s	t_p	s_{ppt}	T_{aMean}	T_{wMean}	Q_{plate}
		-	m/s	˚C	˚C	bar	sec	sec	gms/litre	˚C	˚C	kg/m²/hr
0	1	aluminium	0	-9	4	3	0.25	9	32.45	-8.91	2.34	10.63
0	2	aluminium	0	-9	4	3	0.25	9	32.45	-9.13	2.30	10.63
0	3	aluminium	0	-9	4	3	0.25	9	32.45	-8.64	2.21	10.63
								Mean		-8.89	2.29	
								Rel. Std. error (%)		8.02	1.25	

Test Results															
Exp nr	Rep nr	Ice Weights (kg)					Icing rates								
							by weight (kg/m2/hr)					by thickness (mm/hr)			
		From 10 min moving average			From end readings		From 10 min moving average			From end readings		assuming uniform ice layer	measured		
		w_{ice15}	w_{iceX15}	w_{ice60}	w_{tot}	w_{plate}	r_{ice15}	r_{iceX15}	r_{ice60}	r_{tot}	r_{plate}	i_p	i_{25}	i_{6-}	i_{6+}
0	1	0.51	0.48	0.99	0.97	0.92	4.16	1.32	2.03	1.97	1.87	2.08	2.24	1.99	3.44
0	2	0.49	0.63	1.12	1.07	0.98	3.99	1.72	2.29	2.18	2.00	2.22	2.65	1.93	4.66
0	3	0.47	0.51	0.99	0.99	0.92	3.88	1.40	2.02	2.01	1.87	2.08	2.47	2.16	3.67
				Mean			4.01	1.48	2.11	2.05	1.91	2.13	2.45	2.02	3.92
				Rel. Std. error (%)			6.84	10.11	7.24	5.08	3.35	3.72	9.60	5.81	30.48

The repeatability analysis is shown in Table 4 in terms of relative standard errors (RSE). The actual temperatures cannot be practically kept constant. The RSE in the air temperature was 8.02%, whereas the RSE in the seawater temperature was only 1.78%.

In case of icing rates by weight, the icing rate by weight excluding the first 15 minutes (r_{iceX15}) shows the greatest RSE at 10.11% and all other measures of the icing rates by weight have much lower RSEs.

In case of icing rates by thickness, the icing rates by thickness for the low icing region (i_{6-}) and that for the whole plate, either by measurement (i_{25}) or by weight measurements assuming a uniform icing layer (i_p) show RSEs under 10%. The icing rate by thickness in the heavy icing region of the plate (i_{6+}) however, shows a relatively high RSE of 30.48%.

Sea spray icing is a complex physical phenomenon having multiple independent variables. The experiment with the repetitions is just an example of how, even in controlled laboratory conditions, and the difference in the methods of measurement, there could be a variation in the recorded measurement of icing rates.

7.2. Experiment 1: Effect of material

Lightness, strength, and easy production make aluminium alloys one of the best choice for structures for several kinds of boats and vessels [26]. Construction of large scale container ships uses high strength and thick steel plates [27]. Fire retardant glass reinforced polyester (GRP) is used for construction of hulls and deck for totally enclosed type of lifeboats [28]. Depending on the possibility of procurement, the materials chosen for this study were aluminium alloy AL 5052, steel alloy S355 NVA/NVE, and GRP supplied by VikingNorsafe.

Al 5052 has a high corrosion resistance in marine atmospheres, and has a thermal conductivity of 138.4 W/m·K (W/m·°C) [29]. S355 has a thermal conductivity of 45 W/m·K [30]. Thermal conductivity of polymer resins and glass fibre typically lie in the range of 0.05-0.18 W/m·K and is dependent on several factors including composition [31], [32]. This value, compared to that of steel and aluminium is extremely small. The exact composition of the GRP plate was unknown, and its thermal conductivity was assumed to be 0.18 W/m·K. Thermal conductivity is also a function temperature, and all values mentioned in this section are for ambient room temperature.

Atmospheric icing research has shown that thermal conductivity of a substrate affects the dynamic ice accretion process significantly [33]. Other parameters such as surface coating and surface finish might significantly affect the icing rates [3]. The aluminium and steel plates used for this test were uncoated. For the purpose of this study, thermal conductivity is assumed to be the dominant parameter of differentiation between the materials and effects due to any other parameters are neglected.

This experiment (exp. 1) with thermal conductivity or material as the variable was conducted without wind. All the set input conditions for this experiment are listed in Table .

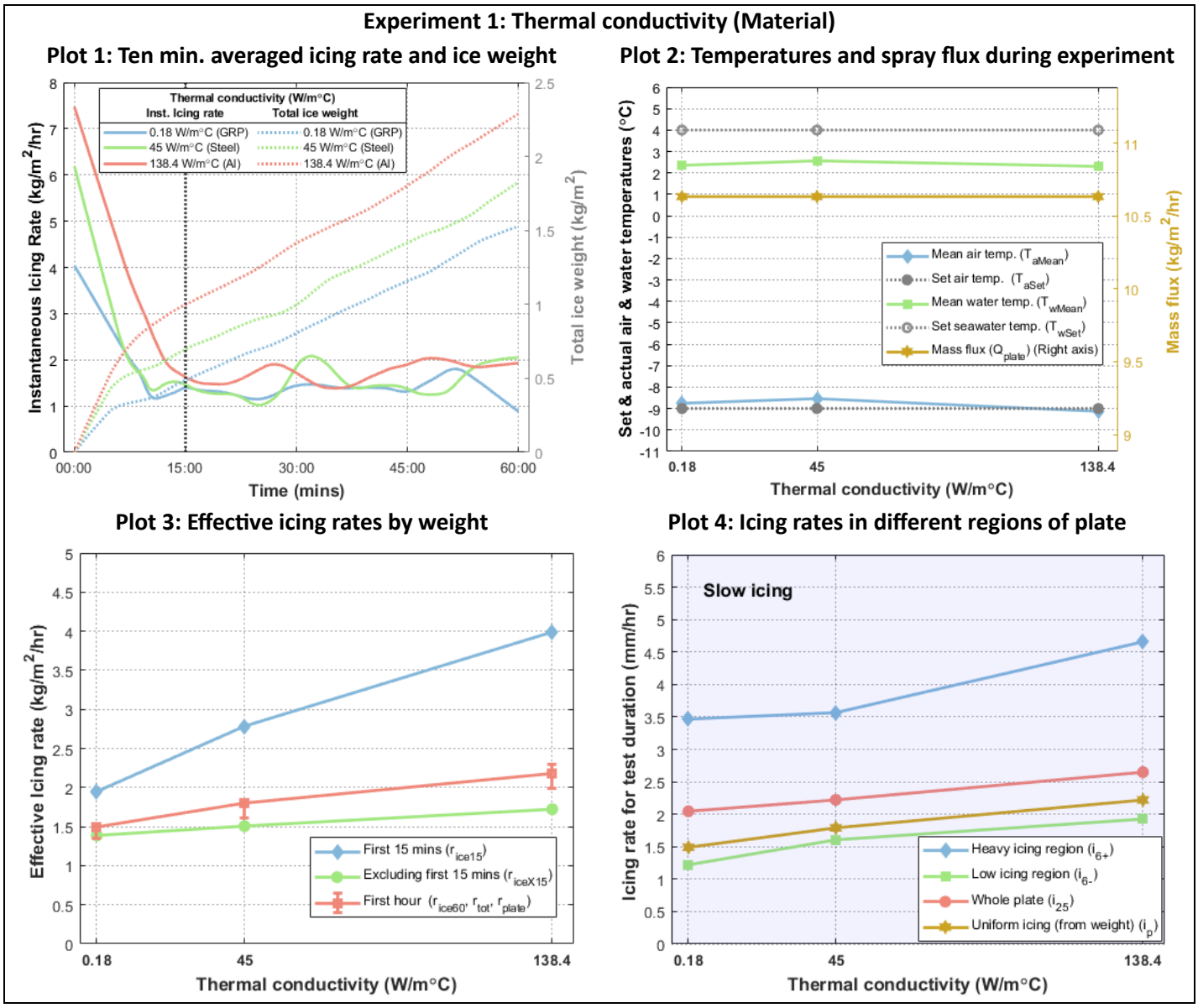

Figure 13: Exp. 1 - Ice weights, temperature & spray flux variations, and icing rates (Variable: Material)

Figure 13 – Plot 3 shows that the mean icing rates for the initial 15 minutes period vary greatly with the thermal conductivity. The Icing rates for the aluminium plate in the initial 15 minutes were close to twice that of the GRP plate. However, if the initial 15 minutes period is neglected, the icing rates have negligible variation with the material. This shows that the material plays an important role only during the initial icing phase, after which, the icing rates are more or less independent of the material of the substrate. This is in agreement to Kulyakhtin 2014, who stated that the average ice growth rate becomes constant after the first few sprays since the heat stored in the substrate is spent in the first few sprays and does not contribute in subsequent spray events [2]. Figure 13 – Plot 1 too, shows how, after 15 minutes, the icing rates for all materials are similar and the ice weight curves for all materials with respect to time are approximately parallel.

Owing to the lack of wind, all materials show slow icing intensity in Figure 13 – Plot 4, irrespective of the region on the plate. The icing thickness in all regions of the plate increases slightly with the increase in the thermal conductivity of the material. However, this increase is quite low. Since the ice thickness was measured only after the culmination of the tests, the icing rates by thickness for the first 15 minutes cannot be commented upon. It is however possible that the small difference in the icing rates by thickness at the end of 1 hour are a result of the unequal icing rates in the initial stage.

Figure 13 – Plot 2 shows that the average temperatures during all the tests in Exp. 1 were stable and deviated by less than a degree between all tests. The seawater temperature was more than a degree lower than the set seawater temperature for all tests.

Summary of results from Exp.1:

Experiment 1 investigates the variation in icing rate due to the material of the freezing surface. The experiment clearly shows that the icing rates in the initial few minutes are dependent on the material, more specifically, the thermal conductivity. As the ice layer builds up, the influence of the material on the icing rate is reduced. The initial ice layer itself insulates the freezing surface such that all materials become 'equal' in terms of further icing. For applications where the initial icing rates are important, for e.g., automation of anti-icing thermal cables, the material is definitely of consequence. In other cases, that require icing rates for a longer period of time, the influence of the material can be neglected as stated by Kulyakhtin 2014 [2].

The plate in the current experimental setup was not insulated, such that the temperature of the freezing surface on the side facing the spray were equal to the temperature at the rear at the start of the test. The temperature inside the hull of a vessel or inside a marine structure, or any other forms of heat sources close to the freezing surface would obviously affect the icing rate, especially in the early phase of the icing period.

7.3. Experiment 2: Effect of wind speed

Wind speed, or relative wind speed is one of the most significant factors contributing to sea spray icing [9]. Wind speed directly affects the evaporative heat transfer coefficient [7]. Higher wind speeds not only lead to faster in-flight cooling of the spray droplets, but also lead to faster freezing of the ice film. Previous research clearly shows that higher wind speeds lead to higher icing rates [8], [9], [15]. Especially during intermittent spray, higher wind speeds lead to faster freezing of the water film between the ice-air interface leading to higher icing rates.

Experiment 2 involved investigating the relation of icing rates to wind speed on and near the freezing surface. In the 4 tests in the experiment, the wind speed was varied for each test with all other parameters constant as shown in Table . Wind speeds were measured near the freezing surface as shown in Figure 6 and were varied from 0-6 m/s in steps of 2m/s. It should be noted that these are the equivalent of relative wind speeds and not the same as U_{10}, which is a standard for forecasting and metrological wind measurement. Relating this experiment to field conditions would require interpretation of these wind speeds in terms of U_{10} and the wind field near and around a ship or marine structure.

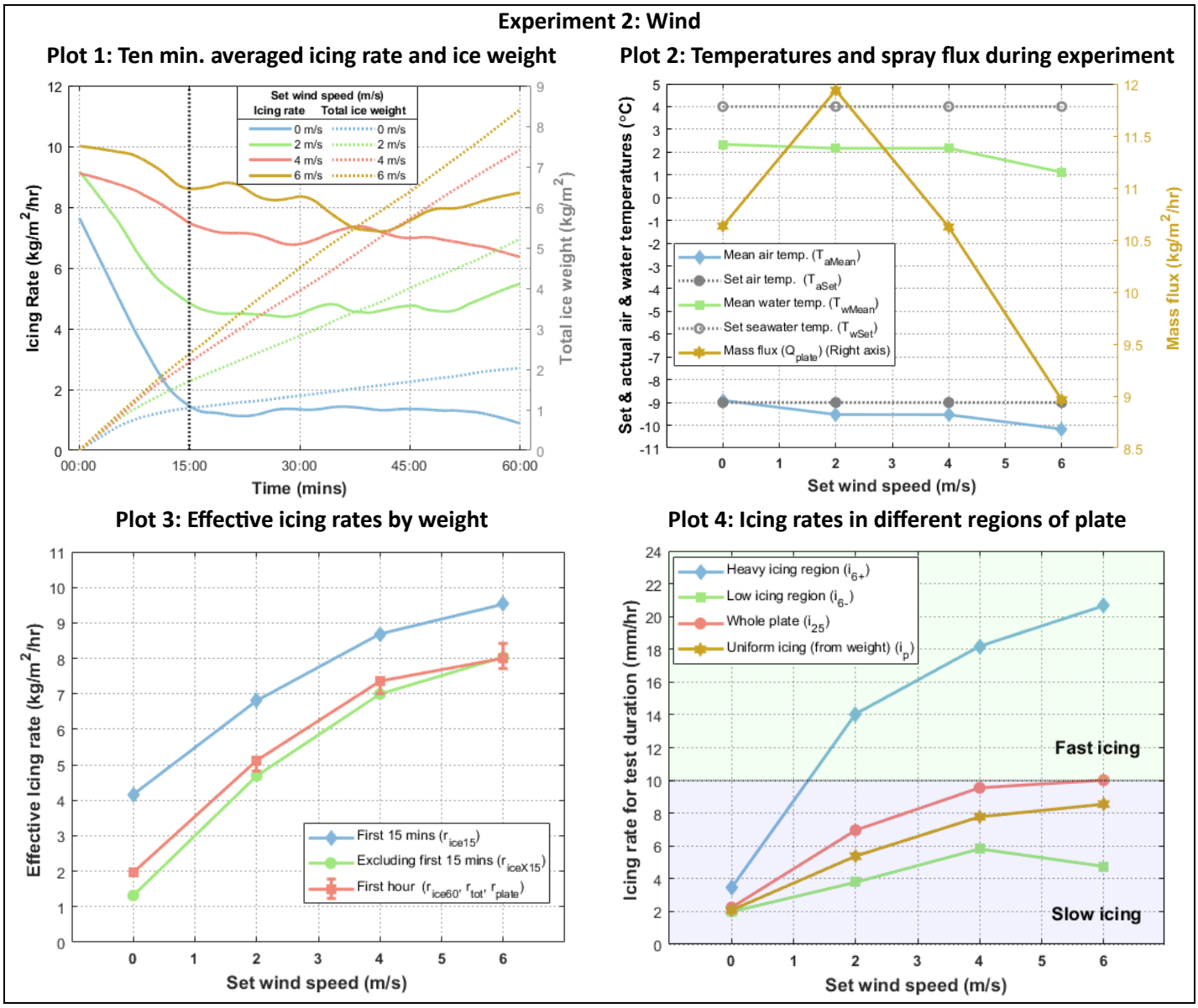

Figure 14: Exp. 2 - Ice weights, temperature & spray flux variations, and icing rates (Variable: wind speed)

Figure 14 – Plots 3 & 4 show how the icing rate increases with the increase in wind speeds. Figure 14 – Plot 3 shows that the icing rates for the first 15 minutes are higher than after the first 15 minutes. The difference however is reduced with increasing wind speeds. This means that as the wind speeds increase, the icing rate becomes less time dependent, at least for the first hour of icing. In case of no wind (which is a hypothetical icing case for field conditions), the rate of icing was 3.15 times higher in the first 15 minutes compared to after it, and 2.05 compared to the icing rate for the complete one hour (including the first 15 minutes), whereas, at 6m/s wind, the initial icing rate was just 1.19 times higher than that excluding the first 15 minutes.

As the wind speed increased from 2 to 6 m/s, the icing rate by weight increased from 5.11 to 8.01 kg/m^2/hr and that by thickness increased from 6.96 to 10.02 mm/hr for the entire plate, and 14.06 to 20.66 mm/hr for the heavy icing region.

Icing rate trends from both, Figure 14 – Plots 3 & 4, show that the change of icing rate with respect to wind speeds is reduced with increase in wind speeds. The icing rate is approaching a constant value at a certain threshold of wind speed.

Figure 14 – Plot 1 confirms this finding. It can be seen that the curves of icing rates and weights for higher wind speeds are closer to each other than the curves for lower wind speeds. From Figure 14 – Plot 1, it can also be seen that the difference in the icing rates in the initial stages, compared to the later stages, is higher for lower wind speeds. This difference is not as visible for higher wind speeds where the time dependence of wind speeds on icing rates becomes lesser. Since all experiments starting from experiment 3, are performed with a wind speed of 6m/s, this 'knee bend' that is seen for 0 and 2 m/s wind, would not be as prominent as in Plot 1 of Figure 12, Figure 13, and Figure 14.

The experimental setup did not allow for testing at higher near surface wind speeds than 6m/s, so the threshold of windspeed when the icing rate stops increasing remains to be found. It must also be considered that higher wind speeds will increase the inflight cooling of incoming spray.

Figure 14 – Plot 4 shows that the heavy icing region on the plate experiences fast-icing already at 2m/s wind. The mean icing rate for the entire plate, approaches fast icing for higher wind speeds. The local variation in the icing rates measured in mm/hr are dependent on the local flux on the freezing surface. Although the total mass flux across the plate surface was measured, the local flux at each of the 25 divisions on the plate was out of the measurement scope. In a way, this is analogous to field conditions where different regions on the ship will have different amounts on incoming spray leading to different icing conditions, but this is not a point of consideration for the current study.

Though the mass flux through the nozzle was constant throughout this experiment, the mass flux measured at the plate varied due to the wind affecting the flow of the droplets and driving some away from the plate. It is interesting to notice although the icing rate increased with wind speeds, Figure 14 – Plot 2 shows that the flux measured at the plate decreased with increase in wind. This means that the icing rates increased even though lesser water impinged on the plate. Due the variation of spray flux for different wind speeds, the flux acts as a covariate, and if ideally kept constant, could give a slightly different curve for the icing rates in Figure 14 – Plots 3 & 4. In ideal experimental conditions, the flux across the plate should remain constant despite of varying wind speeds. The drop in the icing rate in the low icing region for 6m/s wind could be attributed lesser spray reaching this region of the plate at higher wind speeds. Figure 14 – Plot 2 also shows that the experiments with the highest wind speed had lower mean air and seawater temperatures than the other tests. This might have resulted into an overestimation of icing rates at higher wind speeds.

Summary of results from Experiment 2:

Experiment 2 concerning relation between the icing rates and wind speeds gives a clear indication that the icing rates are highly dependent on wind speeds. For further analysis, the role of the covariates, i.e., the air and water temperatures, and especially the spray flux, needs to be evaluated.

The mean icing rate in terms of weight was almost 4 times higher at 6m/s wind than without wind. The icing rate in terms of thickness was approximately 5 times higher for 6m/s wind compared to no wind

irrespective of the region on the plate. This confirms that wind plays a significant role in determining the icing rates due to sea spray icing.

7.4. Experiment 3: Effect of Air Temperature

Experiment 3 investigates the role of air temperature for sea spray icing rates. Along with wind speed, air temperature is one of the two most significant factors for determining icing severity [9]. Lower air temperatures lead to quicker freezing of the water film between sprays, leading to higher icing rates. Experiment 3 consisted of 3 tests at different set air temperatures, under the freezing temperature of -1.8°C at 32.9ppt salinity (Eq. (1)), with the other conditions constant as given in Table .

$$Freezing\ point\ of\ saline\ water = -0.002 - 0.0524 \cdot s_{ppt} - 6 \times 10^{-5} \cdot s_{ppt}^2 \qquad \textit{Ref:}\ [9] \qquad \textit{Eq. (1)}$$

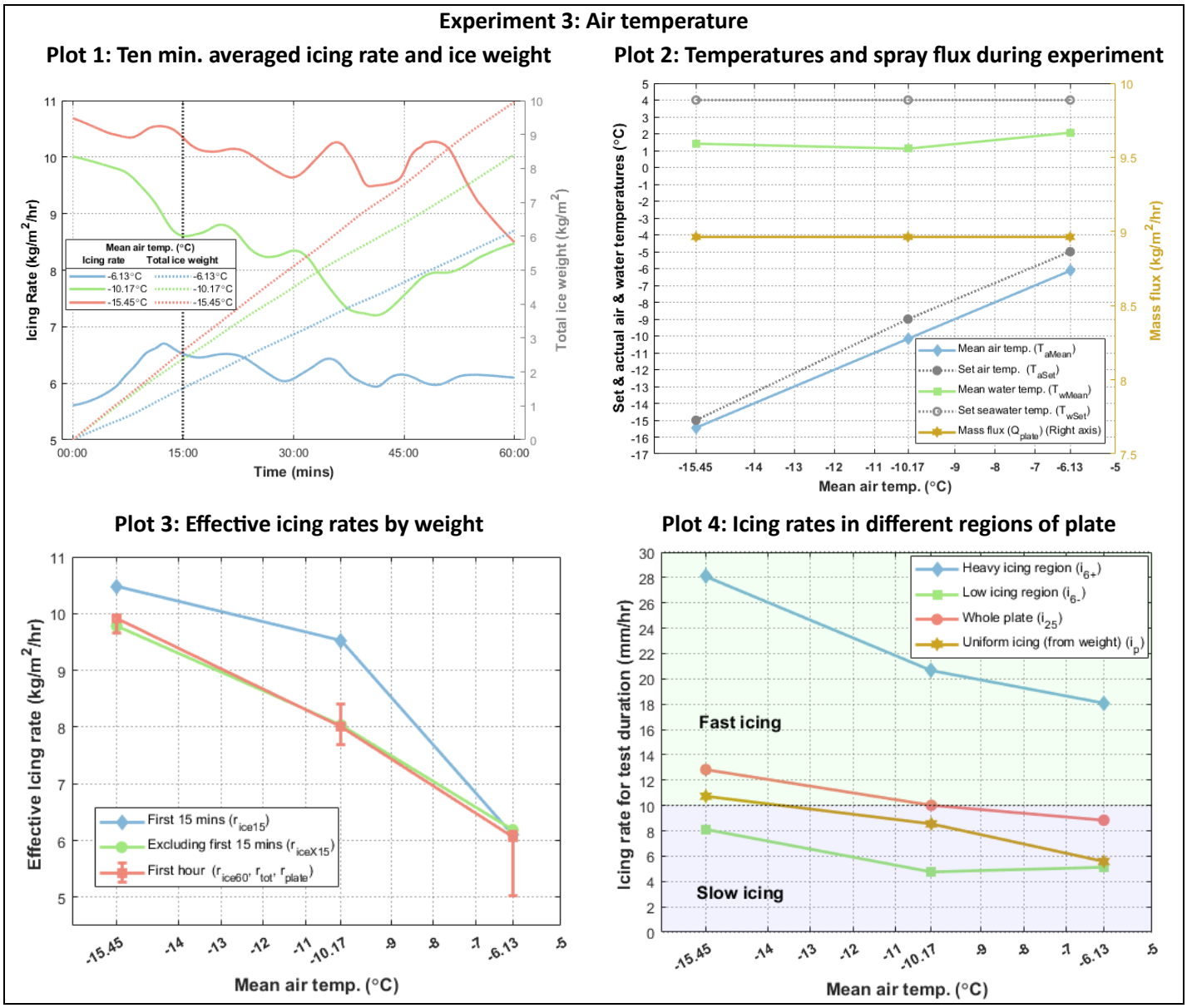

Figure 15: Exp. 3 - Ice weights, temperature & spray flux variations, and icing rates (Variable: Atmospheric temperature)

The three tests in this experiment were carried out at set air temperatures of -15°C, -9°C, and -5°C with recorded mean air temperatures of -15.45°C, -10.17°C, and -6.13°C respectively. Since this experiment focussed on air temperatures, for which the measured values were available throughout all the tests, the graphs in Figure 15, unlike the other experiments, are plotted against the measured mean air temperatures rather than the set air temperatures.

Figure 15 – Plots 3 & 4 show a clear trend where the icing rate increases with decrease in air temperature. Except for the initial 15 minutes, all measures of icing rates in terms of weight show almost a linear increase with the decrease in temperature for the range of temperatures tested. The icing rate in terms of weight increased from 6.06 kg/m^2/hr at a mean air temperature of -6.13°C to 9.92 kg/m^2/hr at -15.45°C corresponding to an increase of 0.41 kg/m^2/hr/°C fall in air temperature if linear relation is assumed. The

icing rates in terms of thickness increased by 4mm/hr for the entire plate, and 10mm/hr in the heavy icing region as the mean air temperature dropped from -6.13°C to -15.45°C.

There is only a small difference in the icing rates in the initial 15 mins as compared to the rest of the test for the tests with lower temperatures. This can also be confirmed from Figure 15 – Plots 1 where the deviations in the icing rates are comparatively low as compared to the experiment with wind at lower wind speeds.

In case of the icing rate in the first 15 minutes, the change of icing rate with temperature is higher for higher temperatures (from -6.13°C to -10.17°C) compared to lower temperatures (from -10.17°C to -15.45°C). The increase in icing rate due to air temperature is more or less linear if the first 15 minutes are neglected. The difference in the initial and overall icing rate in case of the highest temperature of -6.13°C however, is almost constant. Reasons for this could be that the marginal difference in the atmospheric temperature to that of the freezing temperature of seawater (4.33°C for the test with mean air temperature of -6.13°C) leads to slow freezing of the impacting seawater and might cause some of the accreted ice to melt in the initial stages when the ice layer is thin. The small difference in temperatures could also lead to lack of adhesion between the ice and the surface causing some of the ice sliding away due to weight in case of vertical surfaces. This was observed in case of the test with -6.13°C as shown in Figure 16. Plot 1 of Figure 15 also shows how, for the test with -6.13°C air temperature, the icing rate actually increases with time in the initial period.

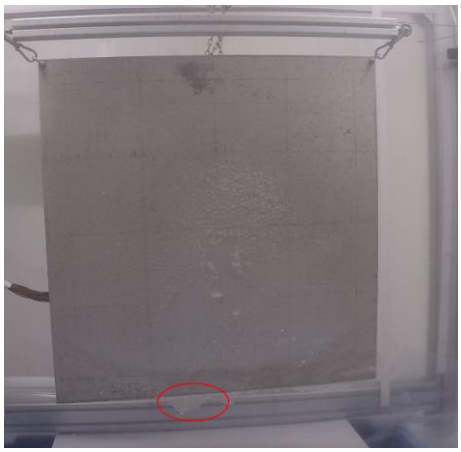

Figure 16: Breakup of initial ice layer at higher temperatures

Another important point to notice in Figure 15 – Plot 3 is that the icing rate in terms of weight has longer error bars for higher temperatures. As mentioned in 6.6, the error bar denotes difference in values due to difference in the interpretation of the weight of ice accreted. This means that the method of calculating the weight of ice accreted plays an important role for higher temperatures. The reason for this is that the formation of ice stalactites was more for higher temperatures. This was confirmed from the pictures from the tests shown in Figure 17.

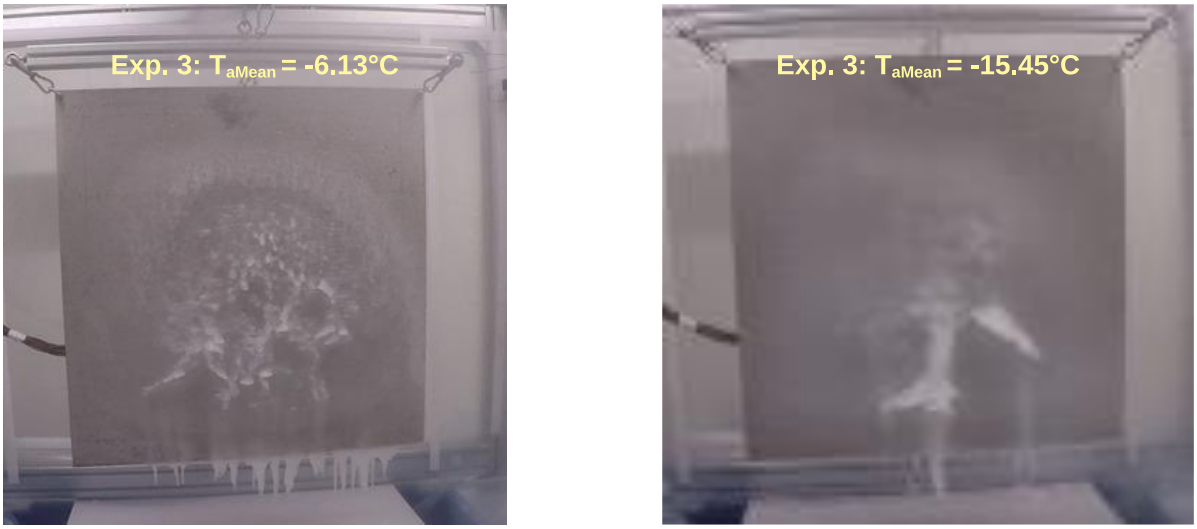

Figure 17: Testing effect of air temperature - More ice stalactites at higher air temperatures

Due to slower freezing for higher temperatures, a considerable amount of impacting spray water trickles down or 'runs off' before freezing, giving rise to more ice stalactites. Depending on the application, either the total weight of ice on the plate with the ice stalactites would be required, or in case a larger surface area is considered, the ice specifically on the projected area would be considered with the ice stalactites ice being a part of another 'cell' during the calculations. However, in case of larger surfaces the middle 'cells' will have a similar amount of water coming in from upper 'cells'.

Figure 15 – Plot 4 shows that the heavy icing region of the plate experiences fast icing rates for all temperatures. This is owing to the fact that the standard wind conditions throughout the experiment were of 6m/s. As the air temperature falls, it is seen that the mean icing rate for the entire plate too, experiences fast-icing.

Figure 15 – Plot 2 shows that the mean air temperature throughout the tests for higher air temperatures was at least a degree lower than the set temperature. This however has no implications on the results of this experiment since the results are reported at the actual mean air temperatures recorded during the individual tests. The seawater temperature was a bit higher for the test with -6.13°C air temperature than that of the other 2 readings, which could suggest some underestimation of the icing rates for this test at the given mean air temperature. All the 3 tests in this experiment had the same spray flux.

Summary of results from Experiment 3:

Atmospheric temperature is one of the most important factors in sea spray icing. The icing rates show a near linear increase due to the decrease in atmospheric temperature. The icing would start at a maximum temperature just lower than the freezing point of seawater, which depends on the salinity (-1.8°C for the salinity of 32.9ppt of the seawater used for this experiment). It was observed from the experiment that the icing rate increased by 0.41 kg/m^2/hr/°C fall in air temperature if linear relation is assumed. In addition, at higher air temperatures close to the freezing point of seawater, freezing of the water film is slow. This

leads to the impinged water trickling down at a higher rate then at lower air temperatures before it freezes. This showed an increase in ice stalactites i.e., more ice hanging below the plate. In certain situations where there is danger of falling ice, it could be said that the ice formed at temperatures closer to the freezing point pose a greater threat. This difference in the ice formed at lower and relatively higher freezing temperature also affects how the total mass of accreted ice is calculated. At temperatures closer to the freezing point, the total mass of ice on the projected surface area of the plate would be relatively lower than if the weight of the ice stalactites is included. This could prove to be important during ship stability calculations.

7.5. Exp. 4: Effect of Sea Temperature

Experiment 4 investigates the role of the surface sea temperature in sea spray icing. Sea temperatures are of moderate significance for sea spray icing [9]. It could be imagined that at constant atmospheric temperatures, lower sea temperatures lead to higher icing rates due to lesser time taken for the water film to freeze owing to lower difference in sea and atmospheric temperatures.

As shown in Figure 18 – Plot 2 (and Plot 2 for all other experiments), the seawater temperature was measured at 2 places, upstream of the nozzle, one in the freezing room, and one in the cooling room. The temperature had to be registered due to two practical difficulties in keeping the seawater temperature constant in the entire system; the first being the rise of temperature due to the pump, and the second being the periodic stagnation of the seawater in the line leading to the nozzle, in the freezing room (more in section 6.2).

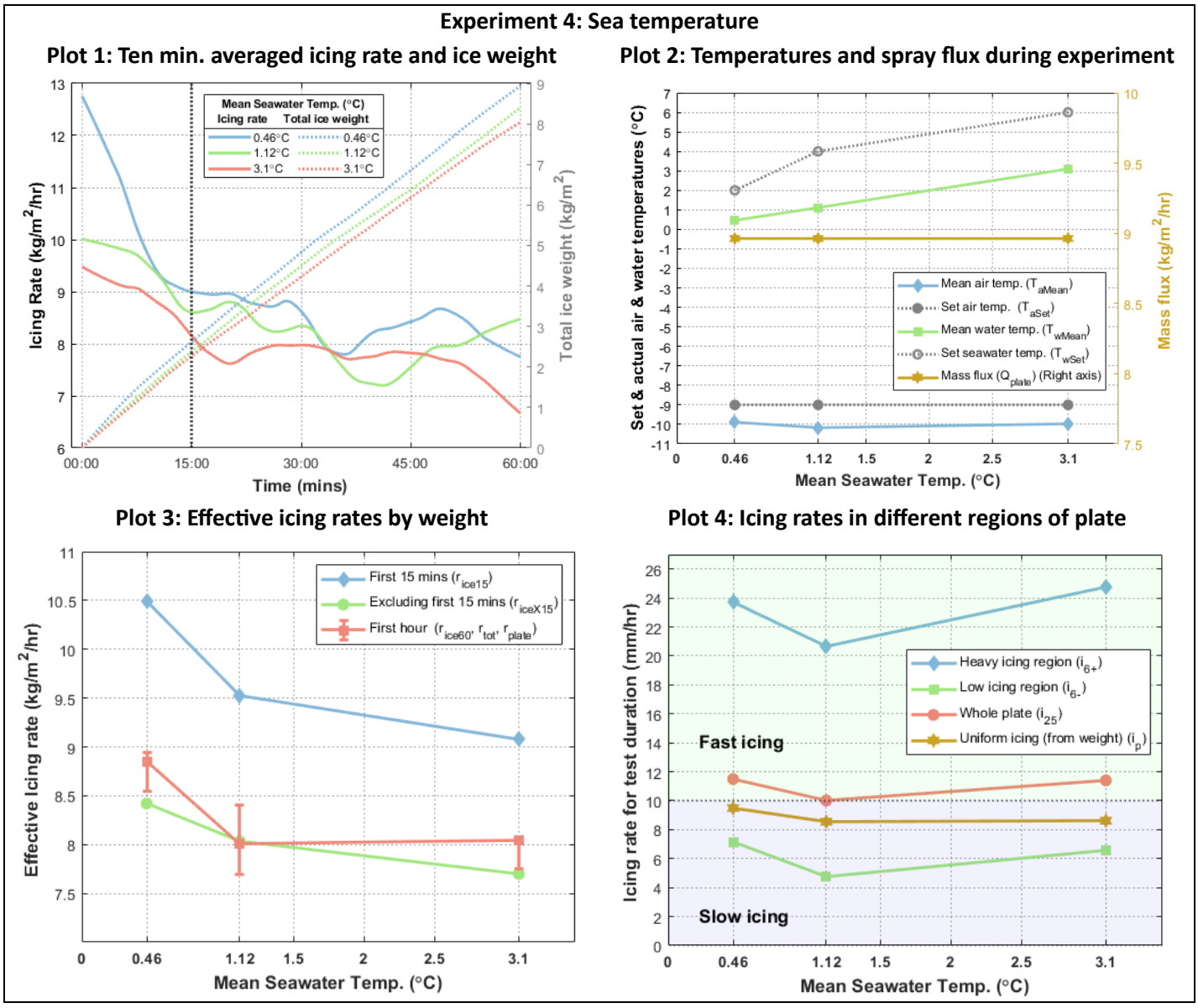

Figure 18: Exp. 4 - Ice weights, temperature & spray flux variations, and icing rates (Variable: Seawater temperature)

The three tests in this experiment were carried out at set seawater temperatures of 2°C, 4°C, and 6°C with recorded mean seawater temperatures of 0.46°C, 1.12°C, and 3.1°C respectively. Since this experiment focussed on seawater temperatures, for which the measured values were available throughout all the tests, the graphs in Figure 18, unlike the other experiments, are plotted against the measured mean seawater temperatures rather than the set seawater temperatures.

Figure 18- Plot 3 shows an increase in the icing rates for the first 15 minutes and the rest of 45 minutes of each test with decrease in seawater temperature. The absolute increase is however, small; 0.72 kg/m^2/hr for a 2.64°C drop in the set seawater temperature; showing that the sea temperature is not as significant as wind and atmospheric temperature in the sea spray icing process. This can also be seen in Figure 18- Plot 1, where the icing rates for all the three tests are very close to each other.

The icing thickness calculated from weight with an assumption of uniform icing over the entire plate shows an increasing trend in Figure 18- Plot 4. The values of all the different measurements of ice thickness differ with only 2-3 mm in corresponding regions over the complete range of seawater temperatures that are tested. It should be pointed out that the unconfirming trend of the physical mean thickness measurements could be a result of complexity for measurements due to uneven ice accretion as shown in Figure 17. This is the reason for inclusion of the data where uniform icing is assumed. In cases where the difference in icing rates does not significantly increase due to change in a certain variable, such as experiment 4, it could happen that the trends for measured ice thickness visible in the graph do not reflect the real trend due to either the practical difficulties in achieving ideal test conditions, or the random selection of points for thickness measurement within individual plate divisions.

The temperatures in Figure 18- Plot 2 show that the mean seawater temperatures were lower than the set seawater temperatures, as the setup did not allow for complete control over the seawater temperatures. This however has no implications on the results of this experiment since the results are reported at the actual mean seawater temperatures recorded during the individual tests.

Summary of results from Experiment 4:

Figure 18- Plot 3 shows a clear trend of higher icing rates with lower seawater temperatures. The difference between the icing rates over the range of mean seawater temperatures tested is, however, not as significant as due to the variation of wind and atmospheric temperatures. This confirms that the seawater temperature is only of moderate significance for sea spray icing.

7.6. Experiment 5: Effect of Spray flux

Depending on weather and spray parameters, ice accretion due to periodic sea spray icing may involve melting and freezing cycles. On each incoming spray in this case, the layer of ice at the ice-air interface melts due to the impinging seawater that is warmer than the ice. Freezing of this layer takes place in between 2 consecutive sprays [3]. The amount of seawater impinging on a freezing surface, i.e., the spray flux, directly affects the amount of ice accretion [34]. In general, the increase in the spray flux impinging on the plate increases the rate of icing up to a certain threshold of flux for the given conditions. However, over this threshold, it is possible that the incoming spray with a larger amount of water might melt or wash away some of the ice; the extreme condition of which is wave washing, where there is no ice accretion as the ice is mechanically removed by sea waves [4]. This suggests that the icing rate depends significantly on the incoming spray flux.

In experiment 5, the spray flux was varied by adjusting the pressure in the system with the control valve as shown in Figure . Each reading corresponds a gauge pressure of 1, 2, and 3 bars respectively measured approximately 1.5m before the nozzle. Finding the threshold of flux at which the icing rate falls was out of scope of the current experiment. Since the droplet size distribution through nozzles are dependent on pressure, this could be considered as another covariate in the experiment. The effect of droplet size is however not considered, rather, the selection of the nozzle is based on the droplet sizes used in previous literature (see section 3.1).

Studying the variation of icing rates due to change in the spray flux is also important since the flux was a covariate in several experiments in the current study due to the fact that the spray flux showed variation due to wind, spray duration, and spray period.

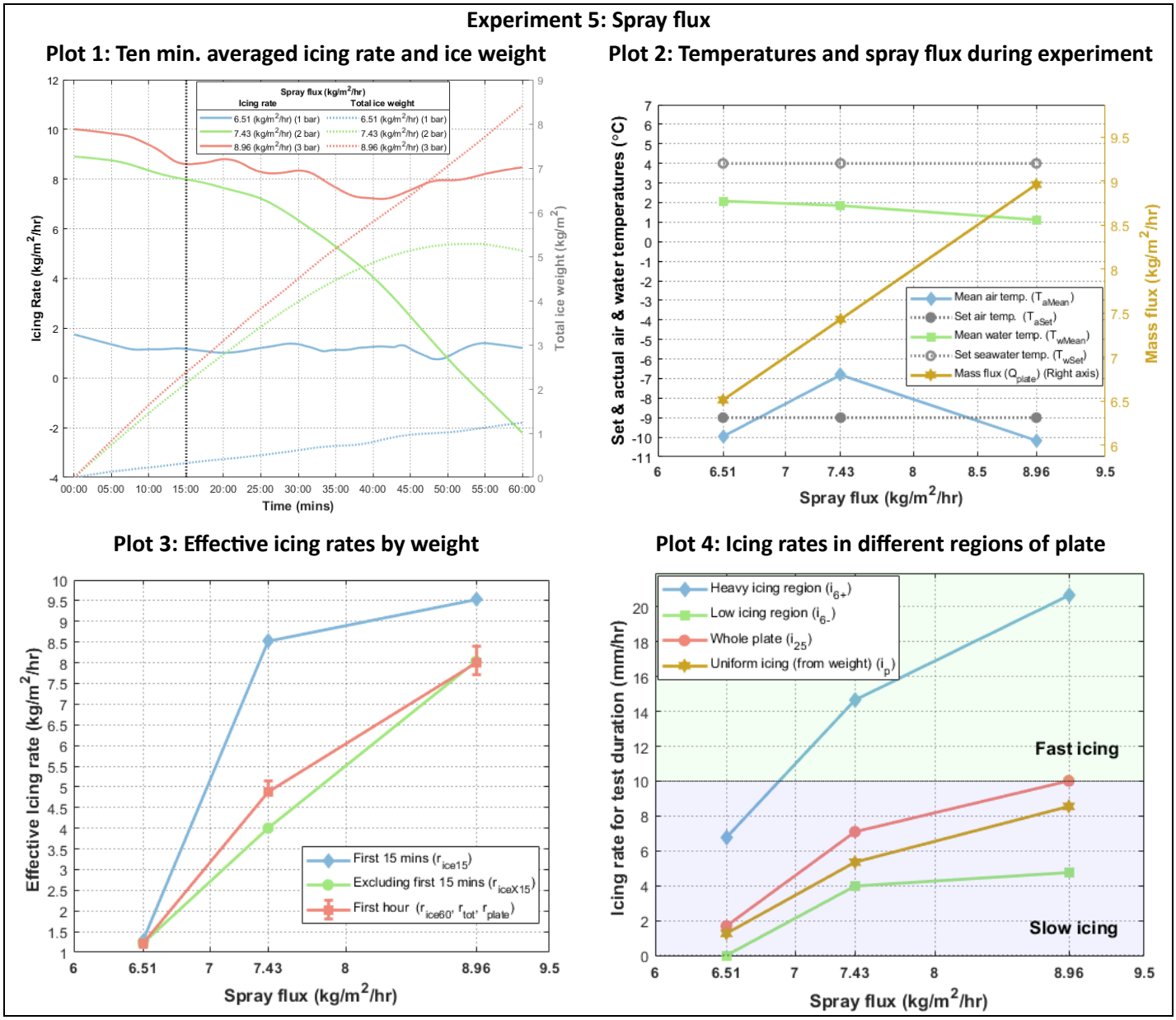

Figure 19: Exp. 5 - Ice weights, temperature & spray flux variations, and icing rates (Variable: Spray flux)

Figure 19 – Plots 3 & 4 show that the icing rate increases with the increase in spray flux. The icing rate by weight for the lowest flux at 1 bar pressure however was unexpectedly low. This could have been due to the fact that the low pressure of just 1 bar in the system did not carry the spray as well as in the other tests with 2 and 3 bars of pressure. This can also be seen in the value of icing rate by thickness that is zero in the low icing region for the test with the least spray flux. This would have led to severe underestimation of ice weights and thereby icing rate.

Additionally, Figure 19 – Plot 2 of the actual conditions in the experiment shows that the air temperature for the second reading was significantly higher than the set temperature. This suggests that the icing rates for this case might be underestimated. This can be an explanation of the dip in the icing rate towards the end of the second test with 2 bars of pressure and a flux of 7.43 kg/m^2/hr in Figure 19-Plot 1.

Summary of results from Experiment 5:

"When researchers selectively report significant positive results, and omit non-significant or negative results, the published literature skews in a particular direction. This is called 'reporting bias', and it can cause both casual readers and meta-analysts to develop an inaccurate understanding of the efficacy of an intervention." [35]

Except for the test with 3 bars of pressure with a flux of 8.96 kg/m^2/hr, the other two results are not reliable. The test with a pressure of 2 bars (flux of 7.43 kg/m^2/hr) showed an unexpected dip in the ice weight at the end of the test, the reason for which could not be pinpointed, but can be a result of the higher mean temperature in the freezing room. More importantly, the test with 1 bar pressure (flux of 6.51 kg/m^2/hr) did not seem to carry the spray well on to the plate. This could have resulted in false spray flux measurement since the entirety of the plate was not exposed to the spray and resulting into a severe underestimation of icing rate.

A suggested improvement while repeating this experiment would be to use higher pressures to vary the spray flux. This was unfortunately not possible for the current setup where a maximum of 3 bar pressure measured 1.5m before the nozzle.

Throughout the current study, there was an indirect variation in the spray flux due to other factors like wind, spray duration, and spray period in the other experiments. Analysis of the effect of the spray flux on icing rates could be done from these readings using statistical procedures.

7.7. Experiment 6: Effect of Spray Duration

Several existing sea spray icing models use the liquid water content (LWC) in kg/m^3 per spray as a variable for estimating icing rates [2], [7], [9]. It is a function of wave height, and researchers have presented various methods to estimate the LWC [6], [36]–[38]. The spray duration, along with the spray period, is dependent on wave and ship characteristics. Overland 1990, points out that icing forecasts provided by weather services is based on meteorological data, but for ship specific forecasts, the vessel length, wavelength, and wave height are all important factors [8].

The aim of having the spray duration as a variable is to investigate how the wave height (along with the wavelength and ship characteristics) play a role in sea spray icing. Although this analysis regarding the wave and ship characteristics is beyond the scope of the current study, experiment 6 investigates the direct relation of the spray duration with sea spray icing.

The spray duration and spray period are complex functions of factors including the wavelength, wave height, wind, ship characteristics, and sailing direction. In general, keeping the spray period constant and increasing the spray duration gives less time for the water film to freeze before the arrival of the next spray. Since the spray frequency or period is kept constant in this experiment, the number of sprays per hour for

all 3 tests are constant at 400 sprays/hour. This experiment assumes that the spray flux per hour would naturally increase owing to the increase in the spray duration of individual sprays. This causes the spray flux to be a covariate in the analysis for spray duration.

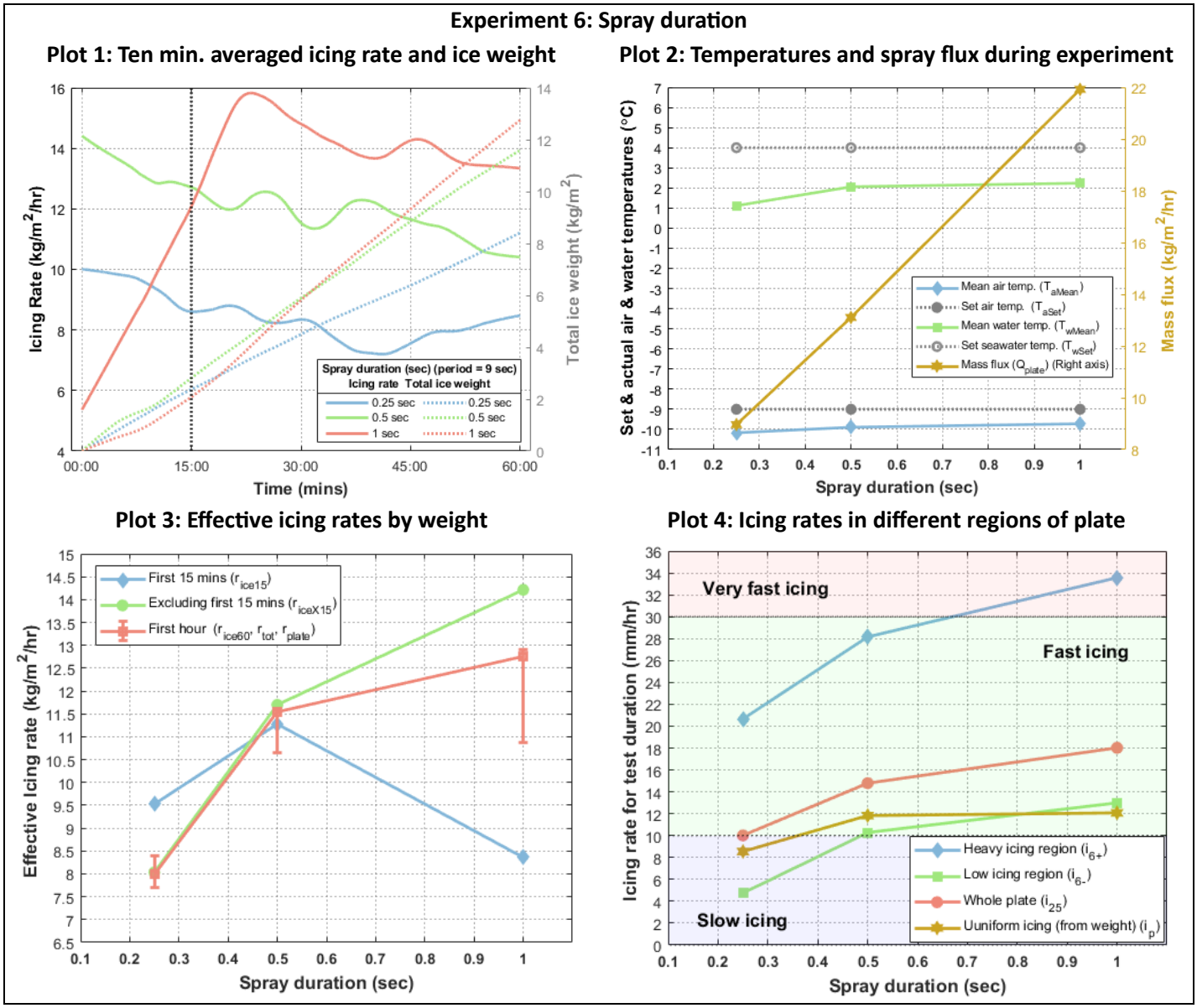

Figure 20: Exp. 6 - Ice weights, temperature & spray flux variations, and icing rates (Variable: Spray duration)

Figure 20 – Plot 3 shows that the mean icing rate recorded in the first 15 minutes goes up when the spray duration goes up from 0.25 seconds to 0.5 seconds. However, at a spray duration of 1 sec, the mean icing rate during the first 15 minutes falls significantly. Increasing the duration of spray adds more flux to the plate. The thin layer of ice formed at the start would be partially washed away due to the incoming spray. The icing rate for the remaining 45 minutes, however, suggests that once the initial ice layer builds up, the icing rate increases much more than when the spray duration is small. This phenomenon can be observed in Figure 20 – Plot 1 where the icing rate for a spray duration of 1 second is the lowest at the start and

steadily increases to a higher icing rate than the smaller spray durations. As seen in experiment 1, as the initial ice layers develop, the effect of the freezing surface on the icing rate decreases.

This is an example why it is important to study the icing rates also in the initial stages of icing. This difference between the initial and later icing rates could help to optimise anti-icing systems. To the best of authors' knowledge, none of the previous models have taken this difference in icing rates in the initial and latter stages of icing into consideration. However, as discussed earlier in experiment 1, when an icing event lasts for a relatively longer duration (several hours), the initial icing rate is of less importance.

The increasing error bars in Figure 20 – Plot 3 also suggest that there is a significant difference between the weights recorded with and without the ice stalactites. This in turn means that as the spray duration (and spray flux) increases, more water flows down and freezes below the projected area of the plate causing larger or more ice stalactites. As discussed earlier, although the ice stalactites can be said to be a part of the next lower 'cell' for calculations, in case of large surfaces, a similar amount water could be expected to enter from the upper 'cell' into the current one.

Figure 20 – Plot 4 for icing thickness rates show the heavy icing region of the plate experiencing 'Very fast icing' for a spray duration of 1 second. It is clear from Figure 20 – Plot 2 that the reason is the close to 2.5-fold increase in the spray flux compared to a spray duration of 0.25 sec. It is clear that the thickness of the accreted ice increases with the spray duration. It can also be noticed that the uniform icing thickness calculated from the weight over the entire plate not as high. This suggests that the icing becomes relatively more non-uniform as the spray duration increases.

Figure 20 – Plot 2 shows the significant increase in spray flux due to increase in the spray duration. To study the variation of icing rates due to change in spray duration, the flux ideally should have been kept constant throughout the experiment. Flux was something that was not directly controlled in the experiments, but changed primarily by changing the pressure in the system, and was further affected by wind. It was thus practically not possible to keep the flux constant. The average temperatures were a lower than the set temperatures indicating slight overestimation of the icing rates.

Summary of results from Experiment 6:

Though this experiment is aimed to study the dependence of icing rates on the spray duration, the significant difference in the spray flux makes it a significant covariate. Further investigation is necessary to form a conclusion about the dependence of the icing rates purely on the spray duration with a constant flux. If it is assumed that the flux would naturally increase as a result of increase in the spray duration, the test clearly shows higher icing rates for higher spray duration. This however would be true up to a certain threshold of spray duration, after which the rate of ice formation could slow down or eventually stop as the heat from incoming water limits the freezing of the water film on the plate. Analysing this threshold could be a suggestion for further research. Using the results for the spray duration for field estimations would necessitate interpretation of this data in terms of ship and wave characteristics.

7.8. Experiment 7: Effect of Spray Period/ Spray Frequency

Spray period is the time between two consecutive sprays. Spray period or spray frequency, just as spray duration, is a complex function of the ship characteristics and sea conditions. The frequency of spray impact on marine surfaces depends on the speed of the vessel relative to the wavelength and direction of the waves [10]. Overland, 1990 also suggests that the number of deck wettings, i.e., the frequency of spray is a function of significant wave height, speed of the vessel, and its length [8]. If the time between 2 consecutive spray events increases, the water film would get more time to freeze completely in between the 2 sprays. Since the spray period is changed, the number of sprays per hour changes for all the 3 tests in this experiment with 1200, 600, and 400 sprays per hour for spray periods of 3, 6, and 9 seconds respectively. Since the spray duration is kept constant, though the flux per spray is constant, the spray flux per hour for higher spray periods will naturally reduce due to the lesser number of sprays. This experiment assumes that the spray flux per hour would naturally decrease owing to the increase in the spray period or the time between 2 consecutive sprays. This causes the spray flux to be a covariate in the analysis for spray period.

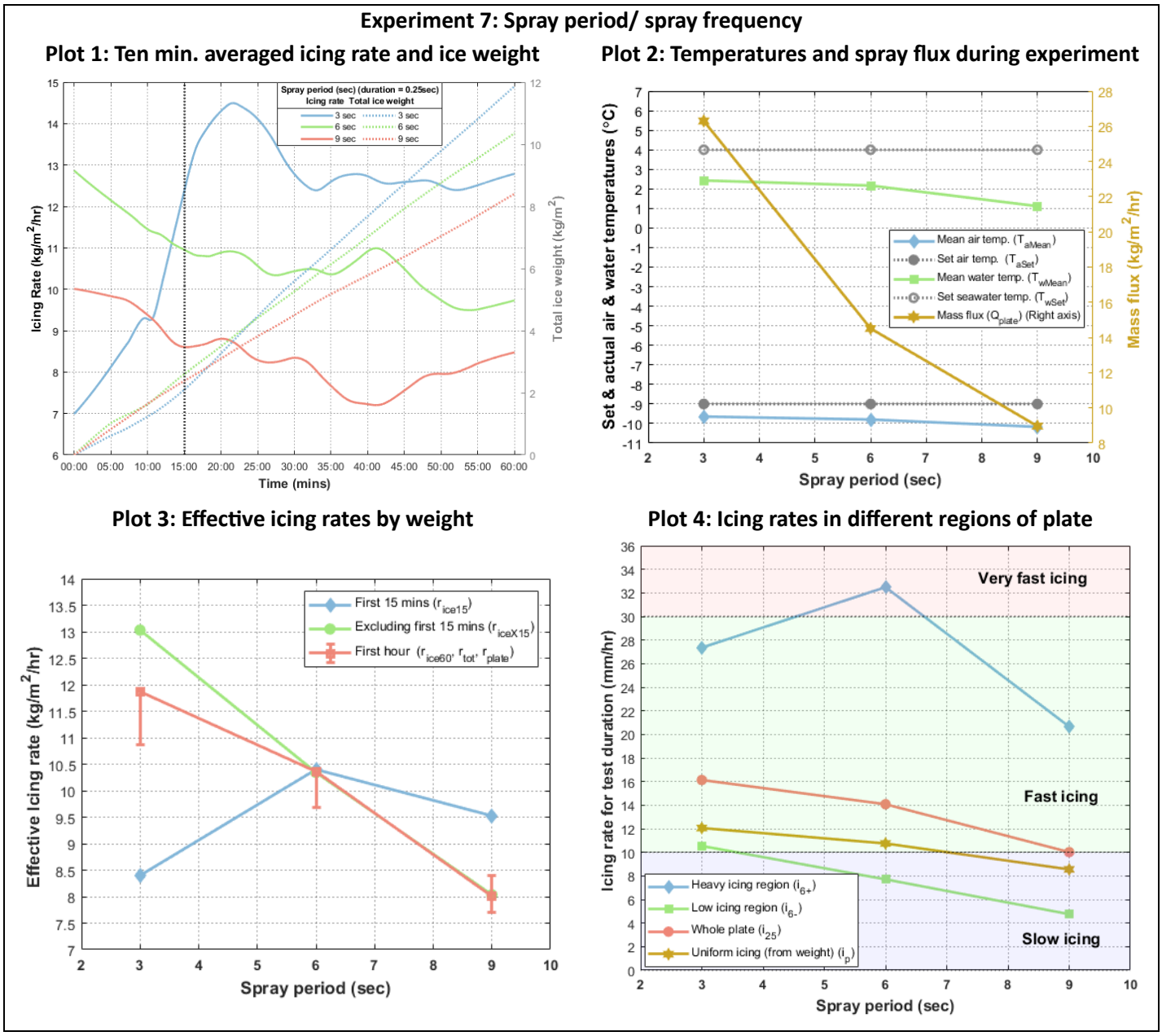

Figure 21: Exp. 7 - Ice weights, temperature & spray flux variations, and icing rates (Variable: Spray period)

Figure 21 – Plot 3 shows that as the spray period increases (as spray frequency decreases), the icing rate in terms of weight decreases. This is a direct result of the decreasing spray flux on the plate per hour. Figure 21 – Plot 2 shows the 3-fold decrease in the spray flux per hour as the spray period increases.

The icing rate in the first 15 minutes for a spray period of 3 seconds is much lower than in the latter part of the test. The reason is similar to the case of higher spray duration in experiment 6. The water film on the plate does not get enough time to freeze completely owing to the less time between incoming sprays and thus keeping the surface relatively warm. However, after the formation of the first few layers of ice, the ice keeps on growing rapidly. This too, as in case for experiment 6 with spray duration, can also be observed in Figure 21 – Plot 1, where the icing rate for the spray period of 3 seconds is initially lower

compared to higher spray periods, but eventually increases steadily to have the highest icing rate. As seen in experiment 1, as the initial ice layers develop, the effect of the freezing surface on the icing rate decreases.

Figure 21 – Plot 4 shows that the icing rate in terms of thickness decreases as the spray period increases, except for the heavy icing region. This could again be attributed to the decrease in spray flux. The ice thickness in the heavy icing region however shows an inconclusive trend. A closer look at Figure 21 – Plot 4 suggests that the difference between the icing rates by thickness in the low and heavy icing regions on the plate are smaller for a spray period of 3 seconds than larger spray periods. This could suggest relatively more even icing on the surface for more frequent sprays.

The seawater temperature measured at the nozzle in Figure 21 – Plot 2 shows a dip for the longer spray period of 9 seconds. This is because the water in the pipe towards the nozzle stays stationary for a longer time in the freezing room. This is an example of why the seawater temperature was recorded at multiple locations and measuring it close to the nozzle is important. Overall, all the readings had lower average temperatures for air and seawater than the set temperatures, suggesting that the icing rates could have been slightly overestimated.

Summary of results from Experiment 7:

Though this experiment is aimed to study the dependence of icing rates on the spray period, the significant difference in the spray flux per hour makes it a significant covariate. Further investigation is necessary to form a conclusion about the dependence of the icing rates purely on the spray duration with a constant flux. If it is assumed that the flux would naturally decrease as a result of decrease in the spray frequency, the test clearly shows higher icing rates for lower spray periods. This however would be true up to a certain minimum threshold of spray period, after which, more frequent sprays could slow down or eventually stop the ice formation as the heat from incoming water limits the freezing of the water film on the plate. Analysing this threshold could be a suggestion for further research. Using the results from the experiment with spray period for field estimations would necessitate interpretation of this data in terms of ship and wave characteristics.

7.9. Exp. 8: Effect of Salinity

To study the variation of icing rate to salinity, 3 tests were conducted in experiment 8. The first reading was taken with fresh water, the next with 2 different batches of seawater with a salinity of 32.45 and 32.90 ppt respectively.

Salts in supercooled sprays lower the nucleation temperature. Thus, increase in salinity lead to lesser icing rates [9]. Stallabrass, 1980 states that a small change in salinity of 5ppt results in variation of the freezing temperature by only 0.25°C; and is hardly of any practical significance for the severity of icing [9]. On the other hand, Kulyakhtin 2014 mentions how salinity plays an important role in ice accretion process at the water film level between consecutive sprays [4]. Kulyakhtin 2014 also mentions how wind generated spray has a significantly lower freezing temperature than seawater owing to higher salinity [4].

Since the freezing temperature, and thus the icing rate is affected by salinity, the experiment with differing values of salinity were performed. This experiment is especially important since multiple batches of saltwater were used for the entire study.

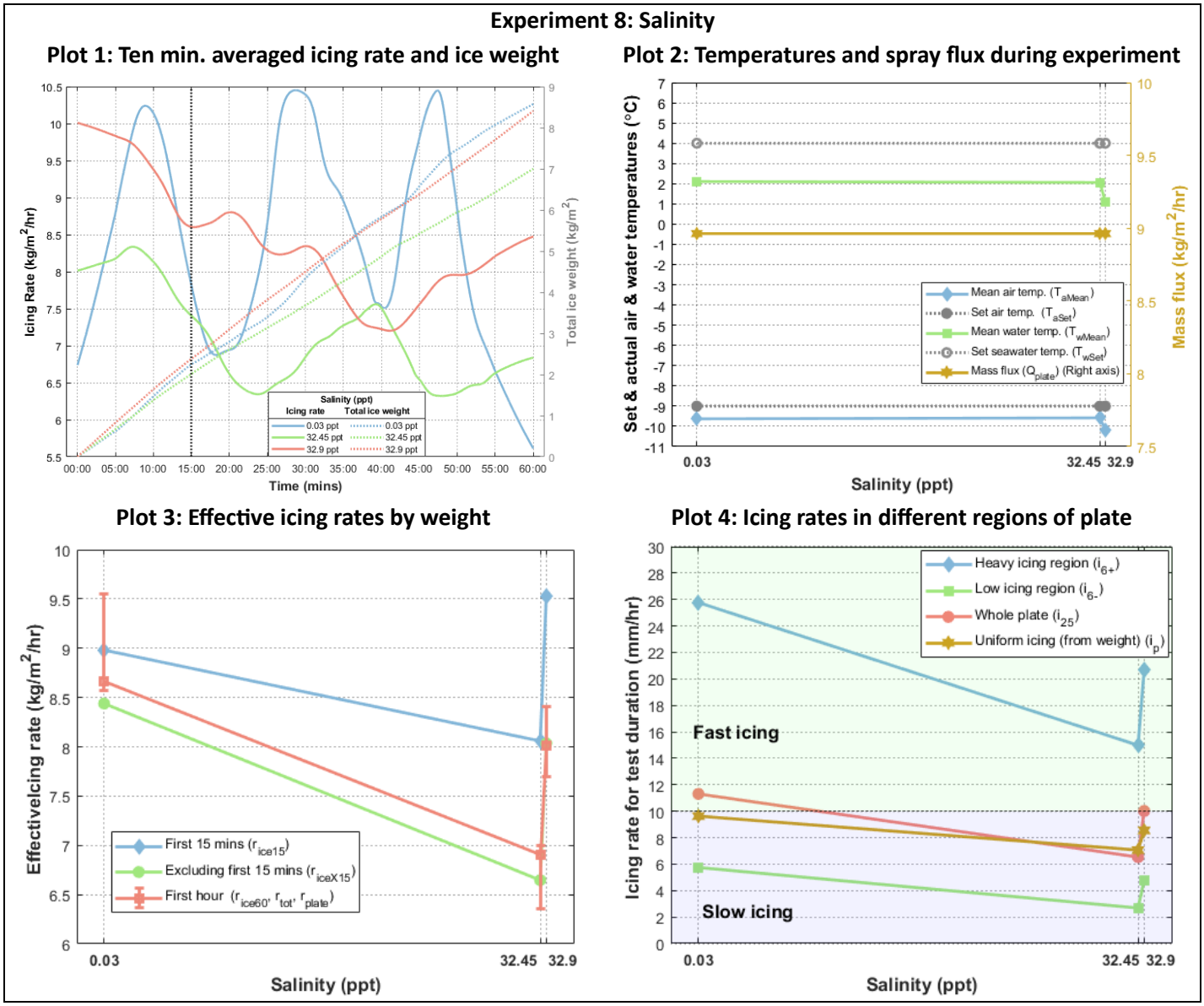

Figure 22: Ice weights, temperature & spray flux variations, and icing rates for Exp. 8 (Variable: Salinity)

Figure 22 shows that icing rates for freshwater and for 32.45ppt salinity in terms of both, thickness (Plot 4) and weight (Plot 3), as expected, go down for the test with seawater. It can also be seen in Figure 22 – Plot 2 that the mean temperatures for both tests are almost equal. However, in the last test with 32.90ppt salinity, the icing rates showed unexpected behaviour. The reason for the increase in the icing rates for this batch of seawater can be clearly seen in Figure 22 – Plot 2, which shows that the mean temperatures, both air, and water, during the experiment were close to 1°C lower than the first 2 readings. Figure 22 – Plot 4 shows that the significant dip in the temperature also caused the ice thickness to increase significantly for the 32.9ppt salinity test. The air and seawater temperatures contribute to icing more than salinity, and

thus the unexpected hop in the curve, also for the ice thickness. These temperatures act as significant covariates for this experiment.

Additionally, it is interesting to see that the icing rate with fresh water in Figure 22 – Plot 1 shows a strong periodic behaviour. Icing rate with fresh water depends purely on air and water temperatures with the other variables constant. The cooling mechanism of any refrigeration system holds the temperature between a certain upper and lower threshold of the set temperature. If the room temperature falls below the lower threshold, the refrigeration system stops and starts again only when the room temperature reaches the upper threshold – explaining the periodic appearance of the icing rate for fresh water. This cyclic nature of the refrigeration system does indeed also affect the icing rates for tests with sea water. However, the periodic appearance of the icing rates is not as prominent in case of saline water. This could be explained by the complex freezing process of periodic sea spray (saline water). At each incoming spray, salt exchange takes place between existing brine pockets and the newly formed brine film, and the freezing temperature of the brine changes due to salt rejection. This phenomenon can be said to dampen the effect of the periodic temperature change of the refrigeration system on the icing rates. This also shows that salinity indeed plays an important role in the calculation of icing rates for periodic sea spray icing.

Summary of results from Experiment 7:

Literature already suggests that higher salinity results in lower icing rates owing to lower freezing temperatures. This was observed from the first 2 readings of freshwater and 32.45ppt salinity. Analysis from the last test with a salinity of 32.9ppt showed lower mean temperatures of air and seawater during the test duration compared to the first 2 tests, and thus led to significantly higher icing rates. Significant variation in the temperatures for the tests make it difficult to reach a conclusion on the effect of salinity considering the effect of air and seawater temperatures on the icing rate is much greater in comparison.

8. Lessons learnt, summary, and future work

This paper presents results from a comprehensive experimental study of sea spray icing, including a detailed description of the experimental setup and lessons learned from the experimentation. Eight parameters governing the sea spray icing process were investigated experimentally. In particular, the initial stages of sea spray icing have been analysed and documented.

Sea spray icing is a complex process, and this also marked complexity under controlled laboratory conductions. Some of the general experiences and lessons learned from the experiments are listed below followed with a summary of observations from the results, and suggestions for future work.

8.1. Lessons learned

- Basis for the selection of the method of measurement of icing rate should be investigated and selected carefully. Variation in the method of measurement could lead to variation in the results. The weight of accreted ice can be measured with or without ice stalactites and could be used in case of different applications. The weight measured by processing the raw data of the test duration and that which is measured after the duration of the test might show some variation depending

on the data processing methods. If not presented as a range, and rather a single value, these variations should be accounted for in the errors.

- Icing rates in the initial stages of an icing event are generally higher than if the initial few sprays are neglected. None of the existing sea spray icing models account for this difference and neglect the higher icing rates at the start. Anti-icing methods requiring real time icing rates could make use of this difference in the icing rates for optimization purposes However, in other cases where long-term icing rates are applicable, the initial icing rates can be neglected. For general experiments with sea spray icing, it is suggested to report variation of icing rates with time.
- As sea temperature affects the icing rates, it is necessary to control and report the temperature of seawater during experiments. Internal heat generation in the pump significantly affects the temperatures of seawater, making it necessary for a heat exchanger between the pump and the nozzle, at least for a similar setup.
- Wind is a major factor affecting ice accretion. Measurements of wind speeds should be done as close as possible to the freezing surface or interpreted in such a manner so as to reflect the real wind speeds that act on the surface. Failing to do this would be a major source of error in the results.
- Because of how temperature control in refrigeration systems works, variations in the air temperature in cold climate laboratories cannot be avoided and the icing rates would have a certain dependence on these variations. This is a challenge for absolute repeatability of such experiments, and thus repeatability analysis should be reported.
- Air bubbles in the pipe leading to the nozzle proved to affect the flow rate through the nozzle. This is especially important while achieving periodic spray through mechanical means. It was experienced that as time progressed, the build-up of air bubbles caused the spray to be visibly weaker, within the 1-hour duration of the tests. This was tackled with the help of a check valve before the nozzle and ensuring the existing air pockets are removed by having continuous spray before the start of periodic spray, thus proving the spray drainage system in Figure 5 to be quite important.

8.2. Summary of observations from the results:

- Material: The material of the test plate affected the initial icing rates, but after some initial sprays, the difference in the icing rates was not significant. This means that for applications such as anti-icing with heating where the heat energy needs to be sufficient to avoid icing at all, information of the initial icing rates in the given condition could be used to optimise the heating systems such that the heat energy is enough to avoid any ice accretion. Whereas in cases where, for example, the total weight of ice accretion is required, the initial icing rates can be ignored since they are applicable only for the first few sprays.
- Wind speed: As expected, the icing rates varied greatly with wind speeds. Increase in wind speed caused increase in the icing rate. The increase in the icing rate for unit increase in wind speed decreases with increase in wind speed. This points to a threshold of windspeed after which the icing rate would not considerably increase. Finding the threshold was out of scope for the current study. Though other variables were constant, the wind resulted in change in spray flux at the

plate. The flux was thus a covariate and the reported icing rates are not purely for wind alone and further analysis of the data is required.

- Air temperature: Decrease in the air temperatures caused significant near-linear increase in the icing rates for the tested temperature range. At higher temperatures below the freezing point for a given salinity, more ice stalactites could be expected. Air temperatures were recorded for every second during the one-hour tests and showed fluctuations that could have affected the icing rates. The mean air temperatures during each test are reported, but the effect of instantaneous variations in the air temperature could be studied further from the data. Higher air temperatures resulted in more stalactites.
- Sea temperature: Icing rates increased with decrease in seawater temperature almost linearly. The variation was not as significant as due to air temperature and wind speed. The seawater temperature showed some amount of fluctuation during the tests. This too, like air temperature was recorded for ever second of the test. The seawater temperature showed only a moderate effect on the icing rates, and the instantaneous fluctuations could be considered to not affect the icing rate as much as the air temperature.
- Spray flux: Results from the experiment with spray flux as the variable was deemed to be not useful due to weak spray at lower pressures. The selection of the pump and piping is suggested to be improved to achieve higher pressures instead of testing with low pressures of 1 -2 bars. The spray flux acted as a covariate for several other experiments where it varied due to either wind, spray duration, or spray period. It could be interesting to analyse the data of these experiments through statistical means to investigate if any conclusion on the role of spray flux can be made.
- Spray duration: Longer spray durations tended to give lower icing rates in the initial stages. However, as time progressed, longer sprays resulted into higher icing rates as the effect of the substrate reduced after the formation of initial ice layers. Spray flux was a significant covariate, and the presented graphs are as result of a combination of spray duration and flux. Longer spray durations resulted in more ice stalactites.
- Spray period: Lower spray periods (more frequent sprays) gave lower icing rates in the initial stages but showed an increase as the icing progressed as the effect of the substrate reduced after the formation of initial ice layers. The spray flux, also here, was a significant covariate and should be considered while reading the results. Shorter spray periods or more frequent sprays give more ice stalactites.
- Salinity: Considering the first two readings in the experiment for salinity, the icing rates for seawater were lower than that of freshwater. The difference, however, was marginally more than the relative standard error in repetitions (experiment 0), suggesting that the salinity plays only a marginal role in the icing rates. In the third reading however, significant temperature deviations from the set temperatures were observed.

8.3. Future work with the experimental data

The current study gives a general idea of the trends for icing rates due to 8 different variables. The study also touches the topic of good practices for sea spray icing experiments by sharing the noteworthy experiences from the whole exercise. The real temperatures during the course of individual tests showed

deviation from the set temperatures. The mean observed temperatures during individual experiments, too, varied when ideally, they should have remained constant. Reporting icing rates with these temperatures could include significant errors. The spray flux proved to be a significant covariate in many experiments. Inclusion of multiple variables that are highly interdependent calls for advanced statistical methods to make a correlation analysis and pinpoint how individual variables affect the icing rate. The huge amount of data collected from the 20 test that are presented in this article, calls for in investigation into the use of machine learning techniques for analysis. Moreover, variables such as spray flux, spray period, and spray duration, are a function of ship and wave characteristics. For the practical use of these variables, results have to be interpreted in terms of metocean conditions and ship characteristics. Lastly, the results have to be compared with existing models to ensure that the experimental data is suitable to be used as a basis for the development of a prediction model.

9. Acknowledgements

- The authors would like to thank all colleagues, friends, and family members that extended help during the construction and for taking measurements during this labour-intensive exercise.
- VikingNorsafe for glassfibre plate

10. References

[1] E. M. Samuelsen and R. G. Graversen, “Weather situation during observed ship-icing events off the coast of Northern Norway and the Svalbard archipelago,” *Weather Clim. Extrem.*, vol. 24, no. 9293, p. 100200, Jun. 2019, doi: 10.1016/j.wace.2019.100200.

[2] A. Kulyakhtin, “Numerical Modelling and Experiments on Sea Spray Icing,” Doctoral thesis. Department of Civil and Transport Engineering. Norwegian University of Science and Technology (NTNU), Norway, 2014.

[3] S. Deshpande, A. Sæterdal, and P.-A. Sundsbø, “Sea Spray Icing: The Physical Process and Review of Prediction Models and Winterization Techniques,” *J. Offshore Mech. Arct. Eng.*, vol. 143, no. 6, pp. 1–12, Dec. 2021, doi: 10.1115/1.4050892.

[4] A. Kulyakhtin and A. Tsarau, “A time-dependent model of marine icing with application of computational fluid dynamics,” *Cold Reg. Sci. Technol.*, vol. 104–105, pp. 33–44, Aug. 2014, doi: 10.1016/j.coldregions.2014.05.001.

[5] I. Horjen, “Numerical modeling of two-dimensional sea spray icing on vessel-mounted cylinders,” *Cold Reg. Sci. Technol.*, vol. 93, pp. 20–35, Sep. 2013, doi: 10.1016/j.coldregions.2013.05.003.

[6] T. W. Forest, E. P. Lozowski, and R. Gagnon, “Estimating marine icing on offshore structures using RIGICE04,” in *Proceedings of the International Workshop on Atmospheric Icing on Structures (IWAIS), Montreal, Canada.*, 2005, no. June.

[7] E. M. Samuelsen, K. Edvardsen, and R. G. Graversen, “Modelled and observed sea-spray icing in Arctic-Norwegian waters,” *Cold Reg. Sci. Technol.*, vol. 134, pp. 54–81, Feb. 2017, doi: 10.1016/j.coldregions.2016.11.002.

[8] J. E. Overland, “Prediction of Vessel Icing for Near-Freezing Sea Temperatures,” *Weather Forecast.*, vol. 5, no. 1, pp. 62–77, Mar. 1990, doi: 10.1175/1520-0434(1990)005<0062:POVIFN>2.0.CO;2.

[9] Stallabrass, “Trawler Icing - a Compilation of Work Done At N. R. C.,” *Mech. Eng. Rep. MD-56, N.R.C. No. 19372 (National Res. Counc. Ottawa Canada)*, 1980.

[10] J. E. Overland, C. H. Pease, R. W. Preisendorfer, and A. L. Comiskey, “Prediction of Vessel Icing,” *J. Clim. Appl. Meteorol.*, vol. 25, no. 12, pp. 1793–1806, Dec. 1986, doi: 10.1175/1520-0450(1986)025<1793:POVI>2.0.CO;2.

[11] C. C. Ryerson, “Superstructure spray and ice accretion on a large U.S. Coast Guard cutter,” *Atmos. Res.*, vol. 36, no. 3–4, pp. 321–337, May 1995, doi: 10.1016/0169-8095(94)00045-F.

[12] J. Stallabrass and P. Hearty, “The Icing of cylinders in conditions of simulated freezing sea spray,” 1967.

[13] A. Dehghani-Sanij, M. Mahmoodi, S. R. Dehghani, Y. S. Muzychka, and G. F. Naterer, “Experimental investigation of vertical marine surface icing in periodic spray and cold conditions,” *J. Offshore Mech. Arct. Eng.*, vol. 141, no. 2, pp. 1–40, 2019, doi: 10.1115/1.4041394.

[14] A. Kulyakhtin and T. Engineering, “Sea spray icing : in-cloud evaporation . Semi- analytical and numerical investigations .,” vol. 42, 2011.

[15] A. Kulyakhtin, O. Shipilova, B. Libby, and S. Løset, “Full-scale 3D CFD Simulation of Spray Impingement on a Vessel Produced by Ship-wave Interaction,” *Proc. 21st IAHR Intl. Symp. Ice*, pp. 1129–1141, 2012.

[16] A. Hyldgård, D. Mortensen, K. Birkelund, O. Hansen, and E. V. Thomsen, “Autonomous multi-sensor micro-system for measurement of ocean water salinity,” *Sensors Actuators A Phys.*, vol. 147, no. 2, pp. 474–484, Oct. 2008, doi: 10.1016/J.SNA.2008.06.004.

[17] A. Dehghani-sanij, Y. S. Muzychka, and G. F. Naterer, “Analysis of Ice Accretion on Vertical Surfaces of Marine Vessels and Structures in Arctic Conditions,” in *Volume 7: Ocean Engineering*, May 2015, pp. 1–7, doi: 10.1115/OMAE2015-41306.

[18] K. F. Jones and E. L. Andreas, “Sea spray concentrations and the icing of fixed offshore structures,” *Q. J. R. Meteorol. Soc.*, vol. 138, no. 662, pp. 131–144, Jan. 2012, doi: 10.1002/qj.897.

[19] S. Brohez, C. Delvosalle, and G. Marlair, “A two-thermocouples probe for radiation corrections of measured temperatures in compartment fires,” *Fire Saf. J.*, vol. 39, no. 5, pp. 399–411, Jul. 2004, doi: 10.1016/J.FIRESAF.2004.03.002.

[20] CSGNetwork, “Water Density Calculator,” 2011. http://www.csgnetwork.com/h2odenscalc.html (accessed Sep. 14, 2022).

[21] Matlab_Documentation, “Filtering and Smoothing Data - MATLAB & Simulink - MathWorks Nordic.” https://se.mathworks.com/help/curvefit/smoothing-data.html (accessed Aug. 16, 2022).

[22] R. D. Brown and T. Agnew, “Characteristics of marine icing in Canadian waters.,” in *Proceedings of the International Workshop on Offshore Winds and Icing*, 1985, pp. 78–94.

[23] X. Chang *et al.*, “Research on ultrasonic-based investigation of mechanical properties of ice,” *Acta Oceanol. Sin.*, vol. 40, no. 10, pp. 97–105, 2021, doi: 10.1007/s13131-021-1890-3.

[24] *ISO 19906:*, 2nd ed. Petroleum and natural gas industries – Arctic offshore structures, 2019.

[25] M. C. Ortiz, L. A. Sarabia, M. S. Sánchez, and A. Herrero, “Quality of Analytical Measurements:

Statistical Methods for Internal Validation," in *Comprehensive Chemometrics*, vol. 1, Elsevier, 2009, pp. 17–76.

[26] S. Ferraris and L. M. Volpone, "ALUMINIUM ALLOYS IN THIRD MILLENNIUM SHIPBUILDING: MATERIALS, TECHNOLOGIES, PERSPECTIVES.," *Fifth Int. Forum Alum. Ships.*, Oct. 2005.

[27] S. SUZUKI, R. MURAOKA, T. OBINATA, S. ENDO, T. HORITA, and K. OMATA, "Steel Products for Shipbuilding," *JFE Tech. REPORT, 241*, Mar. 2004.

[28] VikingNorsafe, "VIKING Norsafe Life-Saving Equipment Norway AS MATHILDA-74," VIKING Doc. No.: TSB-0045, Rev. No. 3, Mar. 2021. Accessed: Aug. 15, 2022. [Online]. Available: https://myviking.viking-life.com/en/Boats-and-davits/Boats/Conventional-lifeboats/p/P0301001030.

[29] RolledMetalProducts, "Aluminum 5052 data sheet." 2017, [Online]. Available: rolledmetalproducts.com/wp-content/uploads/docs/Aluminum5052.pdf.

[30] A. A. Bhatti, Z. Barsoum, H. Murakawa, and I. Barsoum, "Influence of thermo-mechanical material properties of different steel grades on welding residual stresses and angular distortion," *Mater. Des.*, vol. 65, pp. 878–889, Jan. 2015, doi: 10.1016/j.matdes.2014.10.019.

[31] G. B Vaggar, S. C Kamate, and P. V Badyankal, "Thermal Properties Characterization of Glass Fiber Hybrid Polymer Composite Materials," *Int. J. Eng. Technol.*, vol. 7, no. 3.34, p. 455, Sep. 2018, doi: 10.14419/ijet.v7i3.34.19359.

[32] S. Wang and J. Qiu, "Enhancing thermal conductivity of glass fiber/polymer composites through carbon nanotubes incorporation," *Compos. Part B Eng.*, vol. 41, no. 7, pp. 533–536, Oct. 2010, doi: 10.1016/j.compositesb.2010.07.002.

[33] L. Li, Y. Liu, Z. Zhang, and H. Hu, "Effects of thermal conductivity of airframe substrate on the dynamic ice accretion process pertinent to UAS inflight icing phenomena," *Int. J. Heat Mass Transf.*, vol. 131, pp. 1184–1195, Mar. 2019, doi: 10.1016/J.IJHEATMASSTRANSFER.2018.11.132.

[34] E. P. Lozowski, K. Szilder, and L. Makkonen, "Computer simulation of marine ice accretion," *Philos. Trans. R. Soc. London. Ser. A Math. Phys. Eng. Sci.*, vol. 358, no. 1776, pp. 2811–2845, Nov. 2000, doi: 10.1098/rsta.2000.0687.

[35] P. Dawson and S. L. Dawson, "Sharing successes and hiding failures: 'reporting bias' in learning and teaching research," *https://doi.org/10.1080/03075079.2016.1258052*, vol. 43, no. 8, pp. 1405–1416, Aug. 2016, doi: 10.1080/03075079.2016.1258052.

[36] I. Horjen and S. Vefsnmo, "Mobile platform stability (MOPS) subproject 02 - icing (MOPS Report No. 15).," 1984.

[37] R. D. Brown and P. Roebber, "The Scope of the ice accfretion problem in Canadian waters related to offshore energy and transportation.," Canadian Climate Centre Report 85-13, 1985.

[38] W. P. Zakrzewski, "Icing of Fishing Vessels. Part I: Splashing a Ship With Spray.," 1986.

14. Appendix 3: Paper 3

A Machine Learning Model for Prediction of Marine Icing

Sujay Deshpande

Dept. of Building, Energy and Material Technology, UiT, The Arctic University of Norway.

Address: C/o UiT, Campus Narvik, Lodve Langesgate 2, 8514, Narvik, Norway

email: Sujay.r.deshpande@uit.no

[This is a reprint of the accepted version of the article. Reprinted with permission from ASME. Strictly for the use of inclusion in the PhD thesis. DOI of published version: https://doi.org/10.1115/1.4064108]

1. Abstract

Marine icing due to freezing sea spray has been attributed to many safety incidences. Prediction of sea spray icing is necessary for operational safety, design optimization, and structural health. In general, lack of detailed full-scale measurements due to the complexity and costs make validation difficult. The next best option is that of controlled laboratory experiments. The current study is the first study in the field of sea spray icing that investigates the use of new data science technologies like machine learning and feature engineering for the prediction of sea spray icing based on data collected from controlled laboratory experiments. A new prediction model dubbed 'Spice' is proposed. Spice is designed 'bottom-up' from experimentally collected data and thus, if the input variables are accurately known, it could be said to highly accurate within the tested range compared to existing theoretical models. Results from the current study show promising trends, however, more experiments are suggested for increasing the range of confident predictions and reducing the skewness of the training data. Results from spice are compared with five existing models and give icing rates in various conditions in the middle of the spectrum of the other models. It is discussed on how validation from two existing full-scale icing measurements from literature prove to be challenging and more detailed measurements are suggested for the purpose of validation.

2. Introduction

Icing on ships and offshore structures occurs from sea spray icing sourced from seawater and atmospheric icing due to precipitation in the form of snow, rain, fog, etc. Sea spray is either wind generated, where seawater droplets from breaking waves are carried to the structure due to wind, or impact generated, where the sea spray is a result of the impact of the ship or structure with waves. Sea spray icing accounts for 80-90% of all offshore icing incidents [1]. 40 fishermen are reported to have died in icing related incidents in the 1960s [2]. Impact generated sea spray is regarded as the most important water source in dangerous icing events [3]–[7]. Icing also affects offshore wind turbines, but is limited to lower levels of the structure and blade tips during azimuthal downward position [8]. Similarly, for other structures like oil rigs, sea spray icing is dominant in the lower parts where sea spray droplets are easily impacted, whereas icing in the upper regions is usually atmospheric icing [9]. Models for predicting sea spray icing are crucial for optimal design of ships and structures operating in cold climate regions [10].

The 1960s-1980s saw extensive work in gathering icing data for use in prediction of dangerous icing events [7]. Icing data was previously gathered from around 7000 questionnaire responses across countries, but

wasn't publicly available [7], [11]. Samuelsen et.al. 2017 report a few cases from the past where the icing data has been made available. Precise icing rate estimation ideally requires detailed information of metocean parameters and ship characteristics during the icing events, which is lacking in existing datasets [7]. This makes the existing full-scale data not detailed enough for validation of computational results [10].

All existing models use observations or empirical equations to estimate several inputs required for predicting sea spray icing. Existing models rely on just 3 studies, each on one particular ship [7]. Estimation of spray flux is the weakest link in existing models, for example, the spray flux used in ICEMOD is 10-1000 times lesser that the spray flux used for RIGICE04, and it is difficult to say which one is better [1]. Spray duration and spray period are also derived from limited observations and different researchers have used different formulations for estimating these [7]. Samuelsen et.al 2017 compare predictions using 2 different formulations of spray flux. Other researchers, like Kulyakhtin, 2014 have arbitrarily chosen one of the formulations and suggest that any formulation could be used. The performance of individual empirical formulations is beyond the scope of the current study. Details of some of the existing models can be found in Appendix A.

Due to different approaches, predictions from existing models show considerable variation [10]. Moreover, the limited comparisons with experimental or full-scale data makes it difficult to say which model is the most accurate [12]. ISO 35106 notes that none of the existing models predict sea spray icing on a wide range of vessels or structures, and that the Overland 1990 model has been traditionally used to estimate icing on small-to-medium sized fishing vessels [12].

Detailed full-scale measurements of sea spray icing are expensive [1], [10]. Only a handful of these exists, and even fewer as published research [1]. Although some researchers like Samuelsen 2017 [7] attempted to validate their models against these datasets, the current study found the datasets not feasible for the purpose of validation. This was also observed by Bodaghkhani et.al. 2016, who point out that the spray parameter measurements are not detailed enough for validation of computational results [13]. One of the reasons being that the icing is heavily dependent on spray flux, i.e., the amount of water impinging on the freezing surface, which varies greatly with the measurement location and could be vastly different at different locations on the same vessel or structure for the same spray event. Taking icing measurements at a different location than the spray measurements would not suffice for validation. A detailed explanation as to why existing datasets could not be used for precise validation is provided in the further sections.

The next best option is to have validation data from controlled experiments – which have also proved to be time intensive [14]. Owing to the lack of detailed data for sea spray icing, Deshpande et.al 2023, carried out controlled experiments with sea spray icing including 20 tests structured into 8 experiments. Each experiment focused on one of 8 crucial variables affecting sea spray icing. The experiments simulated sea spray icing conditions in a cold climate laboratory. Seawater from a cooling chamber at 2°C to 6°C was sprayed onto a plate in a freezing chamber at -5°C to -15°C with a nozzle. Wind was simulated with a fan in the freezing chamber. Effects on icing rates by varying air and seawater temperatures, wind speed, material, spray duration and period, salinity, and flux were examined. The weight of the ice accreted on the plate was monitored per second for each hour-long test. For complete details, interested readers are encouraged to refer to Deshpande et. al. 2023. Data for each experiment was presented. Due to the vast

nature of the data gathered, the current study explores the use of new techniques including machine learning to analyze and make sense of the data from the experiments. Adding to the aforementioned challenges in full scale icing measurement, gathering comparable and varied full-scale data is difficult, especially as each variable necessitates measurements under diverse weather conditions. Scaling effects from lab experiments must ideally be confirmed via full-scale tests. Future research could explore suitable full-scale measurement techniques.

Applications of machine learning algorithms have grown exponentially in the past few years. The technology makes it possible to make sense of large amounts of data that at the first look could fail to show any logical relationships. Machine learning has been recently used in icing severity predictions in the aerospace industry [15], [16]. Icing on aircraft blades is purely atmospheric icing where the physical icing process, variables involved, and icing severity is completely different to that of sea spray icing. To the best of the author's knowledge, this is the first study wherein a data-driven machine learning model is implemented for the purpose of sea spray icing predictions.

The current study proposes a sea spray icing prediction method based on the experimental data by Deshpande et.al. 2023 using machine learning and feature engineering techniques and is an extension of the previous study. Post-publication, 10 additional repetitive tests were conducted. First, the data is analyzed, followed by implementing some machine learning models without feature engineering, comparing predictions on unseen data. The advantages and disadvantages of these models are discussed in short. Finally, a model, hereafter called the 'SPICE' model (prediction model for Sea sPray ICE) is described and implemented with more complexities added in terms of feature engineering in the chosen machine learning model. SPICE is proposed to serve as a new model for prediction of sea spray icing based on experimentally validated data. Predictions from SPICE are compared to existing models for 9 hypothetical cases to see the effects of certain variables on the predictions. Attempts to validate the model based on two full-scale datasets proved insufficient as the datasets were found to be inadequately detailed. Advantages, limitations, and scope for further improvement of SPICE are discussed. The theory behind individual machine learning models is beyond the scope of the current study, but some elementary details are provided for readers not familiar with the subject. Problems with the use of current spray flux formulations are discussed and suggestions for future research are presented. The SPICE model is, after further improvements, intended to be deployed as a user-friendly application for general use for icing predictions, and as a python package for use in further research.

3. The SPICE model

The SPICE model comprises four Python classes: data processor, transformer, predictor, and feature calculator, along with their methods. An instance of the data processor manages initial raw data processing. An instance of the transformer computes and integrates new features during feature engineering before the prediction model. The predictor class is a container for the trained ML object and is used for predictions and post-processing. The feature calculator is an addition for cases where the original variables required for predictions are unavailable. The usage of all classes elaborated in appropriate sections.

Assembling together the methods developed for data processing, feature engineering, the machine learning model, and the feature calculator in subsections 4, 5, 6, and 7 respectively, the software architecture for the SPICE model was developed for which the flowcharts are presented in Figure and Appendix D. The model is a combination of four different applications:

- **Spice Data Processor:** This is used for preprocessing raw data and arranging the data in a format that can be used further by the machine learning model. Details about the data processor are covered in section 4.
- **Spice Transformer:** This is used for Feature Engineering. The Spice transformer generates additional data (transforms the dataset) for the ML model. It generates several new columns as a combination of existing input and is used in training and predictions. The need for the Spice Transformer has basis in the nature of the experimental data and in explained in section 4.4. Details of the Spice Transformer are covered in section 5.
- **Spice Predictor:** This is the core ML part of the application which is used while training the ML model and for making predictions from new and unseen input data. While section 4.4 discusses the preliminary ML model evaluation, details of the Spice Predictor are covered in section 6.
- **Spice Feature Calculator:** Any ML model requires identical input variables for prediction as during training. In Spice, certain prediction inputs (e.g., spray period) can't be directly measured with onboard instrumentation, necessitating estimation from related factors like wavelength, ship speed, and heading using existing formulations from literature. While making predictions, if obligatory variables are absent from the input, the SPICE Feature Calculator is called to estimate them from available data. The flowchart for the Spice Feature Calculator is shown in Figure 12 and its details are covered in section 7.

Figure shows the flowchart of the SPICE algorithm.

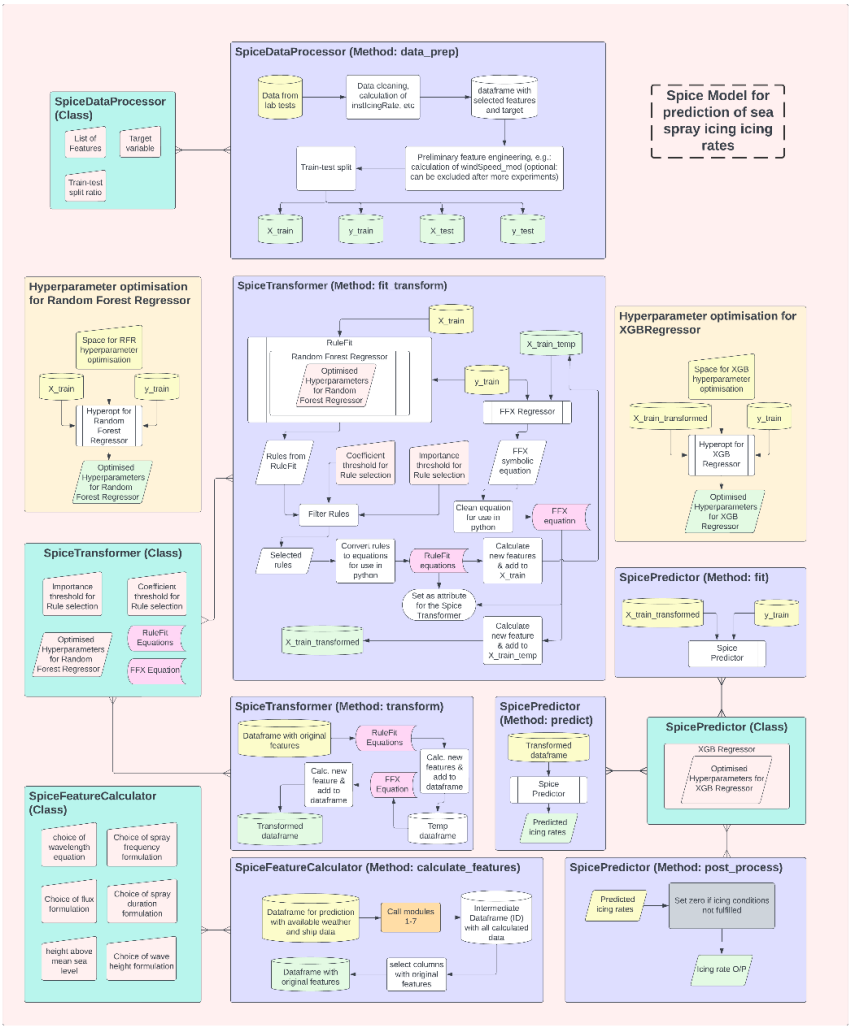

Figure 1: Flowchart of the Spice model

4. Data and the Spice Data Processor

This section gives details about the data used in the current study and how it was processed.

4.1. Data selection, features, and target.

The experimental setup consisted of two climate-controlled chambers for simulating sea spray icing conditions. Seawater from the cooling chamber was sprayed onto a plate in the freezing chamber, on which the ice accretion was measured, with a nozzle. The spray duration and period were controlled with a PLC (Programmable Logic Control) valve. Spray flux was varied with the pump pressure, but also varied due to other factors such as spray duration and spray period. Salinity was varied using different batches of seawater and fresh water. The temperatures in the climate chambers were varied and controlled with the refrigeration mechanism. A fan in the freezing chamber simulated variable wind speeds with a regulator. The detailed setup, procedure, and further details of the experiments and the data collected can be found in Deshpande et.al. 2023.

Data was recorded every second for each hour-long test. The parameters that were controlled, measured, and used in the study, i.e., 'features' for the ML models are: thermal conductivity of the substrate material, air temperature, seawater temperature, salinity of seawater, spray flux, spray duration, spray period, and wind speed. The weight of accreted ice was measured and the instantaneous icing rate, also the 'target' for the ML models, was calculated from 10-minuite averaged values of the weight of ice accreted.

The refrigeration mechanism introduced air and seawater temperature variations in each test, acting as covariates across all experiments. This hindered drawing conclusions on effects of some of the tested variables on the icing rate directly from the experimental data. Other variables remained constant per test, enabling inclusion of data from every second. It was already proven that the effect of the material diminishes after initial few minutes (15 mins kept as reference) [14], allowing removal of 'material' from the list of features if the initial few minutes are neglected. Data from two 'bad' experiments [14] along with the initial 15 mins of each test were excluded. Additionally, the last 15 minutes of each test were omitted to prevent errors in the 10-minute moving average icing rate calculation.

Technical limitations made it possible to test a maximum near-surface windspeed of only 6m/s [14] which was low for application, especially in cases where ships sail into the wind. As a part of preliminary feature engineering, the wind speed was transformed to a variable called windSpeed_mod (u_{mod}) from Eq. (3) which describes a log wind profile. The near-surface wind speeds were measured at 9mm over the plate surface [14]. The experimental setup in Deshpande et.al 2023 allows us to assume a roughness length of 0.001m for a ground with an ice sheet on its surface [17]. The resulting u_{mod} is in theory the hypothetical u_{10} for the experiments, but as the test object was stationary, it is, for the case of this study it is assumed to be comparable to the relative wind speed for a moving ship. The validity of this technique is discussed in section 9.

$$\frac{u_z}{u_{z0}} = \frac{\ln(z/z^*)}{\ln(z_0/z^*)} \qquad \textit{Ref: [18]} \qquad \textit{Eq. (1)}$$

4.2. Exploratory data analysis

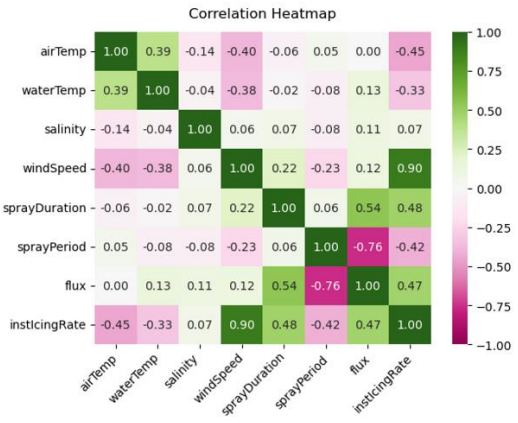

Figure 2: Correlation heatmap of the data

Figure 2 shows the correlations between the variables in the data. Notably, higher wind speeds strongly corelate with higher icing rates with a correlation coefficient of 0.9, while salinity has a minimal impact.

Contrary to theoretical expectations [4], experimental data shows a slight positive correlation between icing rate and salinity, observed previously also by Ryerson 1995 [19]. Deshpande et.al. 2023 acknowledge potential variability even under controlled conditions (Experiment 0). Such variations might contribute to the positive salinity-icing rate correlation, suggesting that errors in salinity wouldn't significantly alter predictions in icing rates. Negative correlations appear for air and water temperatures, and spray period, indicating higher icing rates with lower values. Conversely, positive correlations are evident for wind speed, flux, and spray duration. Some features exhibit a high multicollinearity, e.g. flux shows high correlation to spray duration and period as these variables directly affect the amount of spray hitting the plate. In a real case, the flux would be also a function of the position on the ship. Air and water temperatures show a relatively high correlation. This could also be true in a real case where the near surface seawater temperatures vary with the air temperature. The relatively high correlation between the wind speed and air temperature can be ignored as they are completely independent variables.

From the correlation analysis, it could be argued to be acceptable to remove salinity, and spray period form the list of features due to the low correlation of salinity with the target variable, icing rate and the high correlation of the spray period to flux. Exclusion of these features was investigated, and the features were retained for better accuracy (more about this in section 6.2).

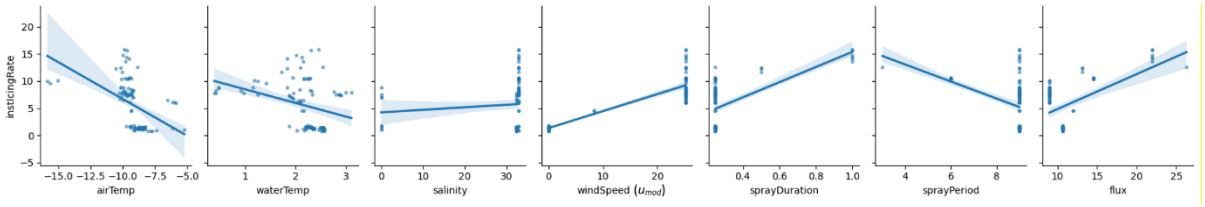

Figure 3: Pair plot for the target variable with 100 random datapoints

Figure 3 shows the pair plot with 100 random samples from the dataset for the target variable instantaneous icing rate (instIcingRate). This gives clarity on how the icing rate is affected by each variable and the extremities of feature values. Notably, air and water temperatures spread quite well, while other features are heavily skewed. This is because features other than the temperatures remained constant for an individual test. More details can be found in Table 1 of Deshpande et.al 2023. It is later seen in section 4.4 why feature engineering techniques were needed to be implemented due to the skewed data.

4.3. Final data preparation

The dataset contained no missing values and was shuffled and split randomly into train and test sets (X_train: all features, y_train: values of instIcingRate for corresponding X_train rows, X_test: all features, y_test: values of instIcingRate for corresponding X_test rows) where 80% of the rows were used for training and 20% for testing with instIcingRate as the target variable and other variables shown in Figure 3 as features. The training dataset is used for training the ML models, whereas the test dataset is used for evaluating the performance of the models. Variable units do not affect predictions, but consistency in units is vital during training and predictions.

Table shows the range of all the features in the training dataset. This is very important, as any predictions made for values outside this range would not be said to be accurate.

Practical usage of the SpiceDataProcesser Class is given in Appendix E.

Table 1: Range of trained data

Features ->	airTemp	waterTemp	salinity	Windspeed (u_{mod})	sprayDuration	sprayPeriod	flux
Units ->	°C	°C	ppt	m/s	sec	sec	kg/m²/hr
Minimum value in training set	-15.92	0.15	0.03	0.00	0.25	3.00	8.96
Maximum value in training set	-4.69	3.32	32.90	25.15	1.00	9.00	26.30

4.4. Preliminary ML model evaluation

Four ML models was assessed using the most commonly used metrics [20]: MAE (Mean Absolute Error: best fit value = 0), MSE (Mean Squared Error: best fit value = 0), and R^2 (R square: best fit value = 1) for the train and test datasets are shown in Table 2. The linear regressor model and three decision tree-based models: (DTR) Decision Tree Regressor, LGBM (Light Gradient Boosting Method) Regressor, and XGB (Extreme Gradient Boosting) Regressor [21] were implemented with the help of the Scikit-learn library [22] with default hyperparameters. The scores in Table 2 are obtained by comparing the predicted instIcingRate values with actual values (y_train or y_test) using the metrics module in Scikit-learn.

Tree-based regression models are preferable over linear regression for skewed and multicollinear datasets [23]. Table 2 confirms this where all metrics show better fits with tree-based models compared to Linear Regression. Thus, linear regression, and additionally DTR, for which the training set shows clear overfitting, are ruled out. XGB Regressor performs best with the lowest MAE and MSE for both sets, serving as a reference (Model 1) for further development. Internal algorithm specifics of individual ML models are beyond the scope of the current study.

Table 2: Model scores during preliminary analysis

	Train set			Test set		
	MAE	r2	MSE	MAE	r2	MSE
Linear Regression	0.494	0.97	0.500	0.489	0.971	0.488
Decision Tree Regressor	0.000	1.000	0.000	0.108	0.994	0.105
LGBM Regressor	0.215	0.994	0.103	0.215	0.994	0.103
XGB Regressor (Model1)	0.169	0.996	0.069	0.191	0.994	0.095

XGB Regressor's strong scores in Table 2 indicate satisfactory predictions for unseen data. However, guidelines for evaluating models (metric thresholds) are arbitrary and may not be appropriate in practice [24]. A limitation of this model was identified when testing for u_{mod} values from 0-20 and can be seen in Figure 6.

Despite good scores, Model 1 showed an unnatural stepped trend in icing rates with wind speed. This is unlikely in reality. Upon examining a tree from the model clarified the reason. Tree based models categorize data based on rules applied on the feature values, leading to stepped outputs. The severity of this tendency depends on training data, and in this case has limited practical value. Wind speeds varied

from 0-6 m/s in steps of 2, and these were constant throughout an individual test. Transforming wind speed to u_{mod} created wider intervals. The model broadly categorized data based on u_{mod} values in the training dataset. The model's categorizations along the average of successive values of u_{mod} was sufficient for the training data. With consistent u_{mod} values in the test dataset, the model makes predictions based on these broad categories, yielding good metrics. However, the model underperforms on dissimilar validation data. For example, the wind speed values present in both, the training and testing dataset were 0,2,4,6 m/s. The model might end up giving similar results if the wind speed in the validation data is 2.5 or 3.5m/s, which could be practically untrue. The case with wind speeds is especially important looking at the mean absolute SHAP [25] values in Figure 4. SHAP (SHapely Additive exPlanations) values show feature influence on predictions, but do not infer any causality [26]. windspeed (u_{mod}) has the highest impact over the prediction, accentuating stepped appearance vs the icing rates. Other variables might show similar trends but to a lesser extent.

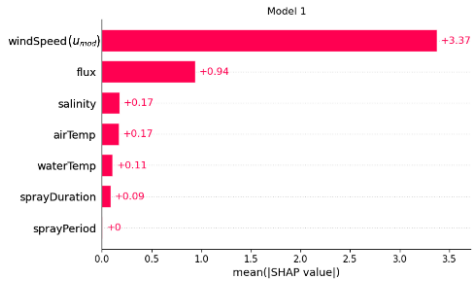

Figure 4: Model 1 mean absolute SHAP values

5. Method: Feature engineering and the Spice Transformer

To address predictions between experimental intervals for dataset variables involved exploring additional methods, including feature engineering. Feature engineering encompasses transforming, generating, selecting, or mapping new features from existing variables [27]. An example is when windSpeed was transformed to (u_{mod}) using domain knowledge. Two algorithms were employed to create new features: RuleFit [28] and FFX (Fast Function eXtraction) symbolic regression [29]. The methodology and positive effects on model predictions using feature engineering with these two algorithms for regression tasks were demonstrated by Cote 2022 [30].

RuleFit, using a tree-based base ML model, generates decision rules as polynomial-like equations from decision paths [31] comprising of combinations of original features. Rules are given coefficient and importance values and selected rules are used as new features while training. The python package for the RuleFit algorithm by Molnar 2016 [32] was used in this study. FFX produces a single equation that best fits the dataset. This equation adds another feature to the dataset. The python package for FFX by McConaghy, 2011 [33] was used in this study. Hyperparameter optimization is used for tuning the learning process. A range of hyperparameters is defined, yielding optimal values for training the ML model. This was done using Hyperopt library in python [34]. Grid search is an alternative approach.

5.1. Implementation of RuleFit

RuleFit permits either Gradient Boosting Regressor or Random Forest Regressor (RFR) as the base model. Here, RFR from scikit-learn library [22] was chosen. Hyperopt was used to get optimized RFR hyperparameters. RuleFit was then executed on training data, producing over 100 rules with varying importance and coefficients. Rules with absolute coefficients and importance over a threshold of 0.02 were selected, resulting in 9 rules. Rules with single variables marked 'linear' were excluded, as they duplicated original variables. Coefficient and importance values are only used for rule selection. Rules were translated into equations for coding, where variables were multiplied. After coding for clarity and interpretability in Python, equations (Table 3) were derived. These equations compute new features from X_train variables, temporarily stored for use in FFX.

Table 3: Selected RuleFit Rules and Equations

Rule.no.	coef	importance	equation
0	0.85	0.16	(windSpeed_mod**1) * (flux**3)
1	-0.58	0.11	(airTemp**2) * (windSpeed_mod**1) * (flux**1)
2	-1.04	0.32	(airTemp**2) * (salinity**2) * (windSpeed_mod**1) * (flux**1)
3	0.26	0.05	(airTemp**2) * (waterTemp**1) * (salinity**1) * (windSpeed_mod**1) * (flux**2)
4	-0.45	0.22	(airTemp**1) * (windSpeed_mod**1) * (flux**1)
5	-0.22	0.11	(airTemp**1) * (windSpeed_mod**1) * (flux**1)
6	0.83	0.29	(windSpeed_mod**1) * (flux**1)
7	-1.64	0.80	(windSpeed_mod**1) * (flux**1)
8	-0.34	0.06	(airTemp**2) * (windSpeed_mod**1) * (flux**1)

Duplicate equations were intended to be removed but were erroneously allowed and discovered at a later stage. However, the power of machine learning models could be seen at a later stage in Figure 5, where the new model does not consider the duplicates as important and do not severely affect the predictions. In any case, duplicates should ideally be removed in future versions.

5.2. Implementation of FFX symbolic regression

The dataframe with existing and new features after RuleFit is used along with y_train to fit the FFX model. The FFX model score was 0.9888. The output of the FFX model is a rather long equation which was cleaned for its use in python and a new feature was calculated. The resulting dataframe is the transformed dataframe that will be used for training the new model. The head of X_train_transformed is shown in Appendix B for better understanding.

Practical usage of the SpiceTransformer Class is given in Appendix E.

6. Method: ML model and the Spice Predictor

Table 2 shows that the XGB Regressor model gave the best results during the preliminary ML model evaluation. The same model is selected for further use. The only difference is that instead of training with X_train, the model is now trained with the X_train_transformed obtained after feature engineering. Additionally, Hyperopt is used for hyperparameter optimization similar to what was done for the RFR

during training of the transformer model. Practical usage of the SpicePredictor Class is given in Appendix E.

6.1. Results after feature engineering

Table 4 compares metrics of the model using SPICE (hereafter called Model 2) to Model1. The scores for Model2 show a 17.13% increase in the MSE for the test set. Using SPICE shows improvement in the predictions over XGB with default parameters without feature engineering.

Table 4: Metrics with and without SPICE

	Train set			Test set		
	MAE	**r2**	**MSE**	**MAE**	**r2**	**MSE**
Model1	0.169	0.996	0.069	0.191	0.994	0.095
Model2 (using SPICE)	0.159	0.997	0.049	0.180	0.995	0.079
% change	6.24	-0.12	28.26	5.73	-0.1	17.13

The mean absolute SHAP values for Model 2 are shown in Figure 5. The new calculated features (see Table 3, and Figure 10) are given more importance than the original features. The highest mean SHAP values is seen for the eqn_5 feature which is a multiple of air temperature, wind speed and flux. These are in fact the variables that are most crucial for the prediction of icing rates.

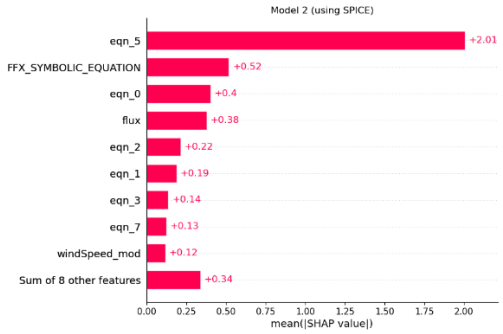

Figure 5: Model 2 mean absolute SHAP values.

Figure 6 compares the predictions of Model2 (using SPICE) to Model 1 for the sensitivity of the models to windspeed (u_{mod}) with constant values for the other features. The implemented feature engineering techniques make the model better at predicting values in between the experimented values of features, in this case, the wind speed. Since new features from the transformed dataframe are used for training, the dependence of the model on individual original features is reduced.

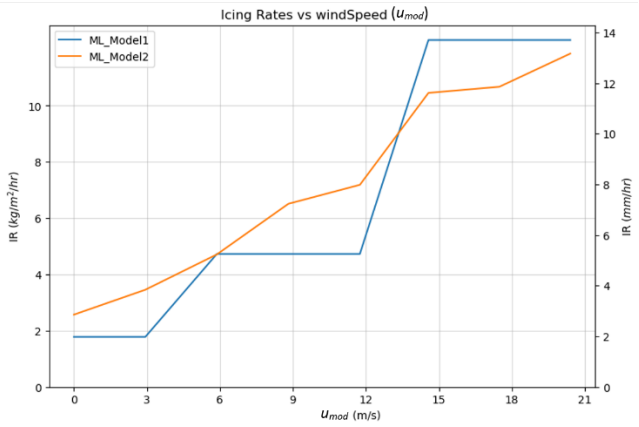

Figure 6: Model1 vs Model 2

6.2. Consideration of dropping out less important features

Similar models with the same feature engineering techniques were made to see the effect of exclusion of certain features that were deemed to be less important by the ML model. The metrics for the different cases are presented in Table 5, where 1 represents inclusion of the feature and 0 represents exclusion.

Table 5: Effect of exclusion of less important features

Sr. nr.	Air Temp	Water Temp	Wind Speed (u_{mod})	salinity	Spray Duration	Spray Period	flux	nr. features	Train set			Test set		
									MAE	r2	MSE	MAE	r2	MSE
1	1	1	1	1	1	1	1	7	0.159	0.997	0.049	0.180	0.995	0.079
2	1	1	1	0	1	1	1	6	0.185	0.995	0.084	0.224	0.991	0.148
3	1	1	1	0	1	0	1	5	0.222	0.993	0.113	0.249	0.990	0.164
4	1	1	1	0	0	0	1	4	0.206	0.994	0.097	0.235	0.991	0.150
5	1	0	1	0	0	1	0	3	0.783	0.875	2.113	0.759	0.880	1.981

It was seen that the first case presented in Table 5 with all features included, also the previously named Model 2, showed the best metrics. Thus, all the original features, even though of less importance to the model, were retained for better accuracy. The practical significance of this is that variables like salinity, if unknown, are set to a certain default value, and this assumption would not have any severe consequences on the prediction; however, the prediction would be marginally better if the accurate values of these variables are known.

7. Method: The Spice Feature Calculator

Until this stage, the model was tested only on arbitrary values of the original features. However, in a real case, many of these values are not straightforward to know. Air and seawater temperatures, and salinity, can be easily measured. As mentioned in section 4.1, the feature u_{mod} is equated with the relative wind speed, which might or might not be directly available depending on the actual case. Spray duration, period, and flux are reliant on complicated ship-ocean dynamics and may not be directly available and current models use some formulations to estimate these. Spice is provided with a feature calculator to estimate the unknown values before the predictor is called. However, a case for minimizing and as far as possible,

not using the feature calculator, especially for the estimation of the spray flux is later argued for. Practical usage of the SpiceFeatureCalculator Class is given in Appendix E.

Formulations for the estimation of some variables are debated in literature and are discussed in the following sections. This study does not vouch for the use of any of these formulations and thus it is possible to use any of the available formulations by setting the choice as an attribute of the object (see Figure) of the feature calculator. These attributes are used wherever necessary inside individual feature calculator modules. Each attribute has an arbitrarily chosen default value.

7.1. Estimation of wind dependent parameters

Wind speed at given height

In the absence of relative wind speed, the wind speed at the given height (u_z) is calculated by the wind power law in Eq. (2), where the height above the mean sea level (z) is retrieved from the attributes of the feature calculator and is set of 5m as a default. The roughness length (z^*) for the calculation in used from Eq. (3). In case submodule A1 is called, it is obligatory to have the values of u_{10}, in the absence of which an error is raised regarding insufficient data and the user is notified.

$$\frac{u_z}{u_{10}} = \frac{\ln(z/z^*)}{\ln(10/z^*)} \quad \text{(z is retrieved from the attributes)}$$ *Module A* *From Eq. (3)* *Eq. (2)*

$$z^* = \begin{cases} 1.87 \times 10^{-4} & for \quad u_{10} < 15m/s \\ 3.92 \times 10^{-3} & for \quad u_{10} \geq 15m/s \end{cases}$$ *Module A2* *Ref: [35]* *Eq. (3)*

Relative wind speed

If the relative wind speed in unknown, the ship speed in the direction of wind is first calculated by Eq. (4), where the ship heading α, if unknown is set to 0° (heading straight into wind), which is inconsequential for stationary ships or structures. If the object is stationary, or in case the absolute ship speed is unknown, V_s is set to zero. Further, the relative wind speed is calculated with Eq. (7).

$$V_{s\alpha} = V_s \cos\alpha$$ *Module B* *Eq. (4)*

$$V_r = u_z + V_{s\alpha}$$ *Module B* *Eq. (5)*

7.2. Estimation of wave dependent parameters

Wave height

Literature provides some methods to estimate the significant wave height (H_s) from the weather data using u_{10}, for example, the formulation by Zakrzewski, 1986 [5], which requires the wind fetch, the Beaufort scale [36], and the formulation by Horjen, 2013 [37] based on the observations of Jørgensen 1985 [38] given in Eq. (6).

$$H_s = \begin{cases} 0.752 u_{10}^{0.723}, & if\ wave\ height\ attribute = 'Horjen' \\ from\ Beaufort\ scale\ using\ u_{10}, if\ wave\ height\ attribure = 'Beaufort' \end{cases}$$ *Module W1* *Ref: [37],[36]* *Eq. (6)*

The Horjen formulation (default) or the Beaufort scale are available in SPICE and can be selected for wave height estimation. In case of the Beaufort scale, the mean of the range of wave heights for the corresponding u_{10} is selected.

Wave Period

Two formulations for estimation of wave period were found in literature. The Zakrzewski, 1986 [5], requires the wind fetch and the Horjen, 2013 [37] formulation based on Horjen 1990 [39] observations given in Eq. (7). In case the local wave period is unavailable, currently, only the Horjen 2013 formulation is used and there is currently no attribute for the selection of wave period equation.

$$T_s = 6.161 H_s^{0.252}$$ *Module W2* *Ref: [37]* *Eq. (7)*

Wavelength

If known, users can directly input wavelength(λ). Alternatively, equations for linear wave theory [40] estimate λ from wave period (Ts). Based on water depth (d), equations for deep ($d/\lambda \geq 0.5$), intermediate ($0.05 < d/\lambda < 0.5$), and shallow waters ($d/\lambda \leq 0.05$) determine λ. Users can set an attribute to choose the corresponding equation in Eq. (8). For intermediate and shallow waters, value of water depth is vital; else, deep waters are assumed. The same happens in case the wave height or wave period is estimated from the above formulations. These calculations assume open, deep waters with fully developed waves. These formulations assume open, deep waters and fully developed waves. In enclosed waters, like fjords, or near land, smaller and steeper waves can be expected [36]. If the intermediate equation is used, an iterative process starts with an arbitrary 100m for λ, refining until successive iterations differ by <0.01m.

$$\lambda = \begin{cases} \frac{gT_s^2}{2\pi} & if\ attribute\ for\ wavelength\ eqn = 'deep' \\ \frac{gT_s^2}{2\pi}\tanh\left(\frac{2\pi d}{\lambda}\right) & if\ attribute\ for\ wavelength\ eqn = 'intermediate' \\ \sqrt{gd}T_s & if\ attribute\ for\ wavelength\ eqn = 'shallow' \end{cases}$$ *Module W3* *Ref: [40]* *Eq. (8)*

Wave phase speed

The wave phase speed is required for calculating time between successive ship-wave collisions and is calculated with Eq. (9).

$$c = \lambda / T_s$$ *Module W4* *Eq. (9)*

Ship speed relative to waves

The ship speed in the direction of waves $V_{s\theta}$ is first calculated with Eq. (9) with the absolute ship speed V_s and the ship heading with respect to waves, θ. θ is assumed to be 0° if unknown (ship heading straight into waves). This is inconsequential for stationary ships or structures. If ship speed is unavailable, V_s is set to 0. The ship speed relative to waves is then calculated with Eq. (11). The value of θ is restricted to 45° due to other formulations.

$$V_{s\beta} = V_s cos\beta$$ *Module C2* *Eq. (10)*

$$V_{rw} = c + V_{s\beta}$$ *Module C1* *Eq. (11)*

Time between successive ship- wave collisions

The time between successive ship-wave collisions t_{col}, can be calculated with Eq. (12) knowing the wavelength λ and the ship speed relative to waves V_{rw}.

$$t_{col} = \frac{\lambda}{|V_{rw}|}$$ *Module C* *Eq. (12)*

7.3. Estimation of feature values

Module 1: Air temperature

Air temperature is an obligatory input to the feature calculator. The feature calculator checks the input data for airTemp and stores it in the temporary dataframe. If airTemp is missing, an error is raised with a notification.

Module 2: 'waterTemp'

If the water temperature is available, it is stored in the intermediate dataframe. If missing, it is set to 2.14 which is the mean of the values the model was trained on, and the user is notified of the assumption. The water temperature was not set as obligatory since it is later concluded that variation in water temperature caused negligible change in the icing rates (see Figure 7).

Module 3: 'salinity'

If the salinity is available it is saved in the intermediate dataframe, else it is set to 32.895 – the mode of what the model was trained on, and the user is notified. It is not made obligatory for the same reasons as for water temperature. Additionally, the freezing temperature of saline water is calculated by Eq. (13).

$$t_f = -0.002 - 0.0524S - 0.00006S^2$$ *Module 3* *Ref: [4]* *Eq. (13)*

Module 4: 'windSpeed_mod'(u_{mod})

As discussed in previous sections u_{mod} is set equal to the relative wind speed (V_r) for a real case. If the relative wind speed is available, this is stored as u_{mod} in the intermediate dataframe. In the absence of the knowledge of the relative wind speed, it is estimated through the submodules. Figure 12 can be referred for the detailed flowchart.

Module 5: 'sprayPeriod'

If available, the spray period is saved in the intermediate dataframe. If absent, the feature calculator checks for the number of sprays per hour (spray frequency) and converts it to spray period or vice versa. If both are missing, sub-modules assess available data to estimate time between successive ship-wave collisions (t_{col}).

Spray is not generated at every ship-wave impact [3]. Zakrzewski, 1986, drew from Panov, 1976 [41], and Aksjutin, 1979 [42], proposing that a Medium Sized Fishing Vessel (MFV) experienced splashing roughly every other wave impact [35]. Horjen, 2013 adopted this for ICEMOD2 [37], as did Kulyakhtin, 2014 for MARICE [43]. Lozowski, 2000, noted spray on every fourth ship-wave impact for a large vessel [3]. This was also used in MINCOG by Samuelsen et.al., 2017 [7]. Ryerson, 2013, on the other hand, suggests spray frequency is independent of wavelength as given in Eq. (14) [44] which is invalid for ship speeds below 1.665m/s.

$$N = 60 * (1.5 + 0.26(1.94V_s - 9)) \qquad \textit{Module 5} \quad \textit{Ref: [44]} \quad \textit{Eq. (14)}$$

Spray period is calculated with Eq. (15) with 'Zakrzewski' as the default attribute. Setting the attribute to 'Ryerson' uses equation Eq. (14) for the number of sprays per hour and converts it to spray period. In the absence of ship speed or if the ship speed is below 1.665m/s, the choice is changed to 'Zakrzewski' and the user is notified. If other observations are made for an individual case, it is possible to set the attribute to an integer value *n*.

$$P_s = \begin{cases} 2 * t_{col}, & if\ attribute\ for\ sprayfreq = 'Zakrzewski' \\ 4 * t_{col}, & if\ attribute\ for\ spray\ freq = 'Lozowski' \\ n * t_{col}, & if\ attribute\ is\ an\ integer = n \end{cases} \qquad \textit{Module 5} \quad \textit{Ref: [35] [3]} \quad \textit{Eq. (15)}$$

Module 6: 'sprayDuration'

In the absence of spray duration in the input, it is estimated through other available data through several sub-modules. Literature presents several formulations for spray duration. Zakrzewski, 1986, referenced Borisenkov, 1972 [45] who suggested a constant 2-second spray duration for a particular vessel, and proposed an equation for t_{dur} with empirical constant c* based on hull shape and size [35]. Zakrzewski, 1987, calculated c* as 20.62 from Borisenkov, 1972 [45], applicable to the specific ship MFV 'Iceberg' [5]. Since c^* was said to be dependent on hull size and shape, the resulting equation in Eq. (17) would be applicable to ships similar to that of MFV 'Iceberg'. Lozowski et.al., 2000 [3], adapted this equation with c^*=10 for consistency with the USCGC Midgett observations by Ryerson, 1995 [19]. Horjen, 2013, proposed Eq. (16) to estimate spray duration for 'Norwegian waters' with relative windspeed between vessel and u_{10} [37]. Samuelsen et.al. 2017 proposed another new formulation based on observations of the 'KV Nordkapp' [7] and is given in Eq. (17).

$$t_{dur(Horjen)} = \frac{\lambda}{2u_{10rel}} \qquad \textit{Module 6} \quad \textit{Ref: [37]} \quad \textit{Eq. (16)}$$

$$t_{dur} = \begin{cases} 20.62\frac{H_s V_{rw}}{u_{10}^2}, if\ spray\ duration\ attribute = 'Zakrzewski' \\ 10\frac{H_s V_{rw}}{u_{10}^2}, if\ spray\ duration\ attribute = 'Lozowski' \\ 0.123 + 0.7007\frac{H_s V_{rw}}{u_{10}}, if\ spray\ duration\ attribute = 'Samuelsen \end{cases} \qquad \textit{Module 6} \quad \textit{Ref: [35] [3] [7]} \quad \textit{Eq. (17)}$$

The Zakrzewski, 1987, Lozowski 2000 (default), and Samuelsen 2017 formulations are available in SPICE and could be used by selecting the appropriate attribute. Any divisions by 0 are set to 0.

Module 7: 'flux' (Spray flux)

Various studies employ Liquid Water Content (LWC) in the wave impact spray for flux estimation [3], [5], [46], [47]. Forest et.al., 2005, noted vast spray flux variations due to different LWC formulations, ranging from 6.94×10^{-7} to 44 kg/m^2/hr at 10m above the mean sea level and attributed this to the difference in climatic factors and spray generation mechanisms used while developing the LWC models [47]. Kulyakhtin, 2014 [1], highlighted flux uncertainty as a key icing prediction challenge, pointing that the flux formulation in ICEMOD gives 10-1000 times less flux than the one in RIGICE04. It is therefore recommended to calculate or measure the flux on a case-to-case basis. Figure 4 , Figure 5, and Table 3 show the critical role of flux in icing predictions. Models reliant on formulations for the estimation of spray flux limit these models only to the type of ship or structure the flux formulation is based on.

If flux is unknown, the feature calculator offers three flux estimation formulations, with a warning to the user if used. Setting the attribute to 'Kulyakhtin' (default) uses the steady version of the spray flux formulation by Kulyakhtin, 2014 [43] derived from Horjen and Vefsnmo 1985 [48], from Eq. (18); where z_{hv} is given in Eq. (19), which makes it valid only for $z > H_s/2$.

$$M_k = \left(6.28 \times 10^{-4} \cdot u_{10} \frac{1 - (1 - 10^{-2} \cdot u_{10}) \exp\left(-\left(\frac{4 \cdot z_{hv} + 2}{9}\right)^2\right)}{\exp(0.0588 \cdot u_{10}^{0.667} \cdot z_{hv}^2)} * \cos(\alpha) \right) * 3600 \qquad \begin{matrix} \textit{Module} \\ 7 \end{matrix} \quad \begin{matrix} \textit{Ref:} \\ \textit{[43]} \end{matrix} \quad \begin{matrix} \textit{Eq.} \\ \textit{(18)} \end{matrix}$$

$$z_{hv} = \left(\frac{2z}{H_s}\right) - 1 \qquad \textit{Module 7} \quad \textit{Ref: [43]} \quad \textit{Eq. (19)}$$

Setting the attribute for the spray flux formulation to 'Horjen' uses the Horjen 2013 [37] formulation for spray flux (Eq. (20)). For simplification, only the alternative for $\alpha = 45°$ from Horjen 2013 is used (invalid for $z > 2.17H_s$), and the water density is kept constant at 1026 kg/m^3.

$$M_h = \left(\left(\frac{1026 H_s^2}{T_s^2 u_{10}^2} \right) \cdot \left(\frac{g T_s}{4\pi} + V_s cos\beta \right) \cdot (-3.0706 \times 10^{-4} z_{hv} + 1.027 \times 10^{-3}) \right) * 3600 \qquad \begin{matrix} \textit{Module} \\ 7 \end{matrix} \quad \begin{matrix} \textit{Ref:} \\ \textit{[37]} \end{matrix} \quad \begin{matrix} \textit{Eq.} \\ \textit{(20)} \end{matrix}$$

Alternatively, setting the attribute to 'Ryerson' uses Eq. (21) where the constant 0.074992 is derived from the mean spray flux per second from the 39 events from the Ryerson 1995 [19] data, omitting three of the smallest and largest values.

$$M_r = 0.074992 * t_{dur} * N \qquad \begin{matrix} \textit{Module} \\ 7 \end{matrix} \quad \begin{matrix} \textit{Ref:} \\ \textit{[19]} \end{matrix} \quad \begin{matrix} \textit{Eq.} \\ \textit{(21)} \end{matrix}$$

8. Results and validation

Nine cases are presented for the validation of the Spice model by comparing the results with Spice to that of five existing models: Overland model (ov), Roebber & Mitten model (rm), (modified) Stallabrass model (st_mod), (modified) MARICE model (ku_mod), and the RIGICE04 model (ri). Details of the existing models and their equations can be referred to in Appendix A. Each case is set up such that only one variable is

varied in the individual case while other variables are constant for that case. For cases 1-7, all features were set within the trained range of the model as given in Table (except that of the variables that easily default to a certain value, like water temperature and salinity). For cases 8 and 9, the spray period, spray duration, and spray flux, are not provided, and thus calculated by the feature calculator.

Table 6: Inputs for cases 1-9 and information about other models

Case nr.	**Air Temp**	**Water Temp**	**salinity**	**u10**	**spray Duration**	**spray Period**	**flux**	**ship speed**	**ship heading wrt wind**	**z**	**Test Variable**	**If model is a function of test variable**					
	(°C)	**(°C)**	**(ppt)**	**(m/s)**	**(sec)**	**(sec)**	**(kg/m^2 /hr)**	**(m)**	**(°)**	**(m)**		**spice**	**ov**	**r&m**	**st_mod**	**ku_mod**	**ri**
1	-10	default	default	0 to 20	1	9	20	default	default	8	**u10**	only if local wind speed unknown	yes	yes	yes	yes	yes
2	-15 to -5	default	default	8	1	9	20	default	default	8	**airTemp**	yes	yes	yes	yes	yes	yes
3	-10	default	default	8	1	9	9 to 24	default	default	8	**spray flux**	yes	no	no	no	yes	through wave parameters
4	-10	0.15 to 3.3	default	8	1	9	20	default	default	8	**water Temp**	yes	yes	yes	yes	no	no
5	-10	default	30 to 32.8	5	1	9	10	default	default	3	**salinity**	yes	yes	yes	yes	yes	yes
6	-10	default	default	5	0.25 to 1	9	10	default	default	3	**spray duration**	yes	no	no	no	only for calc of flux	through wave parameters
7	-10	default	default	5	0.25	3 to 9	10	default	default	3	**spray period**	yes	no	no	no	only for calc of flux	through wave parameters
8	-10	default	default	10	default	default	default	0 to 10	default	3	**ship speed**	only if local wind speed unknown	no	no	yes	no	no
9	-10	default	default	10	default	default	default	5	0 to 90	3	**ship heading wrt wind**	only if local wind speed unknown	no	no	yes	no	no

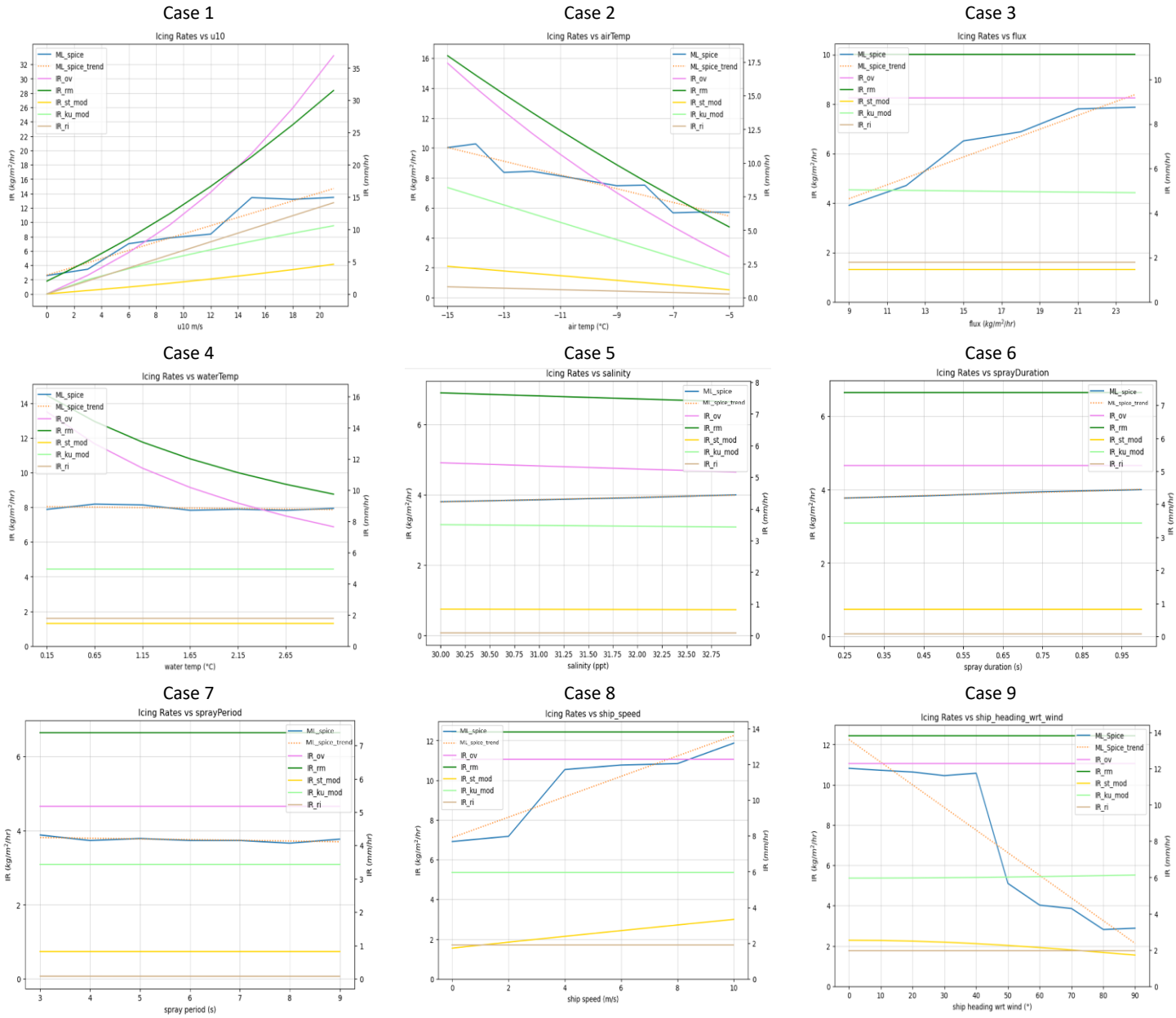

Figure 7: Results of spice compared with other models for various inputs

The right segment of Table 6 shows whether icing rates are a function of the tested variable in all the presented models. Diverse model approaches make direct comparison difficult. It was discussed in previous sections how the skewed data and tree-based models lead to a stepped output. This behavior was vastly reduced with feature engineering, though complete removal might require a vast number of additional tests. Hence, Figure 7 also presents the trend of the predictions with Spice. The purpose of the trend is to give a rough idea of the behavior of the model and a linear fit was considered. The aim eventually however is to ideally have more data so as to completely avoid the stepped output.

Figure 7 reveals considerable disparities in icing rate predictions by different models. Cases 1-3 depict icing rate variations due to three key variables: wind speed, air temperature, and spray flux. All models exhibit

increased icing rates with increasing u_{10} wind speed. Predictions with SPICE lie in the middle of the spectrum of existing models, closest to that of RIGICE04. While most models project zero icing at zero wind speed, R&M and Spice show some minimal icing. For R&M, Eq. (24) yields positive polynomial values at zero predictor, while for Spice, any input flux maintains slight icing. If the flux was unknown, and thereby calculated with the feature calculator, the flux value at zero wind would be zero, giving no icing. It is thus important to know the feature values for an accurate prediction.

Case 2 shows a clear tendency of increasing icing rates with decreasing temperatures. However, the dependence of icing on the air temperature varies vastly from model to model. Predictions with Spice lie somewhere in between all models. At higher temperatures however, Spice shows the highest icing rates.

In Case 3, only Spice predicts increasing icing rates solely with varying spray flux, where spray duration and period are constant. Spice's ability to achieve this is notable, while other models fail to show similar trends. Notably, in the presented models, flux is not considered by the Overland and R&M models, while the rest incorporate various formulations involving wind speed, wave parameters, ship speed, and height from the mean sea level. This limitation could lead to incorrect estimates of icing rates in existing models, particularly in cases where wave parameters remain constant due to steady wind conditions as the theoretically calculated flux at the fore and aft of the vessel would be constant.

Cases 4-7 explore less impactful variables according to the ML model: water temperature, salinity, spray duration, and spray period. Notably, the Overland and R&M models show high sensitivity to water temperature; and despite the Overland model's criticism about this by Makkonen et.al. 1991 [49], it still remain in use[1]. For the other variables, models either neglected them or exhibited minimal changes in icing rates within the tested range for a constant flux. While Spice did show minor variations in predicted icing rates due to these, the absolute change was negligible. The limited range of tested spray duration (max 1 sec compared to 5.57 sec observed by Ryerson 1995 [19]) underscores the need for more experimental data to confidently predict a wider input range. Similarly, the negligible but opposing trend in icing rates with changing salinity aligns with observations by Ryerson 1995. Importantly, minor measurement errors in these variables have negligible effects on predictions, overshadowed by dominant factors like wind speed, air temperature, and flux.

For cases 8 and 9, only the modified Stallabrass model considers ship speed and heading. RIGICE04 and MARICE are designed for structures, while Overland and R&M, although developed for vessels, disregard ship speed. Spice relies on local wind speed information, specifically u_{mod}, which is compared to relative wind speed. In these cases, Spice's feature calculator estimated windspeed (u_{mod}), spray duration, period, and flux. This involved estimating wave parameters from u_{10}, leading to values outside tested ranges for spray-related variables. While an ML model performs well within its training range, extrapolating beyond it lacks certainty, especially when validation data is absent. Section 8.2 covers the inability of using existing datasets for validation. Thus, the certainty of absolute icing rates for these cases cannot be determined, yet their trends for both cases, in terms of the direction of the slopes, match the modified Stallabrass model, albeit with substantially different magnitude for case 9. Higher ship speeds result in elevated icing rates, likely due to increased relative wind speed, while lower rates coincide with specific ship headings, associated with reduced relative wind speed and flux. Notably, Spice generally yields higher icing rate values than the modified Stallabrass model.

8.1. Importance of accurate knowledge of flux

The correct estimation of flux is emphasized in the previous sections as well as by researchers in previous studies [1]. The feature calculator in Spice is provided in situations where a rough estimation of icing rates would suffice. However, for accurate predictions, especially where icing predictions are critical for design and safety purposes, the aim should be to avoid using the feature calculator as much as possible, at least for more important features like wind speed and flux. The feature calculator could be used in case of unknown salinity, water temperature, spray duration, and spray period, which showed comparatively negligible effects on the icing rate, with minor loss of accuracy.

Figure 8 presents an example where the predictions are heavily dependent on the choice of flux formulation. The 3 different choices of flux show great variation in the icing rates against wind speed, for a constant air temperature of -10°C and other parameters set to default. Additionally, many of the values for spray duration, spray period, and especially flux, were seen to be out of range of the tested data – thus calling for additional experimental data to increase the range of confident predictions.

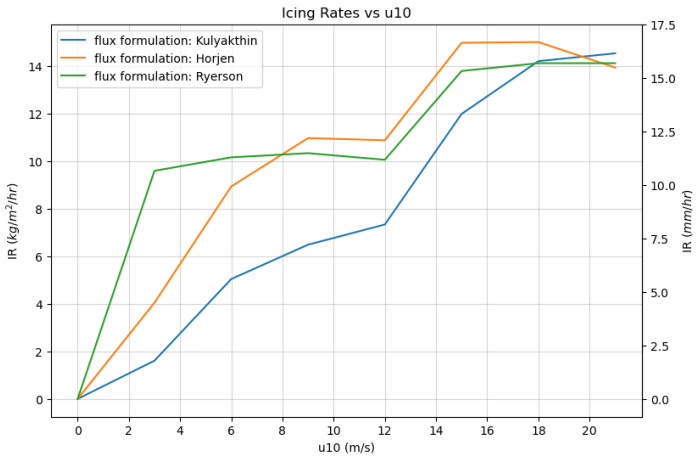

Figure 8: Variation in icing rate prediction by flux formulation

8.2. Why currently available datasets could not be used for precise validation

Due to complexities and expenses, few comprehensive icing and spray datasets are accessible [1], [10] and even fewer are published. Two openly accessible datasets containing extensive icing rates and related metocean and ship data were explored for validation attempts in real scenarios.

Ryerson 1995 [19] gives a detailed description of 39 spray impacts and the total ice accreted in an icing event that lasted for 100 hours. However, using this data directly for validation poses challenges. Ice measurements are given at four locations, but only one table includes flux observations. Real flux experienced at the four locations would clearly have been different due to observed differences in icing thickness, even at the same height. The measured ice thickness often exceeded model predictions in Figure 9. Despite lasting only about 2 minutes cumulatively, the 39 spray impacts span 100 hours, and icing measurements cover the entire period rather than after each event. Ryerson 1995 reported fluxes ranging from 5.22×10^{-4} to 18.62 18.62 kg/m^2 per event [19]. With such high fluxes, there's a possibility that some accreted ice might be removed in a dynamic process involving multiple accretion and ablation episodes

during an icing event [19]; which cannot be captured due to the nature of Ryerson's data. Another graph shows very high wind speeds throughout the 100-hour period. Although most models mostly neglect wind generated spray, it could affect the observations over a 100-hour period where wave impact generated spray lasted for cumulatively only 2 minutes. The graph for the main deck level at the starboard bulkhead shows ice thickness decreasing when wind speed reduces and air temperatures fall below freezing, suggesting potential effects due to wind generated flux.

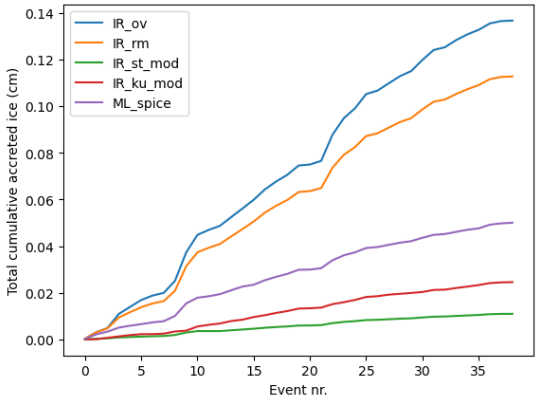

Figure 9: Total cumulative calculated ice for Ryerson 1995 [19] data.

The closest comparison could thereby only be achieved with other models as shown in Figure 9. (The consolidated Ryerson 1995 data used as inputs for this calculation is presented in Appendix C.) This graph converts predicted icing rates to thickness and presents accumulated ice after each spray impact, and eventually, the maximum predicted ice thickness with different models for the Ryerson 1995 data. However, even among the models, the closest match to Ryerson 1995 data is limited to specific observations at the 02-level starboard bulkhead. This comparison does not provide substantial validation insight for any model, including Spice, in real case scenarios.

In another set of full-scale data, Samuelsen et al. 2017, for their MINCOG model, present a case with 37 spray events, of which 14 have an icing rate of 0.33 cm/hr [7]. However, scrutiny of the metocean data reveals significant variations in other parameters within these 14 cases. Air temperature varies from -20.2°C to -1.9°C, water temperature from -1.3°C to 6.6°C, u_{10} from 9.3m/s to 25.2 m/s, wave height from 1.5m to 12m, ship speed from 1 m/s to 8.6 m/s, among others, for individual cases. It is unclear whether these presented icing rates are observed or calculated by MINCOG. Nevertheless, the exact same icing rate for cases with such huge variations of other variables is questionable. It could be a possibility that several parameters are presented in the form of mean values over larger periods of time. In either case, comparison of the predicted icing rates by any model with this dataset, as presented, did not serve the purpose of validation for a real case.

9. Discussion

9.1. On the estimation of flux

Kulyakhtin 2014 names flux estimation as the biggest cause in sea spray icing prediction errors [1]. Figure 8 shows the stark differences in icing rates from three flux estimation formulations. Additionally, Ryerson

1995 from their detailed study of flux and icing measurements mention that the observed flux data was attempted to be written as general equations as a function of other parameters, but most relationships were complex and not significant [19]. This observation clearly discourages the use of any formulations for estimation of spray flux. Despite this, researchers have been using the handful of available flux formulations. Models using these formulations, often in the form of LWC, would, at most, predict icing rates for similar ships and the exact locations as ones from the flux measurements. Any attempts to generalize these types of ice prediction models over different types and sizes of ships or structures or using them to estimate the distribution of ice would provide inaccurate results. This effectively deems all theoretical models as inaccurate or limited to very specific cases. The problem was visible while attempts to validate models against full scale data, since the ice thickness and flux were measured at different locations. This calls for a radical change in how future models approach the estimation of spray flux. CFD techniques and real-time measurement of spray flux at the desired locations are suggested for future research.

9.2. Advantages of the Spice model and scope for improvement

- Being developed 'bottom-up' from data from controlled experiments, predictions with Spice could be said to be highly accurate within the tested range if the input variables are accurately known. This claim about the accuracy can be made owing to the high model scores while predicting icing rates for the completely unseen test data. Dominant variables like air temperature, wind speed, and spray flux significantly affect icing rates, with others having minor impacts. One could argue that some additional variables, like humidity, are not captured and could affect the icing rates in full-scale testing. Kulyakhtin 2011 proved that the in-cloud humidity can be neglected as other terms have a much higher effect on the mass of accreted ice [50].
- Spice can be made available as an easy-to-use package in python, or even a deployed version which could be integrated with other systems. This makes Spice extremely user-friendly in comparison to existing models.
- Spice has the ability for continuous improvement by retraining the model with data from additional tests for e.g., for increasing the prediction range or including melting rates.
- Spice can be used as a transient model and could be integrated with the ships' systems to make real-time icing predictions. The problem, however, lies in the measurement of flux. Investigations into whether instruments such as rain gauges could be used at critical points for the real-time estimation of spray flux is suggested for future research.
- Existing models ignore precipitation as a source of flux, and if accurately known, Spice can estimate combined sea spray and rain-induced icing rates, given its broader training on both salt and freshwater experiments.
- Technical limitations with generation of high windspeeds in the lab necessitated the preliminary feature engineering technique using the u_{mod} variable. Predicted icing rates using this technique in Spice fall between those of other models, and ideally should be validated in full scale.
- Spice is built 'bottom-up' from data from controlled laboratory experiments and is thus experimentally validated in the laboratory. This is already an advantage over existing models; however, full scale application of the model could be restricted due to pending full scale validation. This is a topic of

ongoing research. Flux estimation using the feature calculator in general remains the biggest uncertainty for accurate predictions. This said, unlike existing models, Spice is developed to be extremely flexible, such that the user is free to use the most appropriate formulation depending on the case or to use input values from any other source or method of choice. In general, the goal should be to make as little use of the feature calculator as possible. Techniques for the reduction of the feature calculator by using Spice in combination with CFD models is part of ongoing research.

- The original MARICE model incorporates CFD to address the problem of unequal flux at different locations at the same height above the sea level but uses existing spray generation formulations and points out that these spray generation formulations are the weakest link [1]. Spice, however, offers independence in specifying spray flux, making it possible to combine CFD or measured flux data for more accurate predictions tailored to specific vessel configurations or environmental conditions.

10. Conclusion

The study introduces a novel sea spray icing prediction model utilizing ML, dubbed 'Spice'. The model is based on controlled experiments involving 30 sea spray icing cases in a cold climate laboratory. Performance of various open-source ML algorithms was assessed. Given the skewed nature of the experimental data, feature engineering techniques were employed, yielding promising results. Results from Spice were compared with five existing models in 9 hypothetical cases, each involving variation of one parameter. Another case compared results with different flux formulations. The study concludes by addressing challenges associated with using currently available full-scale data for validation purposes. A comprehensive flowchart of Spice and its development is provided for replicability. This is the first study in the field of sea spray icing wherein a data-driven machine learning model is implemented for the purpose of icing predictions.

The Deshpande et al. 2023 experiments lacked definitive conclusions on the impact of certain independent variables due to several covariates. Earlier findings established that material does not affect icing rates beyond initial sprays, while icing rates rise with wind speed and decline with temperature [14]. This study concludes that higher spray flux contributes to increased icing rates within the tested range. Furthermore, variations in water temperature, salinity, spray duration, and period exhibit negligible effects on icing rates compared to dominant factors like air temperature, wind speed, and flux.

Some of the findings from this study are presented below:

- Air temperature, wind speed, and spray flux stand out as the dominant parameters affecting icing rate predictions. ML methods confirm their combined importance, aligning with logical reasoning, for e.g., high wind speeds and flux won’t cause icing unless temperature is below the freezing point.
- Existing models employ spray duration and period solely to estimate flux, not as independent variables. Independently, these variables show minimal impact on icing rates for a constant time-averaged flux within the tested range.
- Linear regression gave poor results and the tree based XGB Regressor predicted the unseen ‘test data’ well. However, the limited number of tests necessitated use of feature engineering techniques for which RuleFit and FFX gave satisfactory results.

- Existing models predict vastly different icing rates. The varying approaches and different purposes of the models makes it difficult for a direct comparison.
- Validation of models with existing full-scale experimental data proved to be challenging. It is difficult to measure flux and icing at a detailed level on a large ship. However, it is essential to have more detailed full-scale tests for validation of prediction models, in the absence of which data from controlled laboratory experiments is the most reliable for development and validation of prediction models.
- A 'general' model for sea spray icing is one that can predict icing for a wide range of applications (e.g., for both, structures and for all sizes of vessels). Resolving the issue of flux estimation on a case-to-case basis through CFD or real-time methods and feeding this to Spice could ensure its universal applicability making it a potential candidate as a truly 'general' model for sea spray icing prediction. This would also ensure prediction of the distribution of ice which is critical for design optimization and research in this direction is already underway.

11. Acknowledgements

The author would like to thank Dr. Edward Lozowski, Dr. Tom Forest, and Dr. Anton Kulyakhtin for sharing the RIGICE04 model and kind email exchanges. The author would also like to thank Tom Yang from Einblick for their time and effort for introducing me to possibilities with machine learning in the Einblick software and assisting me with the case in the initial stages. Finally, the author would like to thank Vedangini Sahajpal for her machine learning lessons in python.

12. Nomenclature

Symbol	Units	Description	Symbol	Units	Description
c	m/s	Wave phase speed	t_f	°C	Freezing point of saline water at salinity S ppt
c^*	-	Empirical constant for spray duration	T_s	sec	Wave period
d	m	Water depth	t_w	°C	Seawater temperature
e		Saturation vapour pressure at given temp (Subscripts: a: at temperature T_a; f: at temperature T_f)	u_{mod}	m/s	Modified wind speed (windspeed_mod) variable used after preliminary feature engineering (see section 4.1)
g	m/s^2	Acceleration due to gravity ($g = 9.81$)	u_z, u_{z0}	m/s	Wind speed at heights z and z_0 for the calculation of wind speed by wind power law
H_s	m	Significant wave height	u_{10}	m/s	Wind speed at height of 10m above sea surface
IR	As per given equation, but eventually converted to mm/hr and $kg/m^2/hr$	Icing rate (Subscripts refer to the model used)	V_r	m/s	Relative wind speed
M	$kg/m^2/hr$	Spray flux (Subscripts refer to the formulation used)	V_{rw}	m/s	Ship speed relative to waves
n	-	Spray generated at every 'n^{th}' ship-wave collision	V_s	m/s	Absolute ship speed

N	/hour	Nr. of sprays per hour or Spray frequency per hour	$V_{s\alpha}$	m/s	Ship speed in wind direction (Into wind is +ve)
PR	m°C/s	Predictor for icing rates by overland	$V_{s\beta}$	m/s	Ship speed in wave direction (Into waves is +ve)
P_s	sec	Spray period	z	m	Height above mean sea level
S	ppt	Salinity of seawater	z^*	m	Roughness length or roughness coefficient for calculating the wind speeds by the wind power law.
t_a	°C	Air temperature	α	°	Ship heading wrt wind (Straight into wind = 0°)
t_d	°C	Droplet temperature at impact	β	°	Ship heading wrt waves (Straight into waves = 0°)
t_{dur}	sec	Spray duration	λ	m	wavelength
t_{col}	sec	Time between successive ship-wave collisions	ρ_{ice}	kg/m^3	Density of ice (Used only for the conversion of icing rates in terms of mass to thickness and set to 900)

13. Appendix A

Details of prediction by existing models used for comparison

Existing models employ diverse approaches and input variables for predicting icing rates. They also serve varying purposes such as RIGICE04 being developed specifically for large stationary structures. This diversity hampers straightforward model comparisons. Nonetheless, selected models were approximated, accommodating coarse assumptions wherever necessary for evaluation of Spice. Conversion of icing rates among mentioned models was done to mm/hr and kg/m^2/hr through straightforward calculations using ice density $\rho_{ice} = 900kg/m^3$ [43], [51].

Overland model

One of the simplest models to date in terms of implementation was proposed by Overland 1986 [52]. In spite of the criticism of Makkonen 1991 [49] towards this model, it is widely used for mapping regions susceptible to sea spray icing [43]. Its popularity stems probably from its simplicity and straightforward implementation. The Overland 1986 model first calculates a predictor (*PR*) from Eq. (22) from which the icing rate is calculated in cm/hr from Eq. (23).

$$PR = \frac{u_{10}(t_f - t_a)}{1 + 0.4(t_w - t_f)} \qquad \textit{Ref: [52]} \quad \textit{Eq. (22)}$$

$$IR_{ov} = 2.73 \times 10^{-2}(PR) + 2.91 \times 10^{-4}(PR)^2 + 1.84 \times 10^{-6}(PR)^3 \text{cm/hr} \qquad \textit{Ref: [52]} \quad \textit{Eq. (23)}$$

Roebber & Mitten model

Roebber and Mitten, 1987 [53] suggested changes to the polynomial of the Overland 1986 model using the same predictor (*PR*) from Eq. (22). This model, referred to as the Roebber & Mitten (R&M) model calculates the icing rate in cm/hr by Eq. (24).

$$IR_{rm} = 0.1982 + 3.07 \times 10^{-2}(Pr) + 1.996 \times 10^{-4}(PR)^2 \text{ cm/hr} \qquad \textit{Ref: [52]} \quad \textit{Eq. (24)}$$

Stallabrass model

The Stallabrass 1980 model [4], based on icing measurements on fishing trawlers and tests on cylinders, is simplified here for comparison. The equilibrium freezing surface temperature is assumed equal to the freezing point of seawater at the given salinity from Eq. (13). Stallabrass 1980 notes droplet supercooling [4], and Kulyakhtin 2014 points out to the impact temperature to be anywhere between the air and sea temperatures [43]. For simplification, droplet temperature at impact (t_d) is set equal to air temperature (t_a). Eq. (25) gives the Stallabrass equation for icing rates in mm, and the model is referred to as the 'modified' Stallabrass (st_mod) model.

$$IR_{st\_mod} = 8.26 \times 10^{-3} H_s V_s (t_f - t_d) + 6.28 \times 10^{-2} V_s^{0.8} \{(t_f - t_a) + 1.73(e_f - 0.9 e_a)\} \quad \textit{Ref: [4]} \quad \textit{Eq. (25)}$$

$$e = \left(\left((1.9226 \times 10^{-7} t + 2.4545 \times 10^{-5}) t + 1.4224 \times 10^{-3}\right) t + 0.044436\right) t + 0.61094 \quad \textit{Ref: [4]} \quad \textit{Eq. (26)}$$

MARICE model

MARICE [43] is a time-dependent sea spray icing model utilizing CFD. The original implementation of this model was done with the help of a freezing equation for each cell in the CFD simulation. Unlike Overland and Stallabrass models that rely mainly on metocean and structural parameters, direct comparison of Spice to MARICE is challenging due to the scale at which equations are applied. However, coarse assumptions are made for comparison. The original extensive set of equations are not presented here; readers can refer to Kulyakhtin 2014 [43]. For comparison, simplifications include a structural diameter of 0.7m (matching test plate length by Deshpande et al. 2013), windward stagnation point at 90°, the Schmidt number, originally computed with CFD, is set to 200, and a steady-state version of Eq. (18) is used instead of CFD-calculated flux. Removal of accreted ice in the wave washing zone is neglected. The results presented here are for coarse comparison, not original MARICE results. The resulting model is termed as 'modified' Kulyakhtin model (ku_mod).

RIGICE04 model

RIGICE04 was developed for estimating icing on offshore structures [47], and was employed for comparison using its Excel format. To facilitate the comparison, these settings were applied: large vertical column flag set at 1, large column diameter at 0.7m, large column top height at 15, large column bottom height at 0, and number of large columns at 1. The met data from section 8 for each condition was inputted in the first row, while the second row was set to arbitrary conditions with temperature above freezing point (1°C) as required by the program. A 1-hour time difference between the rows yielded hourly icing output. Default relative humidity (80%) and atmospheric pressure (1013.25 bar) from the accompanying metocean data file were maintained. Outputs were in kg of ice and ice thickness as functions of height above mean sea level, as bottom height was set at 0. Ice thickness was converted to mass/m^2 using 900 kg/m^3ice density. Only the first and last values are calculated in Rigice04, and the rest linearly spaced for simplicity. Icing rates with the RIGICE04 model are denoted as 'IR_ri'.

14. Appendix B

X_train_transformed

Figure 10 shows the head (first 5 rows) of the X_train_transformed dataframe for better understanding of how the dataframe looks like after transformation.

	airTemp	waterTemp	salinity	windSpeed_mod	sprayDuration	sprayPeriod	flux	eqn_0	eqn_1	eqn_2	eqn_3	eqn_4	eqn_5	eqn_6	eqn_7	eqn_8	FFX_SYMBOLIC_EQUATION
24068	-9.179672	2.492790	32.445	0.000000	0.25	9.0	10.632562	0.000000	0.000000	0.000000e+00	0.000000e+00	-0.000000	-0.000000	0.000000	0.000000	0.000000	1.528963
106434	-10.319809	1.812036	32.450	25.150839	0.25	9.0	8.962926	18109.308744	24007.427125	2.527988e+07	1.265252e+07	-2326.344076	-2326.344076	225.425104	225.425104	24007.427125	6.968692
41728	-9.459251	2.100834	32.895	25.150839	0.25	9.0	8.962926	18109.308744	20170.459674	2.182607e+07	1.249359e+07	-2132.352685	-2132.352685	225.425104	225.425104	20170.459674	7.769986
81055	-9.548292	2.293249	32.895	25.150839	0.25	6.0	14.513829	76895.061680	33280.197510	3.601187e+07	3.643753e+07	-3485.460643	-3485.460643	365.034970	365.034970	33280.197510	10.811456
45242	-9.622191	2.064517	32.895	16.767226	0.25	9.0	10.623468	20102.965866	16492.080990	1.784577e+07	1.189844e+07	-1713.963200	-1713.963200	178.126087	178.126087	16492.080990	6.974929

Figure 10: X_train_transformed dataframe head

15. Appendix C

Consolidated Ryerson 1995 data

Data from multiple tables from Ryerson 1995 [19] were used in the calculation of icing rates in Figure 9. Some data could be used directly, while some had to be converted to the inputs required by Spice. The consolidated data used as inputs to Spice and other models in Figure 9 are presented in Table 7.

Table 7: Consolidated Ryerson data used for calculations in Figure 9

Spray no.	Spray duration	Ship speed	Wind speed	Ship heading	Wave height	Ship heading	flux per event
	tdur	Vs	umod	wrt wind (α)	H_s	wrt waves (β)	
1	0.87	8.24	10.30	90.00	1.52	110.00	0.09
2	4.53	8.24	15.44	30.00	0.91	50.00	18.60
3	2.80	8.24	15.44	30.00	0.91	50.00	0.03
4	3.90	6.18	26.77	20.00	1.52	30.00	0.93
5	1.93	6.18	26.77	20.00	1.52	30.00	0.08
6	1.57	5.15	29.86	20.00	1.52	30.00	0.14
7	1.77	6.18	21.62	10.00	1.83	20.00	18.70
8	1.17	6.18	20.59	10.00	1.83	20.00	0.13
9	5.20	6.18	20.59	10.00	1.83	20.00	0.58
10	12.33	6.18	20.59	10.00	1.83	20.00	17.80
11	5.57	6.18	24.71	0.00	2.44	0.00	0.08
12	2.77	8.24	17.50	30.00	-	-	0.01
13	2.30	8.24	17.50	30.00	-	-	0.03
14	3.80	8.24	20.59	40.00	2.13	50.00	0.04
15	3.67	8.24	20.59	40.00	2.13	50.00	0.57
16	3.83	8.24	20.59	40.00	2.13	50.00	0.01
17	4.47	8.24	20.59	40.00	2.13	50.00	0.50
18	3.43	8.24	20.59	40.00	2.13	50.00	0.02
19	2.93	8.24	20.59	40.00	2.13	50.00	0.05
20	3.97	8.24	20.59	40.00	2.13	50.00	0.08
21	0.47	8.24	19.56	60.00	2.13	80.00	0.00

22	1.47	8.24	21.62	30.00	2.44	40.00	0.16
23	7.70	11.33	25.74	20.00	1.52	0.00	1.08
24	4.87	11.33	25.74	20.00	1.52	0.00	0.90
25	2.97	11.33	25.74	20.00	1.52	0.00	0.04
26	4.23	11.33	25.74	20.00	1.52	0.00	0.12
27	1.00	11.33	25.74	10.00	1.52	50.00	0.03
28	2.17	11.33	25.74	10.00	1.52	50.00	0.04
29	2.10	11.33	25.74	10.00	1.52	50.00	0.39
30	1.53	11.33	25.74	10.00	1.52	50.00	0.12
31	3.30	11.33	25.74	10.00	1.52	50.00	0.99
32	2.93	11.33	25.74	10.00	1.52	50.00	0.09
33	0.83	11.33	25.74	10.00	1.52	50.00	0.18
34	2.10	11.33	25.74	10.00	1.52	50.00	0.02
35	2.13	11.33	22.65	40.00	1.52	90.00	0.05
36	2.53	11.33	17.50	10.00	1.52	90.00	0.00
37	3.60	11.33	17.50	10.00	1.52	90.00	0.08
38	1.33	11.33	17.50	10.00	1.52	90.00	0.03
39	0.87	1.03	7.21	30.00	1.52	90.00	0.01

16. Appendix D

Supporting flowcharts: The Spice development process and The Feature Calculator.

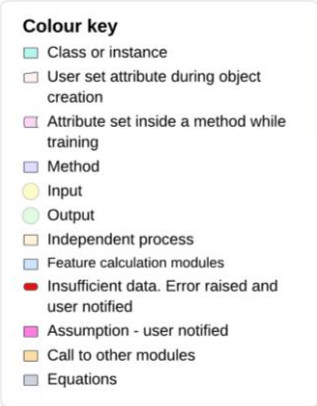

Figure 11: Color keys for the Spice algorithm

Figure 11 explains the color keys used in the flowcharts for clarity. The flowchart for the Spice Feature Calculator is shown in Figure 12.

Figure 13 shows the flowchart for the development of the Spice model, including the training, testing, and validation processes. Figure 14 shows the flowchart for the usage of spice as an end-user of the application. The simplicity of the flowchart in Figure 14 indicates the user-friendliness of the Spice model once it is deployed for use.

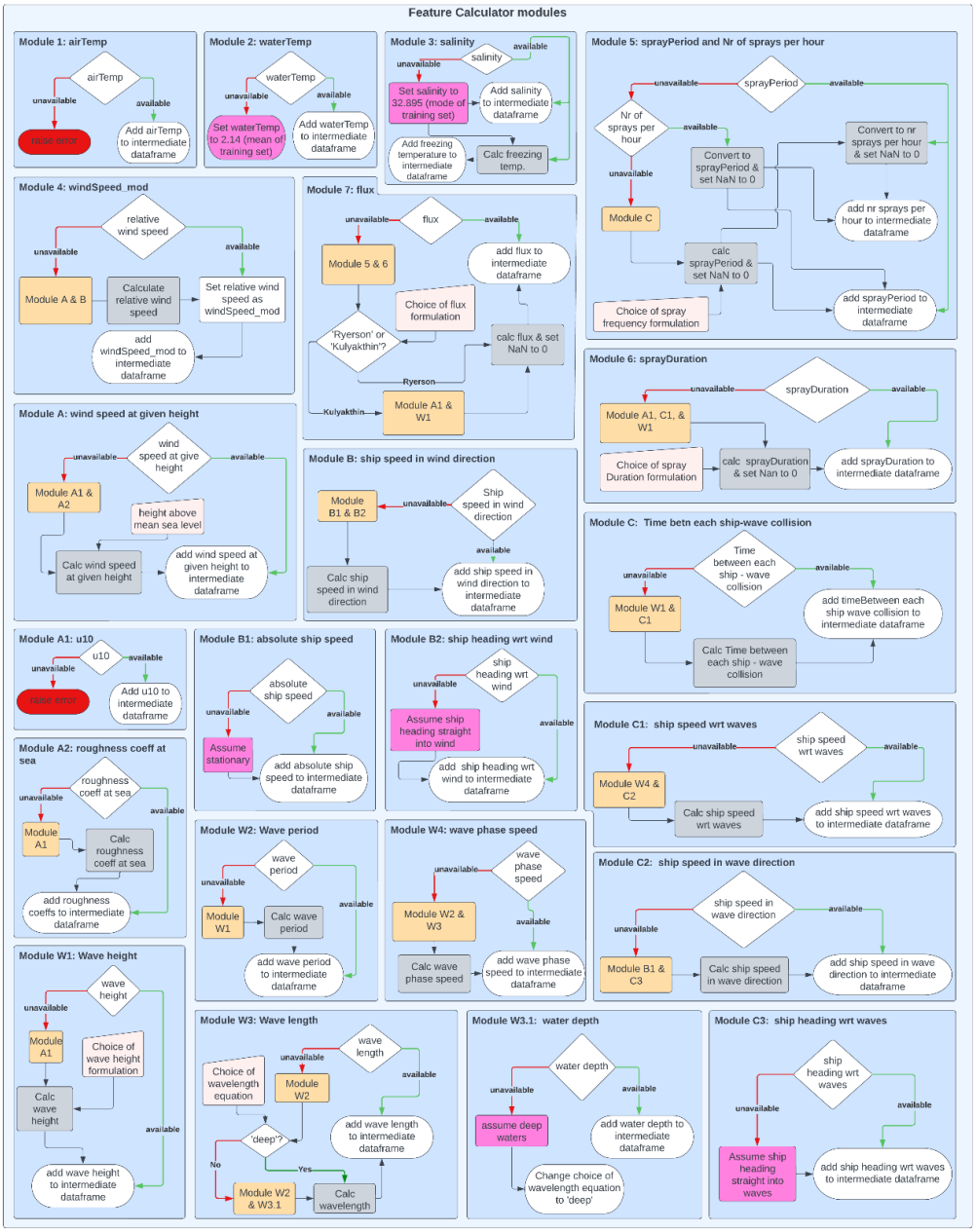

Figure 12: Flowchart for the Spice feature calculator modules

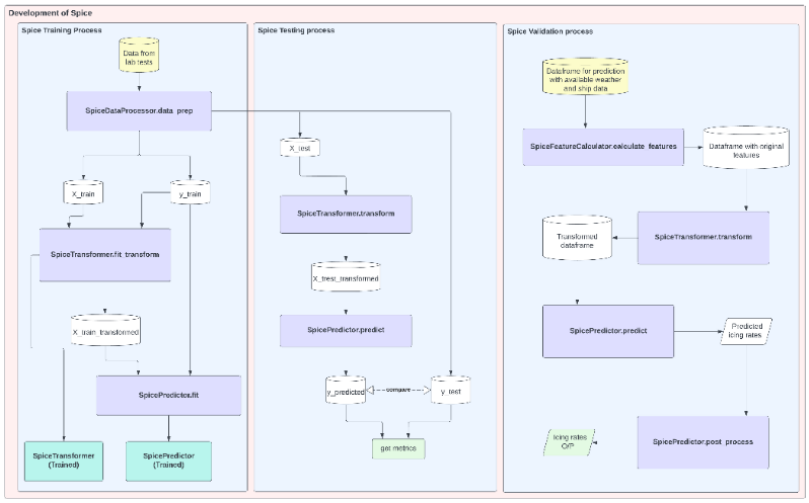

Figure 13: Flowchart for the development of the Spice model

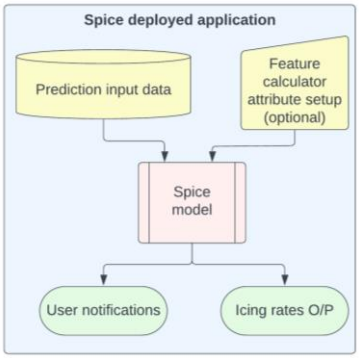

Figure 14: Flowchart for the use of the Spice model when deployed

17. Appendix E

Usage of classes in the Spice model framework

17.1. Use of the SpiceDataProcessor Class

The SpiceDataProcesser Class is provided with a method ‘data_prep’ for obtaining the train-test sets from lab data (Figure). Feature and target names along with the train-test split ratio are set as attributes. The data processer class can be used to retrain the model whenever more experimental data is available.

17.2. Use of the SpiceTransformer Class

The SpiceTransformer class inherits properties from scikit-learn's BaseEstimator and TransformerMixin classes. An instance of this class is created, specifying coefficient and importance thresholds for rule selection as attributes. The 'fit_transform' method trains the transformer object using X_train and y_train, yielding the transformed training dataframe, X_train_transformed. The object is pickled for future use, and retraining can be done by calling the method again. Due to ML's stochastic nature, rules and FFX equations may vary, even with the same dataset. Once the transformer is trained, the ‘transform’ method is called to transform any dataframe with the original features to a dataframe with features including all equations during testing, validation, and general use.

17.3. Use of the SpicePredictor Class

The SpicePredictor class is a container for the ML model for which XGB Regressor was selected after initial assessment. Training is performed by calling the 'fit' method with X_train_transformed and y_train. The trained instance can be pickled. Subsequent 'fit' calls retrain the model, with potential variations due to ML stochasticity. Predictions are made using the 'predict' method (flowchart in Figure). As experiments by Deshpande et.al. 2023 lacked 'no icing' conditions, post-processing predictions is necessary for which the 'post_process' method is called. This sets the predicted icing rate to zero if air temperature exceeds

water freezing point or if spray flux is zero. The condition for zero icing for zero wind was considered, but the possibility of precipitation-induced flux prevents its implementation.

17.4. Use of the SpiceFeatureCalculator class

The SPICE feature calculator class utilizes the 'calculate_features' method to handle situations where original feature values are absent during prediction, and rough approximations suffice. With the available input data, the feature calculator stores calculations in an intermediate dataframe and eventually returns a dataframe containing estimated original feature values. The 'calculate_features' method encompasses multiple functions organized into modules (as depicted in Figure 12). Table 8 outlines module divisions. Main modules (Modules 1 to 7), one for each feature, assess feature values in inputs, while 15 sub-modules are called as needed based on available data. Equations for parameter estimation are detailed in subsequent sections. Missing obligatory inputs triggers an error, notifying users of assumptions made to proceed.

Table 8: Division of feature calculator modules

Feature calculation	1, 2, 3, 4, 5, 6, 7
Wind parameters	A, A1, A2
Ship parameters wrt wind	B, B1, B2
Wave parameters	W1, W2, W3, W3.1
Ship parameters wrt waves	C, C1, C2, C3

18. References

[1] A. Kulyakhtin, “Numerical Modelling and Experiments on Sea Spray Icing,” Doctoral thesis. Department of Civil and Transport Engineering. Norwegian University of Science and Technology (NTNU), Norway, 2014.

[2] J. Stallabrass, “Meteorological and oceanographic aspects of trawler icing off the Canadian east coast.,” 1971.

[3] E. P. Lozowski, K. Szilder, and L. Makkonen, “Computer simulation of marine ice accretion,” *Philosophical Transactions of the Royal Society of London. Series A: Mathematical, Physical and Engineering Sciences*, vol. 358, no. 1776, pp. 2811–2845, Nov. 2000, doi: 10.1098/rsta.2000.0687.

[4] Stallabrass, “Trawler Icing - a Compilation of Work Done At N. R. C.,” *Mechanical Engineering Report MD-56, N.R.C. No. 19372 (National Research Council, Ottawa Canada)*, 1980.

[5] W. P. Zakrzewski, “Splashing a ship with collision-generated spray,” *Cold Reg Sci Technol*, vol. 14, no. 1, pp. 65–83, Jun. 1987, doi: 10.1016/0165-232X(87)90045-0.

[6] A. Kulyakhtin, O. Shipilova, B. Libby, and S. Løset, “Full-scale 3D CFD Simulation of Spray Impingement on a Vessel Produced by Ship-wave Interaction,” *Proc. of the 21st IAHR Intl. Symposium on Ice (2012)*, pp. 1129–1141, 2012.

[7] E. M. Samuelsen, K. Edvardsen, and R. G. Graversen, “Modelled and observed sea-spray icing in Arctic-Norwegian waters,” *Cold Reg Sci Technol*, vol. 134, pp. 54–81, Feb. 2017, doi: 10.1016/j.coldregions.2016.11.002.

[8] L. Battisti, R. Fedrizzi, A. Brighenti, and T. Laakso, “Sea Ice and Icing Risk for Offshore Wind Turbines,” in *OWEMES 2006*, Citavecchia, Italy: OWEMES, 2006, pp. 20–22.

[9] A. R. Dehghani-Sanij, S. R. Dehghani, G. F. Naterer, and Y. S. Muzychka, “Sea spray icing phenomena on marine vessels and offshore structures: Review and formulation,” *Ocean Engineering*, vol. 132, pp. 25–39, Mar. 2017, doi: 10.1016/j.oceaneng.2017.01.016.

[10] S. Deshpande, A. Sæterdal, and P.-A. Sundsbø, “Sea Spray Icing: The Physical Process and Review of Prediction Models and Winterization Techniques,” *Journal of Offshore Mechanics and Arctic Engineering*, vol. 143, no. 6, pp. 1–12, Dec. 2021, doi: 10.1115/1.4050892.

[11] R. D. Brown and P. Roebber, “The Scope of the ice accretion problem in Canadian waters related to offshore energy and transportation.,” Canadian Climate Centre Report 85-13, 1985.

[12] *ISO 35106: Petroleum and natural gas industries — Arctic operations — Metocean, ice, and seabed data*. 2017.

[13] A. Bodaghkhani, S.-R. Dehghani, Y. S. Muzychka, and B. Colbourne, “Understanding spray cloud formation by wave impact on marine objects,” *Cold Reg Sci Technol*, vol. 129, pp. 114–136, Sep. 2016, doi: 10.1016/j.coldregions.2016.06.008.

[14] S. Deshpande, A. Sæterdal, and P.-A. Sundsbø, “Experiments with sea spray icing: Investigation of icing rates. (paper accepted for publication),” *Journal of Offshore Mechanics and Arctic Engineering*, 2023.

[15] S. Li, J. Qin, and R. Paoli, “Data-Driven Machine Learning Model for Aircraft Icing Severity Evaluation,” *Journal of Aerospace Information Systems*, vol. 18, no. 11, pp. 876–880, Nov. 2021, doi: 10.2514/1.I010978.

[16] S. Li, J. Qin, M. He, and R. Paoli, “Fast Evaluation of Aircraft Icing Severity Using Machine Learning Based on XGBoost,” *Aerospace*, vol. 7, no. 4, p. 36, Mar. 2020, doi: 10.3390/aerospace7040036.

[17] E. S. Miles, J. F. Steiner, and F. Brun, “Highly variable aerodynamic roughness length (z0) for a hummocky debris-covered glacier,” *Journal of Geophysical Research: Atmospheres*, vol. 122, no. 16, pp. 8447–8466, Aug. 2017, doi: 10.1002/2017JD026510.

[18] G. M. Masters, *Renewable and Efficient Electric Power Systems.* Hoboken, New Jersey: Wiley-Interscience, 2004.

[19] C. C. Ryerson, “Superstructure spray and ice accretion on a large U.S. Coast Guard cutter,” *Atmos Res*, vol. 36, no. 3–4, pp. 321–337, May 1995, doi: 10.1016/0169-8095(94)00045-F.

[20] D. Chicco, M. J. Warrens, and G. Jurman, “The coefficient of determination R-squared is more informative than SMAPE, MAE, MAPE, MSE and RMSE in regression analysis evaluation,” *PeerJ Comput Sci*, vol. 7, pp. 1–24, Jul. 2021, doi: 10.7717/PEERJ-CS.623/SUPP-1.

[21] T. Chen and C. Guestrin, “XGBoost: A Scalable Tree Boosting System”, doi: 10.1145/2939672.2939785.

[22] F. Pedregosa FABIANPEDREGOSA *et al.*, “Scikit-learn: Machine Learning in Python Gaël Varoquaux Bertrand Thirion Vincent Dubourg Alexandre Passos PEDREGOSA, VAROQUAUX, GRAMFORT ET AL. Matthieu Perrot,” *Journal of Machine Learning Research*, vol. 12, pp. 2825–2830, 2011.

[23] S. Chowdhury, Y. Lin, B. Liaw, and L. Kerby, “Evaluation of Tree Based Regression over Multiple Linear Regression for Non-normally Distributed Data in Battery Performance”.

[24] J. A. Colton and K. M. Bower, “Some misconceptions about R2,” *International Society of Six Sigma Professionals, EXTRAOrdinary Sense*, vol. 3, no. 2, pp. 20–22, 2002.

[25] A. Bodaghkhani, Y. S. Muzychka, and B. Colbourne, “Three-Dimensional Numerical and Experimental Simulation of Wave Run-Up Due to Wave Impact with a Vertical Surface,” *Journal of Fluids Engineering, Transactions of the ASME*, vol. 140, no. 8, pp. 1–12, 2018, doi: 10.1115/1.4039369.

[26] S. Lundberg, “SHAP documentation - Rev.45b85c18.” Accessed: Mar. 07, 2023. [Online]. Available: https://shap.readthedocs.io/en/latest/example_notebooks/overviews/Be careful when interpreting predictive models in search of causal insights.html

[27] G. Dong and H. Liu, *Feature Engineering for Machine Learning and Data Analytics*. CRC Press - Taylor and Francis Group , 2018.

[28] J. H. Friedman and B. E. Popescu, “Predictive Learning via Rule Ensembles,” *Source: The Annals of Applied Statistics*, vol. 2, no. 3, pp. 916–954, 2008, doi: 10.1214/07-AOAS.

[29] T. McConaghy, “FFX: Fast, Scalable, Deterministic Symbolic Regression Technology,” pp. 235–260, 2011, doi: 10.1007/978-1-4614-1770-5_13.

[30] D. Cote, “Demonstrating the power of feature engineering .” Accessed: Mar. 07, 2023. [Online]. Available: https://medium.com/@dave.cote.msc/demonstrating-the-power-of-feature-engineering-part-ii-how-i-beat-xgboost-with-linear-regression-e63aeb6a15f8

[31] C. Molnar, *Interpretable Machine Learning . A guide for making Black Box models Explainable*. https://christophm.github.io/interpretable-ml-book/, 2023.

[32] C. Molnar, “Python package for RuleFit.” Accessed: Mar. 07, 2023. [Online]. Available: https://github.com/christophM/rulefit/blob/master/LICENSE

[33] T. McConaghy, “Python package for FFX,” Solido Design Automation Inc. Accessed: Mar. 07, 2023. [Online]. Available: https://github.com/natekupp/ffx/blob/master/LICENSE

[34] J. Bergstra, B. Komer, C. Eliasmith, D. Yamins, and D. D. Cox, “Hyperopt: a Python library for model selection and hyperparameter optimization,” *Comput Sci Discov*, vol. 8, no. 1, p. 014008, Jul. 2015, doi: 10.1088/1749-4699/8/1/014008.

[35] W. P. Zakrzewski, “Icing of Fishing Vessels. Part I: Splashing a Ship With Spray.,” in *Proceedings of the 8th Int. IAHR Symposium on Ice, Iowa City, August 18–22, 1986, Vol. 2 (1986), pp. 179-194*, 1986.

[36] N. M. L. and A. UK, “The Beaufort Scale,” 2010.

[37] I. Horjen, “Numerical modeling of two-dimensional sea spray icing on vessel-mounted cylinders,” *Cold Reg Sci Technol*, vol. 93, pp. 20–35, Sep. 2013, doi: 10.1016/j.coldregions.2013.05.003.

[38] T. S. Jørgensen, “Sea spray characteristics on a semi-submersible drilling rig - STF60 F 85015,” 1985.

[39] I. Horjen, “Numerical modeling of time-dependent marine icing, anti-icing and de-icing,” Trondheim University, Norway, 1990.

[40] B. Massey and J. Ward-Smith, *Mechanics of Fluids*, Eighth. Taylor & Francis, 2006.

[41] A. Kovrova, C. Korotun, and V. Panov, “Gidrometeorologicheskiye usloviya obledeneniya na sudakh v arkticheskikh moryakh. (Hydrometeorological conditions of icing on ships in the Arctic seasa),” *Arkticheskii i Antarkticheskii Nauchno-lssledovatiel’skii lnstitut, Leningrad*, 1969.

[42] L. R. Aksjutin, “Icing of Ships. Leningrad: Sudostroenye (in Russian),” p. 126, 1979.

[43] A. Kulyakhtin and A. Tsarau, “A time-dependent model of marine icing with application of computational fluid dynamics,” *Cold Reg Sci Technol*, vol. 104–105, pp. 33–44, Aug. 2014, doi: 10.1016/j.coldregions.2014.05.001.

[44] Ryerson, “Icing Management for Coast Guard Assets,” U.S. Army Engineer Research and Development Center, Hanover, New Hampshire, USA, 2013.

[45] Y. P. Borisenkov, “On the theory of spray icing of ships. In: Arkticheskii i Antarkticheskii Nauchno-Issledovatelskii Institut. Trudy 298. Leningrad: Gidrometeoizdat (in Russian), 34-43.,” 1972.

[46] E. M. Samuelsen, “Prediction of ship icing in Arctic waters - Observations and modelling for application in operational weather forecasting,” UiT, The Arctic University of Norway (Doctoral Thesis), 2017.

[47] T. W. Forest, E. P. Lozowski, and R. Gagnon, “Estimating marine icing on offshore structures using RIGICE04,” in *Proceedings of the International Workshop on Atmospheric Icing on Structures (IWAIS), Montreal, Canada.*, 2005.

[48] I. Horjen and S. Vefsnmo, “A Kinematic and Thermodynamic Analysis of Sea Spray (in Norwegian), Offshore Icing—Phase II. Norwegian Hydrodynamic Laboratory (NHI). Report STF60 F85014,” 1985.

[49] L. Makkonen, R. D. Brown, and P. T. Mitten, “Comments on ‘Prediction of Vessel Icing for Near-Freezing Sea Temperatures,’” *Weather Forecast*, vol. 6, no. 4, pp. 565–567, Dec. 1991, doi: 10.1175/1520-0434(1991)006<0565:COOVIF>2.0.CO;2.

[50] A. Kulyakhtin and S. Løset, “Sea spray icing : in-cloud evaporation . Semi- analytical and numerical investigations .,” in *The 14th International Workshop on Atmospheric Icing of Structures, Chongqing, China, May 8 - May 13, 2011 SEA*, Chongqing, China, 2011.

[51] L. Makkonen, “Salinity and growth rate of ice formed by sea spray,” *Cold Reg Sci Technol*, vol. 14, no. 2, pp. 163–171, Aug. 1987, doi: 10.1016/0165-232X(87)90032-2.

[52] J. E. Overland, C. H. Pease, R. W. Preisendorfer, and A. L. Comiskey, “Prediction of Vessel Icing,” *Journal of Climate and Applied Meteorology*, vol. 25, no. 12, pp. 1793–1806, Dec. 1986, doi: 10.1175/1520-0450(1986)025<1793:POVI>2.0.CO;2.

[53] P. Roebber and P. Mitten, *Modelling and measurement of icing in Canadian waters*. Report (Canadian Climate Centre), no. 87-15., 1987.

15. Appendix 4: Paper 4

Investigation into using CFD for estimation of ship specific parameters for the SPICE model for prediction of sea spray icing. Part 1: The proposal

Sujay Deshpande*, Per-Arne Sundsbø

Department of Building, Energy, and Material Technology. UiT, The Arctic University of Norway.
*Corresponding author: Sujay Deshpande
Address: C/o UiT, Campus Narvik, Lodve Langesgate 2, 8514, Narvik, Norway.
e-mail: sujay.r.deshpande@uit.no

[This is a copy of the submitted version of the article to a journal]

[Unavailable in the restricted version of the thesis due to embargo]

16. Appendix 5: Paper 5

Investigation into using CFD for estimation of ship specific parameters for the SPICE model for prediction of sea spray icing. Part 2: Verification of SPICE2 with full scale test.

Per-Arne Sundsbø, Sujay Deshpande*

Department of Building, Energy, and Material Technology. UiT, The Arctic University of Norway.
*Corresponding author: Sujay Deshpande
Address: C/o UiT, Campus Narvik, Lodve Langesgate 2, 8514, Narvik, Norway.
e-mail: sujay.r.deshpande@uit.no

[This is a copy of the submitted version of the article to a journal]

[Unavailable in the restricted version of the thesis due to embargo]

17. Appendix 6: Full-page versions of intricate flowcharts from Paper 3

Full Page Versions of unclear flowcharts from Paper 3

This attachment is for the sole purpose of presenting clearer full-page pictures of the flowcharts already presented in Paper 3 which were deemed to be unclear due to poor image quality. Paper 3 (another attachment) is a reprint of the accepted version of the article, reprinted with permission from ASME, strictly for the use of inclusion in the PhD thesis. DOI of published version: https://doi.org/10.1115/1.4064108.

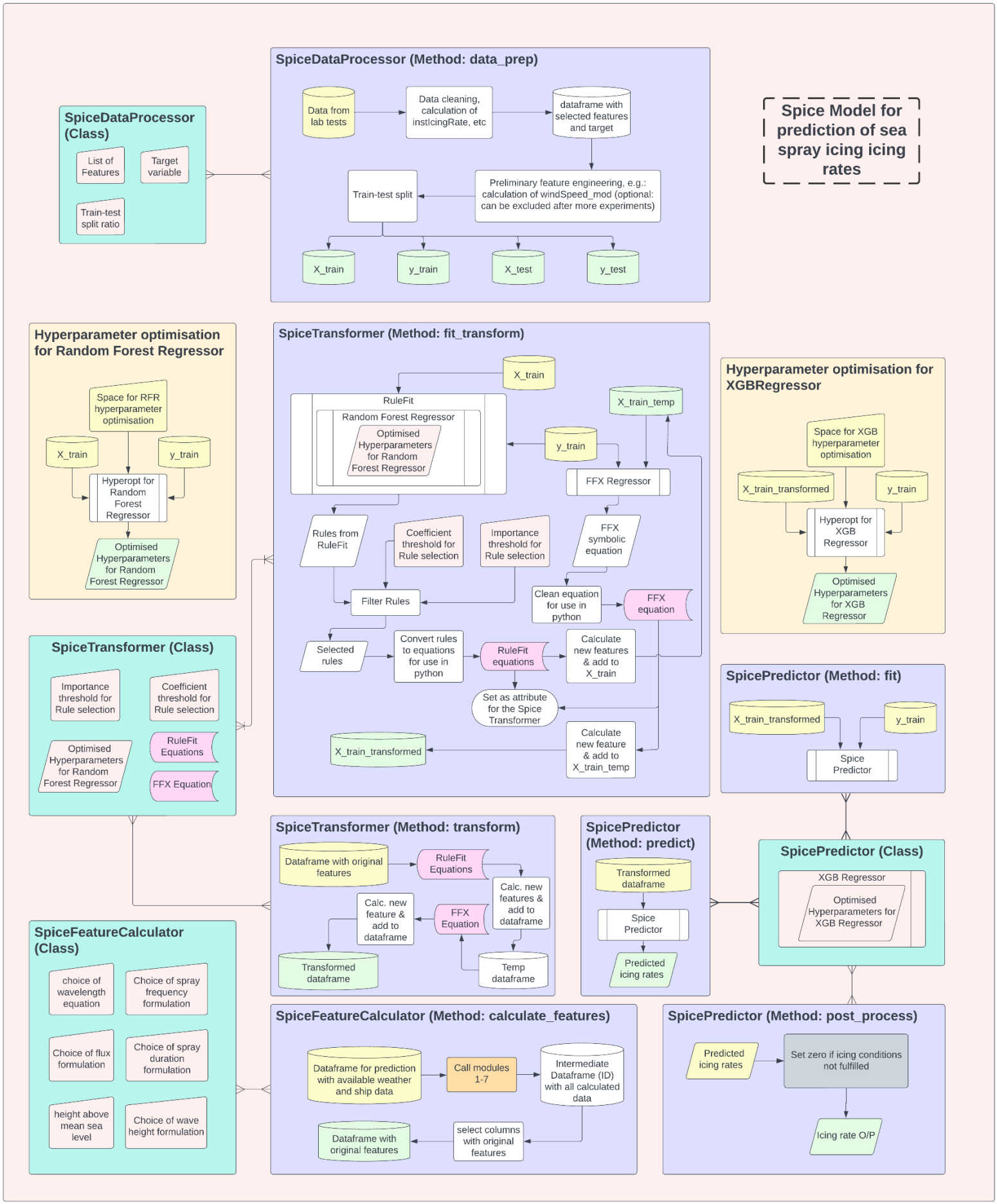
Spice Model for prediction of sea spray icing icing rates
SpiceDataProcessor (Class)
List of Features
Target variable
Train-test split ratio
SpiceDataProcessor (Method: data_prep)
Data from lab tests
Data cleaning, calculation of instIcingRate, etc
dataframe with selected features and target
Preliminary feature engineering, e.g.: calculation of windSpeed_mod (optional: can be excluded after more experiments)
Train-test split
X_train
y_train
X_test
y_test
Hyperparameter optimisation for Random Forest Regressor
Space for RFR hyperparameter optimisation
X_train
y_train
Hyperopt for Random Forest Regressor
Optimised Hyperparameters for Random Forest Regressor
SpiceTransformer (Method: fit_transform)
X_train
RuleFit
Random Forest Regressor
Optimised Hyperparameters for Random Forest Regressor
X_train_temp
y_train
FFX Regressor
Rules from RuleFit
Coefficient threshold for Rule selection
Importance threshold for Rule selection
FFX symbolic equation
Filter Rules
Clean equation for use in python
FFX equation
Selected rules
Convert rules to equations for use in python
RuleFit equations
Calculate new features & add to X_train
Set as attribute for the Spice Transformer
X_train_transformed
Calculate new feature & add to X_train_temp
Hyperparameter optimisation for XGBRegressor
Space for XGB hyperparameter optimisation
X_train_transformed
y_train
Hyperopt for XGB Regressor
Optimised Hyperparameters for XGB Regressor
SpiceTransformer (Class)
Importance threshold for Rule selection
Coefficient threshold for Rule selection
Optimised Hyperparameters for Random Forest Regressor
RuleFit Equations
FFX Equation
SpicePredictor (Method: fit)
X_train_transformed
y_train
Spice Predictor
SpiceTransformer (Method: transform)
Dataframe with original features
RuleFit Equations
Calc. new features & add to dataframe
Calc. new feature & add to dataframe
FFX Equation
Transformed dataframe
Temp dataframe
SpicePredictor (Method: predict)
Transformed dataframe
Spice Predictor
Predicted icing rates
SpicePredictor (Class)
XGB Regressor
Optimised Hyperparameters for XGB Regressor
SpiceFeatureCalculator (Class)
choice of wavelength equation
Choice of spray frequency formulation
Choice of flux formulation
Choice of spray duration formulation
height above mean sea level
Choice of wave height formulation
SpiceFeatureCalculator (Method: calculate_features)
Dataframe for prediction with available weather and ship data
Call modules 1-7
Intermediate Dataframe (ID) with all calculated data
Dataframe with original features
select columns with original features
SpicePredictor (Method: post_process)
Predicted icing rates
Set zero if icing conditions not fulfilled
Icing rate O/P

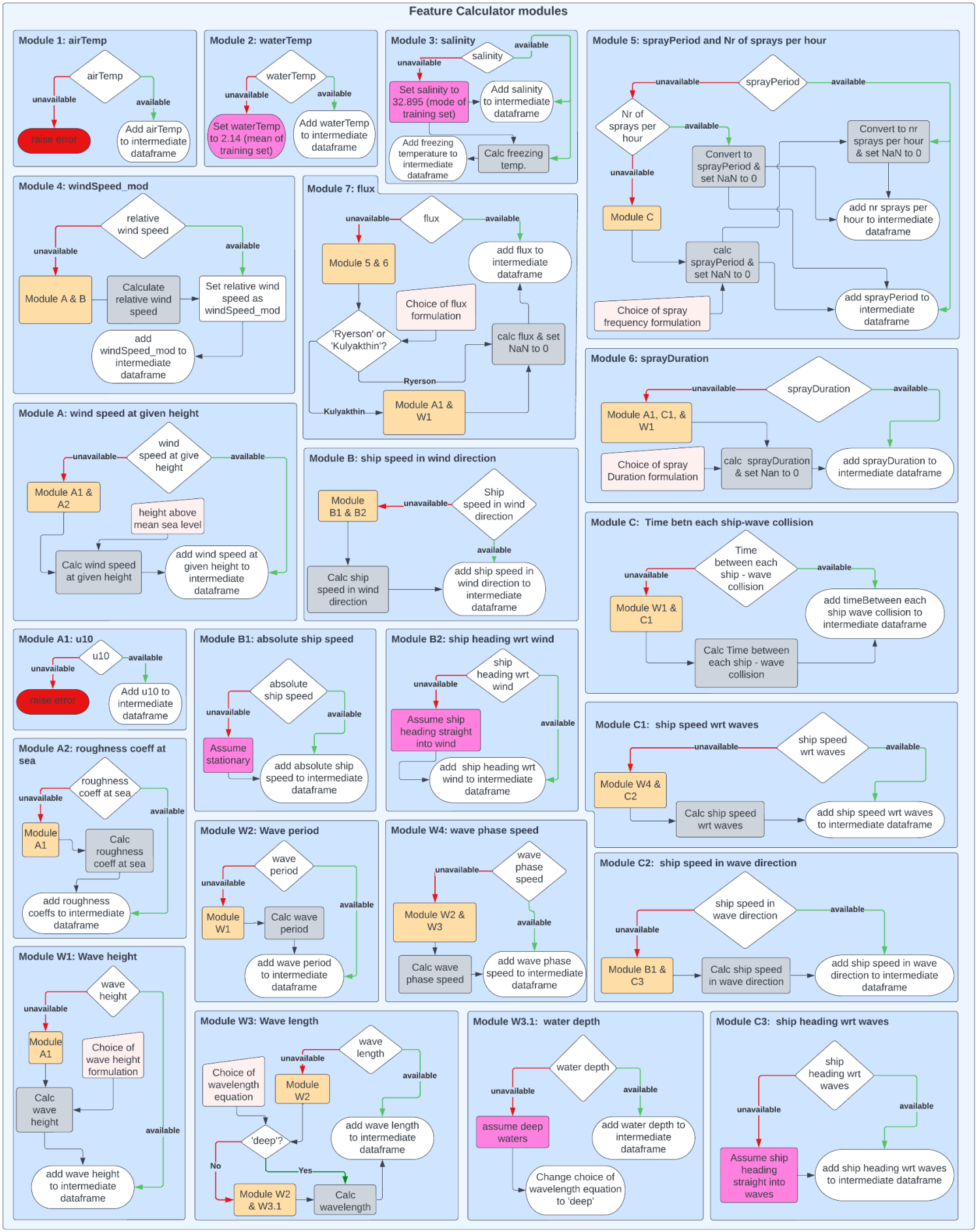
Feature Calculator modules
Module 1: airTemp
airTemp
unavailable
available
raise error
Add airTemp to intermediate dataframe
Module 2: waterTemp
waterTemp
unavailable
available
Set waterTemp to 2.14 (mean of training set)
Add waterTemp to intermediate dataframe
Module 3: salinity
salinity
available
unavailable
Set salinity to 32.895 (mode of training set)
Add salinity to intermediate dataframe
Add freezing temperature to intermediate dataframe
Calc freezing temp.
Module 5: sprayPeriod and Nr of sprays per hour
sprayPeriod
unavailable
available
Nr of sprays per hour
Convert to sprayPeriod & set NaN to 0
Convert to nr sprays per hour & set NaN to 0
Module C
add nr sprays per hour to intermediate dataframe
calc sprayPeriod & set NaN to 0
Choice of spray frequency formulation
add sprayPeriod to intermediate dataframe
Module 4: windSpeed_mod
relative wind speed
Module A & B
Calculate relative wind speed
Set relative wind speed as windSpeed_mod
add windSpeed_mod to intermediate dataframe
Module 7: flux
flux
Module 5 & 6
add flux to intermediate dataframe
Choice of flux formulation
'Ryerson' or 'Kulyakthin'?
calc flux & set NaN to 0
Ryerson
Kulyakthin
Module A1 & W1
Module 6: sprayDuration
sprayDuration
Module A1, C1, & W1
Choice of spray Duration formulation
calc sprayDuration & set Nan to 0
add sprayDuration to intermediate dataframe
Module A: wind speed at given height
wind speed at give height
Module A1 & A2
height above mean sea level
Calc wind speed at given height
add wind speed at given height to intermediate dataframe
Module B: ship speed in wind direction
Module B1 & B2
Ship speed in wind direction
Calc ship speed in wind direction
add ship speed in wind direction to intermediate dataframe
Module C: Time betn each ship-wave collision
Time between each ship - wave collision
Module W1 & C1
add timeBetween each ship wave collision to intermediate dataframe
Calc Time between each ship - wave collision
Module A1: u10
u10
raise error
Add u10 to intermediate dataframe
Module B1: absolute ship speed
absolute ship speed
Assume stationary
add absolute ship speed to intermediate dataframe
Module B2: ship heading wrt wind
ship heading wrt wind
Assume ship heading straight into wind
add ship heading wrt wind to intermediate dataframe
Module C1: ship speed wrt waves
ship speed wrt waves
Module W4 & C2
Calc ship speed wrt waves
add ship speed wrt waves to intermediate dataframe
Module A2: roughness coeff at sea
roughness coeff at sea
Module A1
Calc roughness coeff at sea
add roughness coeffs to intermediate dataframe
Module W2: Wave period
wave period
Module W1
Calc wave period
add wave period to intermediate dataframe
Module W4: wave phase speed
wave phase speed
Module W2 & W3
Calc wave phase speed
add wave phase speed to intermediate dataframe
Module C2: ship speed in wave direction
ship speed in wave direction
Module B1 & C3
Calc ship speed in wave direction
add ship speed in wave direction to intermediate dataframe
Module W1: Wave height
wave height
Module A1
Choice of wave height formulation
Calc wave height
add wave height to intermediate dataframe
Module W3: Wave length
wave length
Choice of wavelength equation
Module W2
'deep'?
No
Yes
add wave length to intermediate dataframe
Module W2 & W3.1
Calc wavelength
Module W3.1: water depth
water depth
assume deep waters
add water depth to intermediate dataframe
Change choice of wavelength equation to 'deep'
Module C3: ship heading wrt waves
ship heading wrt waves
Assume ship heading straight into waves
add ship heading wrt waves to intermediate dataframe